

# Update Offshore Wind Atlas

## Implementing a variable sea surface roughness

J.A.J. Donkers

17 November 2010



# Update Offshore Wind Atlas

Implementing a variable sea surface roughness

Thesis Report

J.A.J. Donkers  
1172484

Petten, Wednesday 17<sup>th</sup> November, 2010



## Abstract

In 2005 the Energy research Centre of the Netherlands (ECN) published its first version of the Offshore Wind Atlas of the Dutch part of the North Sea [3]. This version has been updated and improved using longer time series and another approach for the calculation of the roughness of the sea surface. In contradiction to other Wind Atlases which are based on measurements [28], use is made of data from the Numerical Weather Prediction model Hirlam. Measurements of wind speeds and directions are only used to validate the Wind Atlas.

For the Offshore Wind Atlas, the Hirlam data is interpolated where for the vertically interpolation use is made of the Businger-Dyer profiles in combination with the Monin-Obukhov length [3]. One of the required parameters for the interpolation is the surface roughness. For land, it can be assumed constant while for sea it is variable. In the previous version of the Offshore Wind Atlas, the sea surface roughness has been determined using Charnock's relation [9], where the so-called Charnock parameter is constant. In the new version, the equation of Hsu is introduced which states that the Charnock parameter is variable and dependent on the wave steepness i.e. the wave height divided by the wave length [19]. Assuming that the North Sea is a shallow sea and using the general wave equation, which relates the sea depth and wave length to the phase velocity of the waves, it was found that the wave steepness can be rewritten in a fraction of the wave height over the wave period multiplied by the square root of the sea depth times the gravitational acceleration. These quantities are derived from measured values which are interpolated to the location of interest. Using this approach, it is tried to improve the prediction of the wind speed distributions for a given location and altitude.

Using wind measurements at several locations it was found that adding the wave data to the computations show a small improvement in the estimation of the wind speed distribution compared to the previous version of the Offshore Wind Atlas. For each measurement location and method, a two parameter Weibull distribution has been made, after which a comparison was done between the various shape and scale parameters. Generally, the scale parameter was overestimated by both versions of the Offshore Wind Atlas compared to the measurements. The cause of this behavior might be found in the data used to make the Atlas. The shape parameter is well predicted by the new version of the Offshore Wind Atlas due to the use of wave data. The influence of the wave data is found to be larger for lower altitudes than for higher altitudes. Besides Weibull distributions, also maps with average wind speeds are given by the Offshore Wind Atlas which are compared to older maps.

## Acknowledgement

In this report use is made of several measured time series for wind speeds and directions as well as wave heights and wave periods. For this, thanks goes to the BMU (Bundesministerium fuer Umwelt, Federal Ministry for the Environment, Nature Conservation and Nuclear Safety) and the PTJ (Projekttraeger Juelich, Project Executing Organisation) for measurements at FINO-1 in the German part of the North Sea, KNMI (Royal Dutch Meteorological Institute) for making data available of measurements at the stations Europlatform, K13- $\alpha$ , Meetpost Noordwijk, IJmuiden, LE Goeree, Vlakte vd Raan and Oosterschelde, the CESAR-database (Cabauw Experimental Site for Atmospheric Research) for data of the Cabauw measurement mast, Rijkswaterstaat for the delivery of data on significant wave heights and wave periods, and of course ECN (Energy research Centre of the Netherlands) for providing the data of measurement mast 1 of the EWTW (ECN Wind turbine Test station Wieringermeer) and data of the measurement mast of OWEZ (Offshore Wind farm Egmond aan Zee). Also thanks to the Royal Hydrographic Service of the Royal Netherlands Navy for providing data of the sea depth in the Dutch Exclusive Economic Zone.

Further more, special thanks goes to dr.ir. H. Bijl of TU Delft and dr.ir. A.J. Brand of ECN for supervising me during my Thesis work.

## Keywords

Wind Atlas, North Sea, Offshore, Sea Surface Roughness

# Contents

|  |      |
|--|------|
| List of Symbols  | xvii |
| List of Abbreviations  | xxi  |
| 1 Introduction   | 1    |
| 1.1 Wind Atlas . . . . .                                     | 1    |
| 1.2 Problem definition . . . . .                             | 1    |
| 1.3 Reading guide . . . . .                                  | 2    |
| I Model  | 5    |
| 2 Introduction to the AVDE model                             | 7    |
| 3 Location and Hirlam input parameters                       | 9    |
| 3.1 Location . . . . .                                       | 9    |
| 3.2 Hirlam data . . . . .                                    | 9    |
| 3.2.1 Background Hirlam . . . . .                            | 10   |
| 3.2.2 Hirlam data for model input . . . . .                  | 11   |
| 4 Surface roughness input                                    | 13   |
| 4.1 Description surface roughness and wind profile . . . . . | 13   |
| 4.2 Surface roughness of the Netherlands . . . . .           | 14   |
| 4.3 Theory of estimating the sea surface roughness . . . . . | 15   |
| 4.3.1 Dimensional Analysis . . . . .                         | 15   |
| 4.3.2 Three methods for the sea surface roughness . . . . .  | 17   |
| 4.4 Data . . . . .   | 19   |
| 4.5 Interpolation of Wave Data . . . . .                     | 20   |
| 4.5.1 Inverse Distance Weighting . . . . .                   | 22   |
| 4.5.2 Gibescu's method . . . . .                             | 23   |
| 4.6 Validation of spatial interpolation methods . . . . .    | 31   |
| 4.6.1 Conclusions spatial interpolation methods . . . . .    | 35   |
| 5 AVDE model   | 37   |
| 5.1 Cell selection . . . . .                                 | 37   |
| 5.2 Time interpolation . . . . .                             | 37   |
| 5.3 Vertical interpolation . . . . .                         | 38   |
| 5.4 Horizontal interpolation . . . . .                       | 38   |
| 5.5 Local adjustments . . . . .                              | 38   |
| 6 Model Output   | 39   |
| 6.1 Time Series . . . . .                                    | 39   |

|                       |  |           |
|-----------------------|--|-----------|
| 6.2                   | Weibull distribution . . . . .                   | 39        |
| 6.3                   | Reference wind speed . . . . .                   | 41        |
| <b>II Validation</b>  |  | <b>43</b> |
| 7                     | Setup validation AVDE model                      | 45        |
| 7.1                   | Calculation methods . . . . .                    | 45        |
| 7.2                   | Stations . . . . .                               | 46        |
| 7.3                   | Selection of time step . . . . .                 | 47        |
| 7.4                   | Basic analysis steps . . . . .                   | 47        |
| 8                     | Onshore Locations                                | 49        |
| 8.1                   | Cabauw . . . . .                                 | 49        |
| 8.2                   | EWTW . . . . .                                   | 52        |
| 9                     | Offshore Locations                               | 55        |
| 9.1                   | OWEZ . . . . .                                   | 55        |
| 9.2                   | FINO-1 . . . . .                                 | 57        |
| 9.3                   | KNMI Sea Stations . . . . .                      | 59        |
| 9.3.1                 | KNMI sea station description . . . . .           | 59        |
| 9.3.2                 | Linear regression . . . . .                      | 61        |
| 9.3.3                 | Mean wind speed . . . . .                        | 62        |
| 9.3.4                 | Weibull parameters . . . . .                     | 63        |
| 10                    | Comparison of stations                           | 67        |
| 10.1                  | Turn over point . . . . .                        | 67        |
| 10.2                  | Map error . . . . .                              | 67        |
| 10.3                  | Order in methods . . . . .                       | 69        |
| 10.4                  | Influence of method on shape parameter . . . . . | 70        |
| 11                    | Selection of method                              | 71        |
| 12                    | Conclusions Validation AVDE model                | 73        |
| <b>III Wind Atlas</b> |  | <b>75</b> |
| 13                    | Set up Calculations Offshore Wind Atlas          | 77        |
| 13.1                  | Grid size and Time period . . . . .              | 77        |
| 13.2                  | Used Methods . . . . .                           | 78        |
| 13.3                  | Comparison . . . . .                             | 78        |
| 13.4                  | Contents new Offshore Wind Atlas . . . . .       | 79        |

|   |         |
|---|---------|
| 14 Results Wind Atlas                                   | 81      |
| 14.1 Mean wind speed . . . . .                          | 81      |
| 14.2 Weibull parameters . . . . .                       | 82      |
| 14.2.1 Scale parameter . . . . .                        | 82      |
| 14.2.2 Shape parameter . . . . .                        | 83      |
| 14.3 Reference wind speed . . . . .                     | 85      |
| 15 Comparison with other wind maps                      | 91      |
| 15.1 Previous version ECN Offshore Wind Atlas . . . . . | 91      |
| 16 Conclusions Offshore Wind Atlas                      | 95      |
| <br>IV Conclusions                                      | <br>96  |
| 17 Conclusions  | 97      |
| 17.1 AVDE model . . . . .                               | 97      |
| 17.2 Validation . . . . .                               | 98      |
| 17.3 Wind Atlas . . . . .                               | 98      |
| 17.4 Closing statements . . . . .                       | 99      |
| 18 Recommendations                                      | 101     |
| <br>Bibliography  | <br>105 |
| A Results Onshore Locations                             | 107     |
| A.1 Results Cabauw . . . . .                            | 107     |
| A.2 Results EWTW . . . . .                              | 108     |
| B Results Offshore Locations                            | 109     |
| B.1 Results OWEZ . . . . .                              | 109     |
| B.2 Results FINO-1 . . . . .                            | 111     |
| B.3 Results Europlatform . . . . .                      | 112     |
| B.4 Results K13- $\alpha$ . . . . .                     | 113     |
| B.5 Results Noordwijk . . . . .                         | 114     |
| B.6 Results IJmuiden . . . . .                          | 115     |
| B.7 Results Licht Eiland Goeree . . . . .               | 116     |
| B.8 Results Vlakte van de Raan . . . . .                | 117     |
| B.9 Results Oosterschelde . . . . .                     | 118     |
| C Surface roughness classes                             | 121     |



## List of Figures

|    |  |    |
|----|--|----|
| 1  | Block representation of the AVDE model . . . . .   | 7  |
| 2  | Three different types of location input. . . . .   | 9  |
| 3  | Example of the use of Hirlam data. . . . .   | 10 |
| 4  | Overview area covered by Hirlam files. . . . .   | 12 |
| 5  | Example wind profiles over sea, grassland and city area. . . . .   | 14 |
| 6  | Roughness map of the Netherlands. . . . .  | 15 |
| 7  | Wind profiles for a rough and calm sea. . . . .  | 16 |
| 8  | Area with known sea depth. . . . .   | 19 |
| 9  | Locations wave data measurement stations. . . . .  | 21 |
| 10 | Graphical overview of the time span of the available data per station. . . . .   | 21 |
| 11 | Flow chart of the AVDE model, extended for the Surface Roughness input. . . . .  | 22 |
| 12 | Sea depth before interpolation (left) and after interpolation using IDW (right). . . . .                               | 24 |
| 13 | Mean-variance relationship for significant wave height measurements. . . . .   | 24 |
| 14 | Mean-variance relationship for significant wave height measurements after variance stabilizing transformation. . . . . | 26 |
| 15 | Covariance of logarithmic wave height vs Euclidean distance. . . . .   | 28 |
| 16 | Average of wave height occurring at equal time of the day. . . . .   | 29 |
| 17 | Monthly averaged mean sea level pattern for measured locations. . . . .  | 30 |
| 18 | Wave height covariance per month vs euclidean distance for 15 measurement stations. . . . .                            | 30 |
| 19 | Time series wave height at IJmuiden Munitiestortplaats. . . . .  | 31 |
| 20 | Time series wave height at IJmuiden Munitiestortplaats. . . . .  | 32 |
| 21 | Scatterplot IJmuiden Minutiestortplaats, wave height, method: IDW. . . . .   | 32 |
| 22 | Scatterplot IJmuiden Minutiestortplaats, wave period, method: IDW. . . . .   | 32 |
| 23 | Scatterplot IJmuiden Minutiestortplaats, wave height, method: Cov. . . . .   | 33 |
| 24 | Scatterplot IJmuiden Minutiestortplaats, wave period, method: Cov. . . . .   | 33 |
| 25 | Scatterplot IJmuiden Minutiestortplaats, wave height, method: Cov Month. . . . .                                       | 33 |
| 26 | Scatterplot IJmuiden Minutiestortplaats, wave period, method: Cov Month. . . . .                                       | 33 |
| 27 | Time series Charnock parameter at IJmuiden Munitiestortplaats. . . . .   | 35 |
| 28 | Flow chart of the AVDE model with focus on the calculation module. . . . .   | 37 |
| 29 | Graphical explanation of calculation of energy content in observed time series. . . . .                                | 40 |
| 30 | Location of validation stations. . . . .   | 46 |
| 31 | Scatterplot Measurement vs Method 1 Charnock, for Cabauw at 80 m height. . . . .                                       | 50 |
| 32 | Weibull distribution of measured and calculated time series for Cabauw at 80 m height. . . . .                         | 51 |
| 33 | Weibull distributions of measurements and methods 1 to 3 for Oosterschelde. . . . .                                    | 64 |
| 34 | Weibull distributions of measurements and methods 1 to 3 for K13- $\alpha$ . . . . .                                   | 65 |
| 35 | Map error versus height method 1 Charnock. . . . .   | 69 |
| 4  | Overview area covered by Hirlam files (repeated). . . . .  | 78 |
| 36 | Average wind speed for 40m height, Method 1: Charnock. . . . .   | 82 |

|    |   |     |
|----|---|-----|
| 37 | Average wind speed for 40m height, Method 2: Hsu IDW Sha. . . . .   | 82  |
| 38 | Average wind speed for 90m height, Method 1: Charnock. . . . .  | 83  |
| 39 | Average wind speed for 90m height, Method 2: Hsu IDW Sha. . . . .   | 83  |
| 40 | Average wind speed for 140m height, Method 1: Charnock. . . . .   | 83  |
| 41 | Average wind speed for 140m height, Method 2: Hsu IDW Sha. . . . .  | 83  |
| 42 | Weibull scale parameter $A$ for 40m height, Method 1: Charnock. . . . .   | 84  |
| 43 | Weibull scale parameter $A$ for 40m height, Method 2: Hsu IDW Sha. . . . .  | 84  |
| 44 | Weibull scale parameter $A$ for 90m height, Method 1: Charnock. . . . .   | 84  |
| 45 | Weibull scale parameter $A$ for 90m height, Method 2: Hsu IDW Sha. . . . .  | 84  |
| 46 | Weibull scale parameter $A$ for 140m height, Method 1: Charnock. . . . .  | 85  |
| 47 | Weibull scale parameter $A$ for 140m height, Method 2: Hsu IDW Sha. . . . .   | 85  |
| 48 | Weibull shape parameter $k$ for 40m height, Method 1: Charnock. . . . .   | 86  |
| 49 | Weibull shape parameter $k$ for 40m height, Method 2: Hsu IDW Sha. . . . .  | 86  |
| 50 | Weibull shape parameter $k$ for 90m height, Method 1: Charnock. . . . .   | 86  |
| 51 | Weibull shape parameter $k$ for 90m height, Method 2: Hsu IDW Sha. . . . .  | 86  |
| 52 | Weibull shape parameter $k$ for 140m height, Method 1: Charnock. . . . .  | 87  |
| 53 | Weibull shape parameter $k$ for 140m height, Method 2: Hsu IDW Sha. . . . .   | 87  |
| 54 | Reference wind speed for 40m height, Method 1: Charnock. . . . .  | 88  |
| 55 | Reference wind speed for 40m height, Method 2: Hsu IDW Sha. . . . .   | 88  |
| 56 | Reference wind speed for 90m height, Method 1: Charnock. . . . .  | 88  |
| 57 | Reference wind speed for 90m height, Method 2: Hsu IDW Sha. . . . .   | 88  |
| 58 | Reference wind speed for 140m height, Method 1: Charnock. . . . .   | 89  |
| 59 | Reference wind speed for 140m height, Method 2: Hsu IDW Sha. . . . .  | 89  |
| 60 | Results previous version Offshore Wind Atlas for an altitude of 90 m. . . . .   | 92  |
| 61 | Mean wind speed new version Offshore Wind Atlas for an altitude of 90m, calculated using<br>method 2 Hsu IDW Sha. . . . . | 92  |
| 62 | Average wind speed for 90m height, Method 2: Hsu IDW Sha. . . . .   | 99  |
| 63 | Weibull scale parameter $A$ for 90m height, Method 2: Hsu IDW Sha. . . . .  | 99  |
| 64 | Weibull shape parameter $k$ for 90m height, Method 2: Hsu IDW Sha. . . . .  | 100 |
| 65 | Reference wind speed for 90m height, Method 2: Hsu IDW Sha. . . . .   | 100 |

## List of Tables

|    |  |    |
|----|--|----|
| 1  | Specification of Hirlam files to be used with the AVDE-model . . . . .   | 11 |
| 2  | Coordinates of wave measurement stations. . . . .  | 20 |
| 3  | Deviations from measured time series of wave height for the different validation stations and used methods. . . . .        | 33 |
| 4  | Deviations from measured time series of wave period for the different validation stations and used methods. . . . .        | 34 |
| 5  | Deviations from measured time series of Charnock parameter for the different validation stations and used methods. . . . . | 34 |
| 6  | The frequency of independent observations $v_M$ as a function of the averaging time $T_{ave}$ . . . . .                    | 41 |
| 7  | Specification measurement site Cabauw. . . . .   | 49 |
| 8  | Regression coefficients Cabauw. . . . .  | 50 |
| 9  | Mean wind speeds Cabauw. . . . .   | 50 |
| 10 | Map error Cabauw. . . . .  | 51 |
| 11 | Weibull scale parameter A Cabauw. . . . .  | 52 |
| 12 | Weibull shape parameter k Cabauw. . . . .  | 52 |
| 13 | Specification measurement site EWTW. . . . .   | 52 |
| 14 | Regression coefficients EWTW. . . . .  | 52 |
| 15 | Mean wind speeds EWTW. . . . .   | 53 |
| 16 | Map error EWTW . . . . .   | 53 |
| 17 | Weibull scale parameter A EWTW. . . . .  | 53 |
| 18 | Weibull shape parameter $k$ EWTW. . . . .  | 53 |
| 19 | Specification measurement site OWEZ. . . . .   | 55 |
| 20 | Regression coefficients OWEZ. . . . .  | 56 |
| 21 | Mean wind speeds OWEZ. . . . .   | 56 |
| 22 | Map error OWEZ . . . . .   | 56 |
| 23 | Weibull scale parameter A OWEZ. . . . .  | 57 |
| 24 | Weibull shape parameter k OWEZ. . . . .  | 57 |
| 25 | Specification measurement site FINO-1. . . . .   | 57 |
| 26 | Regression coefficients FINO-1. . . . .  | 58 |
| 27 | Mean wind speeds FINO-1. . . . .   | 58 |
| 28 | Map error FINO-1 . . . . .   | 58 |
| 29 | Weibull scale parameter A FINO-1. . . . .  | 58 |
| 30 | Weibull shape parameter k FINO-1. . . . .  | 59 |
| 31 | Specification measurement site Europlatform. . . . .   | 59 |
| 32 | Specification measurement site K13- $\alpha$ . . . . .   | 60 |
| 33 | Specification measurement site Meetpost Noordwijk. . . . .   | 60 |
| 34 | Specification measurement site IJmuiden. . . . .   | 60 |
| 35 | Specification measurement site Licht Eiland Goeree. . . . .  | 61 |
| 36 | Specification measurement site Vlake van de Raan. . . . .  | 61 |

|    |   |     |
|----|---|-----|
| 37 | Specification measurement site Oosterschelde. . . . .   | 61  |
| 38 | Regression coefficients KNMI stations. . . . .  | 62  |
| 39 | Mean wind speeds at KNMI stations. . . . .  | 62  |
| 40 | Map error KNMI stations . . . . .   | 63  |
| 41 | Weibull scale parameter $A$ for KNMI stations. . . . .  | 63  |
| 42 | Weibull shape parameter $k$ for KNMI stations. . . . .  | 64  |
| 43 | Turn over points from mean wind speed for stations with multiple measurement heights. . . . . | 67  |
| 44 | Sample mean and variance of the map error for potential wind speeds. . . . .                  | 68  |
| 45 | Sample mean and variance of the map error for true wind speed. . . . .                        | 69  |
| 46 | Used calculation methods. . . . .   | 69  |
| 47 | Results of the RMSE analysis for the selection of the best method. . . . .                    | 71  |
| 48 | Overview results of measurements for the location Cabauw. . . . .                             | 107 |
| 49 | Overview results of method 1: Charnock for the location Cabauw. . . . .                       | 107 |
| 50 | Overview results of measurements for the location EWTW. . . . .                               | 108 |
| 51 | Overview results of method 1: Charnock for the location EWTW. . . . .                         | 108 |
| 52 | Overview results of measurements for the location OWEZ. . . . .                               | 109 |
| 53 | Overview results of method 1: Charnock for the location OWEZ. . . . .                         | 109 |
| 54 | Overview results of method 2: Hsu IDW Shallow for the location OWEZ. . . . .                  | 109 |
| 55 | Overview results of method 3: Hsu IDW General for the location OWEZ. . . . .                  | 110 |
| 56 | Overview results of method 4: Hsu Cov Shallow for the location OWEZ. . . . .                  | 110 |
| 57 | Overview results of method 5: Hsu Cov General for the location OWEZ. . . . .                  | 110 |
| 58 | Overview results of measurements for the location FINO-1. . . . .                             | 111 |
| 59 | Overview results of method 1: Charnock for the location FINO-1. . . . .                       | 112 |
| 60 | Overview results of measurements for the location Europlatform. . . . .                       | 112 |
| 61 | Overview results of method 1: Charnock for the location Europlatform. . . . .                 | 112 |
| 62 | Overview results of method 2: Hsu IDW Shallow for the location Europlatform. . . . .          | 113 |
| 63 | Overview results of method 3: Hsu IDW General for the location Europlatform. . . . .          | 113 |
| 64 | Overview results of method 4: Hsu Cov Shallow for the location Europlatform. . . . .          | 113 |
| 65 | Overview results of method 5: Hsu Cov General for the location Europlatform. . . . .          | 113 |
| 66 | Overview results of measurements for the location K13- $\alpha$ . . . . .                     | 113 |
| 67 | Overview results of method 1: Charnock for the location K13- $\alpha$ . . . . .               | 113 |
| 68 | Overview results of method 2: Hsu IDW Shallow for the location K13- $\alpha$ . . . . .        | 114 |
| 69 | Overview results of method 3: Hsu IDW General for the location K13- $\alpha$ . . . . .        | 114 |
| 70 | Overview results of method 4: Hsu Cov Shallow for the location K13- $\alpha$ . . . . .        | 114 |
| 71 | Overview results of method 5: Hsu Cov General for the location K13- $\alpha$ . . . . .        | 114 |
| 72 | Overview results of measurements for the location Noordwijk. . . . .                          | 114 |
| 73 | Overview results of method 1: Charnock for the location Noordwijk. . . . .                    | 114 |
| 74 | Overview results of method 2: Hsu IDW Shallow for the location Noordwijk. . . . .             | 115 |
| 75 | Overview results of method 3: Hsu IDW General for the location Noordwijk. . . . .             | 115 |
| 76 | Overview results of method 4: Hsu Cov Shallow for the location Noordwijk. . . . .             | 115 |

|     |   |     |
|-----|---|-----|
| 77  | Overview results of method 5: Hsu Cov General for the location Noordwijk. . . . .           | 115 |
| 78  | Overview results of measurements for the location IJmuiden. . . . .                         | 115 |
| 79  | Overview results of method 1: Charnock for the location IJmuiden. . . . .                   | 115 |
| 80  | Overview results of method 2: Hsu IDW Shallow for the location IJmuiden. . . . .            | 116 |
| 81  | Overview results of method 3: Hsu IDW General for the location IJmuiden. . . . .            | 116 |
| 82  | Overview results of method 4: Hsu Cov Shallow for the location IJmuiden. . . . .            | 116 |
| 83  | Overview results of method 5: Hsu Cov General for the location IJmuiden. . . . .            | 116 |
| 84  | Overview results of measurements for the location Licht Eiland Goeree. . . . .              | 116 |
| 85  | Overview results of method 1: Charnock for the location Licht Eiland Goeree. . . . .        | 116 |
| 86  | Overview results of method 2: Hsu IDW Shallow for the location Licht Eiland Goeree. . . . . | 117 |
| 87  | Overview results of method 3: Hsu IDW General for the location Licht Eiland Goeree. . . . . | 117 |
| 88  | Overview results of method 4: Hsu Cov Shallow for the location Licht Eiland Goeree. . . . . | 117 |
| 89  | Overview results of method 5: Hsu Cov General for the location Licht Eiland Goeree. . . . . | 117 |
| 90  | Overview results of measurements for the location Vlakte van de Raan. . . . .               | 117 |
| 91  | Overview results of method 1: Charnock for the location Vlakte van de Raan. . . . .         | 117 |
| 92  | Overview results of method 2: Hsu IDW Shallow for the location Vlakte van de Raan. . . . .  | 118 |
| 93  | Overview results of method 3: Hsu IDW General for the location Vlakte van de Raan. . . . .  | 118 |
| 94  | Overview results of method 4: Hsu Cov Shallow for the location Vlakte van de Raan. . . . .  | 118 |
| 95  | Overview results of method 5: Hsu Cov General for the location Vlakte van de Raan. . . . .  | 118 |
| 96  | Overview results of measurements for the location Oosterschelde. . . . .                    | 118 |
| 97  | Overview results of method 1: Charnock for the location Oosterschelde. . . . .              | 118 |
| 98  | Overview results of method 2: Hsu IDW Shallow for the location Oosterschelde. . . . .       | 119 |
| 99  | Overview results of method 3: Hsu IDW General for the location Oosterschelde. . . . .       | 119 |
| 100 | Overview results of method 4: Hsu Cov Shallow for the location Oosterschelde. . . . .       | 119 |
| 101 | Overview results of method 5: Hsu Cov General for the location Oosterschelde. . . . .       | 119 |
| 102 | Roughness classes as defined for the LNG3+ database. . . . .                                | 121 |



## List of Symbols

### General

|            |                                |       |
|------------|--------------------------------|-------|
| $N$        | Number of elements in a vector | [-]   |
| $V_{wind}$ | Wind speed                     | [m/s] |
| $V_{calc}$ | Calculated wind speed          | [m/s] |
| $V_{meas}$ | Measured wind speed            | [m/s] |
| $z$        | Altitude                       | [m]   |
| $\kappa$   | Von Karman constant            | [-]   |
| $\sigma$   | Standard deviation             | [m/s] |

### Hirnam Data

|             |  |                      |
|-------------|--|----------------------|
| $P_0$       | Pressure at sea level                                    | [Pa]                 |
| $P_{10}$    | Pressure at 10 m altitude                                | [Pa]                 |
| $T_{2m}$    | Temperature at 2m altitude                               | [K]                  |
| $T_{n2}$    | Temperature at pressure level $n2$                       | [K]                  |
| $u_{10}$    | Longitudinal wind speed component at 10 m altitude       | [m/s]                |
| $v_{10}$    | Latitudinal wind speed component at 10 m altitude        | [m/s]                |
| $u_{n2}$    | Longitudinal wind speed component at pressure level $n2$ | [m/s]                |
| $v_{n2}$    | Latitudinal wind speed component at pressure level $n2$  | [m/s]                |
| $\rho_{n2}$ | Air density at pressure level $n2$                       | [kg/m <sup>3</sup> ] |

### Surface Roughness

|                |  |                     |
|----------------|--|---------------------|
| $a$            | Wave amplitude   | [m]                 |
| $C$            | Phase velocity   | [m/s]               |
| $C_d$          | Drag coefficient   | [-]                 |
| $d$            | Sea depth  | [m]                 |
| $g$            | Gravitational acceleration of the Earth                            | [m/s <sup>2</sup> ] |
| $H$            | Wave height  | [m]                 |
| $h$            | Height   | [m]                 |
| $h_{ref}$      | Reference height, usually equal to the measurement height          | [m]                 |
| $k_p$          | Wave number corresponding to the peak frequency                    | [-]                 |
| $L$            | Wave length  | [m]                 |
| $m$            | Charnock parameter   | [-]                 |
| $Re_h$         | Vertical Reynolds number related to sea depth indicated by $h$     | [-]                 |
| $Re_X$         | Horizontal Reynolds number related to the wind fetch $X$           | [-]                 |
| $T$            | Wave period  | [s]                 |
| $u_*$          | Friction velocity  | [m/s]               |
| $\tilde{u}_*$  | Normalized friction velocity                                       | [m/s]               |
| $U$            | Wind speed   | [m/s]               |
| $U_{ref}$      | Wind speed at reference altitude, usually the measurement altitude | [m/s]               |
| $U(z)$         | Wind speed at altitude $z$   | [m/s]               |
| $X$            | Wind fetch   | [m]                 |
| $z_0$          | Surface roughness length   | [m]                 |
| $\tilde{z}_0$  | Normalized roughness length  | [m]                 |
| $\alpha_{ch}$  | Charnock parameter (constant)                                      | [-]                 |
| $\nu_a$        | Kinematic viscosity of air   | [m <sup>2</sup> /s] |
| $\nu_w$        | Kinematic viscosity of water                                       | [m <sup>2</sup> /s] |
| $\sigma_\zeta$ | Standard deviation of surface waves                                | [m]                 |

### Spatial Interpolation

|                |   |     |
|----------------|---|-----|
| $d_i$          | Euclidean distance between point of interest and sample point | [m] |
| $n$            | Number of locations for which a measured value is available   | [-] |
| $p$            | Smoothness parameter  | [-] |
| $x_0$          | Location of point of interest                                 | [-] |
| $x_i$          | Location sample point   | [-] |
| $\hat{z}(x_0)$ | IDW: Estimated value at point of interest $x_0$               | [-] |
| $z(x_i)$       | IDW: Measured value at sample point $x_i$                     | [-] |
| $\lambda_i$    | IDW: Weight assigned to sample point $i$                      | [-] |

### Variance Stabilizing Transformation

|               |                                    |     |
|---------------|------------------------------------|-----|
| $c$           | Constant                           | [-] |
| $E[Y]$        | Mean value of $Y$                  | [-] |
| $f(Y)$        | A function of $Y$                  | [-] |
| $V[Y]$        | Variance of $Y$                    | [-] |
| $Y$           | Random variable                    | [-] |
| $\bar{Y}$     | Average of random variable $Y$     | [-] |
| $\alpha$      | Constant                           | [-] |
| $\beta$       | Constant                           | [-] |
| $\mu$         | Mean value                         | [-] |
| $\Omega(\mu)$ | Variance as function of mean $\mu$ | [-] |
| $\sigma^2$    | Variance                           | [-] |

### Multivariate Normal Distribution

|               |  |     |
|---------------|--|-----|
| $LH$          | Logarithm of significant wave height                           | [-] |
| $\hat{X}_c$   | Best estimate of Multivariate Normal Distributed random vector | [-] |
| $X$           | Random vector  | [-] |
| $\mathcal{N}$ | Indicator of normal distribution                               | [-] |
| $\Sigma$      | Covariance matrix  | [-] |

### Covariance

|             |   |     |
|-------------|---|-----|
| $x_i$       | Measured variable at station $i$            | [-] |
| $\hat{x}_i$ | Average of measured variable at station $i$ | [-] |
| $\alpha$    | Constant                                    | [-] |
| $1/\beta$   | Characteristic distance or decay parameter  | [m] |

### AVDE output

|             |   |       |
|-------------|---|-------|
| $C_d$       | Drag coefficient                        | [-]   |
| $D$         | Wind direction at altitude of interest  | [deg] |
| $L$         | Monin-Obukhov length                    | [m]   |
| $P$         | Air pressure at altitude of interest    | [Pa]  |
| $T$         | Air temperature at altitude of interest | [K]   |
| $U$         | Wind speed at altitude of interest      | [m/s] |
| $u_*$       | Friction velocity                       | [m/s] |
| $z_{0,avg}$ | Average surface roughness               | [m]   |

**Distributions**

|                 |   |                                   |
|-----------------|---|-----------------------------------|
| $A$             | Scale parameter of Weibull distribution   | [m/s]                             |
| $E$             | Wind energy content   | [m <sup>4</sup> /s <sup>4</sup> ] |
| $dV$            | Wind speed interval of wind speed histogram                                     | [m/s]                             |
| $F_{e,V_{ref}}$ | Chance that maximum wind speed occurs once in 50 years                          | [-]                               |
| $f$             | Frequency of occurrence   | [-]                               |
| $f(u)$          | Weibull Probability distribution function as function of wind speed             | [-]                               |
| $k$             | Shape parameter of Weibull distribution   | [-]                               |
| $M$             | Number of independent wind speed observations                                   | [-]                               |
| $N$             | Number of dependent wind speed observations                                     | [-]                               |
| $P(...)$        | Probability of (...) where (...) contains an equality                           | [-]                               |
| $T$             | Measurement period  | [s]                               |
| $T_{ave}$       | Averaging time  | [s]                               |
| $V_c$           | Wind speed at the center of a wind speed bin of a histogram                     | [m/s]                             |
| $V_m$           | Mean wind speed   | [m/s]                             |
| $V_{ref}$       | Reference wind speed, the wind speed that occurs statistically once in 50 years | [m/s]                             |
| $\alpha$        | Gumbell parameter $\alpha$  | [-]                               |
| $\beta$         | Gumbell parameter $\beta$   | [-]                               |
| $\Gamma(...)$   | Gamma function  | [-]                               |
| $\nu_m$         | Frequency of independent observations   | [Hz]                              |



## List of Abbreviations

|        |   |
|--------|---|
| AVDE   | Aanbod voorspeller duurzame energie, Wind power forecasting model, HIRLAM post-processor                    |
| BMU    | Bundesministerium fuer Umwelt, Federal Ministry for the Environment, Nature Conservation and Nuclear Safety |
| BUFR   | Binary Universal Form for the Representation of meteorological data   |
| CESAR  | Cabauw Experimental Site for Atmospheric Research   |
| Cov    | Covariance  |
| DTU    | Technical University Denmark  |
| GRIB   | Gridded Binary storage format   |
| IEC    | International Electrotechnical Commission   |
| EEZ    | Exclusive Economic Zone   |
| ECN    | Energy research Centre of the Netherlands   |
| EWTW   | ECN Wind turbine Test site Wieringermeer  |
| HIRLAM | High Resolution Limited Area Model  |
| IDW    | Inverse Distance Weighting  |
| KNMI   | Koninklijk Nederlands Meteorologisch Instituut, Royal Dutch Meteorological Institute                        |
| LE     | Licht Eiland  |
| LGN3+  | Landelijk Grondgebruiksbestand Nederland versie 3+, Dutch land use database version 3+                      |
| MND    | Multivariate Normal Distribution  |
| NWP    | Numerical weather prediction model  |
| OWEZ   | Offshore Wind farm Egmond aan Zee   |
| PDF    | Probability Density Function  |
| PTJ    | Projekttraeger Juelich, Project Executing Organisation  |
| RMSE   | Root Mean Squared Error   |
| SRNWP  | Short Range Numerical Weather Prediction  |
| STRACO | Soft Transition Condensation scheme (Part of Hirlam)  |
| URL    | Uniform Resource Locator  |
| VST    | Variance Stabilizing Transformation   |
| WGS    | World Geodetic coordinate System  |



# 1 Introduction

Since the end of the 1970's the interest in wind energy production has increased rapidly. For the Netherlands, where the land for wind turbine placement is scarce and where wind regimes are not that favorable, it is important to know what the wind climate is on both land and sea area. In the past, locations with generally high wind speeds were given a name to indicate this. Nowadays it is very common to take measurements for at least a year at a location of interest. This, however, is very cost intensive and therefore less expensive methods are required [28].

Two of these methods are described in the following section 1.1. Here the 'Wind Atlas Method' is shortly discussed as well as the 'Numerical Wind Atlas' as has been developed by ECN. This thesis will focus on the update of the Offshore Wind Atlas of ECN and specifically on the improvements of the estimation of the wind speed distribution. This will be further explained in section 1.2. The last section of this chapter will give an overview of the set-up of this report.

## 1.1 Wind Atlas

Several methods are available to find the wind climate at a given location. A well known method is the 'Wind Atlas Method' as described by Troen [47]. This method makes use of a time series of 10-min or hourly averaged wind speed and wind direction measurements from which all local effects are removed. These effects are from obstacles like buildings, terrain use like forests, crops, grass, rural areas and water surfaces, and effects of the orography like hills, mountains or flat terrain. After removal of these local effects, a general time series is found on which the local effects at the location of interest are introduced. This results in a new time series that contains information about the wind climate at the location of interest. Note however that this method has its limitations. For instance, for an increase in the distance between the point of measurement and the point of interest, the accuracy of the estimated wind climate decreases.

A second method makes use of Numerical Weather Prediction models (NWP). These models generally give predictions of the weather for the next 48 hours which are used for weather forecasting. Since these models are run several times a day, it is possible to select only the first part of each calculation run for the calculation of time series. For the update of ECN's Offshore Wind Atlas, this method will be used where the data is from the Hirlam NWP model provided by the Royal Dutch Meteorological Institute (KNMI).

In the past a model was designed by ECN for the prediction of the output power of wind turbines and solar cells. This model was called 'Aanbod Voorspeller Duurzame Energy' or shortly AVDE [4]. Although the developments of the solar part of the model have stopped, the wind part is still developing and currently a stand alone version of the wind part of AVDE is still in use. As input use is made of the result of a numerical weather prediction model and the generated output is a prediction of the power generated by a given wind turbine at a given location. Besides power prediction the AVDE model can also be used for the generation of time series. Using these time series, it is possible to make a Wind Atlas which contains information about wind distributions and wind speeds for a large area. It can then be used in finding locations for the placement of wind turbines or wind farms.

## 1.2 Problem definition

In the past, ECN published an Offshore Wind Atlas based on data of the period 1997 to 2002. Currently, new data is available and an update of the ECN Offshore Wind Atlas

could be made which is the main goal of this thesis work. The starting point of the project consists of new data and the old version of the AVDE model. In addition, the old model has to be updated and improved as well to become more suitable for the development of a Wind Atlas. For the model two goals are set:

- 1 Improve the accuracy of the prediction of wind speed distributions
- 2 Make the AVDE model faster and more suitable for field analysis

In order to improve the accuracy of the predicted wind speed distributions, only a few adjustments can be made. Because the Hirlam model is not controlled by ECN but by KNMI, adjustments to this model are not possible. So, in order to improve the predicted wind speed distributions, a solution has to be found which focuses on the AVDE model.

One of the parameters that can be adjusted in the AVDE model is the so called ‘surface roughness’. It is a parameter that contains information about the state of the surface which is used for the calculation of the wind speed at a given altitude. Important to know is that for a given location on land this parameter is constant in time and above sea it is usually assumed to be constant, but in reality, it is variable in time. In the old version of the AVDE model the surface roughness above sea, or sea surface roughness, was assumed to be constant. In the new version a variable sea surface roughness is introduced. The focus of this thesis will therefore lie on the implementation of a variable sea surface roughness. It is expected that this will give a better estimation of the wind speed distribution compared to the use of a constant sea surface roughness parameter. So the main question of this thesis work is:

Is it possible to improve the prediction of the wind speed distributions for a given location and altitude using a variable sea surface roughness?

Several subquestions can be derived as well. For instance: ‘What are possible methods to calculate the sea surface roughness, and what is their influence on the prediction of the wind speed?’ Also, because ECN already made a version of the Offshore Wind Atlas, a comparison can be made with this old version. The question that can be asked here is: ‘Can it be said that the wind climate is changing and in what way is it changing?’

These questions will all be answered in the remainder of this report. The following section will describe how the report is set up.

### 1.3 Reading guide

This report has been divided into four parts which are: Model, Validation, Wind Atlas and Conclusions. In the first part, Model, the AVDE model is described. It starts in chapter 2 with the introduction of general flow chart of the AVDE model consisting of input, calculation module and output. Each of these three items will be further elaborated. In chapters 3 and 4, the input of the location, Hirlam data and surface roughness is presented. The calculation module, or AVDE model, is described in chapter 5. Here the various calculation steps are presented which results in the output of the model as is presented in chapter 6

The second part of this report, Validation, will focus on the validation of the AVDE model using 11 measurement locations. The part starts with a chapter in which the setup of the validation process is explained, chapter 7. The 11 measurement locations can be separated into two main groups, the onshore locations and offshore locations. The results of the onshore locations are discussed in chapter 8 and the results of the offshore locations are presented in chapter 9. Because there could be commonalities between the stations, a comparison is made of the results for each station and presented in chapter 10. After these

results, in chapter 11, a selection is made of the best method to calculate the sea surface roughness followed by the conclusions of the validation of the AVDE model in chapter 12.

The third part, Wind Atlas, will present the average wind speed, Weibull shape and scale parameter and reference wind speed for the area of the Netherlands and a part of the North Sea, specifically the Dutch Exclusive Economic Zone (EEZ). It will start with chapter 13 where it is described how the results will be computed. In chapter 14 the results will be presented where also a comparison is made with other and older versions of Wind Atlases for the region of interest. The part will close with the conclusions found for the Wind Atlas in chapter 16.

The fourth and last part, Conclusions, consists of two chapters, 17 and 18, in which the conclusions of the report will be summarized and recommendations for further research will be given.



Part I

Model



## 2 Introduction to the AVDE model

As mentioned in the introduction, the AVDE model will be used for the development of the Wind Atlas. Although most part of this model will remain a black box where calculations happen, it is necessary to give an outline of several parts of the model. The AVDE model interpolates the results of a NWP model to a specified location and altitude. As input it needs the location and altitude, the results of a NWP model, in this case from the Hirlam NWP model, and surface roughness parameters. The output consists of time series of several parameters, direction dependent Weibull distributions of the wind speed and the reference wind speed. In figure 1 the basic setup is given. As can be seen, on the left side of the figure the different types of input are presented.

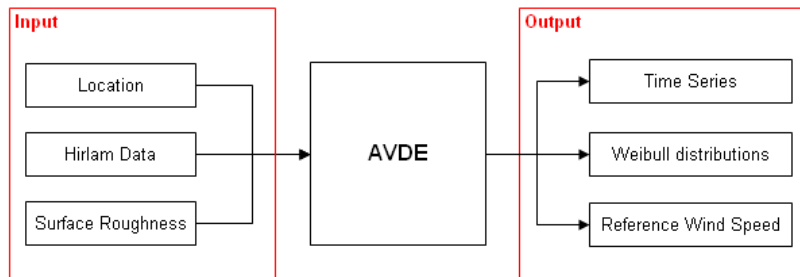


**Figure 1:** Block representation of the AVDE model

First is there the specification of the location of interest. Here the coordinates and the required altitude are given. In addition, for point analysis, it is possible to include information about obstacles near the location as well. For field analysis, this option is not included.

The second input is the result of a Numerical Weather Prediction (NWP) Model. Since use is made of output from HIRLAM (HIGH Resolution Limited Area Model), which is maintained by the Royal Dutch Meteorological Institute (KNMI), it is referred to as the Hirlam data. This Hirlam data is a collection of files, each containing a weather forecast of 48 hours. The model runs four times a day so that only the first six hours of data is used in the calculations. This inherently results in the fact that there are about 1460 files needed to create a time series of one year. Note that the area covered by the Hirlam data limits the area of the Wind Atlas and that the Hirlam model cannot be adjusted by ECN.

The third input indicated is called 'surface roughness'. The surface roughness gives a measure of the influence of the surface on the wind speed. Close to the ground, the influence is large while at altitudes above 1 km the influence is minimal. Above land, the surface roughness is assumed to be fixed since it is related to the land use. For instance, a city has a high surface roughness due to the different type of buildings while a runway has a low surface roughness since it is flat. For water and specifically seawater, two approaches can be taken. The roughness can be assumed constant, which is an assumption usually applied using the Charnock relations [9], and the roughness can be considered as a variable [19] [32] [45]. In the old version of AVDE the sea surface roughness was assumed to be a constant while in the new version a variable sea surface roughness will be introduced. This will be further explained in chapter 4.

In the middle of the figure the box is presented where the calculations are done by the AVDE model. This part is referred to as the calculation module where various calculations take place in order to calculate the wind speed for a given location and moment in time, based on the input.

The output of the AVDE model also consists of three parts: Time Series, Weibull distributions and Reference wind speed. The time series is a direct result of the calculation module where the Weibull distributions and reference wind speeds are derived from post processing the time series. Both the Weibull distributions and the reference wind speeds are given per wind direction sector.

In the following chapters the block diagram presented in figure 1 will be discussed in further detail. Chapter 3 will present what type of data is required for 'Location' and 'Hirlam Data'. In chapter 4 an extensive explanation will be given of the methods used to calculate a variable sea surface roughness, followed by the implementation of it into the AVDE model which will be given in chapter 5. For validation of the AVDE model, the found output will be compared to measurements taken at several locations. This will be presented in chapter 7.

### 3 Location and Hirlam input parameters

As presented in the introduction of the previous chapter, the AVDE-model can be divided in three parts: the input, the calculation module and the output. This chapter will focus on the input of the model and specifically on the input of the location and Hirlam data which contain the basic input data for the calculation module. They also introduce limitations onto each other which should be dealt with by the AVDE-model.

#### 3.1 Location

The first input is the specification of the location of interest. The location can either be a specific point (fig 2.a) or a group of points. The group of points can consist of the locations of the intersections of a grid (fig 2.b), or this group of points can be a collection of random locations (fig 2.c). Each location is specified by a longitude, latitude and altitude where the input of the altitude is separated from the input of the longitude and latitude. As a consequence the given altitude input applies to all locations specified. It is also possible to specify multiple altitudes. The reason for separating the altitude from the longitude and latitude is a construction to simplify the programming of the calculation module. For each point the longitude and latitude must be given in accordance to the World Geographic coordinate System (WGS) and the altitude must be given in meters.

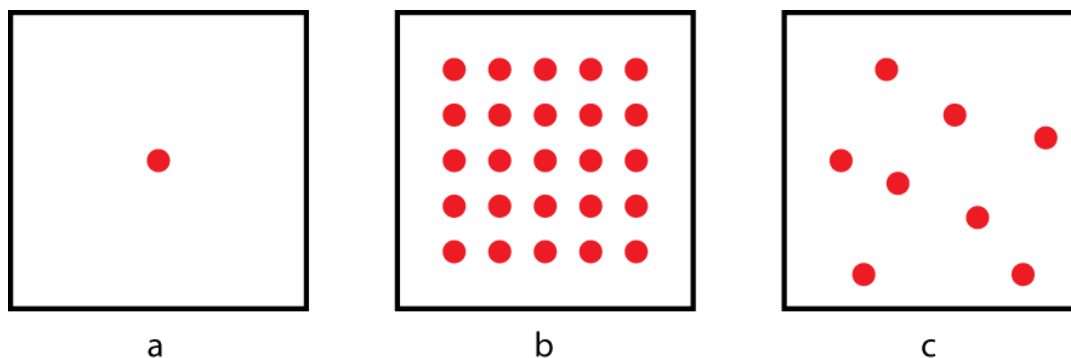


**Figure 2:** Three different types of location input: a) point b) group of points, grid intersections c) group of points, random.

One of the goals of this thesis work, is to deliver wind maps with average wind speeds. Based on these wind maps it can be determined where the suitable locations are to place wind turbines. For this, the average wind speed at hub height of a wind turbine is required. Currently, newly installed wind turbines have a hub height between 70m and 90m. Since it can be expected that in the future wind turbines will be larger, the highest value is chosen here. In addition, two extra levels are included to get values close to the tip of the turbine blades assuming a blade length of 50 m. In total, for the wind atlas three altitudes will be considered: 40m, 90m and 140m. Of course, it is also possible to select other altitudes, note however that the maximum altitude has a limit depending on the Hirlam data.

#### 3.2 Hirlam data

In the introduction it was already mentioned that use is made of Hirlam Data. Hirlam stands for HIGH Resolution Limited Area Model which is a numerical weather prediction model (NWP) used to predict the weather on short term, up to 48 hours ahead. The results of this model are widely used and presented. Examples of the use of Hirlam data can

be found at the weather bulletins on television and in newspapers where pressure and temperature maps are given (see fig. 3).

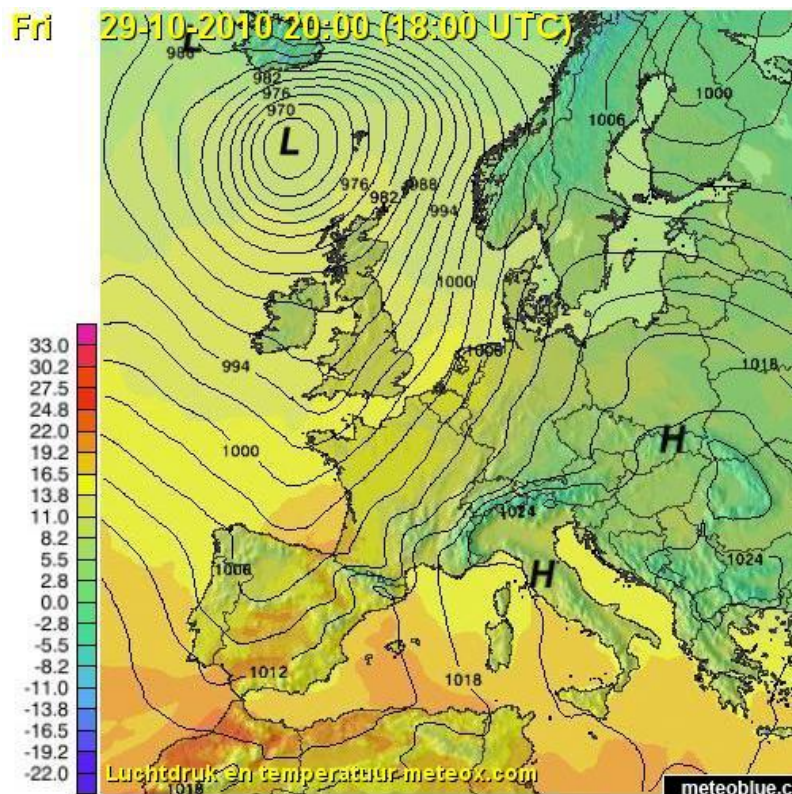


**Figure 3:** Example of the use of Hirlam data as presented by Meteox [34].

As mentioned in the introduction, the Hirlam model runs every six hours, producing a prediction for the following 48 hours after initialization. Since the Hirlam model is not controlled by ECN but by a third party, KNMI, it is not possible to change the results from the Hirlam model. However, to give an overview of what the Hirlam model is, some background information will be given in section 3.2.1. Hereafter, the possible Hirlam data formats for the AVDE-model will be discussed in section 3.2.2 where also some limitations on the area for the Wind Atlas are discussed.

### 3.2.1 Background Hirlam

This section is intended to give some background information about the Hirlam model which is the source of the Hirlam data. The information given will be very general, where possible, references are given to documents in which a specific part of the model is explained.

As mentioned, the Hirlam model is controlled by KNMI. The history of the Hirlam model dates back to 1985 where the first Hirlam project has been established in order to provide a system for short range weather forecasting [18]. In cooperation with multiple European weather institutes, the Hirlam model is being maintained, for operational use, and improved to make better short term predictions of the weather. The basic set of the model consists of the continuity, temperature, momentum, specific humidity and cloud water equations [48]. These equations are discretized using semi-Lagrangian discretization. In addition, several schemes are used to solve the system of equations. A half implicit Coriolis scheme is used as well as a de-centering scheme and a filter. All to speed up the calculation

time while maintaining the stability of the system of equations.

All boundaries of the Hirlam model are over-specified and specified by a ‘host model’ which covers a larger area on a coarser grid [48]. Between the ‘host model’ and the Hirlam model a relaxation zone is created where the data of the ‘host model’ on the coarse grid is transferred to the Hirlam model which is on a finer grid. This is needed because both models evolve independently. Near the top of the atmosphere the vertical velocity is assumed to be zero although there is no physical basis for this assumption. It does, however, reduce the amount of standing waves due to reflections near the boundary. Several parameterization schemes are used to take several physical processes into account. These processes are: Turbulence [46], Clouds and Condensation [53] [22] [7] [23], Radiation [43], Surface and Soil Processes separated in soil and vegetation [39], snow [15] [16] and lakes [36] [26], and Orography [42].

The input for the Hirlam model, besides the ‘host model’, consists of observation data. Measurements of wind speeds, pressure, temperature, moist, density, etc, are pre-processed and stored to form a Climate Database from which the data can be extracted to feed the Hirlam model. Use is made of four dimensional variational data assimilation [20] after which a filter is applied [30]. The filtered data is used for boundary conditions and to initialize the Hirlam model. Note that also the ‘host model’ is used to specify boundary and initial conditions [48].

The output of the Hirlam model for grid point information is stored in BUFR-format (Binary Universal Form for the Representation of meteorological data) while horizontally distributed data is stored in GRIB-format (GRIdded Binary).

### 3.2.2 Hirlam data for model input

The AVDE-model can be fed with six different types of Hirlam files, stored in the GRIB-format, each with their own resolution and boundaries. The data stored in the different Hirlam files is generally the same. Starting at the lowest level, which is at an altitude of 2m, the temperature  $T_{2m}$  is given. At 10 m height, the pressure  $P_{10}$  and wind speed vectors in  $x$  and  $y$  direction are given,  $u_{10}$  and  $v_{10}$  respectively. On a higher altitude, indicated by pressure, the wind speed vectors  $u_{n2}$  and  $v_{n2}$  are given as well as the air temperature  $T_{n2}$  and the air density  $\rho_{n2}$ . Since the altitude of the second level is a pressure altitude, it has a variable geometric height. This means that equations should be included in the model to calculate this geometric height.

For each of the parameters a time series is available. However, for the two lowest altitudes, the time step is equal to one hour. For the higher levels, the time step is equal to three hours. For this reason, a time interpolation step has to be included in the AVDE model as well.

Each of the six different types of Hirlam files has its own specification of covered area and grid resolution. An overview of these domains is given in table 1. For the given resolutions it can be assumed that 0.1 deg is approximately 11 km.

**Table 1:** Specification of Hirlam files to be used with the AVDE-model

| Name                       | Domain NW-corner  |                    | Domain SE-corner  |                    | Resolution<br>[deg] |
|----------------------------|-------------------|--------------------|-------------------|--------------------|---------------------|
|                            | Latitude<br>[deg] | Longitude<br>[deg] | Latitude<br>[deg] | Longitude<br>[deg] |                     |
| Hirlam55                   | 54.000            | 3.000              | 49.500            | 8.000              | 0.5                 |
| Hirlam22 re-sampled to H55 | 54.000            | 3.000              | 49.500            | 8.000              | 0.5                 |
| xHirlam                    | 54.000            | 3.000              | 50.900            | 6.100              | 0.1                 |
| Hirlam22 small domain      | 54.000            | 2.800              | 49.800            | 7.600              | 0.2                 |
| Hirlam22 large domain      | 56.000            | 2.200              | 50.400            | 7.600              | 0.2                 |
| Hirlam22 meteo domain      | 53.600            | 3.200              | 50.200            | 7.400              | 0.2                 |

For the Wind Atlas three types are available which are Hirlam55, Hirlam22 re-sampled to H55 and Hirlam22 large domain. From table 1 it can be found that this results in two different areas since Hirlam55 and the re-sampled Hirlam22 cover the same area. As mentioned previously, this introduces boundaries to the area covered by the Wind Atlas. To put this in perspective, in figure 4 the Netherlands is given as well as the Dutch Exclusive Economic Zone (EEZ) and the two areas covered by the three types of Hirlam files. It can be seen that the for Hirlam55 not the entire EEZ is included while large parts of Belgium and Germany are included. On the other hand, Hirlam22 files cover the entire EEZ and the Netherlands and a smaller part of Belgium and Germany.

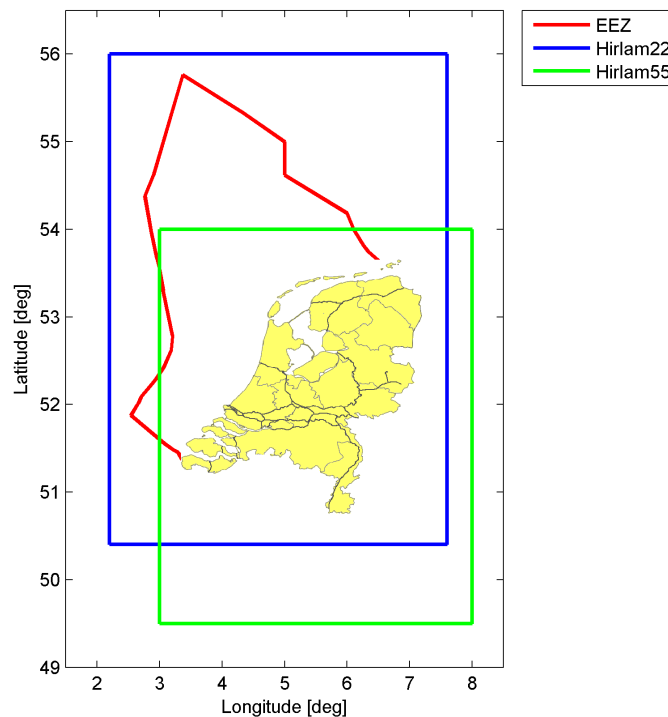


**Figure 4:** Overview area covered by Hirlam files.

For each of the indicated types of Hirlam files, a different amount of data is available with respect to the time period they cover. The Hirlam55 data is available from June 2001 until 16 June 2002. For the re-sampled Hirlam22 data, the period is 17 June 2002 until 18 November 2003. As from 18 November 2003 only Hirlam22 files are available.

## 4 Surface roughness input

Following the model presented in the introduction of this part, given in figure 1, this chapter will give an extensive overview of the third input parameter, the surface roughness. The methods used for the determination of the surface roughness at a given place and time are presented. In section 4.5, a part of the AVDE model will be expanded through which the implementation of the used methods to find the surface roughness will be shown.

First, in section 4.1 an explanation will be given of the surface roughness, what it is and the effect on the logarithmic wind profile. The surface roughness can be estimated for land as well as for sea surfaces, the approach, however, is quite different. For land the surface roughness is determined from the land use, as will be explained in section 4.2, while for a sea, the surface roughness can be derived from the wave height, wave period and sea depth as will be discussed in section 4.3. Due to the limited amount of wave data (i.e. wave height, wave period and sea depth) available, two spatial interpolation techniques, Inverse Distance Weighting (IDW) and Gibescu's method, will be presented in section 4.5 of this chapter. The last section, section 4.6 will focus on the validation and applicability of the used interpolation techniques.

### 4.1 Description surface roughness and wind profile

An important input parameter for the model presented in the introduction is the surface roughness. The surface roughness is a parameter which is used in the modeling of the wind speed profile which is done using the Businger-Dyer wind profiles as will be shown in chapter 5 [6]. For the purpose of explaining what the surface roughness is, and what happens if it changes, the equation for a logarithmic wind profile will be used which is given by:

$$U = U_{ref} \frac{\log\left(\frac{h}{z_0}\right)}{\log\left(\frac{h_{ref}}{z_0}\right)} \quad (4.1)$$

where  $U$  is the wind speed at a given height  $h$ ,  $U_{ref}$  the wind speed at reference height  $h_{ref}$  and  $z_0$  the surface roughness.

The surface roughness is defined as the height at which the wind speed is equal to zero. As such, it is not a physical quantity although it can be considered as a length-scale representation of the roughness of a surface. In addition, it gives a measure of the skin friction of the surface.

The difference in roughness between two surfaces can be found in the amount and size of obstacles on the surfaces. As such, it is easy to imagine that grassland has a lower roughness than a city. It can be expected that the surface roughness for grass land is considerably lower than for a city and that the wind profile over these two surfaces are different. This difference is shown in figure 5. For the given wind profiles in this figure, use is made of equation (4.1) with  $U_{ref}$  of 15 m/s at an altitude  $h_{ref}$  of 200 m. For each curve in the figure only the surface roughness is changed where three characteristic values are selected corresponding to water surface ( $z_0 = 0.001\text{m}$ ), grass land ( $z_0 = 0.03\text{m}$ ) and city ( $z_0 = 2.0\text{m}$ ). As can be seen in figure 5, a high value of the surface roughness has a large impact on the wind speed profile. It reduces the wind speed near the surface considerably compared to the cases where lower values of the surface roughness are used. This is because a rough surface slows down the wind speed more than a smooth surface. For each type of land use, a different value for the surface roughness can be found, ranging from 0.001 m for very smooth surfaces like runways, to 2.0 m for very rough surfaces like cities.

An overview of commonly used values is given in table 102 of appendix C.

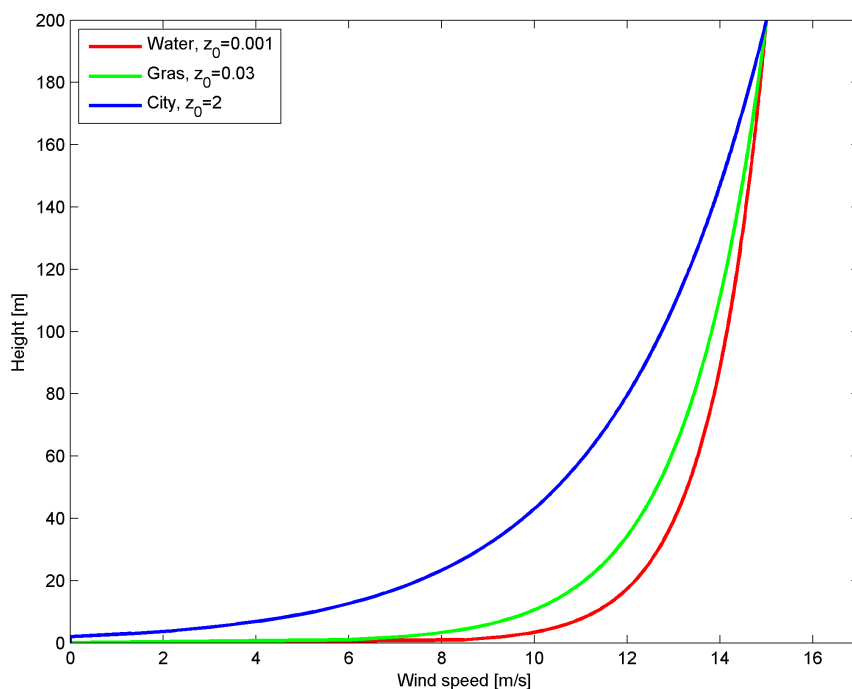


**Figure 5:** Example wind profiles over sea, grassland and city area where the wind speed is calculated using equation (4.1) and  $U_{ref}$  of 15 m/s at an altitude  $h_{ref}$  of 200 m.

## 4.2 Surface roughness of the Netherlands

Considering the area of interest for the Wind Atlas, the surface roughness for the land and sea area need to be known. For land it can be assumed that the relative changes of the land use, with respect to time, are small. The basic structure of, for instance, city's and forests are not likely to change very fast. As such, the surface roughness can be considered as a constant.

For the Netherlands a roughness map has been made during the KNMI Hydra project [25]. This map is freely available and has been derived from the land use database LGN3+ made by Alterra [50] which uses 46 classes to define the land use (see table 102 in appendix C). The map indicates for each segment of 100x100m an average surface roughness based on the land use. The map is shown in figure 6. Note that for Belgium and Germany the map shows no changes in color. This is due to the fact that for these two countries no roughness values were found, a value of 0.03 m is chosen instead which represents grass land.

Although the roughness map also shows a constant roughness for the sea surface, it will not be used in the calculations. This is due to the fact that the motion of the sea surface is influenced by several natural occurring processes. As such, the sea surface roughness is a variable and not a constant. The processes that primarily influence water motion are: gravity, wind stress, atmospheric pressure and seismicity. Secondary processes are coriolis force and internal friction [37]. The build up of sea surface waves, however, is greatly dependent on the wind speed and on the duration of it. Also, since the sea has a finite depth, it can be expected that it also influences the wave heights, especially for shallow seas.

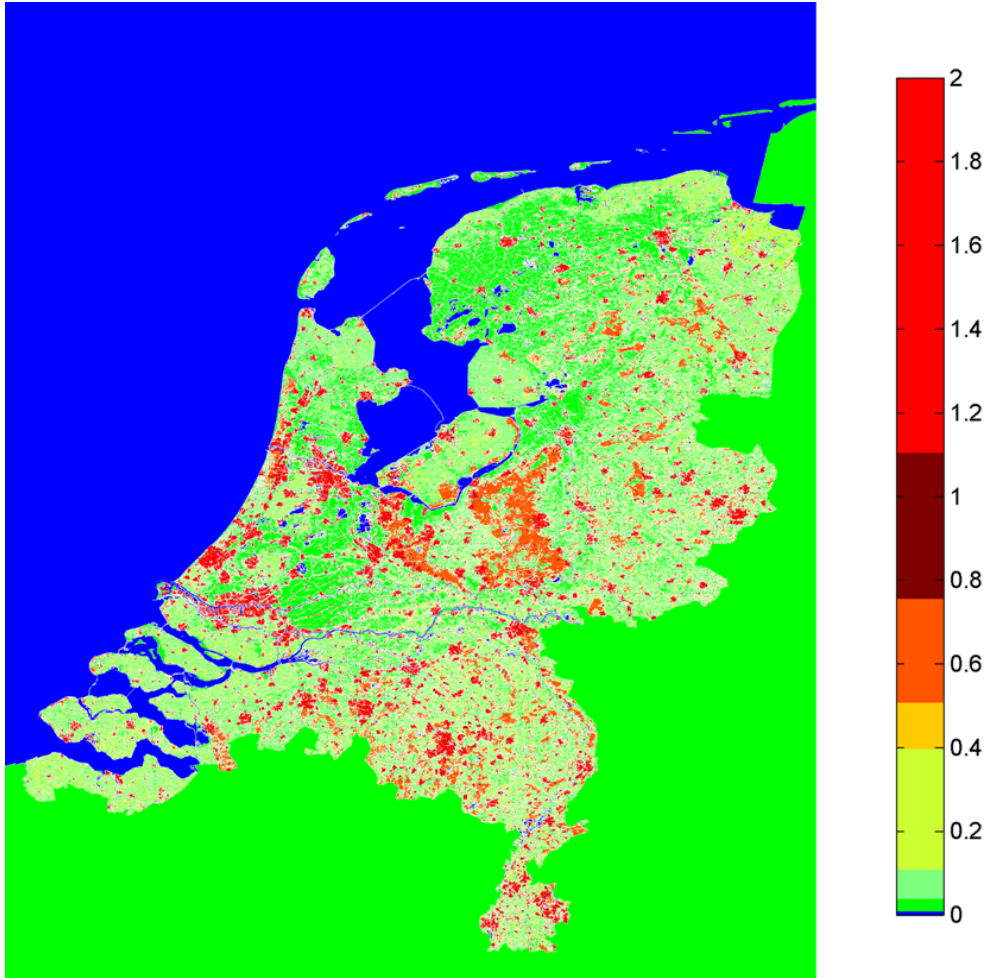


**Figure 6:** Roughness map of the Netherlands.

### 4.3 Theory of estimating the sea surface roughness

As will be discussed in this section, there are multiple ways to calculate the sea surface roughness. Three examples will be given of which one is selected to be used in the AVDE model. As will be shown, additional measurements of sea state parameters are needed for these calculations as well. The availability of data, however, is usually not very large as will be shown in section 4.4. As a consequence, a solution has to be found for compensating the lack of data which will be presented in section 4.5.

#### 4.3.1 Dimensional Analysis

Waves occurring at the sea surface have an influence on the wind speed at a certain altitude above the water level and vice versa. When the sea is rough, the roughness length  $z_0$  will be high, which means that there is a large influence of the surface on the wind speed. When the roughness length is low, which occurs when the sea is calm, then the effect of the surface on the wind speed is also low. In addition, when a wind profile is considered as given in figure 7, it can be seen that a rough sea, having a high roughness length, gives a less steep slope of the wind profile compared to a calm sea which would have a steep slope of the wind profile.

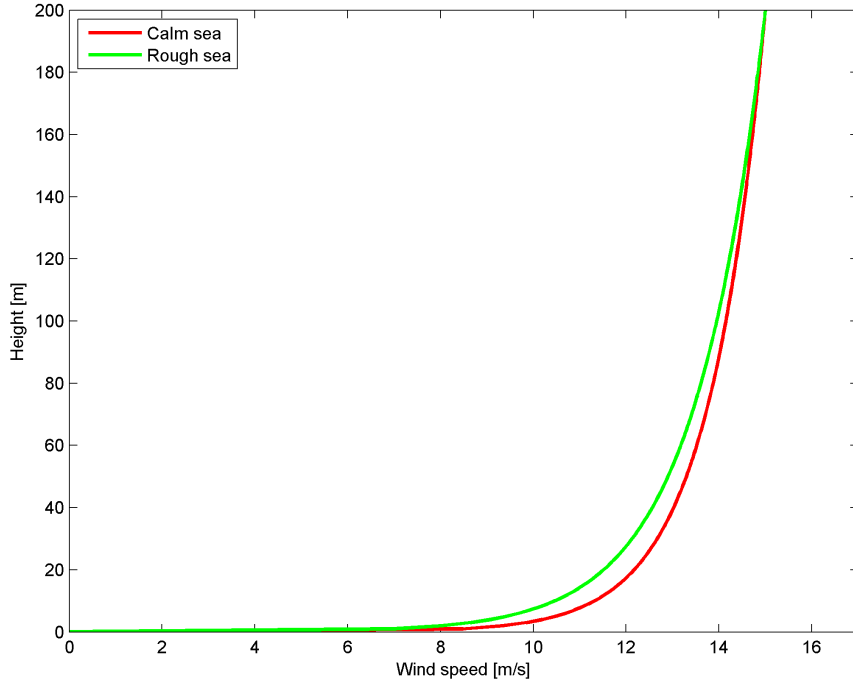


**Figure 7:** Wind profiles for a rough and calm sea.

In the past several researchers tried to find a relation to estimate the sea surface roughness. Most of these started with similarity theory. According to Massel [32], dimensional analysis can be used in order to find a more precise and systematic insight in the dependence of the surface roughness on the wind speed. From this dimensional analysis, it was found that the roughness length at the sea surface should be determined from:

$$\tilde{z}_0 = \Pi_1(\tilde{u}_*, Re_X, Re_h). \quad (4.2)$$

The tilde above the roughness length  $z_0$  and friction velocity  $u_*$  indicate that these are normalized variables given by:  $\tilde{z}_0 = \frac{gz_0}{u_*^2}$  and  $\tilde{u}_* = \frac{u_*}{\sqrt[3]{g\nu_a}}$ . The Reynolds numbers  $Re_X$  and  $Re_h$  are given by:  $Re_X = \frac{u_*X}{\nu_a}$  and  $Re_h = \frac{u_*h}{\nu_w}$ , which are a ‘horizontal’ Reynolds number with  $X$  a distance over open sea, and a Reynolds number related to the sea depth which is here given by  $h$ . The variables  $\nu_a$  and  $\nu_w$  are respectively the kinematic viscosity of air and water.

For deep and shallow waters, relation (4.2) can be simplified. For deep waters it reduces to:

$$\tilde{z}_0 = \Pi_2(\tilde{u}_*, Re_X). \quad (4.3)$$

And for shallow waters

$$\tilde{z}_0 = \Pi_3(\tilde{u}_*, Re_h) \quad (4.4)$$

can be found.

### 4.3.2 Three methods for the sea surface roughness

Following the approach of dimension analysis, three examples can be found in literature which give a solution for the surface roughness. The first solution presented here has been found by Charnock [9] in 1955:

$$z_0 = \alpha_{ch} \frac{u_*^2}{g}. \quad (4.5)$$

In this equation is  $u_*$  the friction velocity of the wind,  $g$  the gravitational acceleration and  $\alpha_{ch}$  the Charnock parameter which is dimensionless. The value of this Charnock parameter was found from a fit on measurements taken in a lake with 16m deep water and a fetch of 1 km. Note that with ‘fetch’ the distance of open water surrounding the measurement point is meant. For the lake where Charnock did his measurements, a value of 0.011 was found for  $\alpha_{ch}$ . In general, when this equation is used, it is assumed that the value for the Charnock parameter  $\alpha_{ch}$  is constant. In reality, however, this parameter is not constant. For instance Garratt [13] found that the Charnock parameter was varying between  $0.3 \cdot 10^{-2}$  and  $8.0 \cdot 10^{-2}$  with an average of  $1.44 \cdot 10^{-2}$  where Garratts measurements were taken over an ocean.

A second example of a solution for the surface roughness was found by Krivitskii and Strekalov:

$$\tilde{z}_0 = 8.65 \cdot 10^{-5} \frac{Re_X}{Re_h}, \quad (4.6)$$

also by the use of wind speed measurements above sea water. This relation, however, gives only a dependence of the friction velocity  $u_*$ , wind fetch  $X$ , and water depth  $h$  and does not include the state of the sea. As such, Kitaigorodski included the dependency of wave height finding the following relation

$$z_0 \approx a \exp\left(-\frac{k_p C}{u_*}\right) \quad (4.7)$$

where  $a$  is a wave amplitude given in meters,  $k_p$  a wave number corresponding to the peak frequency of the waves (dimensionless) and  $C$  is the phase velocity. When the effect of varying steepness of the various waves in the spectrum is included, the  $a$  in equation (4.7) can be given as a function of the standard deviation of surface wave height  $\sigma_\chi$  given in meters. The relation is then extended to:

$$z_0 \approx 0.3 \sigma_\chi \exp\left(-\frac{k_p C}{u_*}\right). \quad (4.8)$$

The third and last equation that will be presented here is the equation found by Hsu [19]. He allowed  $\alpha_{ch}$  in Charnock’s equation (4.5) to be a function of the wave steepness  $H/L$  formed by a wave height  $H$  and a wave length  $L$  both given in meters. He suggests from dimensional consideration:

$$z_0 \propto \left(\frac{H}{L}\right) \frac{u_*^2}{g} \quad (4.9)$$

Although the sea depth is not directly visible in this function, it is needed to calculate the wave length. Using the general wave equation given by equation (4.10) which relates the wave length  $L$ , gravitational velocity  $g$  and the sea depth  $d$  to the phase velocity  $C$ , Hsu’s

equation can be rewritten for shallow and deep sea. Note that for this, the general wave equation must also be rewritten for shallow and deep sea as well.

$$C = \sqrt{\frac{gL}{2\pi} \tanh\left(\frac{2\pi d}{L}\right)} \quad (4.10)$$

For a deep sea, where it is assumed that  $d > L/2$ , the term  $\frac{2\pi d}{L}$  is equal or larger than  $\pi$  which results in  $\tanh \approx 1$ . For a shallow sea, where it is assumed that the sea depth  $d$  is smaller than  $L/20$ , the term  $\tanh(x) \approx x$ . So for a deep sea the general wave equation reduces to:

$$C = \sqrt{\frac{gL}{2\pi}}, \quad (4.11)$$

while for a shallow sea it reduces to:

$$C = \sqrt{gd}. \quad (4.12)$$

By combining equation (4.9) with equation (4.11) Hsu's equation for deep water can be found:

$$z_0 = \frac{1}{2\pi} \left( \frac{\sqrt{Hg}}{C} \right)^2 \frac{u_*^2}{g}. \quad (4.13)$$

For shallow water an additional equation is needed which relates the phase velocity  $C$  of the waves to the wave length  $L$  and wave period  $T$  of the waves. This equation is given by:

$$C = \frac{L}{T}. \quad (4.14)$$

Now combining equations (4.9), (4.12) and (4.14), Hsu's equation for shallow water can be found:

$$z_0 = \frac{H}{T\sqrt{gd}} \frac{u_*^2}{g}. \quad (4.15)$$

Although it is usually assumed that the North Sea is a shallow sea, it does not necessarily mean that Hsu's shallow sea equation is always applicable. This is due to the fact that the wave length  $L$  is varying in time while the sea depth remains constant. Note however that equations (4.9), (4.10) and (4.14) can be solved iteratively to find a roughness length.

The relative differences between the three given examples can be found in the complexity. Starting with Charnock's relation (4.5), this is the simplest relation because it makes use of a constant value for the Charnock parameter. For this reason, it does not include any information on the state of the sea at a given time. The example of Kitaigorodski, which is the most complex relation for the sea roughness given here, also shows a dependency on the state of the sea. This equation however, contains variables that are not easily found like the wave number  $k_p$  and the standard deviation of the surface waves  $\sigma_\chi$ . In addition, using this equation, for a deep sea, there is always an iterative method required to calculate the phase velocity  $C$  using the general wave equation (4.10). Hsu's equation (4.9), on the other hand, includes information about the sea state by stating that the Charnock parameter is a function of the wave steepness. By rewriting Hsu's equation for a deep and shallow sea,

it can be found that for a shallow sea the sea depth is also an important factor to include. Taking the above in consideration, the equation's of Hsu will be used in the AVDE-model. Reason for this is that it includes the state of the sea as well as the sea depth. In addition, the equation contains three variables, wave height  $H$ , wave period  $T$  and sea depth  $d$ , which are relatively easy found because these are already measured for providing ships information about the state of the sea.

#### 4.4 Data

From the previous section it was found that by using Hsu's equation for shallow sea and deep sea, equations (4.15) and (4.13), three unknown variables were introduced. These are the wave height  $H$ , the wave period  $T$  and the sea depth  $d$ . It was also mentioned that these variables are relatively easy to find because they are needed for shipping. Note that from these three, only the sea depth can be assumed to be time independent. Changes of the sea floor, and thus the sea depth, due to changing currents are not taken into account. The wave height and wave period are time dependent and therefore time series are required for the calculations.

The sea depth of the North Sea is measured by the navies of the countries surrounding the North Sea. For the Netherlands Exclusive Economic Zone (EEZ), a part of the North Sea where the Netherlands have the exclusive right to exploit the natural resources and the duty to maintain nature, the sea depth measurements are done by the Hydrografic Service of the Royal Netherlands Navy [38]. For research purposes the service makes the sea depth data available. In figure 8 an overview is given of the availability of the sea depth data provided by the Hydrografic Service. As can be seen, there is still a part of the EEZ for which no data is available. In section 4.5 a method will be given to find the sea depth also for the parts within the EEZ for which no measurement data is available.

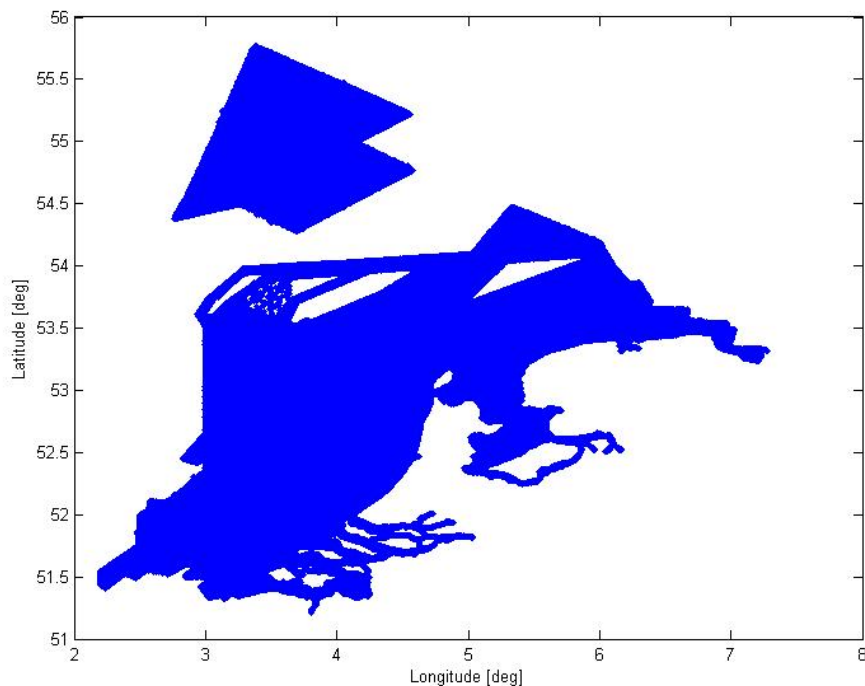


**Figure 8:** Area with known sea depth [38].

The wave height and wave period are measured mainly for shipping. Based on the data of wave height and wave period, a captain can make a decision whether or not it is safe to enter a port. For this reason, at multiple locations, mostly close to large sea routes, these two variables are measured. This can either be done with buoys or with fixed installations. The fixed installations are usually only used in places where other measurements are taken as well, for instance meteorological measurements, like wind speed, wind direction and temperature measurements, or other hydrological measurements, like water temperature and water velocities. The only difference between measuring with buoys and a fixed installation is that the buoys do not measure at a precisely fixed location because they float. This, however, does not influence the measurements very much. The collection and publication of data is maintained by Rijkswaterstaat, part of the Dutch Ministry of Infrastructure and Environment, and is freely available.

The locations where measurements of wave height and wave period take place are given in table 2 and figure 9. As can be seen, a lot of the measurement points are located near the coast in the south-west part of the area of interest.

**Table 2:** Coordinates of wave measurement stations.

| Nr | Station                     | Latitude [deg] | Longitude [deg] | Sea depth [m] |
|----|-----------------------------|----------------|-----------------|---------------|
| 1  | Brouwershavensegat 2        | 51.7686        | 3.6173          | 9.3           |
| 2  | Domburgse Rassen            | 51.6203        | 3.3992          | 10.7          |
| 3  | Eurogeul DWE                | 51.5654        | 3.0001          | 10.7          |
| 4  | Eurogeul E5                 | 51.5904        | 3.2536          | 26.6          |
| 5  | Eurogeul E13                | 52.0036        | 3.4413          | 29.5          |
| 6  | Lichteiland Goeree          | 51.5533        | 3.4011          | 5.2           |
| 7  | Schouwenbank                | 51.7468        | 3.3056          | 28.2          |
| 8  | Stroommeetpaal IJmond       | 52.4650        | 4.5179          | 15.2          |
| 9  | Stroommeetpaal Maasmond     | 51.9932        | 4.0079          | 16.9          |
| 10 | Aukfield Platform           | 56.3997        | 2.0656          |               |
| 11 | Eierlandse Gat              | 53.2769        | 4.6617          | 26.7          |
| 12 | Euro platform               | 51.9986        | 3.2764          | 30.3          |
| 13 | IJmuiden minutiestortplaats | 52.5500        | 4.0583          | 24.9          |
| 14 | K13- $\alpha$ platform      | 53.2178        | 3.2203          | 27.8          |
| 15 | Schiermonnikoog Noord       | 53.5956        | 6.1667          | 18.4          |
| 16 | FINO 1                      | 54.0239        | 6.5906          | 30.0          |

Besides the number of points, it is also important to look at the amount of data that for each point is available. Based on the available Hirlam data, as presented in chapter 3, the period of interest ranges from June 2001 till the end of December 2009. To check the amount of wave data available a plot is shown in figure 10 where the start and end date of the measuring periods are given. Here it can be seen that not for every station wave data is available for the full period of interest. In the beginning of the period, only eight locations show that there is data available increasing to 15 stations at the end of the period. Some notes must be made about the data of the location Aukfield Platform. Firstly, this location is outside the area of interest but it is located furthest off-shore compared to the other stations. Secondly, the quality of the data is questionable. The measurements show large discontinuities which has a negative effect on the total data set. For this reason, the data of Aukfield Station is excluded from the data set.

Since there are only fifteen measurement points available, spatial interpolation of time series is needed to find wave data at other locations in the area of interest. Two methods that can be used will be presented in the following section.

## 4.5 Interpolation of Wave Data

In the previous section it was found that for the sea depth as well as for the wave height and wave period a solution must be found to overcome the problem of missing data. Before

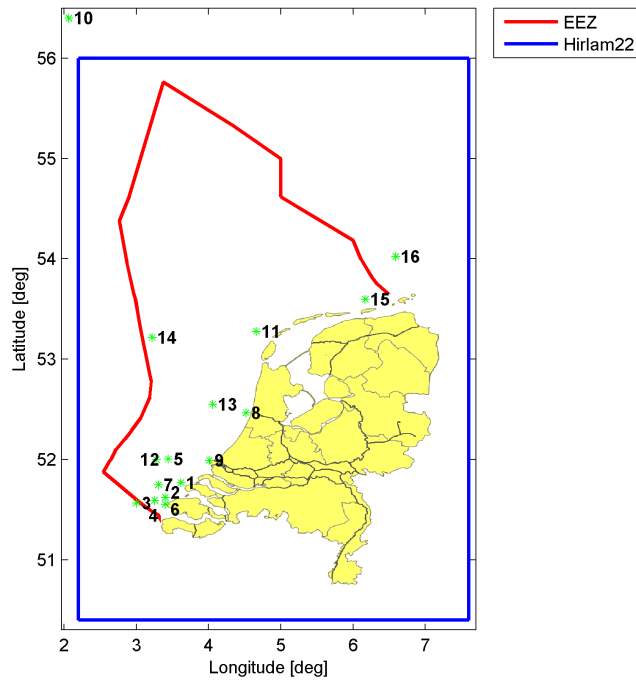


**Figure 9:** Locations wave data measurement stations. Given numbers coincide with numbers in table 2

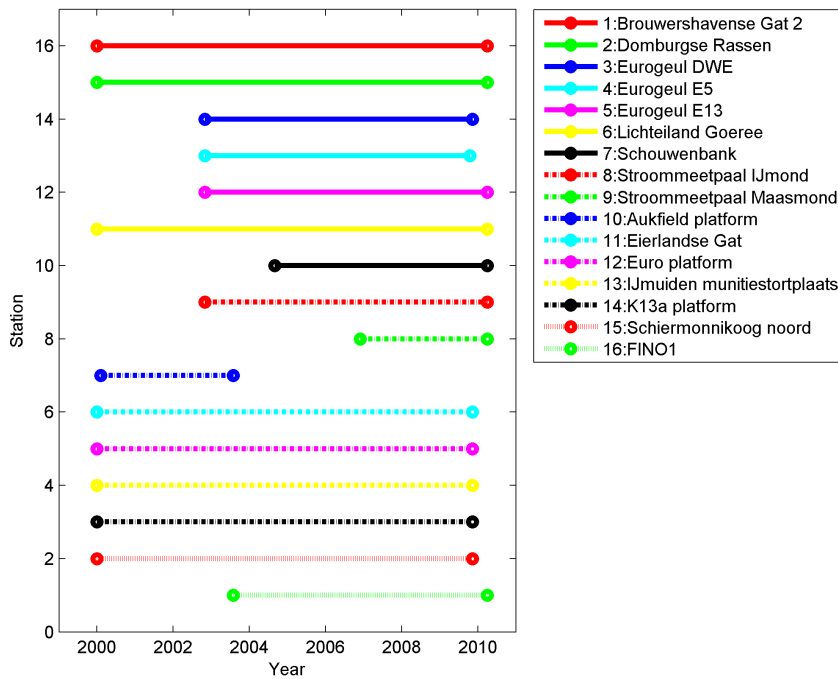


**Figure 10:** Graphical overview of the time span of the available data per station [35]. The line on top corresponds to the first legend entry.

the interpolation methods are introduced, it is important to know where in the flow chart of the AVDE model the various steps take place to find the surface roughness. In figure 11 the model of the introduction is repeated where the surface roughness is further divided in

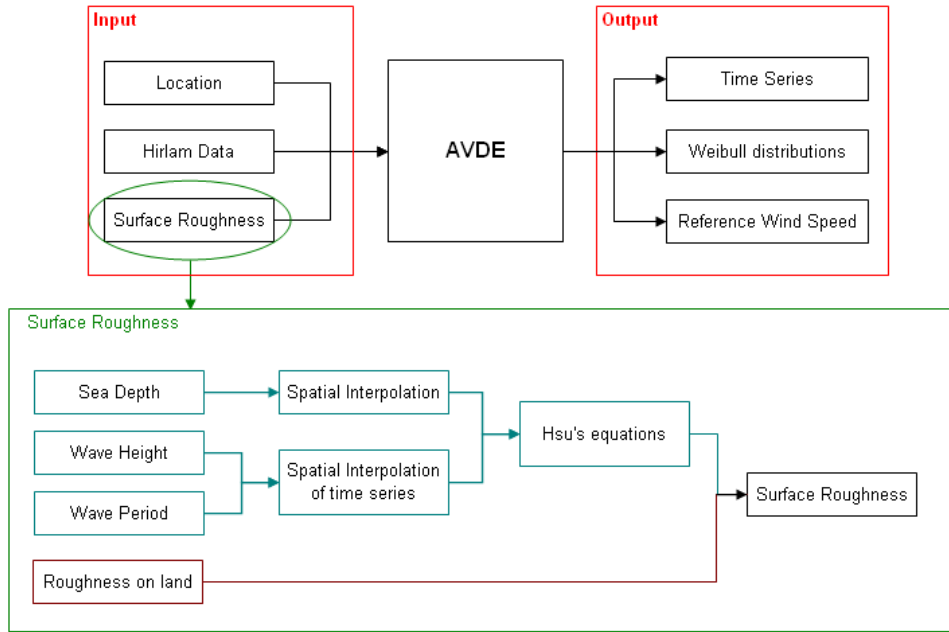


**Figure 11:** Flow chart of the AVDE model, extended for the Surface Roughness input.

several steps.

On the left side of the figure the input data is given, needed to calculate the surface roughness. Going from top to bottom, the three inputs for the sea surface roughness are given which are sea depth, wave height and wave period. The fourth input is the roughness data for locations above land. As stated previously, the roughness above land is dependent on the use of the land and since the use of land is rarely changing, it is assumed to be constant. The figure also indicates that there are extra steps needed to find the sea surface roughness. The data is first interpolated to the point of interest, after which Hsu's equation is applied to find the surface roughness.

In this section two interpolation methods will be presented. The first one is called Inverse Distance Weighting (IDW) [29] which will be used for the interpolation of the sea depth as well as for the interpolation of the wave height and wave period time series. The second one is derived from a method proposed by Gibescu, Ummels and Kling for the spatial interpolation of time series of wind speeds [14]. This last method makes use of the correlation between the several measured time series. As such, it can only be used for the spatial interpolation of wave height and wave period.

These techniques have been chosen because these are very computational friendly, i.e. the calculation time is not very long compared to other, more complex techniques as described by Li and Heap [29].

#### 4.5.1 Inverse Distance Weighting

Inverse Distance Weighting or IDW is a simple form of Kriging [29]. Kriging is a collective noun for various methods of spatial interpolation which were originally used in geology for determining the amount of coal that could be mined from coal mines. Currently Kriging is used in many other disciplines as well, for instance for the determination of the amount of cod in a specific area of the sea, or for the elevation of mountainous terrain.

The basic equation for Kriging is given in equation (4.16):

$$\hat{z}(x_0) = \sum_{i=1}^n \lambda_i z(x_i). \quad (4.16)$$

In this equation is  $\hat{z}(x_0)$  the estimated value at the point of interest  $x_0$ ,  $z$  the observed value at sample point  $x_i$ ,  $\lambda_i$  is the weight assigned to the sample point and  $n$  is the number of sample points.

The different types of Kriging can be distinguished from the way the weight  $\lambda$  is calculated. As mentioned, a simple form will be used which is Inverse Distance Weighting. For the weight the following relation is used:

$$\lambda_i = \frac{\frac{1}{d_i^p}}{\sum_{i=1}^n \frac{1}{d_i^p}}. \quad (4.17)$$

Here  $d_i$  is the Euclidean distance between the point of interest and the sample point,  $n$  is the number of sample points and  $p$  is a power parameter. When the power parameter is equal to one, linear interpolation is applied. When the power parameter is higher than one, a weighted moving average is applied. Furthermore, for increasing  $p$  the smoothness of the surface increases. In general, a value of four is used since it gives the best result concerning the smoothness of a surface. Note that in the case that the distance between a point of interest and an observed point is equal to zero, the weight corresponding to the observed point needs to be equal to one, and the weight of all other observation points should be equal to zero.

Using this method for the spatial interpolation of the sea depth gives the result as presented in figure 12. On the left side the situation is given before the interpolation, on the right side the result after interpolation. Note that only the sea depth within the EEZ will be used, other data is therefore removed. This includes the water in the province Zeeland and the water of IJsselmeer, Markermeer and Wadden region. Reason for this is that there is either no open connection between the measurement stations where the wave data is measured, or the tides of the sea let to much area fall dry which occurs in the Wadden region. In both cases the use of wave data would be incorrect and there is no need to know the sea depth in these regions.

#### 4.5.2 Gibescu's method

A second interpolation method that will be used for the interpolation of time series is Gibescu's method [14]. It was originally used for the spatial interpolation of wind speed time series, where multiple measured time series of wind speeds were used to estimate the time series at a location of interest. However, for wave data it can be used as well. The method is based on the assumption that the available data, after variance stabilizing transformation, forms a multivariate normal distribution. A model can be found to estimate a time series at a given location. In the remainder of this section, the various steps of Gibescu's method will be explained.

##### ***Variance Stabilizing Transformation***

In order to find out if a variance stabilizing transformation is necessary, the variance and mean are calculated for each location of the data set. By plotting the variance as a function of the mean, it is possible to find a relation between them. As can be seen in figure 13, there is a clear linear relationship between the two. This relationship is the so-called heteroscedasticity which is the behavior that needs to be suppressed.

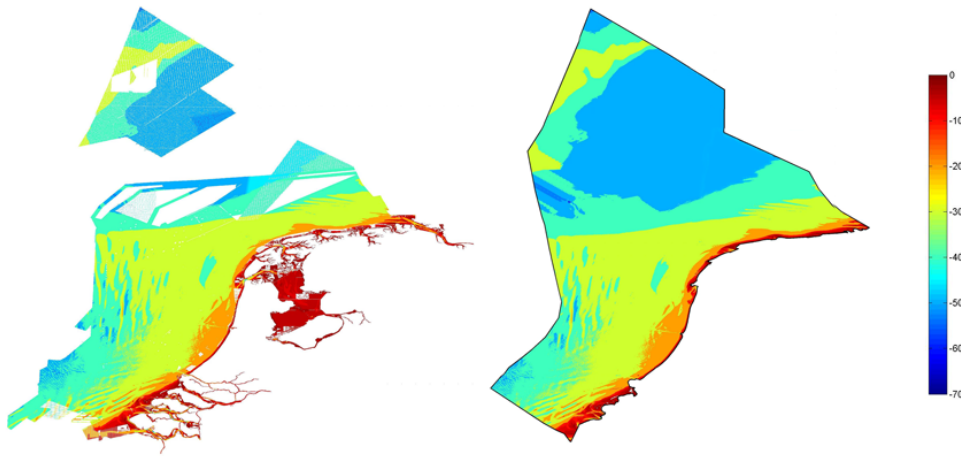


**Figure 12:** Sea depth before interpolation (left) and after interpolation using IDW (right).

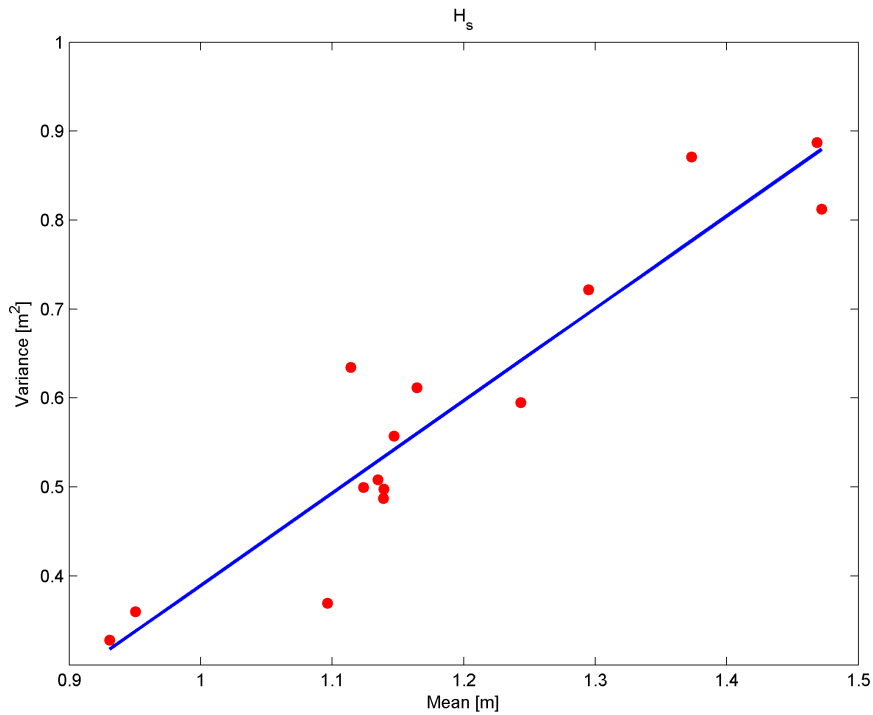


**Figure 13:** Mean-variance relationship for significant wave height measurements.

To suppress this heteroscedasticity, a variance stabilizing transformation can be applied. The goal of this transformation is to get an approximately constant variance which will simplify the regression model presented later in this section by allowing a single, mean independent value for the variance valid for all locations. Here a short overview of the theory will be given as can be found in Brockwell and Davis [5].

Assume a random variable  $Y$  with mean  $E[Y]$  and variance  $V[Y]$  given by:

$$E[Y] = \mu \quad (4.18)$$

$$V[Y] = E[(Y - \bar{Y})^2] = \sigma^2 = \Omega(\mu), \quad (4.19)$$

where  $\bar{Y}$  denotes the average of random variable  $Y$  and  $\Omega(\mu)$  indicates that the variance  $\Omega$  can be written as a function of the mean  $\mu$ . A first-order Taylor series expansion can be used to approximate a function  $f(Y)$  that has a constant variance:

$$f(Y) \approx f(\mu) + (Y - \mu)f'(\mu). \quad (4.20)$$

The approximation can be rewritten after which the expectation is taken on the left and right hand side of the equation.

$$f(Y) - f(\mu) \approx (Y - \mu)f'(\mu) \quad (4.21)$$

$$[f(Y) - f(\mu)]^2 \approx (Y - \mu)^2 (f'(\mu))^2 \quad (4.22)$$

$$V[f(Y)] \approx V(Y)[f'(\mu)]^2 = \Omega(\mu)[f'(\mu)]^2 \quad (4.23)$$

Now, combine

$$f(\mu) = \int \frac{1}{[\Omega(\mu)]^{1/2}} d\mu \quad (4.24)$$

with equation (4.23), gives:

$$V[f(Y)] \approx \left[ \frac{\partial}{\partial \mu} \int [\Omega(\mu)]^{1/2} \left[ \frac{1}{\Omega(\mu)} \right]^{1/2} d\mu \right]^2 = \left[ \frac{\partial}{\partial \mu} \int d\mu \right]^2 = \left( \frac{\partial}{\partial \mu} (\mu + c) \right)^2 = 1, \quad (4.25)$$

where  $c$  is a constant. Thus, taking this transformation on  $Y$  gives a random variable with an approximately constant variance.

Now assume a function for the variance:

$$\sigma^2 = \alpha^2 \mu^{2\beta} = \Omega(\mu), \quad (4.26)$$

in which  $\alpha$  and  $\beta$  are constants.

With this assumed function, two cases can be considered:

**Case 1:**  $\beta \neq 1$

$$f(\mu) = \int \frac{1}{[\Omega(\mu)]^{1/2}} d\mu = \int \frac{1}{\alpha \mu^\beta} d\mu \quad (4.27)$$

$$f(\mu) = \frac{1}{\alpha} \left[ \frac{\mu^{-\beta+1}}{-\beta+1} \right] = c \mu^{1-\beta} \quad (4.28)$$

**Case 2:**  $\beta = 1$

$$f(\mu) = \int \frac{1}{[\Omega(\mu)]^{1/2}} d\mu = \int \frac{1}{\alpha\mu} d\mu \quad (4.29)$$

$$f(\mu) = \frac{1}{\alpha} \log(\mu) \quad (4.30)$$

To find out which of these two cases applies, the value of  $\beta$  should be estimated which can be done by applying a linear regression on:

$$\log(\sigma) = \log(\alpha) + \beta \log(\mu) \quad (4.31)$$

which can be derived from equation (4.26).

In general, when a value for  $\beta$  close to one is found, the logarithmic transformation is applied since this is an easy transformation. For the wave height, a value for  $\beta$  of 1.0792 is found and for the wave period a value of 0.9784 is found. Assuming that both values are close to one, the logarithmic transformation of case 2 is applied. The logarithmic wave height  $LH_s$  can now be found with equation (4.32). The same equation can be used to transform the wave period.

$$LH_s = \frac{1}{\alpha} \log(H_s) \quad (4.32)$$

The result of the transformation can be seen in figure 14. It is clear that the average variance is close to the value one which results in the fact that  $LH_s$  can be assumed to be multivariate-normal distributed.

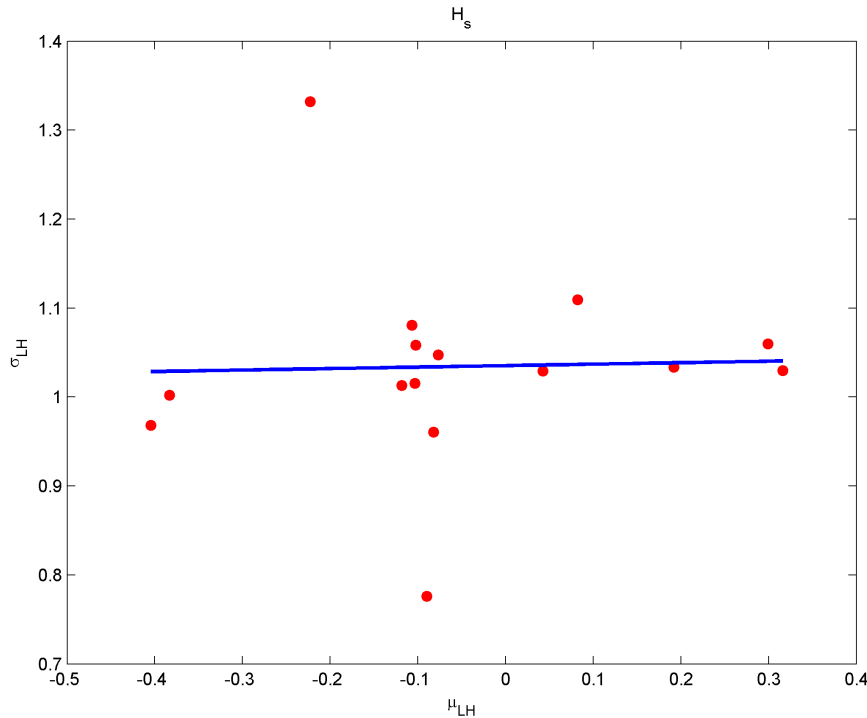


**Figure 14:** Mean-variance relationship for significant wave height measurements after variance stabilizing transformation.

### **Multivariate Normal Distribution**

In order to find an estimate of the wave height and wave period at a given location, use is made of the characteristics of a multivariate normal distribution. Following the explanation given by Brockwell and Davis [5], a random vector  $X$  can be considered which is distributed according to the multivariate normal distribution with mean  $\mu$  and covariance matrix  $\Sigma$ . Suppose that  $X$  is a concatenation of the calculated data set (subscript  $c$ ) and the observed data set (subscript  $o$ ):

$$X = \begin{pmatrix} X_c \\ X_o \end{pmatrix}. \quad (4.33)$$

For the mean and covariance matrix similar partitions can be made:

$$\mu = \begin{pmatrix} \mu_c \\ \mu_o \end{pmatrix}, \quad (4.34)$$

$$\Sigma = \begin{pmatrix} \Sigma_{cc} & \Sigma_{co} \\ \Sigma_{oc} & \Sigma_{oo} \end{pmatrix}. \quad (4.35)$$

If the determinant of  $\Sigma_{oo}$  is larger than zero, then the conditional distribution of  $X_c$  given  $X_o$  is again multivariate normal and given by:

$$\mathcal{N}(\mu_c + \Sigma_{co}\Sigma_{oo}^{-1}(X_o - \mu_o), \Sigma_{cc} - \Sigma_{co}\Sigma_{oo}^{-1}\Sigma_{oc}). \quad (4.36)$$

The best estimate for  $X_c$ , given a specific location and time, can now be found as:

$$\hat{X}_c = E(X_c|X_o) = \mu_c + \Sigma_{co}\Sigma_{oo}^{-1}(X_o - \mu_o). \quad (4.37)$$

Now assume that  $\hat{X}_c$  is the estimate of the logarithmic wave height at a given location, it can be seen that it is formed by a mean value  $\mu_c$  to which an error value  $\Sigma_{co}\Sigma_{oo}^{-1}(X_o - \mu_o)$  is added. The mean value  $\mu_c$  can be calculated from the mean values of the observed data using some form of spatial interpolation. Here, again, use is made of Inverse Distance Weighting (see section 4.5.1). For the estimation of the error value, the two covariance matrices  $\Sigma_{co}$  and  $\Sigma_{oo}$  can be determined based on the observations and the relative distance between the stations as will be explained later on. The last term in the equation  $(X_o - \mu_o)$  is the error value of the observations which can easily be determined.

### **Covariance matrices**

The covariance matrices  $\Sigma_{co}$  and  $\Sigma_{oo}$  are determined from the observed data. In general, the covariance between two time series can be found with:

$$Cov(x_i, x_j) = E((x_i - \bar{x}_i)(x_j - \bar{x}_j)^T) = \overline{x_i \cdot x_j} - \bar{x}_i \cdot \bar{x}_j. \quad (4.38)$$

In this equation is  $x_i$  a measured variable at station  $i$  and  $x_j$  a measured variable at station  $j$ . Note that the result of this equation is a square matrix with on the diagonal the variances and off-diagonal the covariances of the measured time series. For the covariance matrix  $\Sigma_{oo}$  this equation can be used directly. The covariance matrix  $\Sigma_{co}$ , however, cannot be found directly from equation (4.38). This is due to the fact that there is no calculated time series yet. Luckily,  $\Sigma_{co}$  can be estimated using covariance matrix  $\Sigma_{oo}$ , the euclidean distance between the different observation points, and the euclidean distance between the observation points and a point of interest. This goes as follows:

After the covariance matrix  $\Sigma_{oo}$  has been found, the Euclidean distances between the ob-

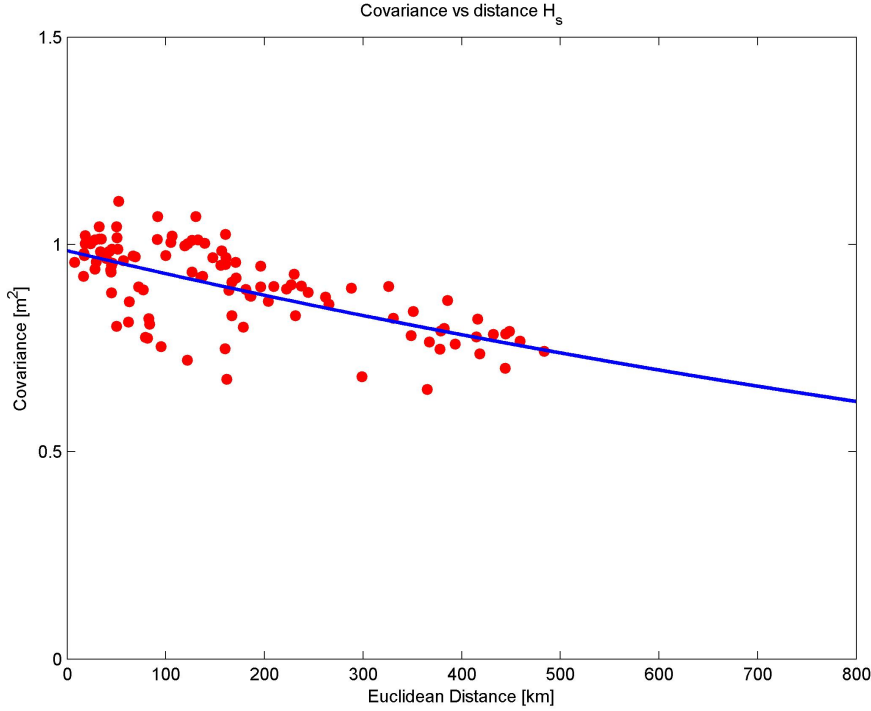


**Figure 15:** Covariance of logarithmic wave height vs Euclidean distance, given for 15 measurement stations.

ervation points is calculated. A plot can be made of the covariance as a function of the euclidean distance which is shown in figure 15. This figure shows that the covariance is decreasing for increasing distance as could be expected from the fact that a point close by will have a larger influence than a point far away.

Next step is to apply an exponential fit on the data in figure 15 in the form of:

$$Cov(x_i, x_j) = \alpha e^{-\beta \|x_i - x_j\|} \quad (4.39)$$

Here  $1/\beta$  is known as the characteristic distance or decay parameter,  $\|x_i - x_j\|$  is the Euclidean distance between two observation points and  $\alpha$  is a constant. Note that the  $\alpha$  and  $\beta$  used here are not related to  $\alpha$  and  $\beta$  given in equation (4.26).

For the calculation of the covariance matrix  $\Sigma_{co}$  equation (4.39) can be used where the euclidean distances are used between the observation points and the point of interest. For stability reasons of equation (4.37), it is important to recalculate covariance matrix  $\Sigma_{oo}$  using equation (4.39) as well. By doing this, the determinant of  $\Sigma_{oo}$  will always be positive definite which results in the fact that  $\Sigma_{oo}$  is always invertible.

The result of this method is only as good as the amount of data available. For the interpolation, 15 measurement stations have been selected. Unfortunately, it happens that not all stations have a measurement at a given moment in time. For this reason, the covariance vector  $\Sigma_{co}$  and covariance matrix  $\Sigma_{oo}$  have to be calculated separately for each moment in time based on the data available for that specific moment in time. In addition, also care should be taken that temporal variations are taken into account as well. For this reason, the wave data should be analyzed to find temporal variations.

### **Back transformation**

Now all variables in equation (4.37) can be determined, it is possible to estimate  $\hat{X}_c$ . Since previously a variance stabilization has been applied,  $\hat{X}_c$  is a variance stabilized value

which has to be transformed back in order to find a real value for  $\hat{X}_c$ . The back transformation is done by equation (4.40):

$$\hat{x}_c = e^{\alpha \cdot \hat{X}_c}, \quad (4.40)$$

which is the inverse of equation (4.32) where  $\hat{X}_c$  is equal to  $LH_s$  and  $\hat{x}_c$  equal to  $H_s$ . Note that the constant  $\alpha$  in this equation is the same as in equation (4.26).

### Temporal Variations

This section will focus on the temporal variations in the available wave data and specifically on the daily and seasonal variations. Starting with the daily effects, in figure 16 the average value is presented of the wave height occurring at the same hour every day. As can be seen, most curves are more or less flat, the plot does not show a daily pattern. This was expected since above sea, the wind speed also shows a more or less constant average during the day. Since the wave height and wind speed influences each other, it was expected that the average wave height would follow the same pattern as the average wind speed.

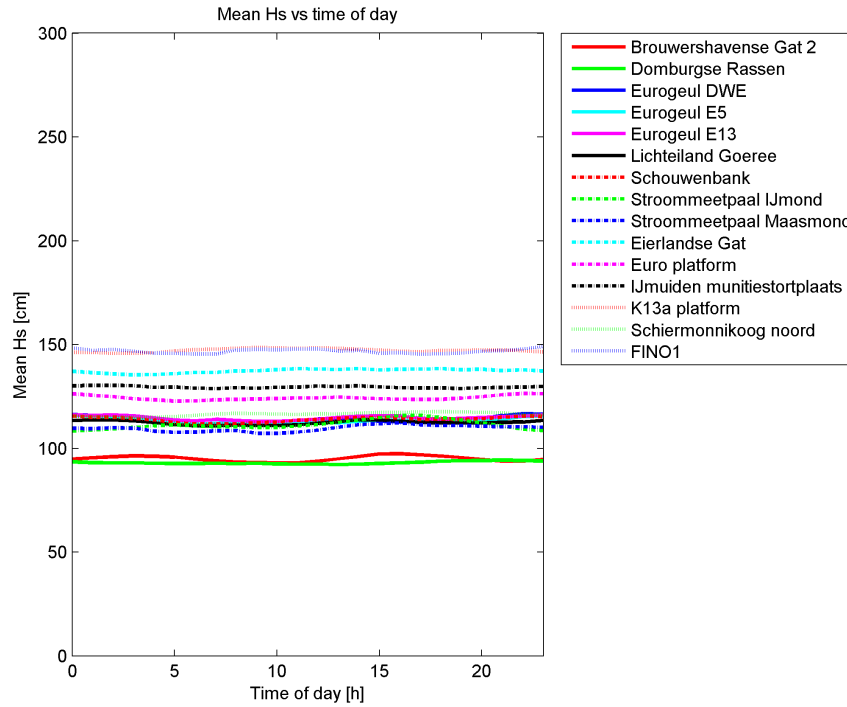


**Figure 16:** Average of wave height occurring at equal time of the day, given for 15 measurement stations.

When the monthly pattern shown in figure 17 is observed, a clear sinusoidal curve can be seen with a maximum at the end of December (month 12) and a minimum around June (month 6). Also note that locations further from the Dutch shore show a higher monthly average than the locations close to the coast. Furthermore, it can be seen that the trend for all locations is similar.

Since a seasonal variation has been found, it can also be expected that this influences the covariance matrix  $\Sigma_{oo}$ . For that reason the covariances per month for the wave height are plotted and given in figure 18. As can be seen here, the covariance is indeed different for each month of the year. As such, it has to be checked what the effect is of the changing covariance matrix on the solution for  $\hat{X}_c$ . This will be further explained in section 4.6.

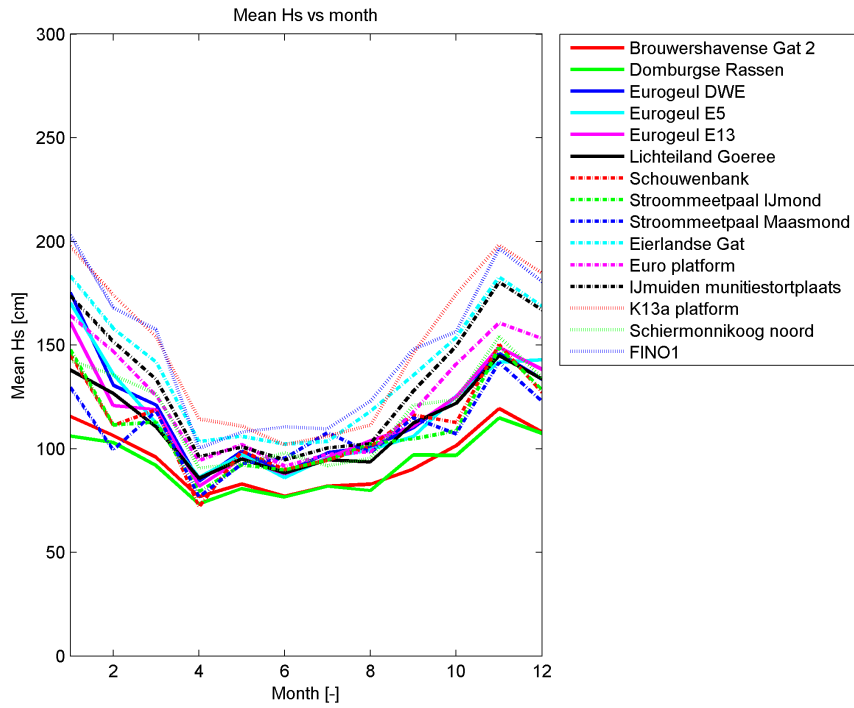


**Figure 17:** Monthly averaged mean sea level pattern for measured locations.

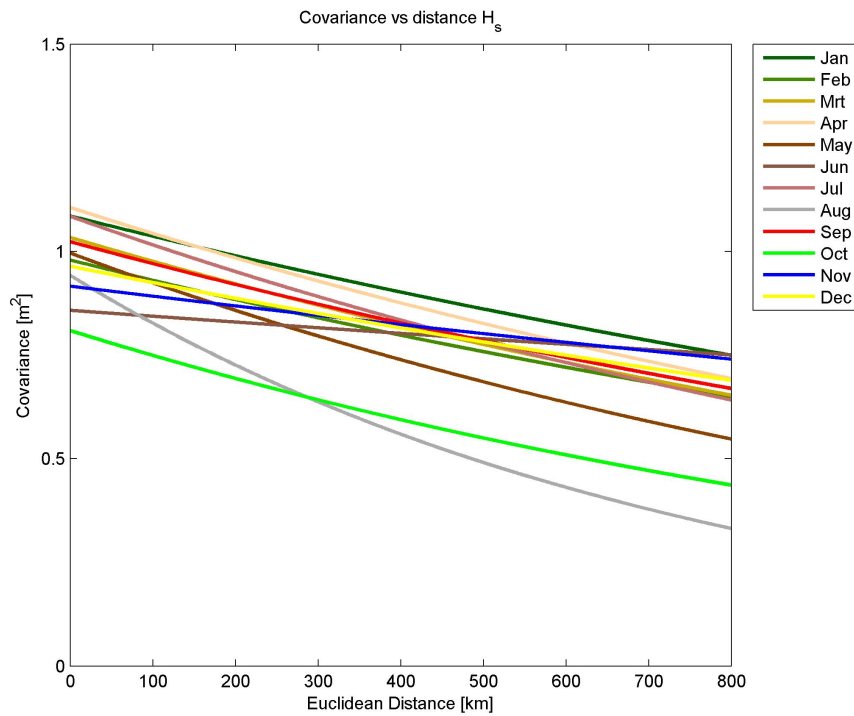


**Figure 18:** Wave height covariance per month vs euclidean distance for 15 measurement stations.

## 4.6 Validation of spatial interpolation methods

In section 4.5 two methods were given for the spatial interpolation of wave data. In addition, for Gibescu's method, it should be checked what the influence is of using a monthly changing covariance matrix. This results in the fact that three methods should be validated:

- 1 Inverse Distance Weighting (IDW)
- 2 Gibescu's method with a single covariance matrix (Cov)
- 3 Gibescu's method with a monthly changing covariance matrix (Cov Month)

For the validation of the above mentioned techniques, use is made of cross validation. One station, the validation station, is taken out of the data set, using the data of the remaining stations to calculate the time series at the validation station. By comparing the measured time series with the calculated time series, the methods can be judged on their accuracy.

In figure 9 the locations of the measurement station were given. Looking at the spread of the stations it can be seen that there are many stations close to the coast while there are only a few which lie further away from the coast. It could therefore be expected that the accuracy of the interpolation decreases with distance to the coast.

In the remainder of this section, the validation of one location will be discussed after which a short overview will follow with the results of the validation at the other measurement stations. The first location that will be left out is IJmuiden Munitiestortplaats.

First the different time series are compared for both wave height ( $H_s$ ) and wave period ( $T_s$ ), in figures 19 and 20. These two plots show that, in general, the calculated time series follow the measured time series quite well although the magnitude is not entirely taken into account. Further more, it is already visible that both of Gibescu's methods give almost equal results.

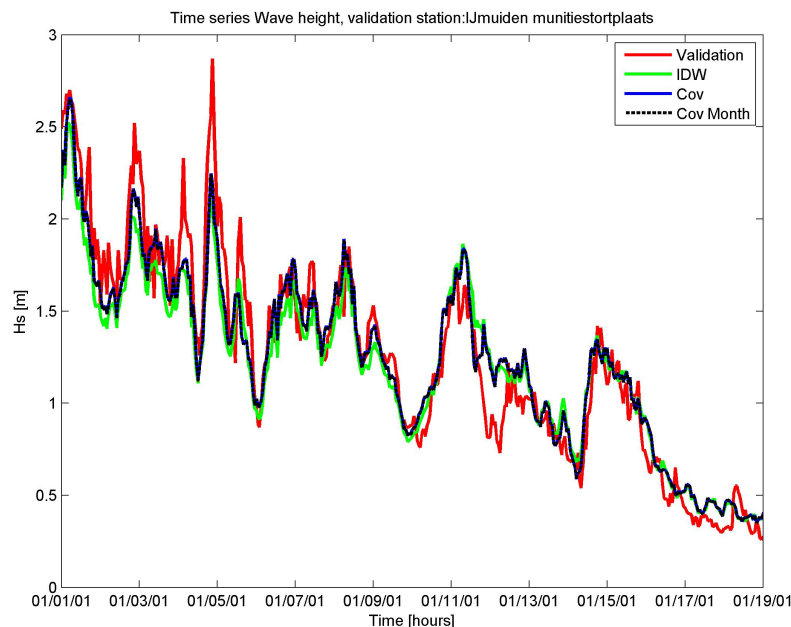


**Figure 19:** Time series wave height at IJmuiden Munitiestortplaats.

Since the plots of the time series only give the result for a small time period, a look is taken at the scatter plots. The various plots for the wave height are given in figures 21, 23 and 25, and for the wave period in figures 22, 24 and 26.

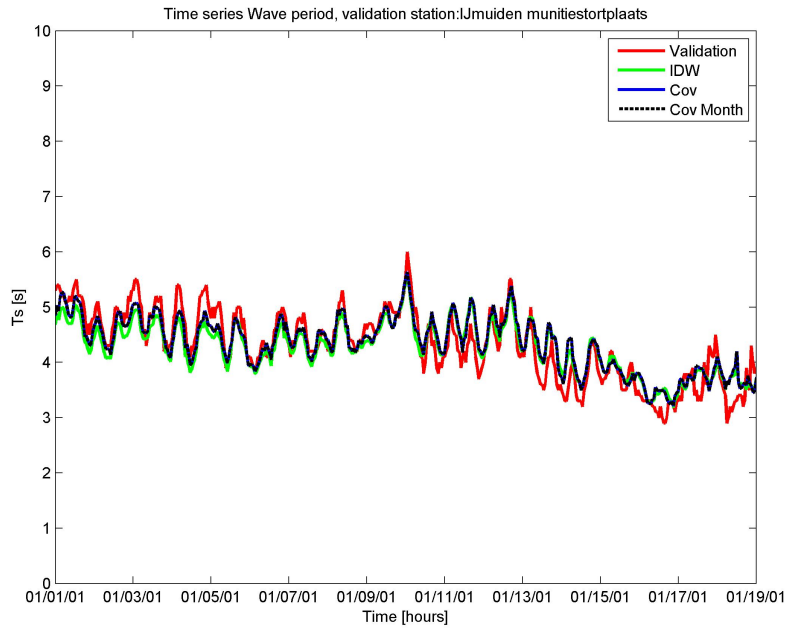


**Figure 20:** Time series wave height at IJmuiden Munitiestortplaats.

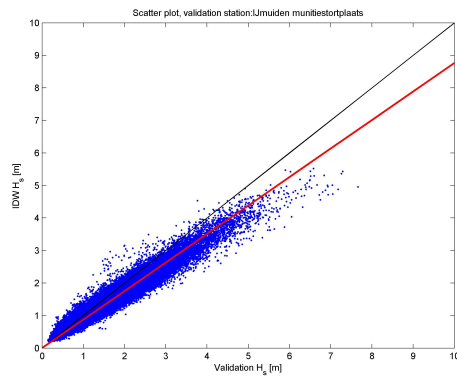


**Figure 21:** Scatterplot IJmuiden Minutiestortplaats, wave height, method: IDW.

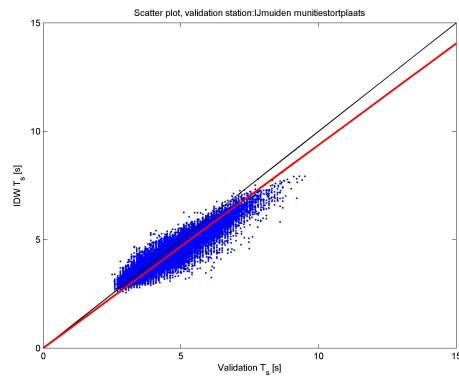


**Figure 22:** Scatterplot IJmuiden Minutiestortplaats, wave period, method: IDW.

From these plots, it can be seen that all methods for this location overestimate the wave height as well as the wave period. The deviations from the optimum where the measured value is equal to the calculated values, are given in table 3 for the wave height and table 4 for the wave period. In these tables an over estimation is represented by a positive value and an under estimation by a negative value. As expected, the largest deviations can be found for locations which are located far from the shore. To check whether these deviations are a problem, the Charnock parameter is calculated for all stations.

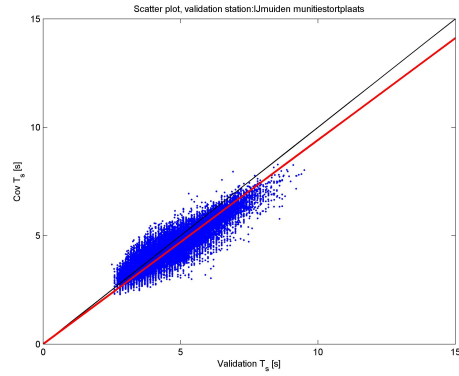
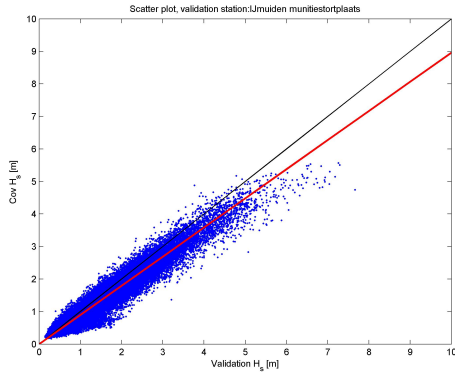


**Figure 23:** Scatterplot IJmuiden Minutiestortplaats, **Figure 24:** Scatterplot IJmuiden Minutiestortplaats, wave height, method: Cov. wave period, method: Cov.

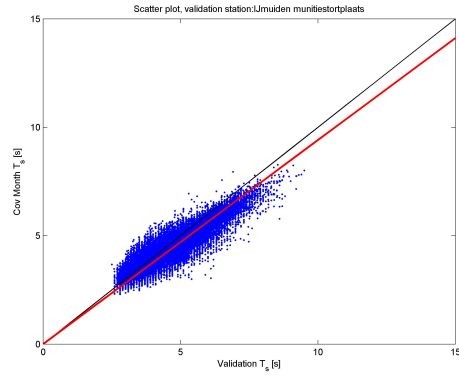
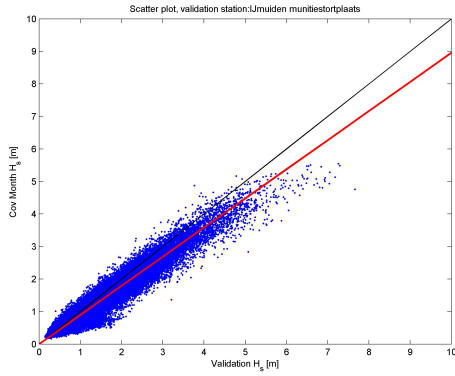


**Figure 25:** Scatterplot IJmuiden Minutiestortplaats, **Figure 26:** Scatterplot IJmuiden Minutiestortplaats, wave height, method: Cov Month. wave period, method: Cov Month.

**Table 3:** Deviations from measured time series of wave height for the different validation stations and used methods.

| Station                     | IDW [%] | Cov [%] | Cov Month [%] |
|-----------------------------|---------|---------|---------------|
| Brouwershavense Gat 2       | 15.511  | 6.134   | 6.124         |
| Domburgse Rassen            | 23.378  | 20.559  | 20.553        |
| Eurogeul DWE                | -8.015  | -0.219  | -0.129        |
| Eurogeul E5                 | -10.102 | -10.623 | -10.606       |
| Eurogeul E13                | -3.270  | -4.164  | -4.173        |
| Lichteiland Goeree          | -8.132  | -16.661 | -16.646       |
| Schouwenbank                | -0.585  | -5.108  | -5.099        |
| Stroommeetpaal IJmond       | 0.296   | 2.287   | 2.317         |
| Stroommeetpaal Maasmond     | 9.200   | 2.933   | 2.937         |
| Eierlandse Gat              | -19.148 | -14.952 | -14.956       |
| Euro platform               | -10.415 | -9.265  | -9.255        |
| IJmuiden munitiestortplaats | -12.341 | -10.362 | -10.406       |
| K13a platform               | -22.172 | -8.531  | -8.171        |
| Schiermonnikoog noord       | -0.472  | 6.405   | 6.798         |
| FINO1                       | -22.178 | -22.463 | -21.946       |

**Table 4:** Deviations from measured time series of wave period for the different validation stations and used methods.

| <b>Station</b>              | <b>IDW</b><br>[%] | <b>Cov</b><br>[%] | <b>Cov Month</b><br>[%] |
|-----------------------------|-------------------|-------------------|-------------------------|
| Brouwershavense Gat 2       | 19.628            | 15.645            | 15.644                  |
| Domburgse Rassen            | 12.702            | 11.887            | 11.886                  |
| Eurogeul DWE                | -4.037            | 1.740             | 1.743                   |
| Eurogeul E5                 | -4.772            | -3.452            | -3.451                  |
| Eurogeul E13                | -3.629            | -5.611            | -5.611                  |
| Lichteiland Goeree          | -7.855            | -12.153           | -12.152                 |
| Schouwenbank                | -1.435            | -4.552            | -4.550                  |
| Stroommeetpaal IJmond       | 4.831             | 7.470             | 7.482                   |
| Stroommeetpaal Maasmond     | -1.462            | -7.230            | -7.231                  |
| Eierlandse Gat              | -8.033            | -5.198            | -5.200                  |
| Euro platform               | -4.307            | -3.267            | -3.267                  |
| IJmuiden munitiestortplaats | -6.303            | -5.870            | -5.870                  |
| K13a platform               | -9.583            | -1.381            | -1.367                  |
| Schiermonnikoog noord       | -2.806            | 2.461             | 2.486                   |
| FINO1                       | -14.236           | -11.508           | -11.494                 |

**Table 5:** Deviations from measured time series of Charnock parameter for the different validation stations and used methods.

| <b>Station</b>              | <b>IDW</b><br>[%] | <b>Cov</b><br>[%] |
|-----------------------------|-------------------|-------------------|
| Brouwershavense Gat 2       | -4.265            | -9.197            |
| Domburgse Rassen            | 8.942             | 7.129             |
| Eurogeul DWE                | -4.185            | -1.704            |
| Eurogeul E5                 | -5.356            | -7.095            |
| Eurogeul E13                | 0.894             | 1.743             |
| Lichteiland Goeree          | -0.170            | -4.924            |
| Schouwenbank                | 0.839             | -0.552            |
| Stroommeetpaal IJmond       | -5.297            | -6.259            |
| Stroommeetpaal Maasmond     | 9.743             | 9.295             |
| Eierlandse Gat              | -7.847            | -6.825            |
| Euro platform               | -6.262            | -6.208            |
| IJmuiden munitiestortplaats | -5.225            | -4.392            |
| K13a platform               | -13.476           | -6.811            |
| Schiermonnikoog noord       | 4.284             | 5.265             |
| FINO1                       | -7.486            | -11.009           |

In figure 27 a part of the Charnock time series is presented including an upper and lower boundary where the value of the Charnock parameter should be between, according to literature [32]. The values of these boundaries are  $0.3 \cdot 10^{-2}$  and  $8.0 \cdot 10^{-2}$ . The figure also includes an average value of  $1.44 \cdot 10^{-2}$  which was found by Garratt [13]. For the calculation of the Charnock parameter, use is made of Hsu's equation given by:

$$m = \frac{H}{T\sqrt{gd}} \quad (4.41)$$

As can be seen from the found plot, the differences between the measured and calculated values are not very large. Also, for this parameter regression plots have been made. From

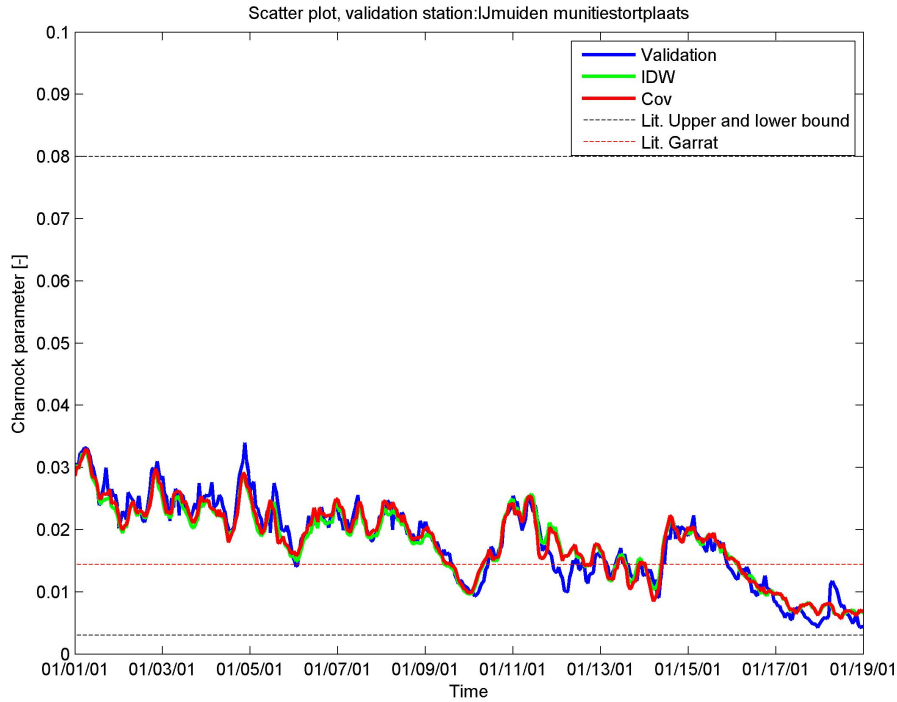


**Figure 27:** Time series Charnock parameter at IJmuiden Munitiestortplaats.

these it follows that the deviation are between  $-10\%$  and  $+10\%$  with two exeptions which go to  $-11\%$  and  $-13\%$ . This can also be seen in table 5. Note that here method 3, Gibescu's method with a monthly change in the covariance matrix, has been left out since it gives the same results as method 2, Gibescu's method with a single covariance matrix. Also note that the found deviations for the Charnock parameter are lower than the deviations found for the individual wave height and wave period.

#### 4.6.1 Conclusions spatial interpolation methods

In the previous sections the results of the validation of the interpolation of the wave height and wave period have been presented. Three different interpolation techniques were used: IDW, Gibescu's method and Gibescu's method with monthly changing covariance matrix. It was found that there was almost no difference for the calculation of the Charnock parameter between the two versions of Gibescu's method. For that reason, the simplest method will be used for the calculation of wind speed time series which is without the monthly change in covariance structure. Since the first method, IDW, shows slightly lower deviations from the measured time series, it will also be used in the calculation of the wind speed time series of the eleven chosen validation points of the Wind Atlas.



## 5 AVDE model

This chapter will discuss some of the aspects of the AVDE model. In figure 28 the flow chart of the AVDE model is given where the calculation module has been divided in five steps: Cell selection, time interpolation, vertical interpolation, horizontal interpolation and local adjustments. In the last step where local adjustments are applied, the sea surface roughness is included in the calculations. The five steps will be briefly discussed.

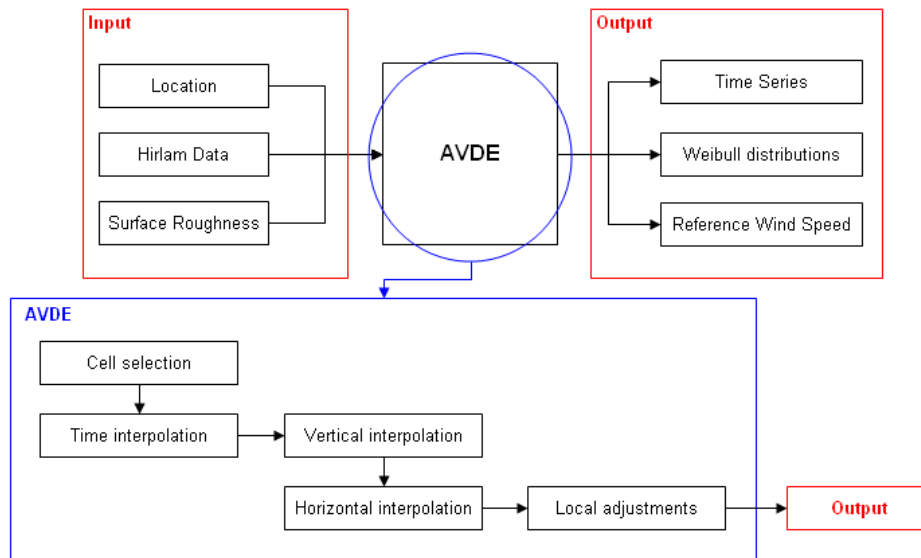


**Figure 28:** Flow chart of the AVDE model with focus on the calculation module.

### 5.1 Cell selection

The first step in the calculation module is the cell selection. A Hirlam file consists of gridded data where each stored variable value has its own place and time specification given by a longitude, latitude, pressure height and time. In this step, only two dimensions are important: the longitude and latitude. For each location of interest, with specified longitude and latitude, four corner points can be found in the Hirlam data which surround the location of interest. All the data available in the Hirlam file for these four points are selected. Of course, if the location of interest coincides with a corner point, only the data for that single point is required for the remainder of the computations.

### 5.2 Time interpolation

The second step is the time interpolation. Depending on the (pressure) altitude, the data in the Hirlam file is stored with a different time step. For the lower levels the time step is one hour while for higher levels the time step is three hours. Reason for this difference is that changes of the state of the atmosphere at higher altitudes are much slower than at ground level. It can therefore be expected that the loss of information due to a larger time step at higher altitudes is minimal. Since in the following calculation steps, it is required that the time step is equal for the two altitudes, time interpolation is needed. In addition, as mentioned in section 3.1, a time step can be specified. If this specified time step is not equal to one hour, the specified time step will be used for the time interpolation resulting

in the fact that time interpolation is needed for both altitudes. Otherwise, if the time step is set to one hour, only for the highest pressure altitude a time interpolation step on the parameters is needed.

### 5.3 Vertical interpolation

In the vertical interpolation step, the interpolation is made to the required altitude. Depending on the difference between the wind speed at low altitude and the wind speed at a higher altitude, two interpolations are possible. First possibility is when the wind speed at high altitude is smaller than the wind speed at low altitude. When this occurs, a linear interpolation is applied. The second possibility is when the wind speed at high altitude is higher than the wind speed at low altitude. When this happens, the Monin-Obukhov methodology is applied with Businger-Dyer wind profiles [52] in accordance to the method of Hegberg [17]. The methodology distinguishes three different atmospheric stability classes based on the Monin-Obukhov length which are stable, neutral and unstable. These stability classes all have their distinct properties and shapes which results in different approximations. For each moment in time, the correct stability class is selected and the corresponding equations are used to estimate the wind speed at the required altitude. Important note is that for this interpolation, only the surface roughness on meso-scale is taken into account. Lengths in the meso-scale ranges from 5 km up to 2000 km. The used surface roughness on meso-scale in the case of a Hirlam22-file is the average surface roughness for an area of 500 km<sup>2</sup>. In the case of a Hirlam55-file the area is 3000 km<sup>2</sup>.

### 5.4 Horizontal interpolation

Now the wind speed is known at the four corner points and at the specified altitude, the horizontal interpolation can be applied. Here a linear interpolation is used between the four points. In some cases this step introduces errors with respect to the Monin-Obukhov length. When this happens, information about which wind profile to apply is lost. It is then assumed that the applicable wind profile is that of the neutral stability class.

### 5.5 Local adjustments

In the local adjustment, the wind speed is corrected for local elements. This is the part where the previously calculated sea surface roughness is included in the calculation module.

## 6 Model Output

Following the block model presented in the introduction to the AVDE model, figure 1, the last item that needs to be discussed is the output. The output consists of numerical data and is given per location and altitude which is the so called point of interest. For each point of interest a time series is generated as well as an analysis on this time series consisting of the directional dependent Weibull parameters and the reference wind speed. In the following sections, these types of output will be discussed.

### 6.1 Time Series

The first output that is given by the AVDE model is a time series which is based on the location, altitude and most importantly, the input of time step and period. The following columns can be found:

- Time stamp consisting out of date, hour and time of year
- Temperature  $T$  [K]
- Pressure  $P$  [Pa]
- Wind speed  $U$  [m/s]
- Wind direction  $D$  [deg]
- Monin-Obukhov length  $L$  [m]
- Friction velocity  $u_*$  [m/s]
- Surface drag coefficient  $C_d$  [-]
- Average surface roughness  $z_{0,avg}$  [m]
- The value of the Charnock parameter  $\alpha_{ch}$  [-]

Although for most applications only the wind speed and wind direction are required, the other variables will be given as well. This is due to the fact that it gives additional information about the state of the atmosphere at a given time. For instance, the Monin-Obukhov length gives a measure of the stability of the atmospheric boundary layer. The surface drag coefficient, average surface roughness and Charnock parameter give an indication of the terrain. Note that above land, the Charnock parameter is constant while above sea, depending on the method applied, this parameter is variable. The surface drag coefficient and average surface roughness are direction dependent and therefore variable in time.

### 6.2 Weibull distribution

Besides the time series, also directional dependent Weibull distributions are given for each location based on the complete time series. Specifically, the two parameter Weibull distribution is used:

$$f(u) = \frac{k}{A} \left(\frac{u}{A}\right)^{k-1} \exp\left(-\left(\frac{u}{A}\right)^k\right) \quad (6.42)$$

Here  $u$  is the wind speed,  $A$  the scale parameter and  $k$  the shape parameter. To fit the data to the two parameters various methods can be used. Here the same method is applied as is used by the Wind Atlas Method [47] made by Risø. There are two reasons for using this method. The first and main reason is that observed histograms usually are not well represented by the Weibull distribution over the whole range of wind speeds. In general, observed histograms, from measured and calculated time series, will show deviations, especially in the lower and higher wind speed regions. These deviations can be caused by the

measurement instruments or, in the case of calculated time series, by numerical errors. Secondly, the method is well known and excepted by many companies.

In order to minimize the effect of the deviations at low wind speeds, the method focuses on wind speeds higher than the mean wind speed. Two requirements are set:

- 1 The total wind energy in the fitted Weibull distribution and the observed distribution are equal
- 2 The frequencies of occurrence of wind speeds higher than the observed average speed are the same for both distributions

The method starts with calculating the frequency distribution of the observed time series in the form of a histogram. The total wind energy content in this histogram is then calculated using

$$E = \sum_{n=1}^N V_c^3 \cdot f \cdot dV, \quad (6.43)$$

where  $E$  is the energy content,  $V_c$  the wind speed of the center of a bin,  $f$  the corresponding frequency of occurrence,  $dV$  the width of the wind speed bin and  $N$  the number of bins. This is also graphically presented in figure 29.

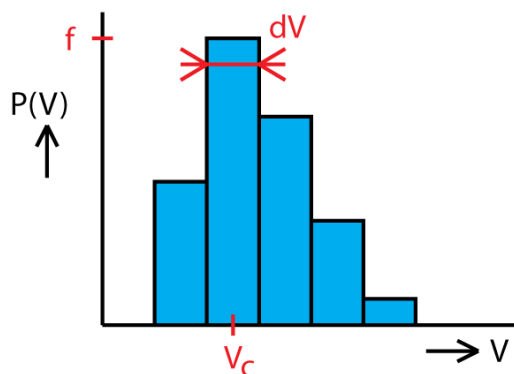


**Figure 29:** Graphical explanation of calculation of energy content in observed time series.

Now the energy content is known, two equations for the scale parameter are used which are based on the two requirements given above:

$$A = \frac{E}{\left(\Gamma\left(1 + \frac{3}{k}\right) \cdot dV\right)^{1/3}}, \quad (6.44)$$

$$A = \frac{V_m}{-\log(P(V > V_m))^{1/k}}. \quad (6.45)$$

$$(6.46)$$

Here  $A$  is the scale parameter and  $k$  the shape parameter of the Weibull distribution,  $\Gamma$  represents the Gamma function and  $P(V > V_m)$  is the probability where the wind speed is higher than the mean wind speed  $V_m$ . By subtracting equation (6.44) and (6.45) an equation for the shape parameter  $k$  can be found which can be solved by a root finding algorithm. The scale parameter  $A$  can be found by applying either equation (6.44) or (6.45). Note that both should give the same result.

### 6.3 Reference wind speed

The reference wind speed has been defined by the standard IEC1400-1ed2 as the extreme 10-min average wind speed at turbine hub height with a recurrence period of 50 years [11]. Various methods can be used to estimate its value. Here only the Gumbel-Bergström method will be discussed.

The Gumbel-Bergström method is a method to find the reference wind speed based on given Weibull shape and scale parameters through the Gumbel distribution. As such, in this method it is recognized that the Weibull distribution is a parent distribution of the Gumbel distribution. Relations are available which link the Weibull parameters  $A$  and  $k$  to the Gumbel parameters  $\alpha$  and  $\beta$ . Additionally, the number of independent observations  $M$  is also required for the calculation of the reference wind speed.

As a first step, the number of independent observations must be determined. Suppose that wind speed has been measured for a period of length  $T$  and an averaging time of  $T_{ave}$ . Then a time series with  $N = T/T_{ave}$  averaged wind speeds is available where the  $N$  observations are dependent. To find independent observations, the time series must be broken down into  $M$  independent sub series which would give  $M = T/T_M$  where  $T_M$  is the time between independent observations in the time series. Instead of using  $T_M$ , use is made of the frequency of independent observations  $\nu_M$ :

$$M = \nu_M T, \quad (6.47)$$

where  $\nu_M = 1/T_M$ . To find a value for the frequency of independent observations, the time series has to be considered again. Now the average time is required between two observations which are correlated for 50% [1]. Using the spectral density function of the time series, a value for  $\nu_M$  can be found. It is, however, also been found that the frequency of independent observations does not strongly depend on the actual spectral density function so that values of a typical spectrum may be used which are given in table 6.

**Table 6:** The frequency of independent observations  $\nu_M$  as a function of the averaging time  $T_{ave}$ .

| $T_{ave}$ [s] | $\nu_M$ [Hz] |
|---------------|--------------|
| 3600          | $2.810^{-5}$ |
| 600           | $7.310^{-4}$ |
| 60            | $1.010^{-3}$ |
| 10            | $4.610^{-3}$ |
| 5             | $7.910^{-3}$ |
| 3             | $1.010^{-2}$ |
| 1             | $2.410^{-2}$ |

Now all required parameters are known, the Gumbel parameters can be found using:

$$\frac{1}{\alpha} = \frac{A}{k} (\log M)^{\frac{1}{k}-1}, \quad (6.48)$$

$$\beta = A (\log M)^{\frac{1}{k}}. \quad (6.49)$$

This estimation of the Gumbel parameters have shown to be a biased extreme value analysis. To overcome this problem, an empirical solution has been suggested which is to increase the found shape parameter  $A$  from the time series with 10% before applying equations (6.48) and (6.49) [10].

The reference wind speed can be found from:

$$V_{ref} = \beta - \frac{1}{\alpha} \log \left( -\log \left( F_{e,V_{ref}} \right) \right). \quad (6.50)$$

Here  $F_{e,V_{ref}}$  is the chance that the maximum wind speed occurs once in fifty years i.e.:

$$F_{e,V_{ref}} = 1 - \frac{1}{50} = 0.98. \quad (6.51)$$

Part II

## Validation



## 7 Setup validation AVDE model

In this chapter the setup is given for the validation of the AVDE model. In the first section, the used methods in the validation process will be presented as well as some limitations that occur due to the available data. Hereafter, the chosen validation stations are presented after which an overview is given of the different steps in the validation process.

### 7.1 Calculation methods

In chapter 4.6 two different methods were given for the spatial interpolation of wave data. These methods are Inverse Distance Weighting and Gibescu's method. In addition, in section 4.3, it was mentioned that there are two ways to calculate the surface roughness. One makes use of the Hsu's shallow sea equation (4.15), while the second method makes use of an iterative solution of Hsu's general equation (4.9), the general wave equation (4.10) and an equation that relates the phase velocity to the wave length and wave period of the waves (4.14). For clarity, these four equations are mentioned below:

$$z_0 = \frac{H}{T} \frac{u_*^2}{\sqrt{gd} g}, \quad (4.15)$$

$$z_0 \propto \left(\frac{H}{L}\right) \frac{u_*^2}{g}, \quad (4.9)$$

$$C = \sqrt{\frac{gL}{2\pi} \tanh\left(\frac{2\pi d}{L}\right)}, \quad (4.10)$$

$$C = \frac{L}{T}. \quad (4.14)$$

Using two different methods, it is tested whether using Hsu's shallow sea equation is valid. Besides using Hsu's equations with different interpolation methods, also the original method used for the first version of the Offshore Wind Atlas is included in the comparison. This gives five different methods in total. The characteristics of these methods are given below:

#### **Method 1** Charnock

- The original method as is used in the first version of the Offshore Wind Atlas
- Can be used above land and water
- Above water: constant estimated roughness and constant value for the Charnock parameter
- Above the Netherlands: known roughness map with resolution of 100x100km [25]
- Above other land areas: estimated roughness

#### **Method 2** Hsu IDW Shallow

- Uses equation of Hsu for shallow sea (4.15) for calculation of sea surface roughness
- Uses Inverse Distance Weighting (IDW) to estimate the wave height and period for a given time and place
- Can only be used within the Dutch EEZ since there sea depth is available
- Above land, Method 1 is applied

#### **Method 3** Hsu IDW General

- Similar to Method 2 only here, instead of the Hsu's shallow sea equation, the general wave equation (4.10) is used in combination with Hsu's equation (4.9) to calculate the Charnock parameter.

#### Method 4 Hsu Cov Shallow

- Similar to method 2 only here, instead of using IDW, Gibescu's method is applied for the spatial interpolation of wave height and wave period time series.

#### Method 5 Hsu Cov General

- Similar to Method 3 only here, instead of using IDW, Gibescu's method is applied for the spatial interpolation of wave height and wave period time series.

Given these characteristics it can be found that methods 2 to 5 are only applicable within the Dutch EEZ.

## 7.2 Stations

For the validation the AVDE model, use is made of validation stations. At these stations, wind speeds and wind directions are measured. On land, two locations have been selected which are the metmast in Cabauw and metmast-1 of the ECN wind turbine test field in Wieringermeer (EWTW). Since the Wind Atlas is mainly focused on the North Sea, nine offshore validation stations have been selected which are the metmast at the Offshore Wind farm Egmond aan Zee (OWEZ), the metmast FINO-1 and the sea stations Europlatform, K13- $\alpha$ , Meetpost Noordwijk, IJmuiden, LE Goeree, Vlakte vd Raan and Oosterschelde. The locations of these stations are indicated in figure 30.

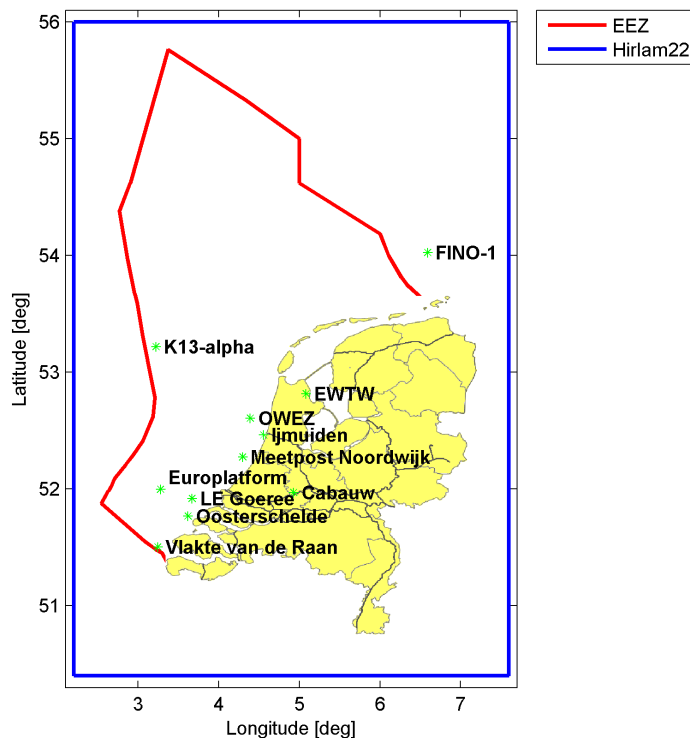


**Figure 30:** Location of validation stations.

As can be seen from this figure, most of the offshore locations are located in the south west corner of the EEZ, near the Dutch coast. Exceptions are station K13- $\alpha$ , located in the west part of the EEZ, and FINO-1 located in the north, outside the Dutch EEZ. Note that only for locations within the EEZ, all five methods described in the previous section will be compared.

### 7.3 Selection of time step

For all the time series calculated, the time step is set to one hour. This value has been chosen because the time resolution of most of the available data, Hirlam data as well as measured wave data and wind speed data, is already available with this time resolution. By keeping this time step for the Hirlam data equal to one hour, the amount of extra data created by time interpolations is minimal. Note that it was mentioned in section 5.2 that the time resolution of the Hirlam data is one hour for the lowest altitudes and three hours for the highest altitudes.

### 7.4 Basic analysis steps

For each of the validation stations a different amount of data is available. This is due to the fact that not all stations were present at the beginning of the Hirlam time series. Also, some stations have been removed or simply have no data available. For the analysis of the measured and calculated time series, however, some common subjects are presented and discussed:

- Specification of the measurement site
- Linear regression between measured and various calculated time series
- Comparison mean values
- Comparison Weibull distributions

In the specification of the measurement site a short description is given of the area surrounding the site. Also the available measurement data is indicated as well as an explanation why a certain part of the dataset is used.

The linear regression is used to find out if, on average, the prediction is equal to the measurements. In this report, a regression of the form  $Y = aX$  will be used where  $Y$  represents the calculated data,  $X$  the measured data and  $a$  the regression coefficient. From this regression coefficient three things can be derived: 1) It can be found if the calculated time series are generally underestimated or overestimated compared to the measured time series, 2) It can be used to locally adjust the calculated time series in order to find a better estimate, and 3) It can be used to find patterns in the deviation found for each station.

Mean values for the wind speed are given for each location for which the total time series are taken into account. The wind direction dependent averages have been calculated as well and are presented in appendices A and B. These, however, will not be discussed further in this report.

The comparison of Weibull distributions is used to find how much the calculated time series deviate from the measured time series. From the comparison it can be found if the calculated time series gives also a good estimate of the wind speed distribution. For this comparison, all wind directions will be taken into account unless stated otherwise. This means that only the distribution of the total length of the time series will be discussed, however, the direction dependent distributions have been calculated as well and the corresponding shape and scale parameters are presented in appendix A and B.

For each measurement site, the best applicable method will be found using the Root Mean Squared Error (RMSE) between the Weibull distribution derived from the measured time series and the Weibull distribution from the calculated time series. The RMSE is calculated with:

$$\hat{E} = \sqrt{\frac{1}{N} \sum_{i=1}^N (\mathbf{P}_{i,meas} - \mathbf{P}_{i,calc})^2} \quad (7.52)$$

where  $\hat{E}$  represents the RMSE,  $\mathbf{P}_{i,meas}$  the probability of occurrence of wind speed  $V_i$  given by the Weibull distribution derived from the measurements,  $\mathbf{P}_{i,calc}$  the probability of occurrence of wind speed  $V_i$  given by the Weibull distribution derived from the calculations and  $N$  the number of wind speeds taken into account. Note that  $\hat{E}$  is a scalar and  $\mathbf{P}_{i,meas}$  and  $\mathbf{P}_{i,calc}$  are vectors of length  $N$ . In the ideal situation where  $\mathbf{P}_{i,calc}$  is equal to  $\mathbf{P}_{i,meas}$  for every  $i$ , the RMSE is equal to zero. In reality, this does not happen therefore the method with the smallest value of the RMSE is selected as the best method. Using this approach, a comparison between the different methods is possible by comparing only the RMSE values. Since we want to know whether methods two to five are performing better than method one, it is counted how many times methods two to five are preferred above method one based on the found values of the RMSE for each method. In this analysis the parameters of the direction dependent Weibull distributions will be included in order to have a decent amount of data to base a conclusion on.

In the following chapters, the results for each location will be discussed, starting with the two land locations Cabauw and EWTW (chapter 8) followed by the sea locations OWEZ, FINO-1, Europlatform, K13- $\alpha$ , Meetpost Noordwijk, IJmuiden, LE Goeree, Vlakte vd Raan and Oosterschelde (chapter 9), where the first two are discussed separately and the other 7 are discussed simultaneously since for those stations only one measurement altitude is available. After the separate results have been discussed, a comparison will be made between the stations in order to find similarities followed by the selection of the best method. The validation part closes with a chapter dedicated to the conclusions of the validation.

## 8 Onshore Locations

In this chapter the results of the two land locations Cabauw and EWTW will be discussed. For Cabauw a complete overview will be given of the steps taken to find the results, for EWTW only the results will be discussed. Each section will start with a short description of the measurement site followed by the results of the linear regression. Then the found mean values are presented as well as the scale  $A$  and shape  $k$  parameters for the complete time series. The conclusions of this chapter will be presented in chapter 12.

### 8.1 Cabauw

In Cabauw a 213m high mast is placed which has been built specifically for meteorological research. The mast is part of the Cesar Observatory where Cesar stands for Cabauw Experimental Site for Atmospheric Research. With measurements taken at this location, research is done to find relations between the state of the atmosphere and the surface conditions. Also, the general weather situation in all seasons is part of the ongoing research.

In the vicinity of the mast, within 400m, the land is open pasture where in the west-south-west direction this extends to a distance of 2 km. Farther away, in the west sector, the landscape is generally very open while in the east sector it is rougher due to low houses, orchards and windbreaks. The north and south side are characterized by pasture and some windbreaks. Further more, within a 20 km radius of the mast, the surface elevation changes are at most a few meters. In addition, there are currently no plans to significantly change the landscape. The measurements taken are, after validation, stored in the Cesar Cabauw Database which is freely available for research purposes [8]. Some specifications of the site and data can be found in table 7.

**Table 7:** Specification measurement site Cabauw.

|                                   |                                  |
|-----------------------------------|----------------------------------|
| Location                          | Lon 4.926199°E , Lat 51.970242°N |
| Measurement Altitude(s)           | 10, 20, 40, 80, 140, 200 m       |
| Available period measurement data | 1 May 2000 - present             |
| Used period measurement data      | 8 June 2000 - 31 December 2009   |
| Source                            | CESAR Cabauw Database [8]        |

As can be seen there is a difference between the period in which data is available and the period that is used for the analysis. In this case, the difference is due to the fact that the amount of Hirlam data is the limiting factor. Since Cabauw is a location on land, only one method can be applied which is method one: Charnock.

#### ***Linear regression***

For each altitude a linear regression is applied between the measured data and calculated data of method one. In figure 31 the result is given for an altitude of 80 m. On the horizontal axis the measured wind speed can be found and on the vertical axis the calculated wind speed. For each value of the measured wind speed, there is a corresponding value of the calculated wind speed which are represented by the blue dots. The black line represents the ideal case where the calculated wind speed coincides with the measured wind speed. The red line shows the result of the regression. As can be seen for this case, the red line is just below the black line indicating that on average the calculated wind speed is over estimated compared to the measurements. The corresponding regression coefficient is found to be 0.996 which is very close to the optimum of one. In table 8 the regression coefficients are given for the other measurement altitudes as well.

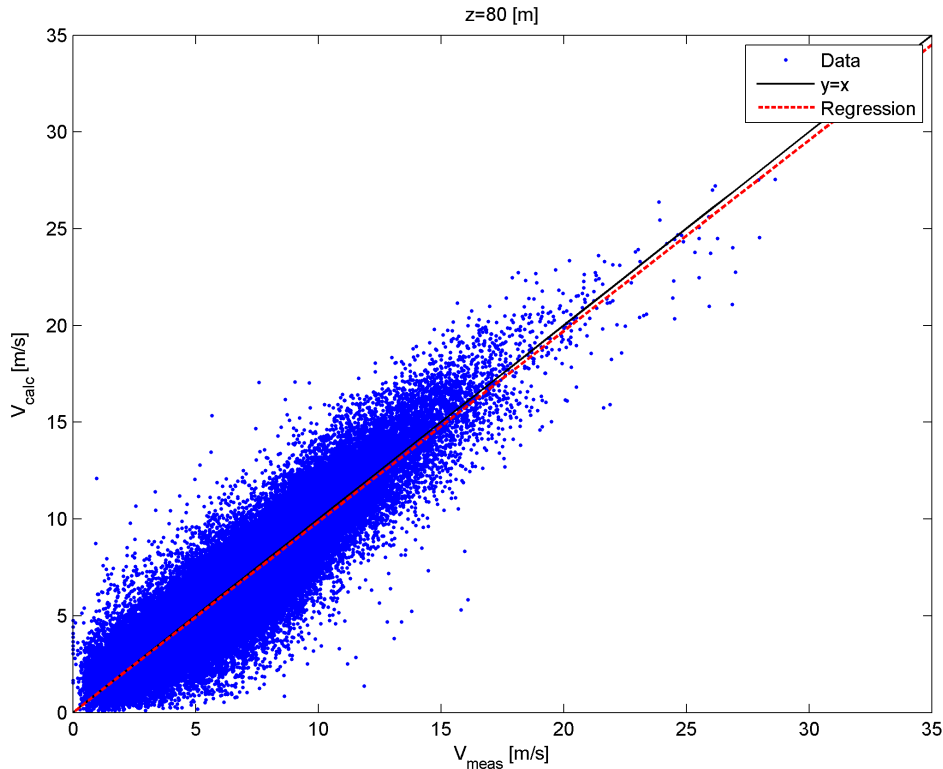


**Figure 31:** Scatterplot Measurement vs Method 1 Charnock, for Cabauw at 80 m height.

**Table 8:** Regression coefficients Cabauw.

| Height [m]         | 10    | 20    | 40    | 80    | 140   | 200   |
|--------------------|-------|-------|-------|-------|-------|-------|
| <b>1: Charnock</b> | 1.085 | 1.082 | 1.056 | 0.996 | 0.950 | 0.927 |

When looking closer to the found results of table 8, it can be seen that the regression coefficients are decreasing for increasing altitude. At an altitude of 77 m it can be expected that the regression coefficient is equal to 1. At this point, which is the turn over point, on average, the estimated time series of wind speeds is equal to the measured time series. Note that the error between the measured and calculated time series is between 8.5% and -7.3% where a positive number corresponds to an over estimation and a negative number corresponds to an under estimation.

### **Mean values**

The mean values found for Cabauw are presented in table 9. As is shown, for low altitudes, the average wind speed is low compared to the average wind speed at high altitudes. This is an expected result for both the measured and the calculated time series since the wind usually follows the shape of a logarithmic wind profile as presented in figure 5. The interesting part about this table is that it shows that for low altitudes the wind speed is over estimated and for high altitudes the wind speed is under estimated. The turn over point, where the predicted average wind speed is equal to the measured average wind speed, can be found at an altitude around 69 m.

**Table 9:** Mean wind speeds Cabauw.

| Height [m]         | 10   | 20   | 40   | 80   | 140  | 200  |
|--------------------|------|------|------|------|------|------|
| <b>Measurement</b> | 4.21 | 4.83 | 5.71 | 6.88 | 7.90 | 8.53 |
| <b>1:Charnock</b>  | 4.80 | 5.34 | 5.99 | 6.77 | 7.49 | 7.98 |

In order to find a confidence interval for the Wind Atlas, the map error is introduced. It is defined as the calculated mean wind speed minus the measured mean wind speed. In table 10 the results are presented. As can be seen, at 10 m altitude, the error is 0.59 m/s decreasing to -0.55 m/s for an altitude of 200 m.

**Table 10:** Map error Cabauw given in [m/s].

| Height [m] | 10   | 20   | 40   | 80    | 140   | 200   |
|------------|------|------|------|-------|-------|-------|
| 1:Charnock | 0.59 | 0.51 | 0.28 | -0.11 | -0.41 | -0.55 |

### ***Weibull distributions***

In figure 32 the Weibull distribution is given for the measured and calculated time series at an altitude of 80 m, including all wind directions. Two important observations can be made from this figure. Firstly, the top of the histogram of the calculated time series is shifted to the lower wind speeds. For wind speeds below 3 m/s and above 10 m/s the histograms are comparable. The second observation that can be made is that the fitted distributions do not show the same behavior as observed for the histograms. This is due to the type of fitting used where the focus of the fitting procedure is on the wind speeds above the mean wind speed as has been explained in section 6.2. For the other altitudes, similar observations can be made.

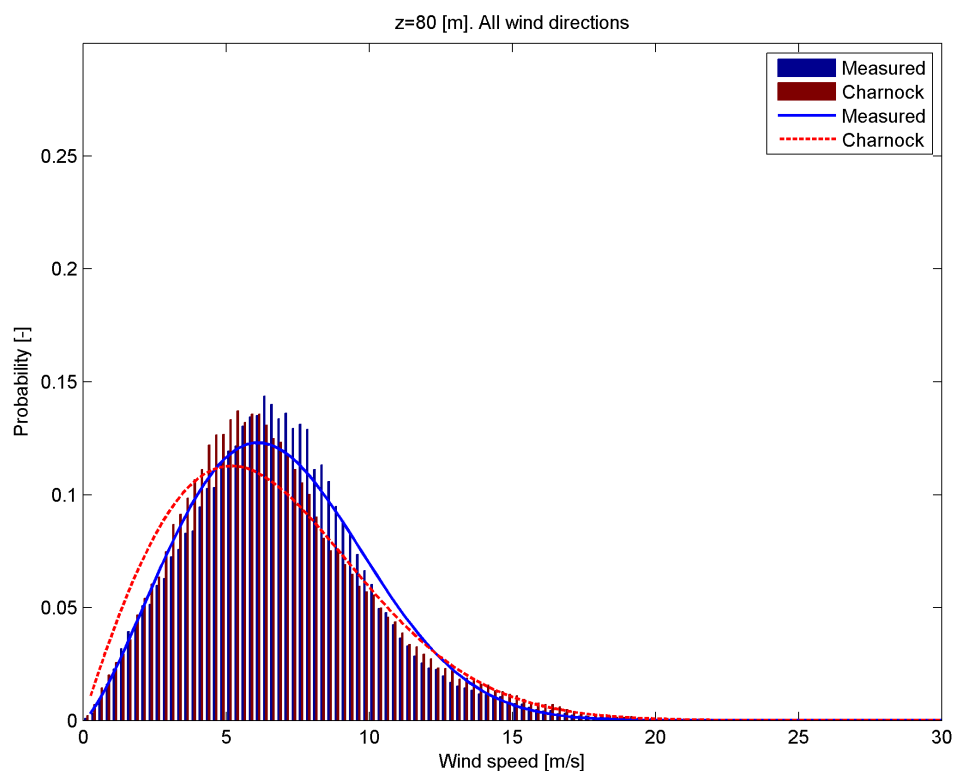


**Figure 32:** Weibull distribution of measured and calculated time series using method 1: Charnock, for Cabauw at 80 m height.

When observing the Weibull parameters of the various distributions given in table 11, it can be found that, for Cabauw, the scale parameter  $A$  is overestimated for altitudes below 70 m and underestimated for higher altitudes. As such, it shows the same behavior found for the mean values and regression analysis. For the shape parameter  $k$  given in table 12 the influence of the land can be found for the measured time series. Looking at  $k$  of the

distribution of the measured time series, it can be seen that for low altitudes  $k$  is small and below a value of 2, and for high altitudes,  $k$  is well above 2. As such, for high altitudes above land, the wind distribution is similar to the distributions found at offshore locations. This is expected behavior because the influence of the land surface roughness decreases with increasing altitude [31]. The values of  $k$  for the calculated time series show a steady but small increase with respect to height.

**Table 11:** Weibull scale parameter A Cabauw.

| Height [m]  | 10   | 20   | 40   | 80   | 140  | 200  |
|-------------|------|------|------|------|------|------|
| Measurement | 4.56 | 5.20 | 6.22 | 7.78 | 9.01 | 9.71 |
| 1:Charnock  | 5.30 | 5.85 | 6.56 | 7.48 | 8.33 | 8.90 |

**Table 12:** Weibull shape parameter k Cabauw.

| Height [m]  | 10   | 20   | 40   | 80   | 140  | 200  |
|-------------|------|------|------|------|------|------|
| Measurement | 1.63 | 1.70 | 1.91 | 2.33 | 2.41 | 2.28 |
| 1:Charnock  | 1.81 | 1.81 | 1.86 | 1.95 | 2.02 | 2.04 |

## 8.2 EWTW

Since June 2003 the first meteorological mast at the ECN Wind Turbine test station Wieringemeer (EWTW) is partly operational [12]. Changes have been made to the set-up of the mast which resulted in the fact that continues measurements at five different altitudes started beginning 2005. The mast is 109 m high and has measurement points at five altitudes as given in table 13. The mast is located in a polder 5 m below sea level. The surrounding area of the mast consists mainly of flat agricultural land. East from the mast there is a dike which is approximately 8 m high on the land side and 3 m high on the ‘sea’ side IJsselmeer. Relevant obstacles in the vicinity are a row of trees approximately 250 m west of the mast, some farmhouses and wind turbines at various locations. These wind turbines have a large influence on the wind direction sectors 60 and 300 degrees. Because this is a land location, only method 1: Charnock is included in the analysis.

**Table 13:** Specification measurement site EWTW. \*Measurements at 70 m stopped in June 2006

|                                   |   |
|-----------------------------------|---|
| Location                          | Lon 5.081069°E , Lat 52.816056°N                    |
| Measurement Altitude(s)           | 25, 45, 70, 85, 108 m                               |
| Available period measurement data | 1 January 2005 - present                            |
| Used period measurement data      | 1 January 2005 - 31 December 2009*                  |
| Source                            | EWTW Meteorological Database maintained by ECN [12] |

### *Linear regression*

In table 14 the regression coefficients are given for the location EWTW. Keeping in mind that values lower than one indicate an over estimation of the wind speed, it can be seen that for almost all altitudes, the wind speed is over estimated though very close to one for altitudes of 25 to 70 m. The altitude at which the regression coefficient is expected to be equal to one is 38 m which is lower than observed for Cabauw. In this case, the maximum over estimating error is found to be 0.7% and the maximum under estimating error is equal to -4.6%.

**Table 14:** Regression coefficients EWTW.

| Height [m] | 25    | 45    | 70    | 85    | 108   |
|------------|-------|-------|-------|-------|-------|
| 1:Charnock | 1.007 | 0.996 | 0.991 | 0.969 | 0.954 |

### **Mean values**

When the mean values given in table 15 are considered, it can be seen that up to an altitude of 70 m, the average wind speed is over estimated by the calculations. Here the turn over point is found to be 80 m which is much higher than the value found from the linear regression.

**Table 15:** Mean wind speeds EWTW.

| Height [m]  | 25   | 45   | 70   | 85   | 108  |
|-------------|------|------|------|------|------|
| Measurement | 5.39 | 6.68 | 7.07 | 7.55 | 8.01 |
| 1:Charnock  | 6.10 | 6.72 | 7.23 | 7.47 | 7.77 |

The map error is also calculated for this location, see table 16. Here it is found that the map error for an altitude of 25 m is 0.71 m/s. This is already larger than the value found for Cabauw at an altitude of 10 m. For the altitude of 108 m, the map error is -0.24 m/s. This is in the same order of magnitude that can be found for the Cabauw location at the same altitude.

**Table 16:** Map error EWTW given in m/s.

| Height [m] | 25   | 45   | 70   | 85    | 108   |
|------------|------|------|------|-------|-------|
| 1:Charnock | 0.71 | 0.04 | 0.16 | -0.08 | -0.24 |

### **Weibull distributions**

In tables 17 and 18 the shape and scale parameters of the various Weibull distributions are given. Again, the over and under estimations of the distributions of the calculated time series are visible in the scale parameter. When looking at the shape parameter, it can be seen that for altitudes above 70 m, the difference between the measured and calculated time series is small. For the lower altitudes on the other hand, the differences are larger, in these cases,  $k$  is overestimated by the model. Also note that, for the measured time series,  $k$  is already above 2 for the lowest altitude. This is due to the fact that EWTW is closer to the sea compared to Cabauw. As such, the influence of the wind coming from the sea is larger at lower altitudes.

**Table 17:** Weibull scale parameter  $A$  EWTW.

| Height [m]  | 25   | 45   | 70   | 85   | 108  |
|-------------|------|------|------|------|------|
| Measurement | 6.45 | 7.31 | 7.96 | 8.46 | 9.05 |
| 1:Charnock  | 6.80 | 7.50 | 8.10 | 8.37 | 8.73 |

**Table 18:** Weibull shape parameter  $k$  EWTW.

| Height [m]  | 25   | 45   | 70   | 85   | 108  |
|-------------|------|------|------|------|------|
| Measurement | 2.01 | 2.03 | 2.19 | 2.22 | 2.30 |
| 1:Charnock  | 2.13 | 2.18 | 2.24 | 2.26 | 2.29 |



## 9 Offshore Locations

In the previous chapter the results of the two onshore locations have been presented. In this chapter, the results of the offshore locations will be discussed. The analysis applied is equal to the analysis done for the two onshore locations. A full description can be found in chapter 7. In chapter 7, it was also indicated that there are 9 offshore locations. For two of these locations, OWEZ and FINO-1, measured time series are available for multiple heights. First an analysis of the OWEZ location will be done, in section 9.1, where all five calculation methods will be used. In section 9.2 the analysis for the FINO-1 location will be presented. Because this station is outside the Dutch EEZ, only one method will be used which is method 1. The remaining 7 stations, which are KNMI stations, will be discussed simultaneously in section 9.3. This is due to the fact that for all these locations only one time series is available which are all given as potential wind speeds.

### 9.1 OWEZ

In 2003 a measurement mast has been erected about 18 km from the Dutch coast at the same latitude of the city Egmond aan Zee. Measurements were taken as a preparation for the Offshore Windfarm Egmond aan Zee [27]. Noordzeewind, a joint venture of Shell and Nuon Duurzame Energie, is responsible for the development, construction and management of the wind farm. In order to gain more knowledge about offshore wind farms, an extensive measurement program has been set-up which focuses on ecology and technology. Wind measurements are therefore taken at the installed metmast. Some specifications of this mast can be found in table 19.

**Table 19:** Specification measurement site OWEZ.

|                                   |                                  |
|-----------------------------------|----------------------------------|
| Location                          | Lon 4.389639°E , Lat 52.606361°N |
| Measurement Altitude(s)           | 21, 70, 116 m                    |
| Available period measurement data | 1 July 2005 - present            |
| Used period measurement data      | 1 July 2005 - 31 December 2009   |
| Source                            | NoordzeeWind [40]                |

As mentioned, the mast is located about 18 km off shore. It can therefore be expected that the influence of land mass is not present. The influence of the wind turbines on the other hand are large [27]. In the wind direction sectors between 135 and 315 degrees the wind is undisturbed, in the other part the wind is disturbed by the wind farm. For this reason, only the undisturbed directions are included in this analysis. As a result of that, the measured and calculated average wind speeds are larger because the undisturbed directions coincide with the dominant wind directions, i.e. the occurrence of wind coming from the undisturbed directions is much higher than the occurrence of wind coming from the disturbed wind directions.

#### ***Linear regression***

In table 20 the regression coefficients can be found for the OWEZ location for the undisturbed wind directions. As can be seen in the table, the regression coefficients decrease for increasing altitude in accordance with the results found for Cabauw and EWTW. Again, for high altitudes, the wind speeds are generally under estimated. For this location the turn over point can be found between 90 and 110 m depending on the method used. In case of an over estimation it can be found that the maximum error is 9.9% which is found for method 1. Note that methods 3 and 5 have a much lower maximum error, in the order of 7.8%. On the side of the under estimation, it can be found that the error for methods 1, 2 and 4 is in the order of -0.6 to -0.2% while for methods 3 and 5 the error is larger, in the order of -1.6 to 1.3%.

**Table 20:** Regression coefficients OWEZ.

| Height [m]           | 21    | 70    | 116   |
|----------------------|-------|-------|-------|
| <b>1:Charnock</b>    | 1.099 | 1.027 | 0.998 |
| <b>2:Hsu IDW Sha</b> | 1.093 | 1.021 | 0.994 |
| <b>3:Hsu IDW Gen</b> | 1.073 | 1.009 | 0.984 |
| <b>4:Hsu Cov Sha</b> | 1.098 | 1.024 | 0.996 |
| <b>5:Hsu Cov Gen</b> | 1.078 | 1.013 | 0.987 |

**Mean values**

In table 21 the mean values are presented for the undisturbed wind speeds. As can be seen, the over estimation of the calculated average wind speeds, relative to the measured average wind speed, at low altitudes is quite large, in the order of 1 m/s. For the altitude of 116 m, also an over estimation can be found, this in contrast with the results from the linear regression where was found that for this altitude the wind speed is generally under estimated. The differences between the calculated means relative to the measured mean, on the other hand is small, in the order of 0.2 m/s as is shown in table 22. Here it can also be found that the mean wind speed is best predicted by method 3.

**Table 21:** Mean wind speeds OWEZ including only undisturbed wind directions.

| Height [m]           | 21   | 70    | 116   |
|----------------------|------|-------|-------|
| <b>Measurement</b>   | 8.64 | 9.79  | 10.31 |
| <b>1:Charnock</b>    | 9.73 | 10.26 | 10.52 |
| <b>2:Hsu IDW Sha</b> | 9.82 | 10.30 | 10.55 |
| <b>3:Hsu IDW Gen</b> | 9.64 | 10.18 | 10.45 |
| <b>4:Hsu Cov Sha</b> | 9.86 | 10.32 | 10.57 |
| <b>5:Hsu Cov Gen</b> | 9.68 | 10.21 | 10.48 |

**Table 22:** Map error OWEZ given in [m/s].

| Height [m]           | 21   | 70   | 116  |
|----------------------|------|------|------|
| <b>1:Charnock</b>    | 1.09 | 0.47 | 0.21 |
| <b>2:Hsu IDW Sha</b> | 1.18 | 0.51 | 0.24 |
| <b>3:Hsu IDW Gen</b> | 1.00 | 0.39 | 0.14 |
| <b>4:Hsu Cov Sha</b> | 1.22 | 0.53 | 0.26 |
| <b>5:Hsu Cov Gen</b> | 1.04 | 0.42 | 0.17 |

**Weibull distributions**

In tables 23 and 24 the Weibull scale and shape parameters are presented for the OWEZ location. The first remarkable thing that is visible looking at the shape parameter  $k$  from the measurements is that it is quite large for low altitudes and decreasing for increasing altitude. This contradicts the findings for all other locations where it is shown that  $k$  is increasing for increasing altitude, especially for the land locations Cabauw and EWTW this behavior is clearly visible. A reason that  $k$  is high for low altitude is because there is a very large fetch where the wind is undisturbed. When looking at  $k$  found for the various calculated time series, it can be seen that method 1 Charnock, does not show the behavior found for the measurements. The other methods, where the influence of the sea depth, wave height and wave period is included, clearly show estimates in line with the measurements. As such, the use of the sea depth and wave parameters have a large influence on the shape parameter of the Weibull distribution. From table 23 it can be found that the influence of the wave parameters and sea depth on the scale parameter is minimal.

**Table 23:** Weibull scale parameter A OWEZ.

| Height [m]           | 21    | 70    | 116   |
|----------------------|-------|-------|-------|
| <b>Measurement</b>   | 9.80  | 11.13 | 11.68 |
| <b>1:Charnock</b>    | 10.96 | 11.54 | 11.84 |
| <b>2:Hsu IDW Sha</b> | 11.08 | 11.62 | 11.89 |
| <b>3:Hsu IDW Gen</b> | 10.87 | 11.49 | 11.79 |
| <b>4:Hsu Cov Sha</b> | 11.12 | 11.65 | 11.91 |
| <b>5:Hsu Cov Gen</b> | 10.92 | 11.51 | 10.92 |

**Table 24:** Weibull shape parameter k OWEZ.

| Height [m]           | 21   | 70   | 116  |
|----------------------|------|------|------|
| <b>Measurement</b>   | 2.60 | 2.49 | 2.35 |
| <b>1:Charnock</b>    | 2.26 | 2.25 | 2.25 |
| <b>2:Hsu IDW Sha</b> | 2.54 | 2.40 | 2.37 |
| <b>3:Hsu IDW Gen</b> | 2.53 | 2.41 | 2.37 |
| <b>4:Hsu Cov Sha</b> | 2.52 | 2.40 | 2.36 |
| <b>5:Hsu Cov Gen</b> | 2.52 | 2.40 | 2.37 |

## 9.2 FINO-1

In the German part of the North Sea, about 50 km from the Dutch coast line, a measurement mast has been placed. The met mast is operated by Germanischer Lloyd (GL) and funded by the German Federal Ministry for the Environment, Nature Conservation and Nuclear Safety (BMU) represented by the Jülich Research Centre (Project Management Organization Jülich, PTJ). It has been designed and build specifically for meteorological and hydrological research to increase the knowledge of the interaction between the sea and the atmosphere and as preparation for various wind farms in the vicinity. The specifications of the mast are presented in table 25.

**Table 25:** Specification measurement site FINO-1.

|                                   |                                     |
|-----------------------------------|-------------------------------------|
| Location                          | Lon 6.590556°E , Lat 54.023889°N    |
| Measurement Altitude(s)           | 33.5, 40, 50, 60, 70, 80, 90, 100 m |
| Available period measurement data | 1 January 2004 - present            |
| Used period measurement data      | 1 January 2004 - 31 December 2009   |
| Source                            | FINO-database, DMU, PTJ [2]         |

The mast measures wind speeds at eight different altitudes between 33.5 and 100 m. Wind directions are measured between 33.5 and 90 m. The mast is placed in 30 m deep water and the closest landmass can be found approximately 45 km to the south of the mast. The nearest wind farm is Alpha Ventus for which the parts above sea level have been erected between June and November 2009. The influence of this wind farm on the measurements is therefore expected to be minimal. Unfortunately there is currently no sea depth information available for the area around this measurement station. For that reason, only method 1: Charnock is included in the analysis.

### ***Linear regression***

In table 26 the regression coefficients can be found for the location FINO-1. As can be seen, for every altitude, the wind speed is generally under predicted. As such, based on the available data, it is not possible to indicate at which altitude the under prediction turns to an over prediction. The found maximum of the under estimation error is -6.1%.

**Table 26:** Regression coefficients FINO-1.

| Height [m]        | 33.5  | 40    | 50    | 60    | 70    | 80    | 90    | 100   |
|-------------------|-------|-------|-------|-------|-------|-------|-------|-------|
| <b>1:Charnock</b> | 0.980 | 0.973 | 0.971 | 0.968 | 0.964 | 0.961 | 0.961 | 0.939 |

**Mean values**

Looking at the mean values given in table 27 it can be said that the averages from the calculations are very close to the averages found from the measurements. For an altitude of 100 m the absolute difference is 0.49 m/s while for the other altitudes the absolute difference is below 0.15 m/s which is a very good estimate. This in contrast with other stations where differences up to 2 m/s can be found. Although a turn over point was not found for the linear regression, it can be found from the average wind speed. The turn over point can be found at an altitude of 43 m. Relative to the other stations seen so far, this is low. For the other stations values between 70 and 90 m were found.

**Table 27:** Mean wind speeds FINO-1.

| Height [m]         | 33.5 | 40   | 50   | 60   | 70   | 80   | 90   | 100  |
|--------------------|------|------|------|------|------|------|------|------|
| <b>Measurement</b> | 8.68 | 8.84 | 9.02 | 9.26 | 9.37 | 9.49 | 9.57 | 9.99 |
| <b>1:Charnock</b>  | 8.73 | 8.85 | 9.00 | 9.13 | 9.24 | 9.34 | 9.42 | 9.50 |

In table 28 the map error is presented. As can be seen, between the altitudes of 60 and 90 m, the map error is only increasing slightly. For altitudes below 60 m, it can be seen that the map error is small, this in contradiction to the altitude of 100 m where the error is rather large compared to the other measurement altitudes. This might be caused by the type of measurement system used to measure the wind speeds. In the top of the FINO-1 metmast a sonic anemometer is used while at the other measurement points use is made of cup anemometers.

**Table 28:** Map error FINO-1 given in [m/s].

| Height [m]        | 33.5 | 40   | 50    | 60    | 70    | 80    | 90    | 100   |
|-------------------|------|------|-------|-------|-------|-------|-------|-------|
| <b>1:Charnock</b> | 0.05 | 0.01 | -0.02 | -0.13 | -0.13 | -0.15 | -0.15 | -0.49 |

**Weibull distributions**

In tables 29 and 30 the values are given for the found Weibull parameters. For the scale parameter the relative absolute differences are small, in the same order of magnitude as was found for the mean values. Also the found shape parameter for the measurements and calculations agree well with each other. As can be seen, the scale parameter of the calculated time series is not changing much with respect to the altitude, this in contradiction to the values found for the measurements. Also the behavior of high  $k$  values for low altitudes, as was found for the OWEZ location, is not observed here. The reason that it does not occur for this location might be because the fetch needed for this behavior is not long enough. In the wind direction where most wind is coming from, the fetch over water surface for the FINO location is approximately 70 km. For the OWEZ location, this distance is over 200 km long.

**Table 29:** Weibull scale parameter A FINO-1.

| Height [m]         | 33.5 | 40    | 50    | 60    | 70    | 80    | 90    | 100   |
|--------------------|------|-------|-------|-------|-------|-------|-------|-------|
| <b>Measurement</b> | 9.70 | 10.33 | 10.24 | 10.62 | 10.58 | 11.21 | 10.79 | 11.33 |
| <b>1:Charnock</b>  | 9.81 | 9.95  | 10.13 | 10.28 | 10.41 | 10.53 | 10.63 | 10.73 |

**Table 30:** Weibull shape parameter  $k$  FINO-1.

| Height [m]  | 33.5 | 40   | 50   | 60   | 70   | 80   | 90   | 100  |
|-------------|------|------|------|------|------|------|------|------|
| Measurement | 2.32 | 2.27 | 2.25 | 2.36 | 2.29 | 2.28 | 2.23 | 2.35 |
| 1:Charnock  | 2.21 | 2.21 | 2.22 | 2.23 | 2.24 | 2.25 | 2.26 | 2.26 |

### 9.3 KNMI Sea Stations

In this section the KNMI sea stations will be discussed simultaneously because they have three aspects in common. The first is already mentioned, which is that each station is part of the KNMI measurement network. Second reason is that for each station only one measurement altitude is available. And thirdly, all wind speeds are given in potential wind speeds.

Following the validation set up described in section 7.4, for each station a short description will be given of the location. This is followed by the discussion of the linear regressions, the mean wind speeds and the Weibull parameters  $A$  and  $k$ .

#### 9.3.1 KNMI sea station description

##### ***Europlatform***

Europlatform is a measurement platform which is located 60 km West of Hoek van Holland [49]. It is part of the measurement network of the Royal Dutch Meteorological Institute (KNMI) which also maintains the measurement data. In table 31 some specifications of the measurement site are given. The measured hourly averaged wind speeds and wind directions are freely available from the KNMI website [24]. Although the measurements are taken at a higher altitude, in this case 29.1 m, the wind speeds are stored as potential wind speed at an altitude of 10 m. The potential wind speed is the wind speed that has been corrected for nearby obstacles and local changes in the land use. Over sea, this potential wind speed is an estimate of the wind speed that could have been measured if measurements were taken at an altitude of 10 m above sea level with a roughness length  $z_0$  equal to 0.002 m. This implies that for the calculated time series, using methods 1 to 5, also the potential wind speeds have to be calculated. Since this transformation has already been implemented in the first version of the AVDE-model, it will not be further discussed. A complete explanation of the potential wind speed can be found in [51].

**Table 31:** Specification measurement site Europlatform.

|                                   |                                  |
|-----------------------------------|----------------------------------|
| Location                          | Lon 3.276388°E , Lat 51.998610°N |
| Measurement Altitude(s)           | 29.1 m                           |
| Available period measurement data | 1 July 1996 - present            |
| Used period measurement data      | 8 July 2001 - 31 December 2009   |
| Source                            | KNMI [24]                        |

##### ***K13- $\alpha$***

This site is an oil platform located approximately 100 km off shore, west northwest of Den Helder. The measurement data is maintained by KNMI so hourly averaged potential wind speeds are available where a  $z_0$  of 0.002 m is used [49]. Given the measurement height of 73.8 m, the platform itself does not significantly influence the measurements [49], the mast in which the measurement equipment is installed on the other hand, does have a significant influence. An over estimation of the wind speed due to the influence of the mast can be up to 8% depending on the wind direction. Information about the length of the available time series as well as some additional information about this measurement location can be found in table 32.

**Table 32:** Specification measurement site K13- $\alpha$ .

|                                   |                                  |
|-----------------------------------|----------------------------------|
| Location                          | Lon 3.219996°E , Lat 53.218334°N |
| Measurement Altitude(s)           | 73.8 m                           |
| Available period measurement data | 1 July 1996 - present            |
| Used period measurement data      | 8 July 2001 - 31 December 2009   |
| Source                            | KNMI [24]                        |

***Meetpost Noordwijk***

Meetpost Noordwijk is a platform located 10 km west of Noordwijk. Since this is also a station for which the measurements are maintained by KNMI, the hourly average wind speeds and wind directions are available, where the wind speed is given as a potential wind speed [24]. Besides the specification given in table 33 it can be mentioned that at this station also hydrological measurements take place. In July 2006 the station has been demolished making meteorological measurements no longer possible, the hydrological measurements on the other hand are still maintained.

**Table 33:** Specification measurement site Meetpost Noordwijk.

|                                   |                                  |
|-----------------------------------|----------------------------------|
| Location                          | Lon 4.296107°E , Lat 52.273892°N |
| Measurement Altitude(s)           | 27.6 m                           |
| Available period measurement data | 1 July 1996 - 5 July 2006        |
| Used period measurement data      | 8 July 2001 - 5 July 2006        |
| Source                            | KNMI [24]                        |

***IJmuiden***

The measurement location IJmuiden is located on a pier at IJmuiden. As such, it can be considered as a land location as well as a sea location. The measurements are taken at a height of 18.5 m which is a few meters above the dunes in the east. Since the measurements are also maintained by KNMI, hourly averaged potential wind speeds are available [51]. For calculating the potential wind speeds a surface roughness  $z_0$  of 0.03 m is used. In table 34 other specifications of measurement location IJmuiden are given.

**Table 34:** Specification measurement site IJmuiden.

|                                   |                                  |
|-----------------------------------|----------------------------------|
| Location                          | Lon 4.555437°E , Lat 52.462903°N |
| Measurement Altitude(s)           | 18.5 m                           |
| Available period measurement data | 1 January 1981 - present         |
| Used period measurement data      | 8 July 2001 - 31 December 2009   |
| Source                            | KNMI [24]                        |

***Licht Eiland Goeree***

Licht Eiland Goeree is located 30 km to the west of Maasvlakte, the entrance to the harbor of Rotterdam [49]. It is in use as a lighthouse where on top of it, in a mast, wind measurements are taking place. The distance between the top of the lighthouse and the measurement location is not very large, some influence of the lighthouse can therefore be expected. Also for this location the measurements are maintained by KNMI, hence again hourly averaged potential wind speeds are available. The used roughness parameter  $z_0$  is equal to 0.002 m. Other specifications of this location are given in table 35.

**Table 35:** Specification measurement site Licht Eiland Goeree.

|                                   |                                  |
|-----------------------------------|----------------------------------|
| Location                          | Lon 3.667220°E , Lat 51.918059°N |
| Measurement Altitude(s)           | 38.3 m                           |
| Available period measurement data | 1 January 1981 - present         |
| Used period measurement data      | 8 July 2001 - 31 December 2009   |
| Source                            | KNMI [24]                        |

***Vlakte van de Raan***

Compared to the other stations for which KNMI is maintaining the measurement data, Vlakte van de Raan is a very young measurement station. It is operational since 1 February 1997. The station is located near to entrance to the Westerschelde, about 2.4 km off shore south west of West Kapelle. Also for this station hourly averaged potential wind speed measurements are available for the time period as mentioned in tabel 36.

**Table 36:** Specification measurement site Vlakte van de Raan.

|                                   |                                  |
|-----------------------------------|----------------------------------|
| Location                          | Lon 3.241642°E , Lat 51.504616°N |
| Measurement Altitude(s)           | 16.5 m                           |
| Available period measurement data | 1 Februari 1997 - present        |
| Used period measurement data      | 8 July 2001 - 31 December 2009   |
| Source                            | KNMI [24]                        |

***Oosterschelde***

Oosterschelde is a measurement station in the North Sea located approximately 7 km from the Dutch shore north west of Nieuw Haarstede. Also for this station the measurements are maintained by KNMI thus hourly averaged potential wind speeds are available. Further specifications can be found in table 37.

**Table 37:** Specification measurement site Oosterschelde.

|                                   |                                  |
|-----------------------------------|----------------------------------|
| Location                          | Lon 3.617302°E , Lat 51.768566°N |
| Measurement Altitude(s)           | 16.5 m                           |
| Available period measurement data | 1 July 1982 - present            |
| Used period measurement data      | 8 July 2001 - 31 December 2009   |
| Source                            | KNMI [24]                        |

**9.3.2 Linear regression**

In table 38 the regression coefficients for the KNMI stations are given. For the stations Meetpost Noordwijk and Oosterschelde the regression shows that, on average, the predictions are very close to the measurements. The maximum deviation found is in the order of 2.5% which follows from the regression term minus one. For the other stations, the deviation is in the order of 4 to 8%. Further, it can be seen that for the stations Europlatform, K13- $\alpha$ , LE Goeree and Vlakte van de Raan, an under estimation occurs while for the stations Meetpost Noordwijk, IJmuiden and Oosterschelde an over estimation can be found.

**Table 38:** Regression coefficients KNMI stations.

| Station              | Europlatform | K13- $\alpha$ | Noordwijk | IJmuiden | LE Goeree | Vlakte vd Raan | Oosterschelde |
|----------------------|--------------|---------------|-----------|----------|-----------|----------------|---------------|
| <b>Height [m]</b>    | 29.1         | 73.8          | 27.6      | 18.5     | 38.3      | 16.5           | 16.5          |
| <b>1:Charnock</b>    | 0.942        | 0.929         | 1.024     | 1.078    | 0.943     | 0.967          | 1.016         |
| <b>2:Hsu IDW Sha</b> | 0.944        | 0.929         | 1.014     | 1.046    | 0.941     | 0.961          | 1.010         |
| <b>3:Hsu IDW Gen</b> | 0.931        | 0.917         | 0.998     | 1.043    | 0.928     | 0.955          | 0.996         |
| <b>4:Hsu Cov Sha</b> | 0.946        | 0.930         | 1.017     | 1.051    | 0.942     | 0.963          | 1.010         |
| <b>5:Hsu Cov Gen</b> | 0.933        | 0.918         | 1.001     | 1.047    | 0.930     | 0.957          | 0.997         |

### 9.3.3 Mean wind speed

Considering the average wind speeds given in table 39, it can be seen that for station Oosterschelde the average wind speed is best predicted by methods 1, 3 and 5. Looking at the other stations, it can be found that methods 2 and 4 always give a higher value than methods 3 and 5. The difference however is small with 0.1 m/s. Further, for station Europlatform, K13- $\alpha$ , LE Goeree and Vlakte van de Raan an under estimation of the average wind speed can be found while for the stations Meetpost Noordwijk and IJmuiden an over estimation is found. A curious thing to note is that for the cases where an under estimation occurs, stations Europlatform, K13- $\alpha$ , LE Goeree and Vlakte van de Raan, the estimation by methods 2 and 4 give a better estimate of the average wind speed. For the cases where over prediction occurs, station Meetpost Noordwijk and IJmuiden, it can be found that methods 3 and 5 give a better estimation of the average wind speed. This might indicate that there is an order in which the methods occur relative to each other. When the values found using methods 2 to 5 are sorted in ascending order, for most cases, the following order of the methods can be found: 3-5-2-4. Note that the measured value is either left or right of this order where left indicates an over prediction and right an under prediction. The position of method 1 in the mentioned order is changing per station, in most cases it can be found between methods 5 and 2.

**Table 39:** Mean wind speeds at KNMI stations.

| Station              | Europlatform | K13- $\alpha$ | Noordwijk | IJmuiden | LE Goeree | Vlakte vd Raan | Oosterschelde |
|----------------------|--------------|---------------|-----------|----------|-----------|----------------|---------------|
| <b>Height [m]</b>    | 29.1         | 73.8          | 27.6      | 18.5     | 38.3      | 16.5           | 16.5          |
| <b>Measurement</b>   | 7.67         | 8.01          | 7.18      | 6.48     | 7.52      | 7.34           | 6.95          |
| <b>1:Charnock</b>    | 7.15         | 7.38          | 7.29      | 7.30     | 7.02      | 7.07           | 6.95          |
| <b>2:Hsu IDW Sha</b> | 7.25         | 7.45          | 7.37      | 7.22     | 7.10      | 7.15           | 7.05          |
| <b>3:Hsu IDW Gen</b> | 7.16         | 7.36          | 7.25      | 7.20     | 7.01      | 7.10           | 6.95          |
| <b>4:Hsu Cov Sha</b> | 7.26         | 7.46          | 7.38      | 7.25     | 7.11      | 7.16           | 7.05          |
| <b>5:Hsu Cov Gen</b> | 7.16         | 7.36          | 7.26      | 7.22     | 7.01      | 7.11           | 6.95          |

In table 40 the map errors are presented for the KNMI stations. Here the largest errors can be found for the station IJmuiden with a maximum of 0.82 m/s using method 1. Note

that for almost all stations the map error found using method 1 is larger than the error found using methods 2 to 5. In the cases that the average wind speed is over estimated, it can be seen that methods 2 and 4 generally give a higher map error than methods 3 and 5. In the case of under estimation, this is the other way around.

**Table 40:** Map error KNMI stations given in [m/s].

| Station              | Europatform | K13- $\alpha$ | Noordwijk | IJmuiden | LE Goeree | Vlakte vd Raan | Oosterschelde |
|----------------------|-------------|---------------|-----------|----------|-----------|----------------|---------------|
| <b>Height [m]</b>    | 29.1        | 73.8          | 27.6      | 18.5     | 38.3      | 16.5           | 16.5          |
| <b>1:Charnock</b>    | -0.52       | -0.63         | 0.11      | 0.82     | -0.50     | -0.27          | 0.00          |
| <b>2:Hsu IDW Sha</b> | -0.42       | -0.56         | 0.19      | 0.74     | -0.42     | -0.19          | 0.10          |
| <b>3:Hsu IDW Gen</b> | -0.51       | -0.65         | 0.07      | 0.72     | -0.51     | -0.24          | 0.00          |
| <b>4:Hsu Cov Sha</b> | -0.41       | -0.55         | 0.20      | 0.77     | -0.41     | -0.18          | 0.10          |
| <b>5:Hsu Cov Gen</b> | -0.51       | -0.65         | 0.08      | 0.74     | -0.51     | -0.23          | 0.00          |

### 9.3.4 Weibull parameters

The Weibull parameters found for the KNMI stations are presented in tables 41 and 42. From the scale parameter, the same behavior can be found as was found for the mean wind speed. For the shape parameter, some notes have to be made. First one is about the  $k$ -values found from the measurements. Considering the fact that Noordwijk and IJmuiden are located near or at the coast, the found shape parameters from the measurements is low, even lower than would be expected on land. This is possible because for the calculation of the potential wind speed by KNMI, use is made of the reference surface roughness for land ( $z_0 = 0.03$ ) and not for sea ( $z_0 = 0.001$ ). For station K13- $\alpha$  the found value for  $k$  is relatively high, possibly because of tower interference at the measurement location. The second observation is that method 1 under estimates the shape parameter in all cases. Differences up to a maximum of 0.6 can be found while on average the difference is around 0.2. Further, it can be seen that the shape parameter predicted by methods 2 to 5 are closer to the values found from the measurements.

**Table 41:** Weibull scale parameter  $A$  for KNMI stations.

| Station              | Europatform | K13- $\alpha$ | Noordwijk | IJmuiden | LE Goeree | Vlakte vd Raan | Oosterschelde |
|----------------------|-------------|---------------|-----------|----------|-----------|----------------|---------------|
| <b>Height [m]</b>    | 29.1        | 73.8          | 27.6      | 18.5     | 38.3      | 16.5           | 16.5          |
| <b>Measurement</b>   | 8.88        | 9.45          | 7.88      | 7.49     | 8.60      | 8.22           | 7.81          |
| <b>1:Charnock</b>    | 8.04        | 8.29          | 8.16      | 8.11     | 7.88      | 7.97           | 7.84          |
| <b>2:Hsu IDW Sha</b> | 8.20        | 8.42          | 8.32      | 8.12     | 8.01      | 8.10           | 7.97          |
| <b>3:Hsu IDW Gen</b> | 8.08        | 8.31          | 8.29      | 8.09     | 7.90      | 8.04           | 7.85          |
| <b>4:Hsu Cov Sha</b> | 8.20        | 8.43          | 8.33      | 8.14     | 8.02      | 8.10           | 7.97          |
| <b>5:Hsu Cov Gen</b> | 8.09        | 8.32          | 8.20      | 8.11     | 7.91      | 8.04           | 7.85          |

**Table 42:** Weibull shape parameter  $k$  for KNMI stations.

| Station       | Europlatform | K13- $\alpha$ | Noordwijk | IJmuiden | LE Goeree | Vlakte vd Raan | Oosterschelde |
|---------------|--------------|---------------|-----------|----------|-----------|----------------|---------------|
| Height [m]    | 29.1         | 73.8          | 27.6      | 18.5     | 38.3      | 16.5           | 16.5          |
| Measurement   | 2.41         | 2.63          | 1.92      | 1.91     | 2.29      | 2.14           | 2.16          |
| 1:Charnock    | 2.02         | 2.07          | 1.90      | 1.80     | 1.99      | 2.07           | 2.02          |
| 2:Hsu IDW Sha | 2.16         | 2.24          | 2.12      | 2.00     | 2.16      | 2.28           | 2.22          |
| 3:Hsu IDW Gen | 2.17         | 2.24          | 2.13      | 2.00     | 2.16      | 2.27           | 2.21          |
| 4:Hsu Cov Sha | 2.16         | 2.23          | 2.10      | 1.98     | 2.15      | 2.27           | 2.22          |
| 5:Hsu Cov Gen | 2.16         | 2.23          | 2.11      | 1.98     | 2.15      | 2.26           | 2.21          |

In order to visualize the differences between the various methods, for stations Oosterschelde and K13- $\alpha$ , a plot will be given of the Weibull distribution of the measurements and methods 1 to 3. Methods 4 and 5 are not included because due to the small differences with methods 2 and 3, the graphs would overlap. In figure 33 the results are presented for the location Oosterschelde. Note that for this location the calculated mean wind speed was very close to the measured mean wind speed for all methods applied. As such, it can be expected that the Weibull distributions are also close to the distribution of the measurements. From visual inspection, however, it seems that the distributions of methods 2 and 3 are closer to the measurements than method 1. This can also be found in the tables 41 and 42, where it can be seen that the shape parameter of method 1 for Oosterschelde is considerably lower than the values found for the measurements and methods 2 to 5. Note that the values of the shape parameter of methods 2 to 5 are closer to the results of the measurement than the value of the shape parameter of method 1.

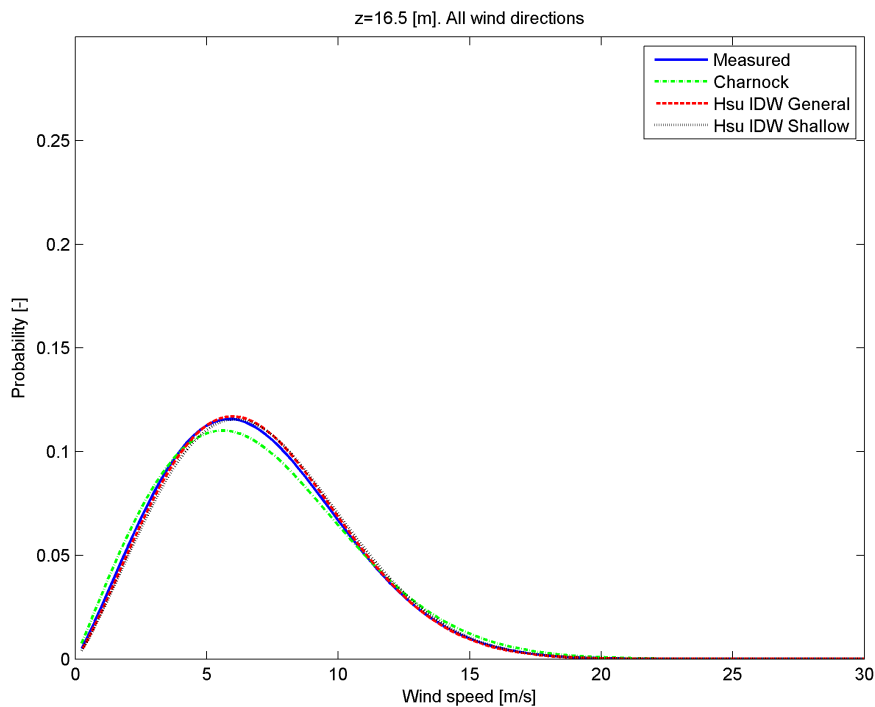


**Figure 33:** Weibull distributions of measurements and methods 1 to 3 for Oosterschelde.

In figure 34 the Weibull distributions are given for the measurements and methods 1 to 3 for station K13- $\alpha$ . For this location, the map error of the mean wind is in the order of -0.6 m/s which is considerably larger than for the Oosterschelde location. As such, a difference between calculated and measured Weibull distribution can be expected. In figure 34, it can be seen that this is true, the peak of the Weibull distribution of methods 1 to 3 are shifted to the left compared to the measurements. Note however, that methods 1 to 3 are close together which is the result of using the same data source, i.e. Hirlam data. Apparently, adding the wave data to the calculations, has a larger influence on the position of the peak of the Weibull distribution, indicated by the value of the shape parameter, than on the value of the scale parameter.

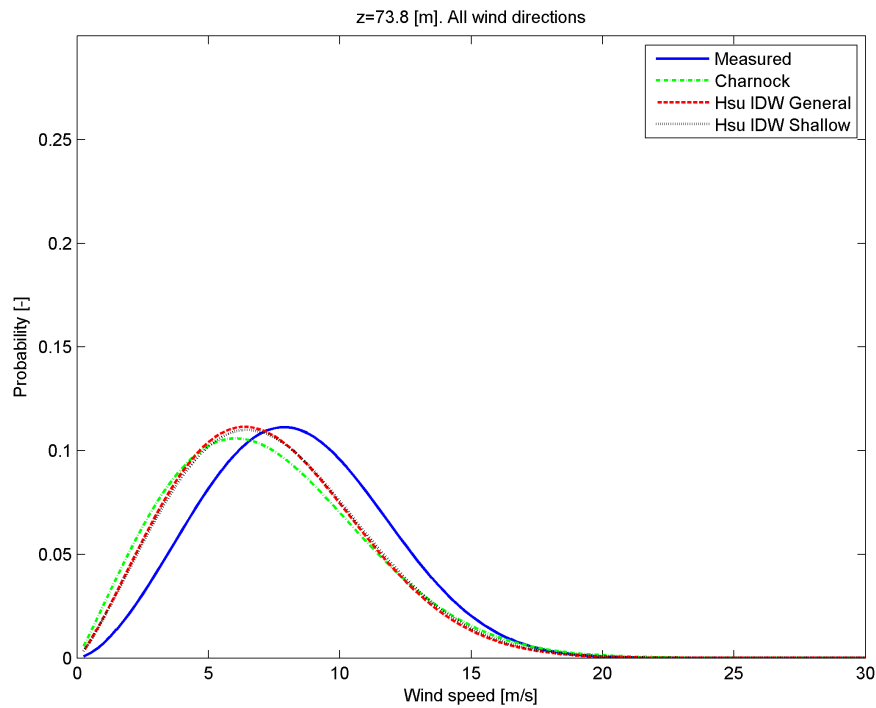


**Figure 34:** Weibull distributions of measurements and methods 1 to 3 for K13- $\alpha$ .



## 10 Comparison of stations

In this section the focus will be on the comparison of the various validation stations. Two questions that need to be answered in this section are:

- What are the commonalities between the locations?
- What is the effect of these on the results of the Wind Atlas?

These questions will be answered in the following subsections. The found turn over points for the four stations, where measurements are available for multiple heights, are discussed followed by a discussion about the map error. The order found for the use of the methods which occurs for all sea stations located in the Dutch EEZ will be presented and last item that will be discussed here is the influence of the method on the shape parameter of the distribution.

### 10.1 Turn over point

As was presented in chapters 8 and 9, there are four stations for which multiple measurement altitudes were available. A common item that occurs for each of these stations is the existence of a turn over point where the estimated average wind speed is equal to the average measured wind speed. For each altitude, however, a different altitude was found for which this occurs as is shown in table 43. Looking only at the altitudes of the turn over point found from the measurements and the calculations using method 1, Charnock, it seems that going west to east, the altitude of the turn over point decreases. When looking from north to south, there is no clear indication of a 'pattern'. Note however that these observations are based on only four points located in a rather large area. As such, it might be that the found pattern of decreasing turn over altitude, going from east to west, is only valid for these four locations. More measurement locations should be included in order to find if this assumption holds.

**Table 43:** Turn over points calculated from the average wind speed of measurements and calculations using method 1 Charnock, at stations with multiple measurement heights.

| Location | Longitude [deg] | Latitude [deg] | Turn over point [m] |
|----------|-----------------|----------------|---------------------|
| Cabauw   | 4.926199        | 51.970242      | 69                  |
| EWTW     | 5.081069        | 52.816056      | 80                  |
| OWEZ     | 4.389639        | 52.606361      | 153                 |
| FINO-1   | 6.590556        | 54.023889      | 43                  |

The consequences of the found result for the Offshore Wind Atlas is that found time series can be adjusted to give a better match of the measurements.

### 10.2 Map error

The map errors found for the different locations can be placed in two groups. The first group consists of the errors found at the KNMI stations for which the potential wind speed has been calculated. The second group consists of the errors found for the stations where measurements were available for multiple altitudes, Cabauw, EWTW, FINO-1 and OWEZ. For both of these groups an average error will be derived including a confidence interval. Note that the results for group one only apply to the cases where the potential wind speed is used. For group two the error will be derived for various altitude groups.

Starting with group one. In table 40 the map errors are given for all the KNMI stations. It is assumed that these errors are part of a normal distribution. Based on this assumption,

an average error and standard deviation can be found as well as a confidence interval. For each used calculation method, methods 1 to 5, a sample mean  $\mu_s$  and standard deviation  $\sigma_s$  have been found which are presented in table 44. When the five methods are compared, it can be seen that method 4 has a sample mean closest to zero and method 2 has the smallest sample variance. As such, these two methods perform better than method 1. Methods 3 and 5 do not perform better than the other methods although they have a smaller variance than method 1, the sample mean is slightly larger. Since it was assumed that the mean map error is normally distributed, a 90% confidence interval  $c_{90}$  for the population mean of the map error can be found as well. This interval is given in table 44 as well. For example, for method 1, the interval is  $-0.14 \pm 0.77$  which means that in 90% of the area of the wind map, the error with the measured wind speed is between -0.91 and 0.63 m/s.

**Table 44:** Sample mean  $\mu_s$  and variance  $\sigma_s$  of the map error for potential wind speeds.

| Method        | $\mu_s$ [m/s] | $\sigma_s$ [m/s] | $c_{90}$ [m/s]   |
|---------------|---------------|------------------|------------------|
| 1:Charnock    | -0.14         | 0.47             | $-0.14 \pm 0.77$ |
| 2:Hsu IDW Sha | -0.08         | 0.42             | $-0.08 \pm 0.70$ |
| 3:Hsu IDW Gen | -0.16         | 0.44             | $-0.16 \pm 0.72$ |
| 4:Hsu Cov Sha | -0.07         | 0.43             | $-0.07 \pm 0.70$ |
| 5:Hsu Cov Gen | -0.15         | 0.44             | $-0.15 \pm 0.73$ |

For group two, the errors have been found for various altitudes. Note that only for one of the four stations it was possible to use all methods. For this reason, this analysis will only focus on method 1 Charnock. In figure 35 the map error is presented relative to the measurement height. An exponential fit is added to show the trend in the graph. As can be seen, there is a very clear relation between the height and the map error. As such, it does not make sense to find an average map error valid for all altitudes. On the other hand, the data available is not enough to give an estimate of the map error at every given altitude. For this reason, three altitude groups are made: 10-50 m, 50-100 m and 100-200 m. For each of these groups the average map error is calculated as well as the variance and the 90% confidence interval. The results are presented in table 45. Note that the first group does not start at zero altitude. This is because at this altitude the wind speed is equal to zero for both the calculated as the measured wind profiles and thus the error is equal to zero. Since it is unknown how the error behaves between 0 and 10 m altitude and wind speed measurements are usually taken from 10 m and higher, the lower value of the first group is set to 10 m.

From table 45 it can be seen that the mean map error is small for the group of 50-100 m. Note that from the regression and mean wind speeds it was found that in this region the turn over point is located. It could therefore be expected that the average map error in this group would be the closest to zero compared to the other groups. For the first group, 10-50 m an average map error of 0.36 m/s was found which corresponds to an over estimation as was found for the regressions and mean wind speeds. A similar observation can be made for the third group, 100-200 m, where an average map error of -0.25 m/s is found which corresponds to an under estimation as was found for the regressions and mean wind speeds as well.

The found values for the standard deviation of the map error for all altitude groups are lower than was found for the case of potential wind speeds. This can be due to various reasons. Most important one is that the samples are small. As such the effect of a location where the errors are large, for instance for the first group where stations IJmuiden and K13- $\alpha$  have relatively high values for the map error compared to the other stations, the influence on the mean map error and the standard deviation is significant. For a better estimation of the map error for the potential wind speed as well as for the true wind speed,

more measurement data should be included at more locations.

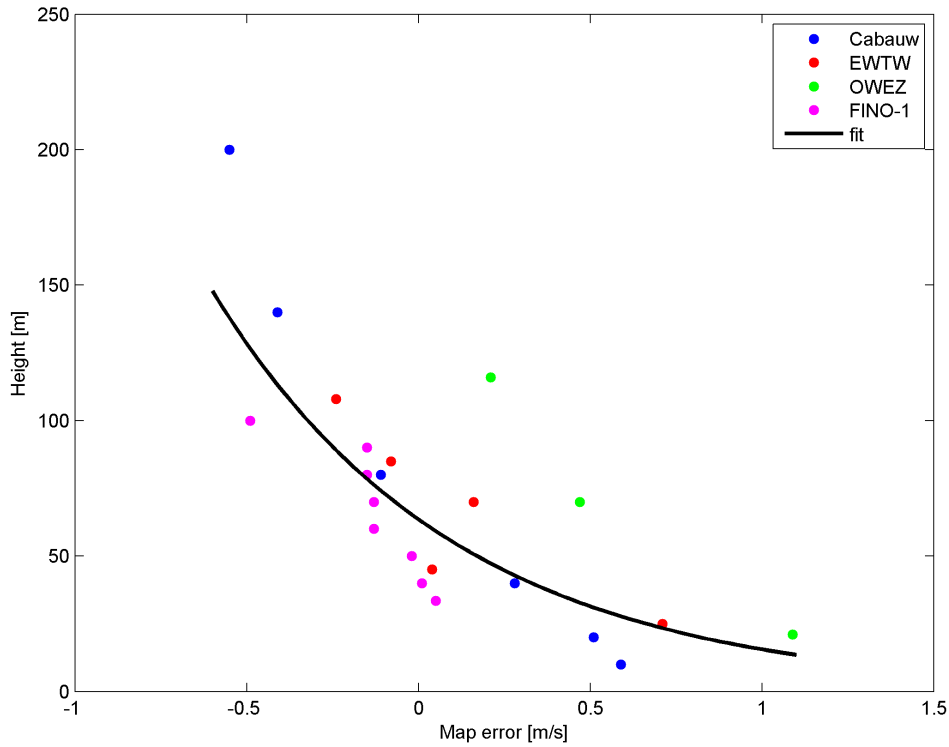


**Figure 35:** Map error versus height for true wind speed found using method 1 Charnock.

**Table 45:** Sample mean and variance of the map error for true wind speed for three different altitude groups based on results of method 1 Charnock.

| Group     | $\mu_s$ [m/s] | $\sigma_s$ [m/s] | $c_{90}$ [m/s]   |
|-----------|---------------|------------------|------------------|
| 10-50 m   | 0.36          | 0.39             | $0.36 \pm 0.64$  |
| 50-100 m  | -0.07         | 0.26             | $-0.07 \pm 0.43$ |
| 100-200 m | -0.25         | 0.33             | $-0.25 \pm 0.54$ |

### 10.3 Order in methods

Another commonality between the station is that for the KNMI station it was found that the methods 2 to 5, all variants using Hsu's equation, appear in a given order relative to each other looking at the mean wind speed. The order in which the methods occur, from low to high mean wind speed, is 3-5-2-4, in table 46 the different methods are given. When looking at the mean wind speeds calculated for the location OWEZ, the same behavior can be found.

**Table 46:** Used calculation methods.

| nr | Name        |
|----|-------------|
| 1  | Charnock    |
| 2  | Hsu IDW Sha |
| 3  | Hsu IDW Gen |
| 4  | Hsu Cov Sha |
| 5  | Hsu Cov Gen |

The positions of the mean wind speed from the measured and calculated time series using method 1, Charnock, are different for each station but again a commonality can be indicated. Where an over estimation occurs, the mean wind speed from the measured time series is left of method 3, while when an under estimation occurs, the mean wind speed from the measured time series is located right of method 4, it is then larger than all estimated mean wind speeds using the different methods of Hsu. The placement of method 1 is very irregular, no clear pattern could be found with respect to the other calculation methods or the measurements. Note that methods 3 and 5 make use of the general wave equation while 2 and 4 use the approximation of the shallow sea. It appears that, using the shallow sea equations, a higher estimation is found with respect to the methods where the general wave equation is used. When looking at the difference between the use of IDW and Gibescu's method for the interpolation of the wave height and wave period, it can be seen that the method where IDW is applied, numbers 2 and 3, always come first relative to the method where Gibescu's interpolation method is applied i.e. method 3 before 5 and method 2 before 4. The reason that this order occurs can be found in the used calculation methods. As was found from the validation of the spatial interpolation methods (subsection 4.6), using IDW would give a slightly higher estimate of the Charnock parameter, and thus the surface roughness, compared to the use of Gibescu's method. Knowing that the surface roughness has a large influence on the shape of the wind profile, and that a higher value of the surface roughness gives a lower wind speed at a given height (see figure 5), it can be expected that methods 2 and 3, where IDW is applied, give a lower average wind speed compared to methods 4 and 5 where use is made of Gibescu's spatial interpolation method.

#### 10.4 Influence of method on shape parameter

When looking at the shape parameter of the Weibull distributions, it can be seen that Method 1: Charnock gives a shape parameter which is generally lower than the shape parameter as was found for the measurements. When using methods 2 to 5, the shape parameter is better estimated which can be related to the use of the equation of Hsu for the sea surface roughness. Especially for the validation station OWEZ, where three heights were analyzed, the shape parameter was well estimated for all heights using methods 2 to 5. For method 1, it was shown that the shape parameter was not well estimated.

Now reconsider the Weibull parameters of station Oosterschelde given in tables 41 and 42. Here the scale parameter is best estimated by method 1, where there is only a difference of 0.03 m/s with the value found for the measurements, followed by methods 3 and 5, where the difference is only slightly larger with 0.04 m/s. Now comparing the shape parameter, it can be seen that using method 1 gives an error of 0.14 with respect to the measurements, while methods 3 and 5 both give an error of 0.05 which is considerable lower and thus better. So, this example clearly shows that the introduction of Hsu's equation mainly effects the shape parameter and only has a small influence on the scale parameter.

## 11 Selection of method

For the selection of the best applicable method, the root mean squared error is calculated between the Weibull distribution of the measurements and the Weibull distributions from the five different calculation methods. Based on these Weibull shape and scale parameters a distribution is constructed for wind speeds between 3 and 25 m/s. The reason for selecting these two values is because they coincide with the cut-in and cut-out wind speeds of a standard wind turbine. The stations which are used in this analysis are the KNMI stations and the OWEZ location for which only the undisturbed wind directions are included.

In order to have a large enough sample, the direction dependent Weibull distributions are included for the cases where the wind speed can be considered to be undisturbed. This means that for most stations 13 different distributions can be created for each method, 12 directional dependent distributions and one of the total time series. Only for the OWEZ location 7 distributions are constructed because 6 wind direction sectors are located in the wake of the wind farm. This gives a total of 112 distributions per method. Note that equation (7.52) is used for this comparison.

Because the goal is to find out which method performs best with respect to the original method, which is method 1, it is counted how many times methods 2 to 5 are preferred above method 1. This means that the methods are compared in pairs of two of which one is method 1. Note that the method with the lowest value for the RMSE is preferred.

In table 47 the results are presented where the fractions are given which indicate how many times a method is preferred above the original method. As can be seen from this table, the preference is different for each station but in half of the cases well above 70.0%. Between the four methods presented, there are small differences but based on the findings of table 47 it can be said that method 2 is the method that performs best.

**Table 47:** Results of the RMSE analysis for the selection of the best method, where the fraction, given in [%], indicates how many times a method is preferred above the use of method 1:Charnock.

| Station            | Method 2    | Method 3    | Method 4    | Method 5    |
|--------------------|-------------|-------------|-------------|-------------|
|                    | Hsu IDW Sha | Hsu IDW Gen | Hsu Cov Sha | Hsu Cov Gen |
| Europlatform       | 84.6        | 61.5        | 92.3        | 61.5        |
| K13- $\alpha$      | 100.0       | 69.2        | 100.0       | 69.2        |
| OWEZ 116 [m]       | 85.7        | 85.7        | 85.7        | 85.7        |
| OWEZ 70 [m]        | 85.7        | 85.7        | 85.7        | 85.7        |
| OWEZ 21 [m]        | 71.4        | 85.7        | 42.9        | 85.7        |
| Ijmuiden           | 61.5        | 61.5        | 61.5        | 61.5        |
| LE Goeree          | 69.2        | 53.8        | 69.2        | 53.8        |
| Noordwijk          | 46.2        | 61.5        | 53.8        | 61.5        |
| Oosterschelde      | 76.9        | 76.9        | 76.9        | 76.9        |
| Vlakte van de Raan | 61.5        | 53.8        | 61.5        | 53.8        |
| Average            | 74.3        | 69.6        | 73.0        | 69.6        |



## 12 Conclusions Validation AVDE model

In this section the conclusions will be given of the validation of the AVDE-model. The results of five different methods for 11 validation stations have been compared to measurements. There were two land locations, Cabauw and EWTW, with multiple measurement altitudes and nine offshore locations. Two of these offshore locations, FINO-1 and OWEZ, have measurements available on multiple altitudes where for the other seven offshore stations of KNMI only one measurement altitude was available. In addition, FINO-1 was located outside the Dutch EEZ.

There were three common subjects that were discussed for each station:

- Linear regression between measured and various calculated time series
- Comparison of mean wind speeds
- Comparison of Weibull distributions

The conclusions for these three subjects will be discussed. This will be followed by the conclusions found from the comparison between the stations as well as the selection of the best method.

For all cases a regression has been applied between the measured and calculated time series where only wind speeds above 4 m/s were taken into account. For the four locations FINO-1, OWEZ, EWTW and Cabauw, it was found that there is a certain altitude at which an under estimation turns into an over estimation. The altitude at which this occurs is the so called turn over point. Going from west to east, it was found that the altitude of the turn over point was rapidly decreasing. Note however that this observation is based on only four points in a rather large area. As such, the correctness of this observation should be checked which can be done by adding additional observation points for which measurements are available at multiple altitudes.

In the comparison of the mean wind speeds, also the existence of the turn over point could be indicated. For most of the considered stations, where it was possible to use all five methods, it was found that the calculated mean wind speed using method 1 Charnock was not the best estimate compared to the use of methods 2 to 5. This could also be found by looking at the map error.

For the determination of the map error, the validation stations were grouped into two groups. The first group consisted of the KNMI stations where the potential wind speeds were calculated and compared. The second group consisted of the stations for which multiple altitudes were analyzed. For the first group it was found that the mean of the map error for method 1, based on a sample of seven stations, is equal to -0.14 m/s with a standard deviation of 0.47 m/s. For methods 3 and 5 the mean map error was slightly larger, -0.16 and -0.15 m/s, respectively. For methods 2 and 4, the mean map error was lower with -0.08 and -0.07 m/s respectively. The standard deviations of methods 2 to 5 were all smaller, in the range of 0.42 to 0.44 m/s. Note that the differences of the map error between the methods are very small and that adding or removing one station of the sample has a large influence on the calculated map error.

For the second group, three altitude groups have been made for which the mean and standard deviation of the map error were calculated. Here only use was made of method 1 Charnock because only for one station in this group it was possible to use all five methods. For the altitude group between 10 and 50 m, a mean map error of 0.36 m/s was found with standard deviation of 0.39 m/s. Note that the positive value of the mean indicates that, generally, the map gives a higher value of the mean wind speed than the mean wind speed calculated from the measurements. The results of the second group, between 50 and 100 m, are -0.07 m/s for the mean map error and 0.26 m/s for the standard deviation. Note that

this group contains the turn over point which results in a low mean map error. For the last group with altitudes between 100 and 200 m, the mean map error is -0.25 m/s and the standard deviation is 0.33 m/s. Note that these results are in agreement with the results of the analysis of the mean wind speed an regression plots.

For the Weibull distributions it was found that the scale parameter calculated using methods 1 to 5 is usually in the same order of magnitude. There are some differences though, with the scale parameter of the measured time series which is due to over an under estimations as was found for the mean wind speed and regression plots. Further, the shape parameter predicted by method 1 is usually lower than the shape parameter found for the measurements. Methods 2 to 5, however, show a better estimate of the shape parameter which is higher than was found using method 1 but closer to the value of the measurements. It appears that using Hsu's equation mainly influences the shape parameter of the Weibull distribution.

In order to select the best method, the root mean squared error (RMSE) is calculated between the Weibull distribution of the measured time series and a calculated time series from methods 1 to 5. Then, for methods 2 to 5, it was counted how many times a method was preferred above method 1 based on the value of the RMSE, i.e., if the RMSE of method 2 was lower than the RMSE of method 1, than method 2 was preferred above method 1. From this analysis it was found that in 74.3% of the cases method 2 was performing better than method 1. On second place, method 4 was preferred in 73.0% of the cases followed by methods 3 and 5 with both a value of 69.6%. For this reason, method 2, Hsu's equation for shallow sea with IDW of the wave data, has been selected for the creation of the Wind Atlas. Note however that differences are small but in all types of analysis used, regression, mean wind speed comparison and Weibull analysis, in most cases it was found that method 2 was performing better compared to the other methods.

Part III

## Wind Atlas



## 13 Set up Calculations Offshore Wind Atlas

In this chapter an explanation is given about the construction of the Offshore Wind Atlas which includes the Dutch Exclusive Economic Zone (EEZ), the Netherlands and small parts of Belgium and Germany. The input parameters will be selected and the consequences of these selections will be discussed. But first a short explanation will be given of what a Wind Atlas is.

A Wind Atlas is a collection of wind data which gives a summary of the wind climate for a given period and given area. The contents are usually the average wind speeds, Weibull shape and scale parameters and reference wind speeds given at several altitudes. Results are usually presented in the form of wind maps which show the distribution of the calculated parameters over a given area.

In part I of this report, the AVDE-model has been described. As mentioned in chapter 3, several input parameters concerning the locations of interest and the Hirlam data have to be given. In section 13.1 the selected grid will be discussed as well as the selected time period because these are closely related. Also the methods used to calculate the wind speeds will be discussed as well as a way to compare results to other wind maps, sections 13.2 respectively section 13.3. In the last section of this chapter, the contents of the new Offshore Wind Atlas will be described.

### 13.1 Grid size and Time period

As presented in subsection 3.2.2 there are six different Hirlam files that can be used as input to the AVDE-model. At ECN only three of these types are available covering two different parts of the Netherlands and surrounding area as presented by figure 4 which is repeated below.

Since it is important to cover the Netherlands as well as the entire EEZ, the largest domain, which is the Hirlam22 domain, will be selected. This immediately puts constraints on the time period that can be included in the calculations. As given in subsection 3.2.2, the time period available for the lower part of this area, where the two domains overlap, is from June 2001 until the end of October 2010. For the other part of the Hirlam22 domain, data is available from 19 November 2003 until the end of October 2010. By using different lengths of time series, errors are introduced which can be visible near the boundaries where the Hirlam55 domain changes to the Hirlam22 domain which is around the latitude of  $54^\circ$ . Because this is unwanted, the time series is shortened which results in the fact that only data is used after 19 November 2003. This also implies that only Hirlam22 files are used for the Wind Atlas. In addition, the wave data is only available until the end of March 2010. In order to make a valid comparison, the time series calculated using different methods should be equal. As such, the selected period for the Wind Atlas is from 19 November 2003 until the end of March 2010.

The spatial resolution of the Wind Atlas is mainly determined by the calculation time. This is due to the fact that for each given point, given by a longitude, latitude and altitude, a time series has to be calculated from which the Weibull parameters and average wind speeds can be derived. Although several attempts have been made to speed up the calculation process of the time series, it appeared to be not possible to reduce the calculation time of one time series to get below 20 to 25 minutes, given the time frame of the thesis work. The advantage of the Wind Atlas, however, is that calculations of time series take place per location. As such, several grid resolutions were chosen which have overlapping grid points. Calculations started at a resolution of  $0.8^\circ$ , which is roughly 88 km, followed by calculations with a resolution of  $0.4^\circ$ , 44 km, and  $0.2^\circ$  or 22 km which was the high-

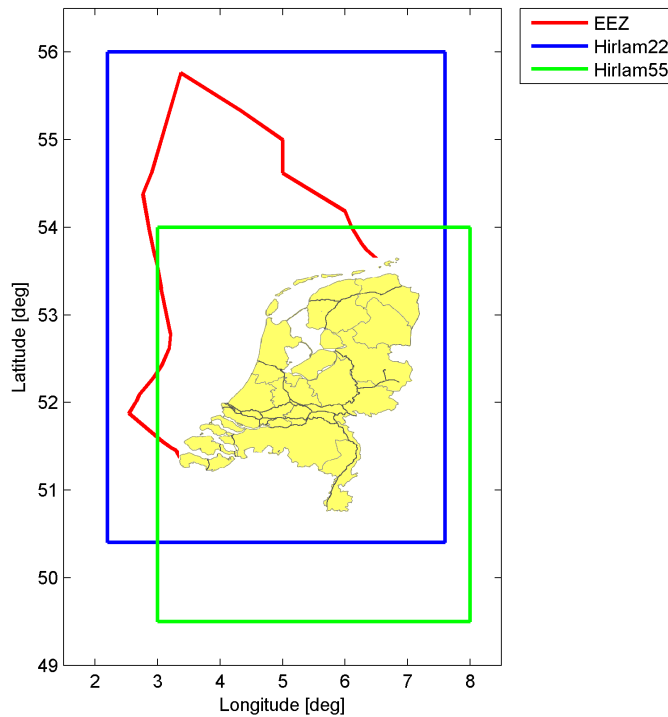


**Figure 4:** Overview area covered by Hirlam files (repeated).

est resolution achievable within the given time frame of the thesis work. By decreasing the resolution in this way, the time series calculated at the coarser grids could be used, reducing the calculation time while making intermediate results possible.

As mentioned in subsection 3.1 three altitudes were given for which the Wind Atlas would be created. These heights are 40, 90 and 140 m, where 90 m is the average hub height of a wind turbine. Based on the assumption that a wind turbine blade has a length of 50 m and anticipating other hub heights, the upper and lower values are selected.

## 13.2 Used Methods

From the validation of the results at 11 measurement stations, it was found which of the 5 described methods is best to use. In more than 74.3% of the considered cases, method 2: Hsu's equation for shallow sea with Inverse Distance Weighting of the wave data is preferred above the use of method 1: Charnock, where a constant value for the sea surface roughness is used. Because method 2 is only applicable in the Dutch EEZ, due to the lack of sea depth data in the other parts of the sea, only results for this area will be given in cases where this method is used. For the land locations and for comparison reasons, method 1 is used to calculate the wind speeds for the Hirlam22 domain as given in figure 4.

## 13.3 Comparison

The calculated wind maps of the Offshore Wind Atlas will be compared to other wind maps. First is there the comparison of the two methods used for the Dutch EEZ. From this comparison it can be found what the influence of using Hsu's shallow sea equation is, for a large area. A second comparison is made with the previous version of the Wind Atlas which con-

sidered a different period. From this comparison it can be found if the wind speeds are changing. If possible, also comparisons will be made with older maps, and maps made by other institutes.

#### 13.4 Contents new Offshore Wind Atlas

The new version of the Offshore Wind Atlas will contain the following information for the three mentioned altitudes of 40, 90 and 140 m:

- 1 Map with spatial distribution of the mean wind speed
- 2 Map with spatial distribution of Weibull scale and shape parameters
- 3 Map with spatial distribution of reference wind speed

These maps are available for the complete time series as well as for each wind direction sector. In addition, per full year of the considered time period, a map is available with the spatial distribution of the average wind speed. Similar maps are made for the monthly mean wind speed. Note, however, that only the results of the full time series are discussed in this report.



## 14 Results Wind Atlas

In this chapter the results of the Offshore Wind Atlas will be presented. For three altitudes the spatial distribution of the average wind speed, Weibull shape and scale parameters and the reference wind speed will be presented. For the calculation of the maps, use is made of two methods: method 1 Charnock and method 2 Hsu's equation for shallow sea with IDW interpolation of the wave data as explained in chapter 13. For each altitude the results of the different methods will be presented side by side, i.e. the results of method 1 will be shown on the left side and the results of method 2 on the right side. Note that method 2 can only be used within the Dutch EEZ, for that reason, the boundaries of the EEZ is also indicated in the results of method 1.

### 14.1 Mean wind speed

The mean wind speed has been calculated based on the full time series. The period starts on 19 November 2003 and lasts until 31 March 2010. The lower boundary of this time period is based on the fact that only Hirlam22 data should be used and the upper boundary is selected based on the fact that wave data is available until this date. The found maps indicating the mean wind speeds for the two methods will be compared. Each color in these plots indicate an average wind speed interval of 0.2 m/s.

In figures 36 to 41 the results are presented of the average wind speed calculated using method 1 Charnock (figures 36, 38 and 40), and method 2 Hsu IDW Shallow (figures 37, 39 and 41).

Several things can be noted about these figures. These are:

- Peaks present above land in wind maps of method 1 Charnock
- Both methods generally give the same mean wind speed, differences are in the order of 0.2 m/s
- The mean wind speed is increasing with height
- Far offshore higher mean wind speeds than onshore

The peaks of the mean wind speed can be seen best in figure 36. The reason that this happens for onshore areas is that on land the surface is changing rapidly because there are a lot of obstacles which influence the wind profile. The terrain is inhomogeneous so that the wind speed can change drastically between the grid points of the used grid. It can be found that the location of the peaks corresponds to the locations of cities. Also note that the grid resolution taken here is 22 km and because the wind speed is changing on a much smaller scale than the selected grid resolution, the transitions between the mean wind speed calculated at one grid point to the mean wind speed calculated for the surrounding grid points is not directly calculated. Instead, the Matlab® software, which has been used to make the plots, uses an interpolation technique to fill the area between the grid points [33]. By using a finer grid above land and in the coastal zone, the size of the peaks in the figure should reduce, not the value corresponding to the peaks. This is due to the fact that when you move away from a city, the influence of the city on the wind speed is reducing. Above sea this behavior does not occur because here the surface is homogeneous, the results will therefore give a smooth plot on a coarser grid.

When comparing the two methods, it can be seen that there are only minor differences. Generally, both methods show the same trends for the different altitudes. Note that this was also found in the analysis of the validation stations. Further, all the plots show an increase in mean wind speed for increasing altitude. Also the mean wind speed near the

coast is generally lower than far offshore as expected. This is due to the fact that in the vicinity of land mass, the wind speed reduces.

Something that also can be seen in the figures of the mean wind speed is the result of selecting a constant surface roughness of 0.03 m for Belgium and Germany. Especially for the part of Belgium, in the south east part of the figure, below the EEZ, it can be seen that the wind speed is more homogeneous compared to the part of the Netherlands. Because cities are not modeled in Belgium and Germany, large fluctuations of the mean wind speed do not occur. The differences that can be seen, however, are small and are most likely caused by the Hirlam model which also includes the surface roughness but then on a coarser grid.

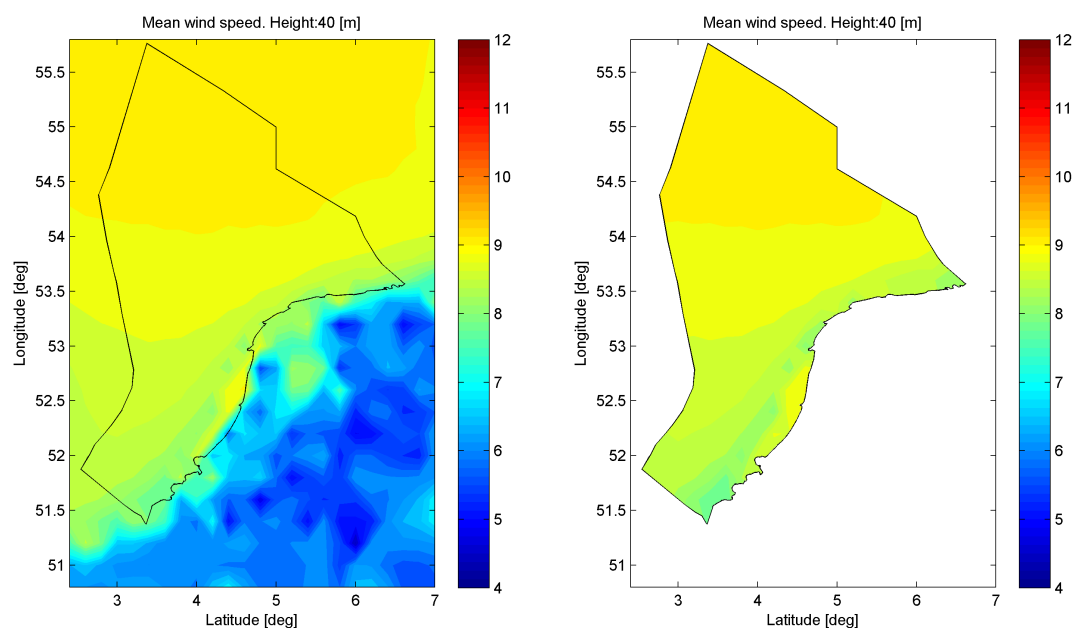


**Figure 36:** Average wind speed for 40m height, Method 1: Charnock. **Figure 37:** Average wind speed for 40m height, Method 2: Hsu IDW Sha.

## 14.2 Weibull parameters

### 14.2.1 Scale parameter

The distribution of the Weibull scale parameter are presented in figures 42 to 47. Each color indicated in the figure represents a difference of 0.2 m/s. Already for the altitude of 40 m a difference between the two plots can be seen. When the upper part of the EEZ is considered, it can be seen that, for all altitudes, method 2 gives a higher estimate of the scale parameter. Note that for the rest of the plot also a higher value of the scale parameter is found. This, however, is not as clear. For the presented plots of method 1 also peaks can be found on the onshore part of the maps. As mentioned, this is due to the fact that at these locations cities are located which have a large influence on the local wind speed. Further, for increasing altitude it can be seen that the scale parameter is increasing as well, where it appears for method 1, above land, the differences between two grid points reduces. This is due to the fact that at higher altitudes, the influence of the surface roughness is less than close to the surface.

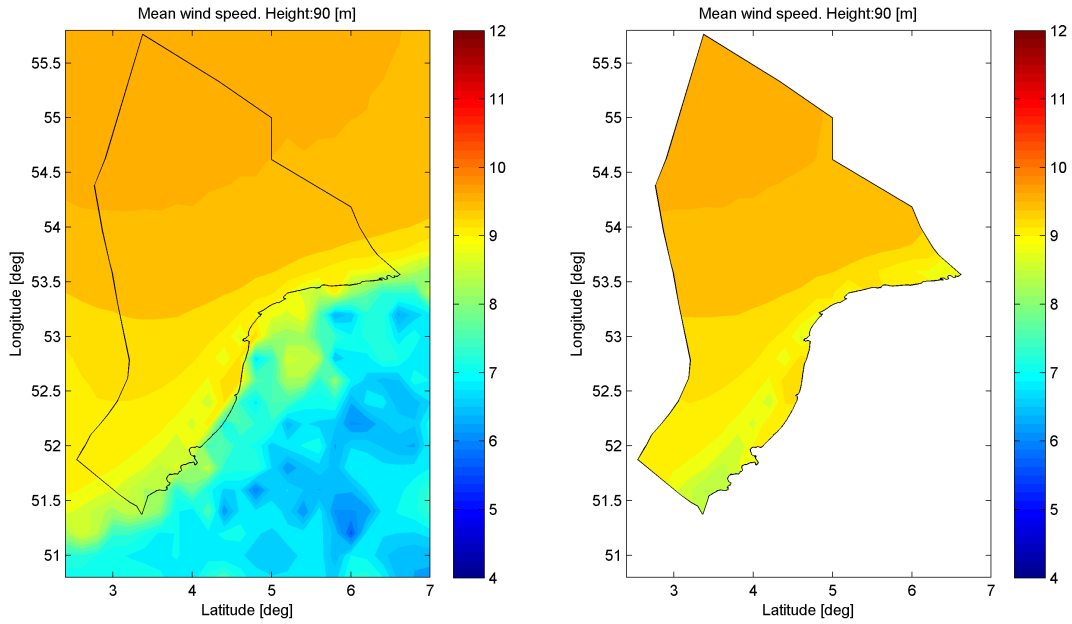


**Figure 38:** Average wind speed for 90m height, **Figure 39:** Average wind speed for 90m height, Method 1: Charnock. Method 2: Hsu IDW Sha.

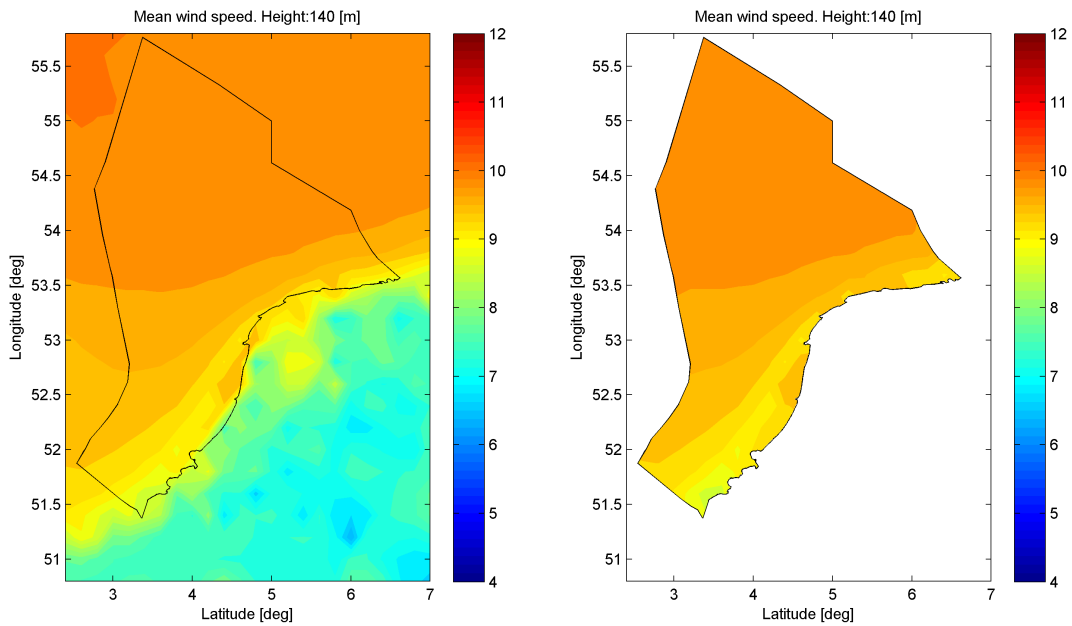


**Figure 40:** Average wind speed for 140m height, **Figure 41:** Average wind speed for 140m height, Method 1: Charnock. Method 2: Hsu IDW Sha.

### 14.2.2 Shape parameter

The shape parameters  $k$  are presented in figures 48 to 53. Again, on the left side the results of method 1 and on the right side the results of method 2. First the results per method will be discussed, followed by a comparison of the two methods.

Starting with method 1 at an altitude of 40 m it can be seen that above sea the shape parameter is roughly between 2 and 2.25. The lowest values can be found near the coast

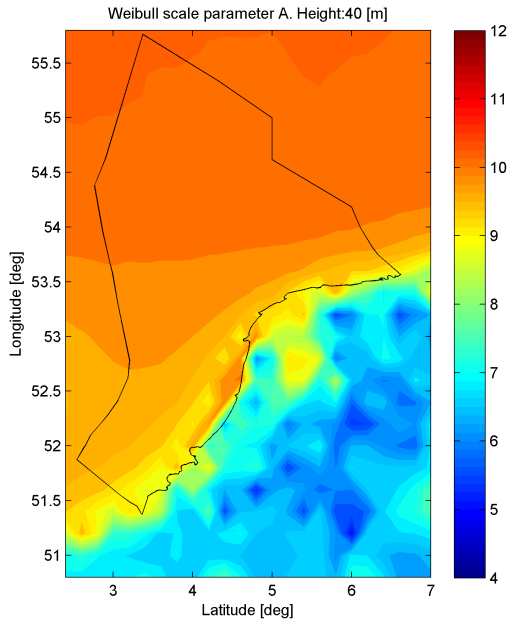


**Figure 42:** Weibull scale parameter A for 40m height, Method 1: Charnock.

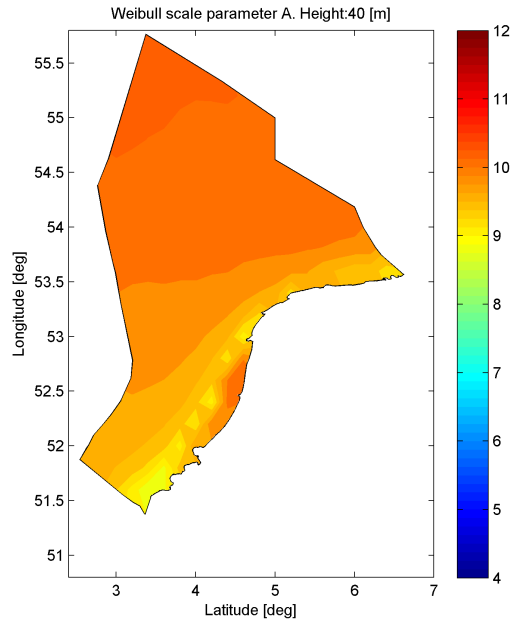


**Figure 43:** Weibull scale parameter A for 40m height, Method 2: Hsu IDW Sha.

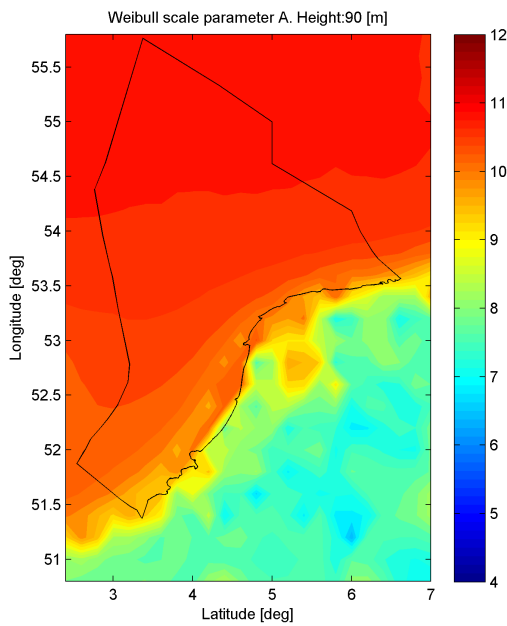


**Figure 44:** Weibull scale parameter A for 90m height, Method 1: Charnock.

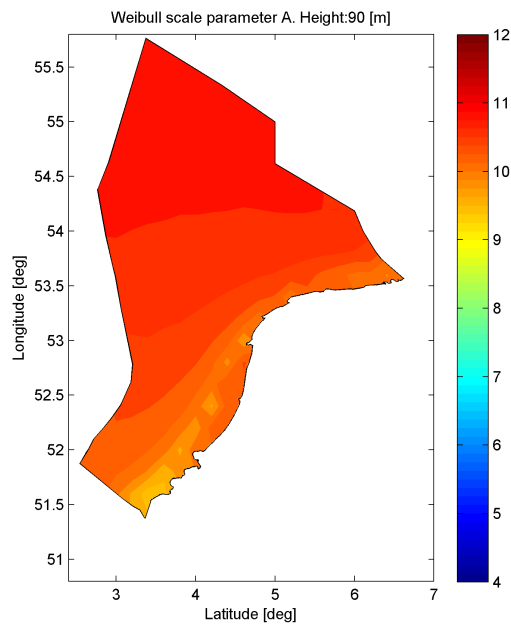


**Figure 45:** Weibull scale parameter A for 90m height, Method 2: Hsu IDW Sha.

while the highest values can be found in the north west corner of the plot. For the land area, the shape parameter is between 1.8 and 2.1 with some peaks going to 2.2, where the lowest values can be found in the south east part of the map and the highest values in the middle of the map just below the EEZ border. It was expected that for regions far inland the shape parameter would be between 1.8 and 2.0. This can also be found in literature [31]. For most regions, this is true except for the few locations in the north west of the land area. The reason for this is currently unknown, there are however two possibilities that could

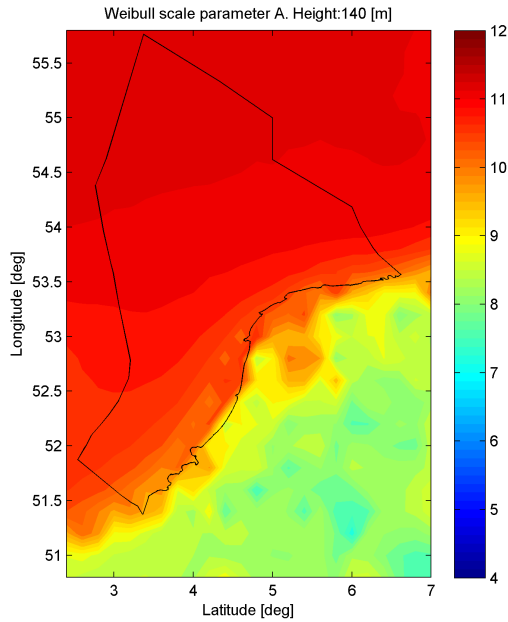


**Figure 46:** Weibull scale parameter  $A$  for 140m height, Method 1: Charnock.

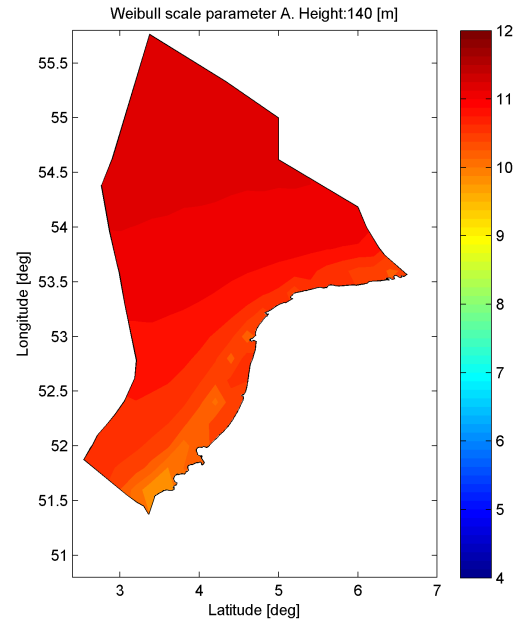


**Figure 47:** Weibull scale parameter  $A$  for 140m height, Method 2: Hsu IDW Sha.

occur. The first one is that there is an error in the calculation of the time series, second possibility is that the Weibull fit is not representing the wind distribution very well.

When looking at the maps for the altitude of 90 m, it can be seen that for method 1 the values of  $k$  are increasing compared to the values for an altitude of 40 m. Onshore, the peaks found for an altitude of 40 m can be found here as well. Just as the rest of the map, their value has increased. Note however that near the coast line in the middle of the map, the scale parameter does not change a lot.

For an altitude of 140 m, the shape parameter has increased again, also for the peaks found onshore. The value of these peaks are around 2.5 which is quite high for a land location. Note however that for Cabauw, at this altitude a shape parameter of 2.4 was found from the measured time series. As such, it is not impossible that these high values can be reached, it is however improbable that it can be estimated correctly by method 1 since it generally gave lower values for the shape parameter compared to the measurements.

For method 2 it can be seen that for an altitude of 40 m the shape parameter is already high, between 2.1 near the coast and 2.35 in the east part of the EEZ. For increasing altitude, however, the shape parameter is decreasing, this in contradiction of the results of method 1 which show an increase in  $k$  for increasing altitude. This decrease in  $k$  for method 2 is caused by the implementation of Hsu's equation for the sea surface roughness.

When both methods are compared, two points can be made. First point is that both methods show low  $k$  near the coast and high  $k$  in the east part of the EEZ. Second point is that for method 1,  $k$  is increasing with increasing height while for method 2,  $k$  is decreasing with increasing height.

### 14.3 Reference wind speed

The reference wind speed is an important parameter for wind turbine designers in order to determine what the maximum loads are on the wind turbine when a turbine is placed in a

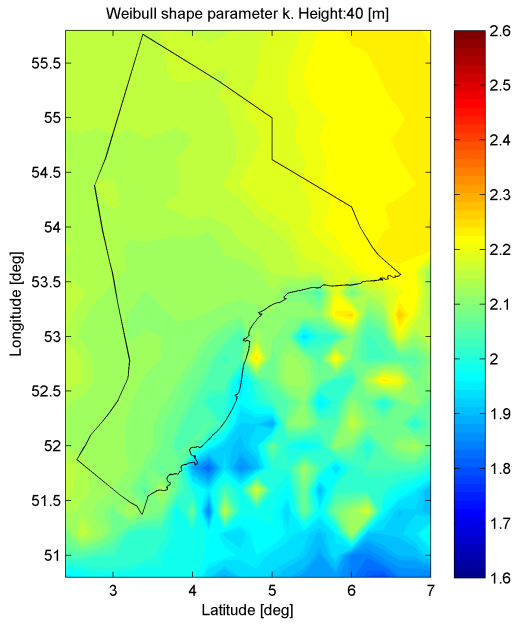


**Figure 48:** Weibull shape parameter  $k$  for 40m height, Method 1: Charnock.

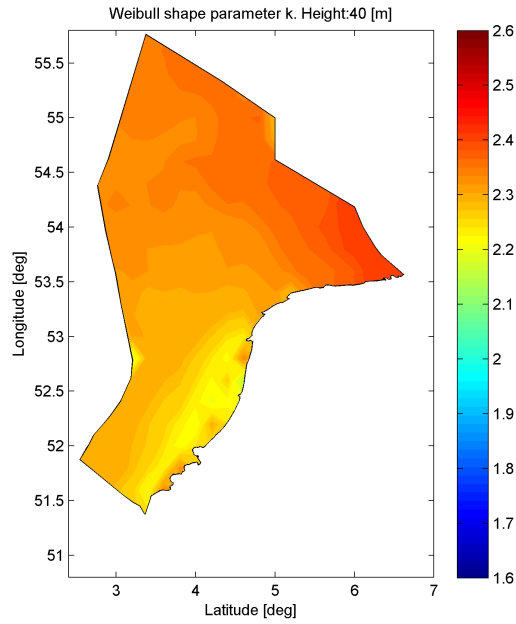


**Figure 49:** Weibull shape parameter  $k$  for 40m height, Method 2: Hsu IDW Sha.

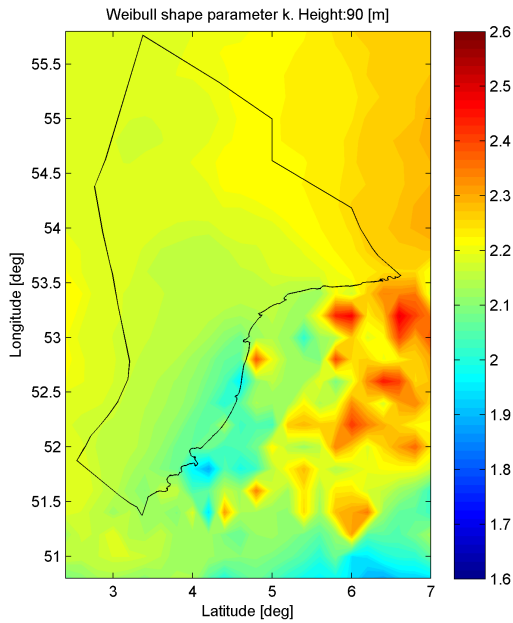


**Figure 50:** Weibull shape parameter  $k$  for 90m height, Method 1: Charnock.

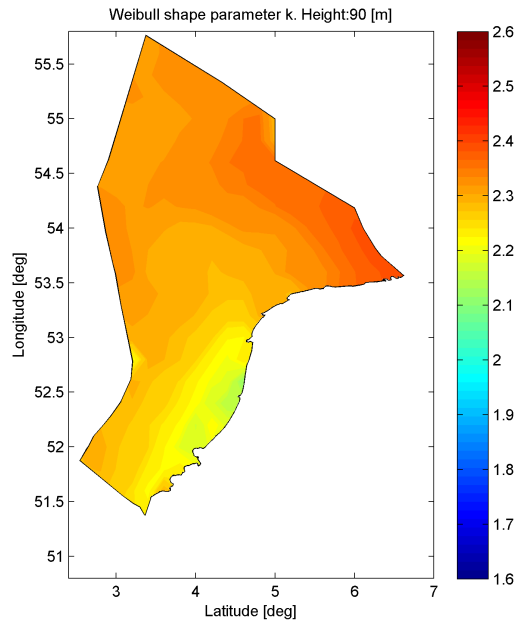


**Figure 51:** Weibull shape parameter  $k$  for 90m height, Method 2: Hsu IDW Sha.

given location, which can occur at least once in 50 years. In the IEC standard IEC-61400-1, three safety classes have been set based on the maximum reference wind speed [21]. These classes are numbered one to three where for class one a reference wind speed of 50 m/s is set, for class two the reference wind speed is 42.5 m/s and for class three the reference wind speed is 37.5 m/s. Based on the reference wind speed calculated for a given site, the wind turbine designer has to design the wind turbine following the rules of the safety class for which the turbine should be build.

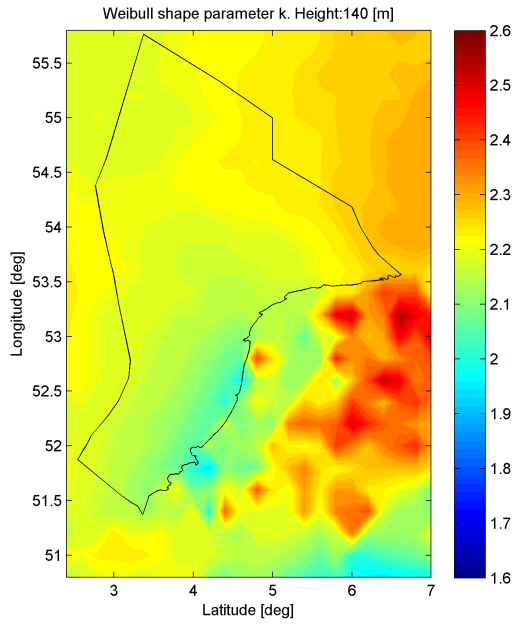


**Figure 52:** Weibull shape parameter  $k$  for 140m height, Method 1: Charnock.

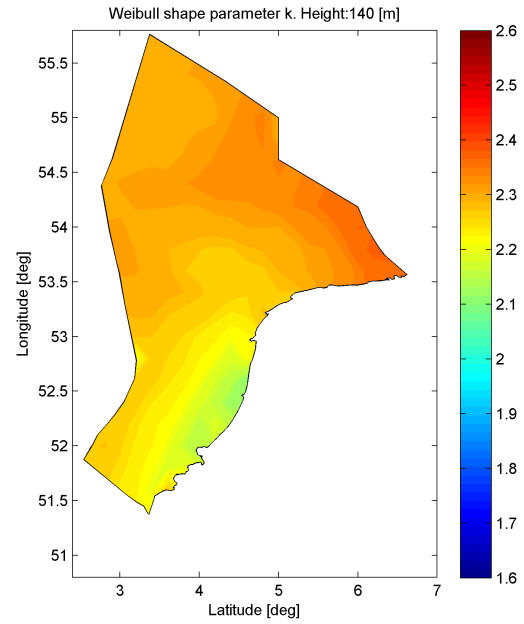


**Figure 53:** Weibull shape parameter  $k$  for 140m height, Method 2: Hsu IDW Sha.

In figures 54 to 59 the results are presented. As can be expected, for increasing height, the reference wind speed is also increasing. For the onshore locations for method 1 it can be seen that the reference wind speed is much lower than for the offshore locations. This is due to the fact that above land the wind speed is already lower than above sea. As such, it can be expected that the reference wind speed is also lower above land.

When the two methods are compared, it can be seen that method 2 gives lower values, in the order of 3 to 5 m/s lower than calculated using method 1. This is probably due to the fact that the calculation of the reference wind speed is based on the found parameters of the Weibull distribution. The large difference that occurs here between the reference wind speeds can be subscribed to the difference in the values of the shape parameter of the Weibull distribution.

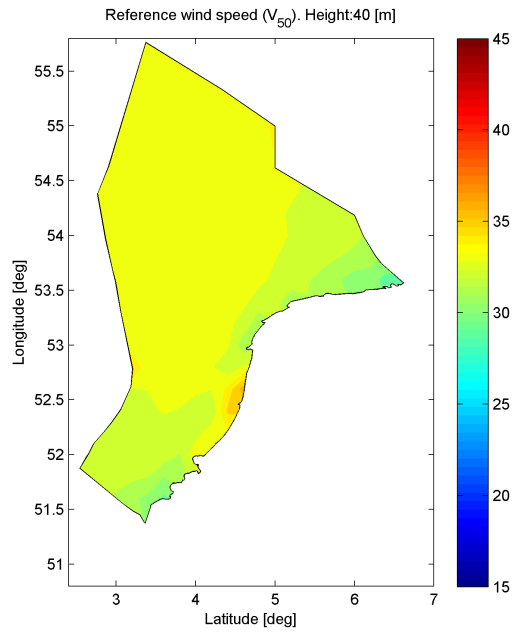
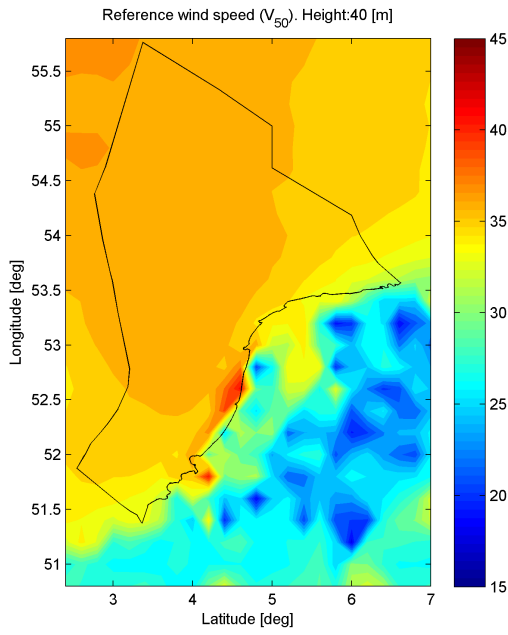


**Figure 54:** Reference wind speed for 40m height, Method 1: Charnock. **Figure 55:** Reference wind speed for 40m height, Method 2: Hsu IDW Sha.

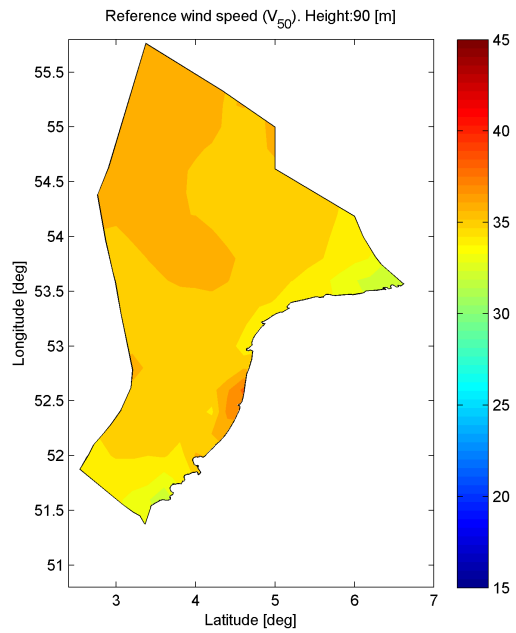
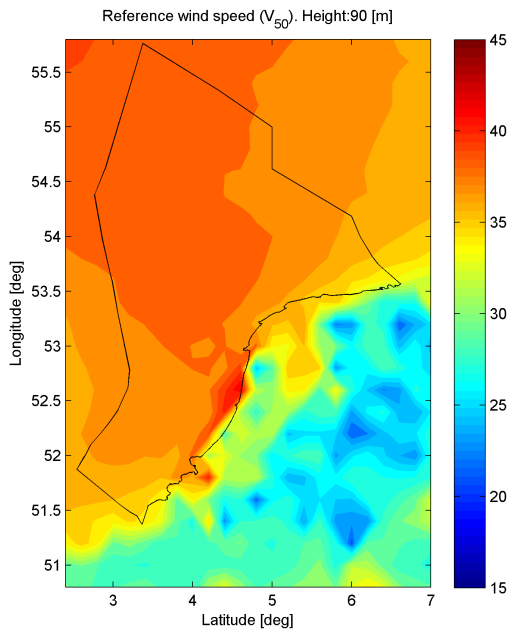


**Figure 56:** Reference wind speed for 90m height, Method 1: Charnock. **Figure 57:** Reference wind speed for 90m height, Method 2: Hsu IDW Sha.

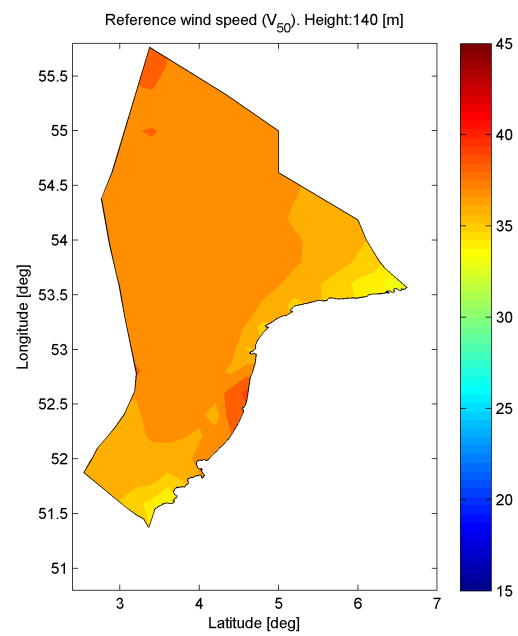
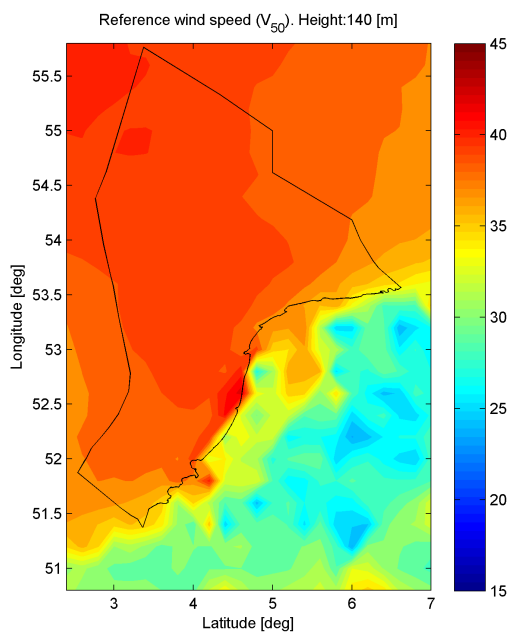


**Figure 58:** Reference wind speed for 140m height, **Figure 59:** Reference wind speed for 140m height, Method 1: Charnock. Method 2: Hsu IDW Sha.



## 15 Comparison with other wind maps

The results of the mean wind speed of the Offshore Wind Atlas will be compared to results found from the previous version of the Offshore Wind Atlas and, if possible, to wind maps made using different methods. Preferably, this comparison is done for equal altitude and resolution. As will be shown, this is not always possible. There are several wind maps freely available, three of these are:

- The European Wind Atlas made by Risø using the wind atlas method [47] [41]
- The wind map made by Senter Novem [44]
- ECN Offshore Wind Atlas [3]

The European Wind Atlas made by Risø has been published in 1989 and is divided into two parts. The first part is an offshore wind atlas indicating the wind speed at five different altitudes, the second part is an onshore wind atlas indicating the wind speed for five different types of land use. There are, however, two reasons why this wind map cannot be used for the comparison. The first reason is that the resolution in which the average wind speed is given ranges from 1 m/s for low altitudes to 1.5 m/s for high altitudes. Because of this, almost the whole area of the Dutch EEZ is covered with the same color making the comparison already impossible. The second reason is that the spatial resolution is quite large, the map comprises the whole continent of Europe and is therefore not on the same scale as the new ECN Offshore Wind atlas. A comparison with the European Wind Atlas is therefore not possible.

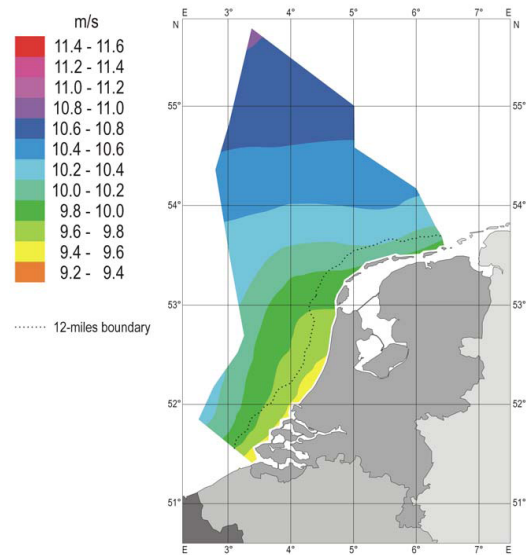
The wind map made by SenterNovem [44] has been created using WaSP [41] which is a program that uses the wind atlas method as described by Troen [47]. The map only includes the Netherlands excluding the Dutch EEZ. In addition, the resolution of this map is very high with 200 x 200 m. The resolution in which the wind speed is given is 0.5 m/s. The time period considered for this wind map is 20 years. Unfortunately, because the spatial resolution of the ECN Offshore Wind Atlas is only 22 x 22 km, it is not accurate enough to be compared with the map of SenterNovem.

The third wind map mentioned is the previous version of the Offshore Wind Atlas which only includes the Dutch EEZ [3]. Four public maps have been made for altitudes of 60, 90, 120 and 150 m. Note that only for an altitude of 90 m a map is available from the new version of the Offshore Wind Atlas. The spatial resolution of the map is in the same order as was used to make the new version of the Offshore Wind Atlas and the resolution of the mean wind speed is 0.2 m/s. The period considered comprises the years 1997 until 2002. The results of the old wind atlas for an altitude of 90 m will be compared to the new version of the wind atlas at the same altitude.

### 15.1 Previous version ECN Offshore Wind Atlas

In figure 60 the previous version of the offshore wind atlas is presented and in figure 61 the result of the new version calculated using method 2. Note that the result of the mean wind speed for methods 1 and 2 were almost identical, for that reason, only a comparison is made between the old map and the new map calculated with method 2.

Mean Wind Speed at the Netherlands' Exclusive Economic Zone (NEEZ)  
 Period: 1997 - 2002  
 Height: 90 m above mean sea level



Copyright (c) 2004 by Energy research Centre of the Netherlands, Petten, the Netherlands

Supported by the Programme 'Duurzame Energie in Nederland' as operated by SenterNovem for the Dutch Ministry of Economic Affairs

**Figure 60:** Results previous version Offshore Wind Atlas for an altitude of 90 m.

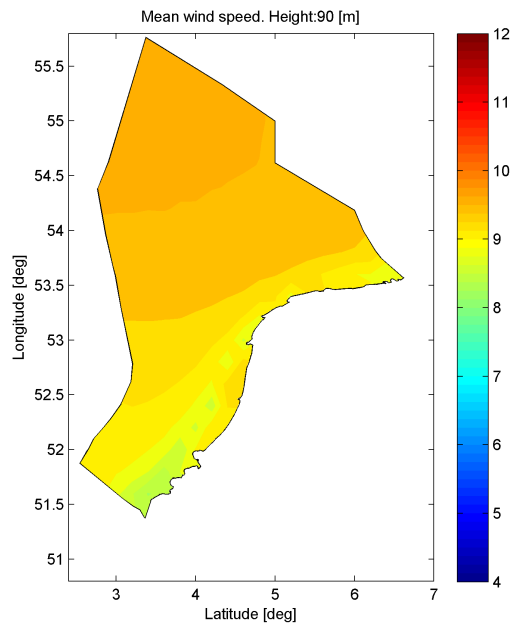


**Figure 61:** Mean wind speed new version Offshore Wind Atlas for an altitude of 90m, calculated using method 2 Hsu IDW Sha.

Although the color scheme used in these plots are different, it can still be seen that there are significant differences between the two plots. In the north part of the EEZ, it can be found for the old map that the wind speed is between 10.6 and 10.8 m/s. The same area in the new wind map gives a wind speed between 9.8 and 10.0 m/s. This is a difference of 0.8 m/s which is rather large. This difference in estimated mean wind speed can be found throughout the whole map. Near the coast, the difference seems to increase to 1 m/s. Note that this does not indicate that either of these maps are wrong. It simply indicates that there is a large difference when two different periods are being compared. There are however some notes that have to be made. First of all, in the summer, the average wind speed is generally lower than in winter. Including an extra summer in a certain period already decreases the average wind speed considerably. For the new version of the Offshore Wind Atlas using method 1, it was found that this decrease in the order of 0.3 m/s is, where the considered period was extended from the end of March 2010 to the end of October 2010. In addition, it is very well possible that in the periods considered for both maps a different amount of storms passed by. Another possibility is that the average wind speed is indeed decreasing. Note however, that this is not directly an indicator that the wind climate is changing. To determine the wind climate, a period of 30 years should be considered. Currently, it is not yet possible to determine this based on the Hirlam data because there is not yet enough data for that.

For the old version of the Wind Atlas, also the map error has been calculated. It was found that the mean map error is -0.17 m/s with a standard deviation of 0.20 m/s. Because the validation for the old map was done using potential wind speeds, it should be compared to the map error of the new wind atlas found for the potential wind speeds. For the new map, the mean map error was -0.14 m/s with standard deviation of 0.47 m/s using method 1 and a mean map error of -0.08 m/s with standard deviation of 0.42 m/s for method 2. When these values are compared, it can be seen that the mean map error of the old map

corresponds well to the mean map error of the new map. The standard deviation of the new wind map however, is twice as large as was found for the old wind map. This is mainly due to the addition of station IJmuiden to the sample for the new map as was stated before.

So, although there is a large difference in found mean wind speed, the maps are both valid for the period they prescribe. The error with the measurements can be considered to be in the same order of magnitude.



## 16 Conclusions Offshore Wind Atlas

For the calculation of the new version of the Offshore Wind Atlas, use is made of two calculation methods, method 1 Charnock and method 2 Hsu's equation for shallow sea with IDW for the spatial interpolation of the wave data. For three altitudes the mean wind speed, the Weibull shape and scale parameter and the reference wind speed have been calculated. The considered altitudes are 40, 90 and 140 m in which the altitude of 90 m represents the hub height of an average wind turbine and the other two altitudes are the highest and lowest possible value for a rotor assuming a blade of 50 m length.

For the mean wind speed it was found that there were only minor differences between the two methods. Both indicated an increase in average wind speed for increasing height. Considering only one altitude, it was found that far offshore, higher wind speeds occur than onshore, where lower wind speeds occur. Note that this is in line with results found in literature [47] [41].

When considering the scale parameter of the Weibull distribution, it was found that there were some differences between the results of methods 1 and 2. The scale parameters calculated using method 2 were slightly higher than those of method 1. This was best visible in the figures for an altitude of 40 m, see figures 36 and 37. For the shape parameter of the Weibull distribution it was found that for method 1 the values are increasing with height. For method 2 however, the shape parameter was decreasing for increasing height. This is a direct effect of the use of the equation of Hsu for the surface roughness. Apparently, using this equation influences the wind speed profile at lower altitudes considerably.

For method 1 it was observed that on land, at an altitude of 140 m, the shape parameter is rather large. It was, however, found from the analysis of the measured time series at the location Cabauw, that high shape parameters can occur onshore. On the other hand, it is improbable that, using method 1, this is a good estimation of the shape parameter since for the other validation stations, usually the shape parameter was lower than the shape parameter from the measured time series. A reason for this difference might be because of the type of Weibull fit used.

Continuing with the reference wind speed, method 1 generally gives a higher value for the reference wind speed than method 2. The reason for this lies in the fact that the reference wind speed is calculated from the scale and shape parameters of the Weibull distribution. Apparently, the shape parameter has a large influence on the value of the reference wind speed. When the found values are compared with the reference wind speeds for the three safety classes set by the IEC standard [21], it can be found that the order of magnitude of the found values is correct.

The calculated map for the mean wind speed at the altitude of 90 m has been compared to the old version of the ECN Offshore Wind Atlas. The new version shows a lower mean wind speed than the old version, in the order of 0.8 to 1.0 m/s. One of the reasons of this difference is that different periods have been considered. It is possible that the amount of storms that occurred in these periods are not equal. Besides this, it is also possible that the average wind speed per year has decreased. It is however not possible to state that the climate has changed because the considered periods are too short. For climate research a period of at least 30 years is needed. When the map errors of the different versions are compared, which are based on time series of potential wind speeds, it can be found that the difference between the results from the map and the results from the measurement is small. For the old version and for the new version created using method 1 the mean map error is almost equal. Because of this, it can be stated that the average wind speed, given by the new version of the wind atlas, is reduced compared to the previous version. In order to find out if the climate is indeed changing, longer time periods have to be considered.



Part IV

## Conclusions



## 17 Conclusions

In the introduction of this report the main goal has been presented for this thesis work which is updating the ECN Offshore Wind Atlas using new available data and the AVDE model. In addition, two sub goals were set:

- 1 Improve the accuracy of the prediction of wind speed distributions
- 2 Make the AVDE model faster and more suitable for field analysis

For the improvement of the prediction of the wind speed distribution, only a few parameters can be changed in the AVDE model. Here is chosen to adjust the parameter corresponding to the surface roughness. Above land, this parameter is constant, above sea it is usually assumed to be constant. However, in reality it is variable. This lead to the main question of this thesis work:

Is it possible to improve the prediction of the wind speed distribution for a given location and altitude using a variable sea surface roughness?

The general conclusion is that, using a variable sea surface roughness, the prediction of the wind speed distribution is improved. Although the improvement is small, with an order of 1 to 2%, it is shown that introducing a variable sea surface roughness is a promising procedure.

In the remainder of this chapter it will be explained how the presented goals are met. First the adjustments of the AVDE model will be discussed after which the results of the validation at eleven different stations is discussed as well as the results of the new Offshore Wind Atlas.

### 17.1 AVDE model

With the introduction of a variable sea surface roughness, the AVDE model has also been updated to be more suitable for field analysis. This latter thing is done by choosing the input of the location in a way that it can be used for point analysis and field analysis by specifying a single point or a group of points either in a grid or randomly spread. In addition, the calculation time for a time series of a single point, for a period of several years, has been reduced from a couple hours to 20 to 25 minutes. For the implementation of a variable sea surface roughness, three equations have been considered which were found in literature which were derived using dimensional analysis. From these equations, the equation of Hsu has been selected because it introduces the state of the sea, in the form of the wave height  $H$ , wave period  $T$  and sea depth  $d$ , in the variable of the surface roughness  $z_0$ . The wave parameters  $H$  and  $T$  are measured at various locations in the North Sea, though mainly in the south west part of the Dutch EEZ. Data from 15 different measurement locations have been included in the calculations. The sea depth is only available for the Dutch EEZ.

Because the values of the wave parameters should be known in all points of the EEZ, two spatial interpolation techniques are introduced. These are Inverse Distance Weighting, which is a simple form of Kriging, and Gibescu's method for spatial interpolation of wind time series has been adopted and applied on the wave data. From a comparison between these two methods, using cross validation, it was found that the differences between the spatial interpolation method were minimal.

## 17.2 Validation

For the validation of the AVDE model, five different methods have been used. Method 1 Charnock is the method that was used in the previous version of the Wind Atlas. Here a constant value for the Charnock parameter is used. Methods 2 to 5 make use of the equation of Hsu, either for shallow sea (methods 2 and 4) or use is made of the general wave equation (methods 3 and 5). For methods 2 and 3 use is made of IDW for the spatial interpolation of the wave parameters where for methods 4 and 5 Gibescu's method is applied. Last item that should be mentioned about these methods is that method 1 is applicable in the complete Hirlam22 domain while the other methods are only applicable within the Dutch EEZ.

For two onshore locations and nine offshore locations time series have been calculated and compared to the measurements. For four stations, Cabauw and EWTW, both onshore, and OWEZ and FINO-1, both offshore, time series for multiple measurement heights were available. Note that only for station OWEZ all methods could be used. Because of this, only the results of method 1 are discussed here. For each of the four stations mentioned an altitude could be indicated for which an under prediction changed into an over prediction, the so called turn over point. This was found from the linear regressions applied, as well as from the comparison of the mean wind speed. Going from west to east over the map the altitude at which this turn over occurs is decreasing from 153 m at the OWEZ location to 43 m for the FINO-1 location. For three different altitude groups, a map error has been defined. The mean map error for the group between 10 and 50 m is 0.36 m/s. For the altitude group of 50 to 100 m the mean map error is -0.07 m/s. Note that in this group the turn over point of most of the stations is located. And for the altitude group of 100 to 200 m, the mean map error is equal to -0.25 m/s.

For the other seven locations, which are offshore KNMI stations, the mean map error for methods 2 and 4 was low, respectively -0.07 and -0.08 m/s. For methods 1, 3 and 5 the values are -0.14, -0.16 and -0.15 m/s, respectively, which is slightly larger.

Considering the Weibull distributions for these validation stations, it was found that method 1 usually under predicts the shape parameter compared to the measurements. It was also found that when Hsu's equation is used, the shape parameter is better estimated, in the order of 6%. For the scale parameter the improvements are lower with an order of 2%.

For the selection of the best method, use is made of a root mean squared (RMSE) analysis on the Weibull distributions. For each used method the RMSE is calculated with respect to the Weibull distribution of the measurements. Then it is investigated if methods 2 to 4 give lower RMSE than method 1 and in how many times of the considered cases this occurs. Based on this analysis, it was found that in 74.3% of the cases, method 2, Hsu's equation for shallow sea with IDW for spatial interpolation, gives the best result. For this reason, it has been selected for the creation of the new version of the Offshore Wind Atlas.

## 17.3 Wind Atlas

As mentioned, method 2 is used for the calculation of the Offshore Wind Atlas. In addition, also method 1 is used to serve as a reference. For three altitudes the mean wind speed, Weibull parameters and reference wind speed has been calculated. These altitudes are: 40, 90 and 140 m.

The results of the mean wind speed showed only minor differences, in the order of 0.2 m/s. As expected, the wind speed is lower inland compared to offshore locations. It was found that the scale parameters found using method 2 were slightly higher compared to the results of method 1. When the shape parameter is considered, it can be seen that method 1

gives a lower value compared to method 2. This coincides with the results of the validation stations. It was also found that for increasing altitude, the shape parameter calculated using method 1, is increasing while the shape parameter calculated using method 2 is decreasing. This is a direct effect of the use of the equation of Hsu for the surface roughness. Apparently, using this equation influences the wind speed profile at lower altitudes considerably.

In the comparison of the mean wind speed of the new version of the Wind Atlas with the old version of the Wind Atlas, for an altitude of 90 m, a difference of 0.8 to 1.0 m/s was observed. This difference is due to the fact that different periods are considered. Also, it can be possible that the average wind speed is indeed decreasing. When the map errors are compared, it can be found that these are in the same order of magnitude for the two different maps. As such, the results can be considered to be valid.

The main figures of the new version of the Offshore Wind Atlas are given in figures 62 to 65 where the mean wind speed, scale and shape parameters and reference wind speed is given for an altitude of 90 m, calculated with Hsu's shallow sea equation.

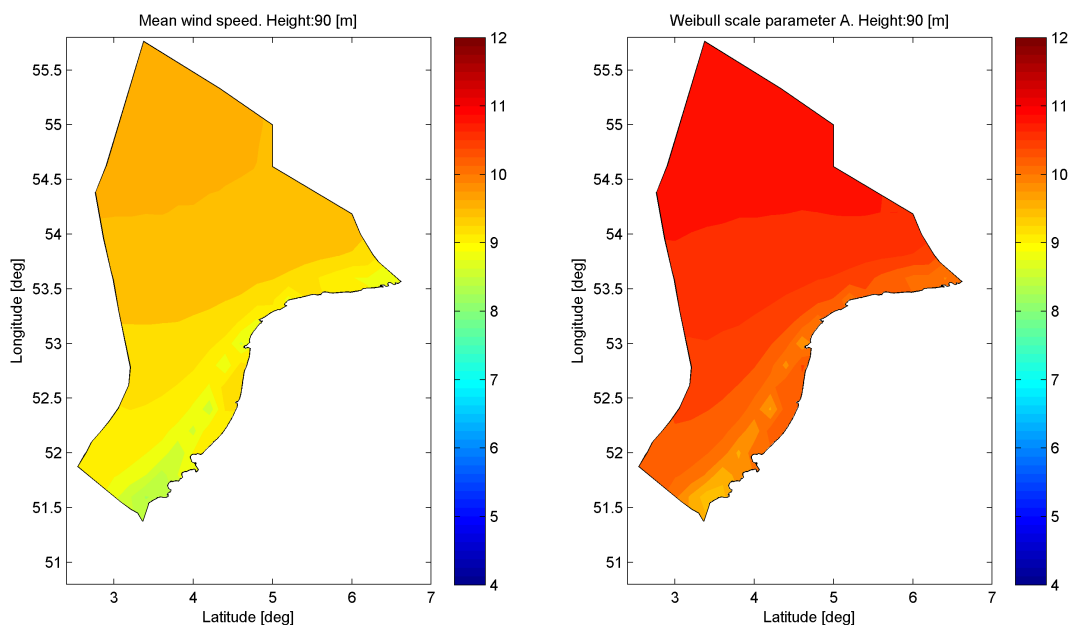


**Figure 62:** Average wind speed for 90m height, **Figure 63:** Weibull scale parameter A for 90m height, Method 2: Hsu IDW Sha.

## 17.4 Closing statements

Now returning to the questions stated in the beginning of this chapter. Starting with the main goal, it can be said that the update is completed. For each grid point in the map a time series is available for three altitudes including an overview of the mean wind speed, direction dependent Weibull parameters, occurrence of wind direction and reference wind speeds. If necessary, for other locations, these results can be calculated as well in a reasonable computation time since it has been significantly reduced for one location and altitude.

From the validation and method selection it was found that Hsu's equation for shallow sea can be used to increase the accuracy of the prediction of wind speed distributions in at least 74.3% of the considered cases. Unfortunately, the improvements are small, in the order of 1

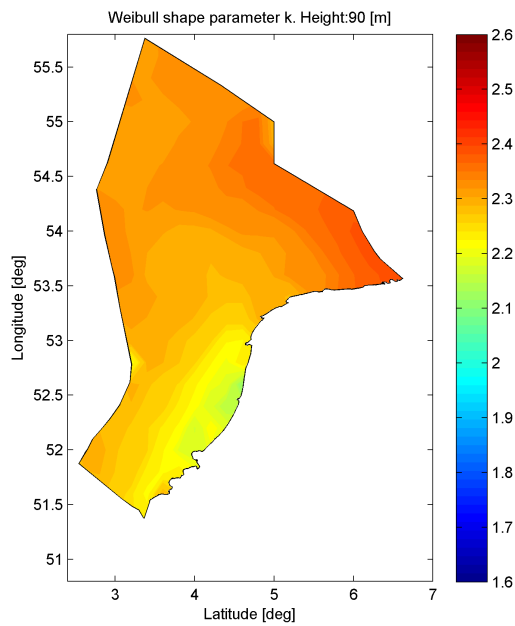


**Figure 64:** Weibull shape parameter  $k$  for 90m height, Method 2: Hsu IDW Sha.

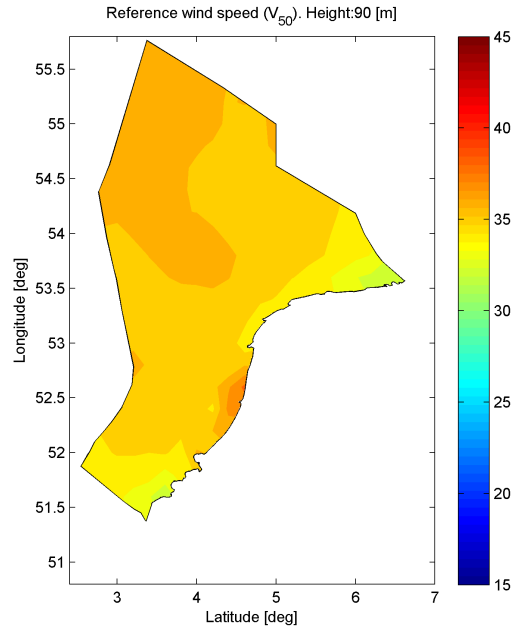


**Figure 65:** Reference wind speed for 90m height, Method 2: Hsu IDW Sha.

to 2% for the mean wind speed and Weibull scale parameter and for the Weibull shape parameter an improvement was found in the order of 5%. What the real effect of these small improvements are, could be determined by looking at the power content of the Weibull distributions. Unfortunately, due to a lack of time, this analysis could not be included in this report and is therefore highly recommended for the possible following up project. Of course, there are some other recommendations that can be considered to improve the results found, using Hsu's equation. These will be presented in the next chapter.

## 18 Recommendations

In this section some suggestions and recommendations are given in order to improve the results of the Offshore Wind Atlas. There are two items that are more or less obvious and two items that are less obvious. The first one has to do with the resolution of the grid. Due to the limited amount of time available, it was not possible to calculate a solution on a finer grid. In order to speed up the calculations it can be considered to use multiple processors to do the calculations. Also the used code of the AVDE model can be further optimized to be more suitable for grid calculations. In addition, to make a comparison with the wind map of SenterNovem [44] possible, the grid resolution should be decreased to at least 1 km instead of the current resolution of 22 km.

The second obvious item is the amount of data available; the wave data as well as the wind speed data for the validation. When wave data is available at more locations, the accuracy of the interpolation increases. This is however hard to come by, since extra measurement installations are needed for that. For the wind speed data, it would be nice to have more sites where measurements are taken at different altitudes. This would seriously increase the confidence in the results found for the mean map error, as well as the results of the turn over point.

A third recommendation that can be made is for the spatial interpolation of the wave parameters. For Gibescu's method two variants are available, one that includes the dependency of the wave parameter at a previous time and one that does not include this. In this report, the simple version is used because it is less time consuming considering the calculation time. In order to give a better estimate of the wave parameters, the dependence on the wave parameter in a previous moment can be included. This should give a better estimate for the wave parameters and therefore a more reliable value for the sea surface roughness.

Fourth recommendation would be to consider different models for the wind profile. Currently, the Monin-Obukhov theory is applied with the Businger-Dyer profiles and the Holt-slag profiles for stable situations together giving three different types of profiles corresponding to stable, neutral and unstable conditions. There are, however, a lot of other approximations available. It might be interesting to find out what the results are if other profiles are used.



## Bibliography

- [1] Bergström, H. (1992): *Distribution of extreme wind speed*. Wind Energy Report WE92:2.
- [2] BMU and PTJ (2010): *FINO database*. URL [fino.bsh.de](http://fino.bsh.de). Password required, free access with acknowledgment.
- [3] Brand, A.J. and T. Hegberg (2005): *Offshore Wind Atlas - Wind resource in the Dutch part of the North Sea*. Confidential ECN-CX-04-136, ECN.
- [4] Brand, A.J. and J.K. Kok (2003): *Aanbodvoorspeller duurzame energie - Deel 2: Korte termijn prognose van windvermogen*. Technical Report ECN-C-03-049, ECN. Appendix C and D are confidential.
- [5] Brockwell, P.J., and R.A. Davis (2006): *Time Series: Theory and Methods*. Springer, 233 Spring Street, New York, second edition.
- [6] Businger, J.A., et al. (1971): *Flux-profile relationships in the atmospheric surface layer*. Journal of Atmospheric Sciences, 28:181–189.
- [7] Calvo, J. (2007): *Kain-Fritsch convection in HIRLAM. Present status and prospects*. HIRLAM Newsletter, 52.
- [8] CESAR (2010): *Cesar Cabauw database*. URL [www.cesar-database.nl](http://www.cesar-database.nl). Password required, free access with acknowledgment.
- [9] Charnock, M. (1955): *Wind stress on a water surface*. Quarterly Journal of the Royal Meteorological Society, 81:639–640.
- [10] Davenport, A.G. (1967): *The dependence of wind loads on meteorological parameters*. Proceedings Second International Conference on Wind Effects on Buildings and Structures . Ottawa.
- [11] Dekker, J. and J. Pierik (1999): *European Wind Turbine Standards II*. Technical Report ECN-C-99-073, European Commission, ECN.
- [12] Eecen, P.J. and J.P. Verhoef (2007): *EWTW Meteorological database, Description June 2003 - May 2007*. Technical Report ECN-E-07-041, ECN.
- [13] Garratt, J.R. (1977): *Review of the drag coefficients over oceans and continents*. Monthly Review, (105):915–929.
- [14] Gibescu, M. and B.C. Ummels and W.L. Kling (2006): *Statistical Wind Speed Interpolation for Simulating Aggregated Wind Energy Production under System Studies*. Wind Energy.
- [15] Gollvik, S. (2001): *A snowmodel intended for ISBA*. Hirlam workshop SRNWP.
- [16] Gollvik, S. (2004): *Surface modelling in Northern Europe*. Hirlam workshop Baltic.
- [17] Hegberg, T. (2002): *Ruimtelijke transformatie van lokale wind*. Report ECN Wind Memo-02-022, ECN.
- [18] Hirlam management group (2010): *Hirlam website*. URL [www.hirlam.org](http://www.hirlam.org). Last visited:.
- [19] Hsu, S.A. (1973): *A Dynamic roughness equation and its application to wind stress determination at the air-sea interface*. Journal of physical oceanography, 4:116–120.

- [20] Huang, X.Y., X. Yang, N. Gustafsson, K.S. Mogensen and M. Lindskog (2002): *Four-dimensional variational data assimilation for a limited area model*. Report 57, Hirlam.
- [21] IEC (2005): *IEC 61400-1 Ed. 3: Wind turbines - Part 1: Design requirements*.
- [22] Ivarsson, K. (2007): *The Rasch Kristjansson large scale condensation. Present status and prospects*. HIRLAM Newsletter, 52.
- [23] Kain, J.S. (2003): *The Kain-ÚFritsch Convective Parameterization: An Update*. Journal of applied meteorology, 43:170–181.
- [24] KNMI (2010): *Uurgegevens potentiële wind*. URL [www.knmi.nl/klimatologie/onderzoeksgegevens/potentiele\\_wind/](http://www.knmi.nl/klimatologie/onderzoeksgegevens/potentiele_wind/).
- [25] KNMI HYDRA (2005): *KNMI HYDRA project website*. URL <http://www.knmi.nl/samenw/hydra/index.html>.
- [26] Kourzeneva, E., P. Samuelsson, G. Ganbat and D. Mironov (2008): *Implementation of Lake Model FLake into Hirlam*. Hirlam newsletter, 54.
- [27] Kouwenhoven, H.J. (2007): *User manual data files meteorological mast NoordzeeWind*. Technical Report NZW-16-S-4-R03, NoordzeeWind/ECN.
- [28] Landberg, L, et al. (2003): *Wind resource estimation - an overview*. Wind Energy, 6:261–271.
- [29] Li J., and A.D. Heap (2008): *A Review of Spatial Interpolation Methods for Environmental Scientists*. Geoscience Australia, Canberra, Australia. GPO Box 378, Canberra, ACT 2601, Australia.
- [30] Lynch, P., R. McGrath and A. McDonald (2007): *Digital Filter Initialization for Hirlam*. Report 42, Hirlam.
- [31] Manwell, J., J. McGowan and A. Rogers (2002): *Wind Energy Explained - Theory, Design and Application*. John Wiley & Sons, West Sussex, England.
- [32] Massel, S.R. (1996): *Ocean surface waves: their physics and prediction*. World Scientific Publishing Co. Pte. Ltd., 1 edition. ISBN 981-02-2109-6(pbk).
- [33] Mathworks (2008): *Matlab V7.7.0.471 (R2008b)*. URL [www.mathworks.com](http://www.mathworks.com).
- [34] Meteox (2010): *Meteox weather information website*. URL [www.meteox.nl](http://www.meteox.nl).
- [35] Ministerie van Verkeer en Waterstaat (2010): *Waterbase database*. URL [www.waterbase.nl](http://www.waterbase.nl).
- [36] Mironov, D.V. (2008): *Parameterization of Lakes in Numerical Weather Prediction. Description of a Lake Model*. COSMO technical report, 11.
- [37] Naeije, M. (2006): *Lecture sheets: Oceans and Ice*. Presentation. Lecture sheets course AE3-E01: Earth and Planetary Observation.
- [38] Netherlands Hydrological Service (2010): *website*. URL <http://www.hydro.nl/>.
- [39] Noilhan, J. and S. Planton (1988): *A Simple Parameterization of Land Surface Processes for meteorological models*. Monthly Weather review, 117:536–549.
- [40] NoordzeeWind (2010): *NoordzeeWind website*. URL [www.NoordzeeWind.nl](http://www.NoordzeeWind.nl). Meteorological data maintained by ECN.

- [41] Risø DTU (2010): *The World of Wind Atlases Ů Wind Atlases of the World*. URL [www.windatlas.dk](http://www.windatlas.dk).
- [42] Rontu, L., K. Sattler and R. Sigg (): *Parametrization of subgrid-scale orography effects in HIRLAM*. Hirlam technical report, 56.
- [43] Savijärvi, H. (1989): *Fast Radiation Parameterization Schemes for Mesoscale and Short-Range Forecast Models*. *Journal of applied meteorology*, 29:437–447.
- [44] SenterNovem (2005): *Windkaart van Nederland op 100m hoogte*. Report, SenterNovem. URL [www.windenergie.nl/site/file.php?file=110](http://www.windenergie.nl/site/file.php?file=110).
- [45] Taylor, P.K. and M.J. Yelland (1999): *The dependence of sea surface roughness on the height and steepness of the waves*. *Journal of physical oceanography*.
- [46] Tijm, A. and G. Lenderink (2003): *Characteristics of CBR and STRACO versions*. Report , Hirlam. URL [http://hirlam.org/index.php?option=com\\_docman&task=doc\\_download&gid=281&Itemid=70](http://hirlam.org/index.php?option=com_docman&task=doc_download&gid=281&Itemid=70).
- [47] Troen, I. and E.L. Petersen (1989): *European Wind Atlas*. Risø National Laboratory, Roskilde.
- [48] Undén, P., et al. (2002): *Hirlam-5 Scientific Documentation*. Report , Hirlam-5 Project. URL [www.hirlam.org](http://www.hirlam.org).
- [49] Verkaik, J.W. (2001): *Documentatie Windmetingen In Nederland*. Technical Report , KNMI.
- [50] Wageningen University and Research center (2010): *Alterra website*. URL [www.alterra.wur.nl/NL/](http://www.alterra.wur.nl/NL/).
- [51] Wever, N. and G. Groen (2009): *Improving potential wind for extreme wind statistics*. Technical Report WR 2009-02, KNMI, De Bilt, The Netherlands. URL <http://www.knmi.nl/samenw/hydra/index.html>.
- [52] Wieringa, J. (1986): *De atmosferische grenslaag*. Technical Report TR-89, KNMI, De Bilt, The Netherlands.
- [53] Zhang, M., W. Lin, C.S. Bretherton, J.J. Hack and P.J. Rasch (2003): *A modified formulation of fractional stratiform condensation rate in the NCAR Community Atmospheric Model (CAM2)*. *J. Geophys. Res.*, 108(D1). 4035,doi:10.1029/2002JD002523.



## A Results Onshore Locations

### A.1 Results Cabauw

**Table 48:** Overview results of measurements for the location Cabauw.

| <i>Measurements</i>  |       | Wind direction sector [deg] |      |      |      |      |      |       |       |       |      |      |      |       |
|----------------------|-------|-----------------------------|------|------|------|------|------|-------|-------|-------|------|------|------|-------|
| Par.                 | H [m] | 0                           | 30   | 60   | 90   | 120  | 150  | 180   | 210   | 240   | 270  | 300  | 330  | Total |
| A [m/s]              | 10    | 3.48                        | 3.51 | 3.63 | 3.81 | 3.79 | 4.03 | 4.96  | 5.75  | 6.28  | 4.77 | 4.41 | 3.98 | 4.56  |
|                      | 20    | 4.10                        | 4.12 | 4.16 | 4.41 | 4.38 | 4.64 | 5.64  | 6.52  | 6.94  | 5.51 | 4.94 | 4.51 | 5.20  |
|                      | 40    | 5.16                        | 5.38 | 5.31 | 5.44 | 5.30 | 5.61 | 6.47  | 7.47  | 7.63  | 6.54 | 6.08 | 5.57 | 6.22  |
|                      | 80    | 6.24                        | 6.66 | 6.76 | 6.95 | 6.89 | 7.19 | 8.29  | 8.97  | 8.73  | 8.06 | 7.35 | 6.84 | 7.78  |
|                      | 140   | 7.07                        | 7.37 | 7.79 | 8.21 | 8.24 | 8.40 | 9.76  | 10.67 | 10.12 | 9.08 | 8.31 | 7.76 | 9.01  |
|                      | 200   | 7.50                        | 7.63 | 8.25 | 8.88 | 8.86 | 8.76 | 10.44 | 11.83 | 11.33 | 9.71 | 8.90 | 8.35 | 9.71  |
| k [-]                | 10    | 1.72                        | 1.81 | 2.14 | 2.10 | 2.36 | 1.97 | 1.92  | 1.89  | 1.82  | 1.66 | 1.89 | 1.88 | 1.63  |
|                      | 20    | 1.81                        | 2.02 | 2.31 | 2.23 | 2.61 | 2.15 | 2.05  | 1.99  | 1.86  | 1.71 | 1.92 | 1.95 | 1.70  |
|                      | 40    | 2.11                        | 2.63 | 2.95 | 2.73 | 3.11 | 2.66 | 2.28  | 2.16  | 1.89  | 1.82 | 2.04 | 2.17 | 1.91  |
|                      | 80    | 2.43                        | 2.75 | 3.31 | 3.13 | 2.79 | 2.87 | 3.00  | 2.64  | 2.05  | 2.07 | 2.18 | 2.46 | 2.33  |
|                      | 140   | 2.45                        | 2.64 | 3.05 | 2.69 | 2.35 | 2.40 | 2.95  | 3.07  | 2.34  | 2.14 | 2.29 | 2.40 | 2.41  |
|                      | 200   | 2.31                        | 2.44 | 2.69 | 2.37 | 2.08 | 2.09 | 2.56  | 3.04  | 2.53  | 2.14 | 2.25 | 2.29 | 2.28  |
| f [%]                | 10    | 5.5                         | 6.1  | 6.3  | 6.9  | 5.8  | 6.1  | 11.4  | 15.7  | 12.6  | 9.3  | 7.6  | 6.5  | 100.0 |
|                      | 20    | 5.5                         | 5.9  | 6.1  | 6.7  | 6.3  | 5.9  | 10.9  | 15.4  | 13.3  | 9.5  | 7.6  | 6.7  | 100.0 |
|                      | 40    | 5.4                         | 6.0  | 6.5  | 7.0  | 5.9  | 5.7  | 9.7   | 15.7  | 14.1  | 9.5  | 7.6  | 6.8  | 100.0 |
|                      | 80    | 5.5                         | 5.8  | 6.3  | 7.3  | 5.7  | 5.5  | 8.7   | 15.5  | 15.2  | 9.8  | 8.0  | 6.9  | 100.0 |
|                      | 140   | 5.5                         | 5.7  | 5.9  | 7.3  | 5.6  | 5.1  | 8.6   | 15.3  | 15.8  | 10.3 | 8.0  | 6.9  | 100.0 |
|                      | 200   | 5.5                         | 5.7  | 5.7  | 7.1  | 5.6  | 5.0  | 7.4   | 13.8  | 17.2  | 11.1 | 8.8  | 7.2  | 100.0 |
| V <sub>m</sub> [m/s] | 10    | 3.17                        | 3.25 | 3.29 | 3.48 | 3.41 | 3.65 | 4.47  | 5.18  | 5.61  | 4.33 | 3.91 | 3.52 | 4.21  |
|                      | 20    | 3.80                        | 3.81 | 3.78 | 4.03 | 3.90 | 4.17 | 5.11  | 5.92  | 6.28  | 5.07 | 4.43 | 4.07 | 4.83  |
|                      | 40    | 4.65                        | 4.81 | 4.75 | 4.86 | 4.67 | 4.93 | 5.83  | 6.80  | 7.02  | 6.06 | 5.48 | 5.00 | 5.71  |
|                      | 80    | 5.53                        | 5.88 | 5.95 | 6.09 | 6.04 | 6.23 | 7.23  | 8.00  | 7.99  | 7.25 | 6.58 | 6.04 | 6.88  |
|                      | 140   | 6.21                        | 6.52 | 6.81 | 7.20 | 7.24 | 7.32 | 8.44  | 9.35  | 9.06  | 8.13 | 7.33 | 6.84 | 7.90  |
|                      | 200   | 6.63                        | 6.76 | 7.19 | 7.82 | 7.87 | 7.74 | 9.04  | 10.30 | 10.03 | 8.70 | 7.84 | 7.33 | 8.53  |

**Table 49:** Overview results of method 1: Charnock for the location Cabauw.

| <i>1:Charnock</i>    |       | Wind direction sector [deg] |      |      |      |      |      |      |       |       |      |      |      |       |
|----------------------|-------|-----------------------------|------|------|------|------|------|------|-------|-------|------|------|------|-------|
| Par.                 | H [m] | 0                           | 30   | 60   | 90   | 120  | 150  | 180  | 210   | 240   | 270  | 300  | 330  | Total |
| A [m/s]              | 10    | 4.04                        | 4.00 | 3.91 | 4.35 | 4.29 | 4.56 | 5.79 | 6.76  | 6.81  | 5.96 | 5.03 | 4.62 | 5.30  |
|                      | 20    | 4.48                        | 4.53 | 4.54 | 4.93 | 4.83 | 5.07 | 6.32 | 7.40  | 7.43  | 6.49 | 5.58 | 5.13 | 5.85  |
|                      | 40    | 5.06                        | 5.23 | 5.34 | 5.66 | 5.57 | 5.77 | 7.05 | 8.18  | 8.17  | 7.14 | 6.22 | 5.75 | 6.56  |
|                      | 80    | 5.77                        | 6.05 | 6.29 | 6.54 | 6.48 | 6.65 | 8.03 | 9.19  | 9.12  | 7.97 | 6.99 | 6.51 | 7.48  |
|                      | 140   | 6.42                        | 6.78 | 7.15 | 7.34 | 7.31 | 7.50 | 8.99 | 10.20 | 10.07 | 8.77 | 7.73 | 7.18 | 8.33  |
|                      | 200   | 6.85                        | 7.24 | 7.72 | 7.86 | 7.85 | 8.05 | 9.67 | 10.91 | 10.72 | 9.28 | 8.20 | 7.65 | 8.90  |
| k [-]                | 10    | 2.04                        | 2.12 | 2.08 | 2.24 | 2.16 | 1.89 | 2.00 | 2.27  | 2.06  | 1.98 | 2.10 | 2.12 | 1.81  |
|                      | 20    | 2.04                        | 2.19 | 2.22 | 2.30 | 2.32 | 2.01 | 1.99 | 2.23  | 1.99  | 1.91 | 2.07 | 2.13 | 1.81  |
|                      | 40    | 2.11                        | 2.38 | 2.47 | 2.42 | 2.52 | 2.15 | 2.04 | 2.23  | 1.96  | 1.88 | 2.06 | 2.18 | 1.85  |
|                      | 80    | 2.25                        | 2.58 | 2.72 | 2.51 | 2.58 | 2.26 | 2.14 | 2.31  | 2.01  | 1.90 | 2.07 | 2.25 | 1.95  |
|                      | 140   | 2.32                        | 2.68 | 2.83 | 2.51 | 2.50 | 2.27 | 2.23 | 2.44  | 2.08  | 1.93 | 2.08 | 2.23 | 2.02  |
|                      | 200   | 2.33                        | 2.63 | 2.82 | 2.43 | 2.37 | 2.22 | 2.29 | 2.53  | 2.13  | 1.94 | 2.05 | 2.21 | 2.04  |
| f [%]                | 10    | 5.4                         | 6.5  | 7.4  | 6.7  | 5.3  | 4.9  | 8.0  | 15.0  | 14.9  | 10.6 | 8.5  | 6.8  | 100.0 |
|                      | 20    | 5.4                         | 6.5  | 7.4  | 6.7  | 5.3  | 4.9  | 8.0  | 15.0  | 14.9  | 10.7 | 8.5  | 6.8  | 100.0 |
|                      | 40    | 5.4                         | 6.5  | 7.4  | 6.7  | 5.3  | 4.9  | 8.0  | 15.0  | 14.8  | 10.7 | 8.5  | 6.8  | 100.0 |
|                      | 80    | 5.4                         | 6.5  | 7.4  | 6.7  | 5.2  | 5.0  | 7.9  | 15.0  | 14.8  | 10.7 | 8.5  | 6.8  | 100.0 |
|                      | 140   | 5.4                         | 6.5  | 7.4  | 6.7  | 5.2  | 5.0  | 7.9  | 15.1  | 14.8  | 10.7 | 8.5  | 6.8  | 100.0 |
|                      | 200   | 5.4                         | 6.5  | 7.4  | 6.7  | 5.2  | 5.0  | 7.9  | 15.0  | 14.9  | 10.6 | 8.5  | 6.8  | 100.0 |
| V <sub>m</sub> [m/s] | 10    | 3.63                        | 3.56 | 3.55 | 3.87 | 3.84 | 4.08 | 5.18 | 6.01  | 6.09  | 5.31 | 4.45 | 4.09 | 4.80  |
|                      | 20    | 4.07                        | 4.06 | 4.12 | 4.41 | 4.32 | 4.53 | 5.70 | 6.62  | 6.71  | 5.86 | 4.98 | 4.57 | 5.34  |
|                      | 40    | 4.59                        | 4.65 | 4.79 | 5.06 | 4.95 | 5.11 | 6.37 | 7.36  | 7.44  | 6.51 | 5.58 | 5.13 | 5.99  |
|                      | 80    | 5.19                        | 5.33 | 5.58 | 5.82 | 5.73 | 5.86 | 7.20 | 8.26  | 8.30  | 7.26 | 6.29 | 5.78 | 6.77  |
|                      | 140   | 5.73                        | 5.95 | 6.29 | 6.51 | 6.45 | 6.56 | 8.00 | 9.09  | 9.10  | 7.97 | 6.94 | 6.37 | 7.49  |
|                      | 200   | 6.09                        | 6.36 | 6.78 | 6.97 | 6.94 | 7.05 | 8.54 | 9.68  | 9.65  | 8.44 | 7.37 | 6.77 | 7.98  |

## A.2 Results EWTW

**Table 50:** Overview results of measurements for the location EWTW.

| <i>Measurements</i>  |       | Wind direction sector [deg] |      |      |      |      |      |      |       |       |      |      |      |       |
|----------------------|-------|-----------------------------|------|------|------|------|------|------|-------|-------|------|------|------|-------|
| Par.                 | H [m] | 0                           | 30   | 60   | 90   | 120  | 150  | 180  | 210   | 240   | 270  | 300  | 330  | Total |
| A [m/s]              | 25    | 6.38                        | 6.66 | 6.18 | 6.50 | 6.12 | 5.99 | 6.36 | 6.29  | 7.10  | 6.82 | 6.16 | 6.11 | 6.45  |
|                      | 45    |                             |      |      |      |      |      |      |       |       |      |      |      | 7.31  |
|                      | 70    | 7.22                        | 7.58 | 6.47 | 7.89 | 7.85 | 7.75 | 7.94 | 8.68  | 8.98  | 8.06 | 6.67 | 7.69 | 7.96  |
|                      | 85    | 7.43                        | 7.40 | 6.45 | 7.51 | 7.65 | 7.93 | 8.99 | 9.47  | 9.75  | 8.68 | 7.43 | 7.85 | 8.46  |
|                      | 108   | 7.79                        | 7.34 | 7.04 | 7.95 | 8.03 | 8.53 | 9.71 | 10.40 | 10.11 | 9.27 | 8.22 | 8.56 | 9.05  |
| k [-]                | 25    | 2.35                        | 2.50 | 2.54 | 2.23 | 2.22 | 2.33 | 2.24 | 1.85  | 1.91  | 1.80 | 1.91 | 2.17 | 2.01  |
|                      | 45    |                             |      |      |      |      |      |      |       |       |      |      |      | 2.03  |
|                      | 70    | 2.16                        | 2.30 | 2.01 | 3.33 | 2.62 | 3.15 | 3.56 | 2.18  | 1.82  | 1.89 | 1.71 | 2.31 | 2.19  |
|                      | 85    | 2.27                        | 2.23 | 1.89 | 2.15 | 2.29 | 2.54 | 3.05 | 2.37  | 2.10  | 2.01 | 2.00 | 2.28 | 2.22  |
|                      | 108   | 2.25                        | 2.28 | 1.90 | 2.23 | 2.25 | 2.57 | 2.99 | 2.58  | 2.07  | 2.10 | 2.11 | 2.50 | 2.30  |
| f [%]                | 25    | 5.5                         | 6.1  | 6.7  | 7.3  | 5.2  | 5.5  | 9.7  | 14.5  | 14.4  | 10.6 | 7.3  | 7.2  | 100.0 |
|                      | 45    |                             |      |      |      |      |      |      |       |       |      |      |      | 100.0 |
|                      | 70    | 6.4                         | 6.1  | 8.3  | 7.0  | 5.4  | 6.0  | 8.2  | 12.7  | 12.2  | 10.0 | 9.1  | 8.4  | 100.0 |
|                      | 85    | 5.7                         | 5.8  | 6.6  | 7.5  | 5.3  | 5.3  | 8.5  | 14.1  | 14.9  | 10.8 | 8.1  | 7.4  | 100.0 |
|                      | 108   | 5.8                         | 5.9  | 6.6  | 7.2  | 5.3  | 5.2  | 8.1  | 13.5  | 15.4  | 11.1 | 8.7  | 7.2  | 100.0 |
| V <sub>m</sub> [m/s] | 25    | 5.75                        | 6.00 | 5.51 | 5.91 | 5.58 | 5.35 | 5.80 | 5.92  | 6.48  | 6.27 | 5.55 | 5.51 | 5.89  |
|                      | 45    |                             |      |      |      |      |      |      |       |       |      |      |      | 6.68  |
|                      | 70    | 6.53                        | 6.84 | 5.98 | 6.87 | 6.92 | 6.78 | 6.94 | 7.85  | 8.37  | 7.44 | 6.15 | 6.77 | 7.07  |
|                      | 85    | 6.71                        | 6.71 | 5.98 | 6.79 | 6.88 | 7.03 | 7.89 | 8.63  | 8.95  | 7.95 | 6.69 | 6.97 | 7.55  |
|                      | 108   | 7.02                        | 6.61 | 6.42 | 7.12 | 7.19 | 7.51 | 8.52 | 9.34  | 9.33  | 8.43 | 7.40 | 7.51 | 8.01  |

**Table 51:** Overview results of method 1: Charnock for the location EWTW.

| <i>1:Charnock</i>    |       | Wind direction sector [deg] |      |      |      |      |      |      |       |      |      |      |      |       |
|----------------------|-------|-----------------------------|------|------|------|------|------|------|-------|------|------|------|------|-------|
| Par.                 | H [m] | 0                           | 30   | 60   | 90   | 120  | 150  | 180  | 210   | 240  | 270  | 300  | 330  | Total |
| A [m/s]              | 25    | 6.08                        | 5.95 | 5.96 | 5.87 | 5.51 | 6.15 | 6.94 | 7.77  | 7.59 | 7.26 | 6.76 | 6.96 | 6.80  |
|                      | 45    | 6.62                        | 6.53 | 6.68 | 6.54 | 6.19 | 6.86 | 7.72 | 8.58  | 8.34 | 7.92 | 7.46 | 7.56 | 7.50  |
|                      | 70    | 7.02                        | 7.04 | 7.24 | 7.09 | 6.74 | 7.45 | 8.37 | 9.28  | 8.96 | 8.52 | 8.03 | 8.06 | 8.10  |
|                      | 85    | 7.21                        | 7.27 | 7.50 | 7.34 | 6.99 | 7.71 | 8.68 | 9.62  | 9.25 | 8.76 | 8.29 | 8.29 | 8.37  |
|                      | 108   | 7.44                        | 7.55 | 7.82 | 7.66 | 7.31 | 8.08 | 9.05 | 10.04 | 9.63 | 9.13 | 8.61 | 8.57 | 8.73  |
| k [-]                | 25    | 2.34                        | 2.48 | 2.56 | 2.31 | 2.26 | 2.35 | 2.30 | 2.33  | 2.12 | 2.00 | 2.19 | 2.31 | 2.13  |
|                      | 45    | 2.37                        | 2.59 | 2.78 | 2.46 | 2.41 | 2.42 | 2.42 | 2.38  | 2.12 | 2.00 | 2.24 | 2.32 | 2.18  |
|                      | 70    | 2.36                        | 2.72 | 2.92 | 2.58 | 2.47 | 2.47 | 2.50 | 2.46  | 2.14 | 2.04 | 2.28 | 2.35 | 2.24  |
|                      | 85    | 2.35                        | 2.78 | 2.97 | 2.61 | 2.50 | 2.46 | 2.55 | 2.50  | 2.14 | 2.03 | 2.30 | 2.35 | 2.26  |
|                      | 108   | 2.34                        | 2.83 | 3.01 | 2.65 | 2.51 | 2.47 | 2.56 | 2.56  | 2.15 | 2.06 | 2.30 | 2.34 | 2.29  |
| f [%]                | 25    | 6.2                         | 6.1  | 6.9  | 6.9  | 5.0  | 5.3  | 7.3  | 14.4  | 14.6 | 10.6 | 8.8  | 7.8  | 100.0 |
|                      | 45    | 6.2                         | 6.1  | 6.9  | 6.9  | 5.0  | 5.3  | 7.3  | 14.3  | 14.6 | 10.6 | 8.8  | 7.8  | 100.0 |
|                      | 70    | 6.2                         | 6.1  | 6.9  | 6.9  | 5.1  | 5.3  | 7.4  | 14.3  | 14.6 | 10.6 | 8.8  | 7.8  | 100.0 |
|                      | 85    | 6.2                         | 6.1  | 6.9  | 6.9  | 5.0  | 5.3  | 7.4  | 14.3  | 14.6 | 10.6 | 8.8  | 7.8  | 100.0 |
|                      | 108   | 6.2                         | 6.1  | 6.9  | 6.9  | 5.1  | 5.3  | 7.4  | 14.3  | 14.6 | 10.6 | 8.8  | 7.8  | 100.0 |
| V <sub>m</sub> [m/s] | 25    | 5.41                        | 5.26 | 5.29 | 5.29 | 4.92 | 5.43 | 6.21 | 7.01  | 6.88 | 6.60 | 6.04 | 6.08 | 6.10  |
|                      | 45    | 5.88                        | 5.77 | 5.88 | 5.86 | 5.49 | 6.06 | 6.88 | 7.75  | 7.59 | 7.24 | 6.63 | 6.61 | 6.72  |
|                      | 70    | 6.25                        | 6.19 | 6.35 | 6.33 | 5.97 | 6.60 | 7.43 | 8.37  | 8.16 | 7.76 | 7.12 | 7.04 | 7.23  |
|                      | 85    | 6.42                        | 6.38 | 6.58 | 6.54 | 6.20 | 6.84 | 7.70 | 8.65  | 8.43 | 8.01 | 7.34 | 7.23 | 7.47  |
|                      | 108   | 6.63                        | 6.61 | 6.86 | 6.81 | 6.47 | 7.16 | 8.03 | 9.01  | 8.77 | 8.31 | 7.63 | 7.49 | 7.77  |

## B Results Offshore Locations

### B.1 Results OWEZ

**Table 52:** Overview results of measurements for the location OWEZ.

| <i>Measurements</i>  |       | Wind direction sector [deg] |      |      |      |      |      |       |       |       |       |       |      |       |
|----------------------|-------|-----------------------------|------|------|------|------|------|-------|-------|-------|-------|-------|------|-------|
| Par.                 | H [m] | 0                           | 30   | 60   | 90   | 120  | 150  | 180   | 210   | 240   | 270   | 300   | 330  | Total |
| A [m/s]              | 21    | 7.38                        | 7.71 | 7.66 | 7.29 | 6.60 | 8.55 | 9.19  | 11.00 | 10.27 | 9.46  | 8.95  | 8.28 | 8.94  |
|                      | 70    | 7.78                        | 8.26 | 8.51 | 8.07 | 7.33 | 9.73 | 10.76 | 12.90 | 11.34 | 10.44 | 9.81  | 9.02 | 10.06 |
|                      | 116   | 8.50                        | 8.71 | 8.75 | 8.44 | 7.84 | 9.66 | 11.60 | 13.60 | 12.21 | 10.93 | 10.09 | 9.35 | 10.55 |
| k [-]                | 21    | 2.61                        | 2.61 | 2.66 | 2.40 | 2.19 | 2.77 | 2.37  | 2.99  | 2.88  | 2.59  | 2.50  | 2.18 | 2.36  |
|                      | 70    | 2.04                        | 2.47 | 2.88 | 2.63 | 2.34 | 2.89 | 2.47  | 2.92  | 2.58  | 2.48  | 2.42  | 2.12 | 2.27  |
|                      | 116   | 2.31                        | 2.61 | 2.74 | 2.63 | 2.32 | 2.48 | 2.42  | 2.71  | 2.49  | 2.33  | 2.37  | 2.09 | 2.18  |
| f [%]                | 21    | 5.8                         | 6.3  | 7.0  | 6.7  | 4.2  | 5.7  | 6.8   | 15.4  | 13.7  | 11.6  | 9.1   | 7.5  | 100.0 |
|                      | 70    | 4.7                         | 5.9  | 6.9  | 7.2  | 4.1  | 4.9  | 7.1   | 16.1  | 14.6  | 11.5  | 9.4   | 7.6  | 100.0 |
|                      | 116   | 5.6                         | 5.6  | 6.4  | 7.0  | 4.5  | 4.9  | 6.9   | 15.0  | 15.6  | 11.7  | 9.5   | 7.3  | 100.0 |
| V <sub>m</sub> [m/s] | 21    | 6.46                        | 6.80 | 6.85 | 6.61 | 5.97 | 7.44 | 8.16  | 9.69  | 9.00  | 8.27  | 7.86  | 7.35 | 7.92  |
|                      | 70    | 6.83                        | 7.25 | 7.49 | 7.20 | 6.52 | 8.48 | 9.38  | 11.36 | 9.98  | 9.12  | 8.63  | 7.98 | 8.88  |
|                      | 116   | 7.43                        | 7.58 | 7.74 | 7.55 | 6.99 | 8.39 | 10.12 | 11.94 | 10.82 | 9.61  | 8.89  | 8.26 | 9.34  |

**Table 53:** Overview results of method 1: Charnock for the location OWEZ.

| <i>1:Charnock</i>    |       | Wind direction sector [deg] |      |      |      |      |      |       |       |       |       |       |      |       |
|----------------------|-------|-----------------------------|------|------|------|------|------|-------|-------|-------|-------|-------|------|-------|
| Par.                 | H [m] | 0                           | 30   | 60   | 90   | 120  | 150  | 180   | 210   | 240   | 270   | 300   | 330  | Total |
| A [m/s]              | 21    | 8.54                        | 8.31 | 8.27 | 7.70 | 7.43 | 8.66 | 10.61 | 12.38 | 11.57 | 10.70 | 9.75  | 9.26 | 9.85  |
|                      | 70    | 8.89                        | 8.75 | 8.83 | 8.28 | 8.08 | 9.21 | 11.21 | 13.05 | 12.17 | 11.22 | 10.21 | 9.60 | 10.38 |
|                      | 116   | 9.03                        | 8.95 | 9.13 | 8.57 | 8.45 | 9.55 | 11.51 | 13.37 | 12.48 | 11.46 | 10.39 | 9.76 | 10.66 |
| k [-]                | 21    | 2.49                        | 2.72 | 2.78 | 2.39 | 2.39 | 2.33 | 2.38  | 2.62  | 2.30  | 2.22  | 2.27  | 2.11 | 2.11  |
|                      | 70    | 2.47                        | 2.81 | 2.87 | 2.51 | 2.52 | 2.35 | 2.39  | 2.57  | 2.28  | 2.24  | 2.23  | 2.07 | 2.11  |
|                      | 116   | 2.45                        | 2.80 | 2.91 | 2.54 | 2.62 | 2.38 | 2.38  | 2.55  | 2.26  | 2.23  | 2.21  | 2.06 | 2.12  |
| f [%]                | 21    | 6.4                         | 6.6  | 7.2  | 6.8  | 4.8  | 5.0  | 7.0   | 14.3  | 14.6  | 11.0  | 8.7   | 7.6  | 100.0 |
|                      | 70    | 6.4                         | 6.6  | 7.2  | 6.8  | 4.8  | 5.0  | 7.1   | 14.3  | 14.6  | 11.0  | 8.6   | 7.6  | 100.0 |
|                      | 116   | 6.4                         | 6.6  | 7.2  | 6.8  | 4.8  | 5.0  | 7.1   | 14.3  | 14.6  | 11.0  | 8.6   | 7.6  | 100.0 |
| V <sub>m</sub> [m/s] | 21    | 7.43                        | 7.26 | 7.28 | 6.94 | 6.55 | 7.59 | 9.33  | 10.92 | 10.31 | 9.48  | 8.65  | 8.20 | 8.78  |
|                      | 70    | 7.74                        | 7.60 | 7.79 | 7.43 | 7.10 | 8.11 | 9.87  | 11.53 | 10.88 | 9.93  | 9.05  | 8.51 | 9.27  |
|                      | 116   | 7.87                        | 7.79 | 8.05 | 7.68 | 7.39 | 8.39 | 10.17 | 11.84 | 11.17 | 10.15 | 9.23  | 8.66 | 9.51  |

**Table 54:** Overview results of method 2: Hsu IDW Shallow for the location OWEZ.

| <i>2:Hsu IDW Sha</i> |       | Wind direction sector [deg] |      |      |      |      |      |       |       |       |       |       |      |       |
|----------------------|-------|-----------------------------|------|------|------|------|------|-------|-------|-------|-------|-------|------|-------|
| Par.                 | H [m] | 0                           | 30   | 60   | 90   | 120  | 150  | 180   | 210   | 240   | 270   | 300   | 330  | Total |
| A [m/s]              | 21    | 8.77                        | 8.73 | 8.70 | 8.22 | 8.01 | 9.13 | 10.89 | 12.39 | 11.60 | 10.73 | 9.82  | 9.32 | 10.10 |
|                      | 70    | 9.01                        | 8.98 | 9.08 | 8.56 | 8.43 | 9.52 | 11.39 | 13.05 | 12.21 | 11.27 | 10.23 | 9.65 | 10.54 |
|                      | 116   | 9.14                        | 9.14 | 9.33 | 8.80 | 8.72 | 9.77 | 11.63 | 13.38 | 12.51 | 11.47 | 10.44 | 9.79 | 10.78 |
| k [-]                | 21    | 2.80                        | 2.95 | 2.96 | 2.63 | 2.68 | 2.56 | 2.65  | 2.96  | 2.59  | 2.44  | 2.48  | 2.27 | 2.38  |
|                      | 70    | 2.61                        | 2.93 | 2.95 | 2.59 | 2.68 | 2.48 | 2.57  | 2.78  | 2.43  | 2.36  | 2.34  | 2.17 | 2.26  |
|                      | 116   | 2.58                        | 2.89 | 2.97 | 2.61 | 2.73 | 2.46 | 2.49  | 2.73  | 2.38  | 2.33  | 2.31  | 2.14 | 2.24  |
| f [%]                | 21    | 6.4                         | 6.6  | 7.2  | 6.8  | 4.8  | 5.0  | 7.0   | 14.3  | 14.6  | 11.0  | 8.6   | 7.6  | 100.0 |
|                      | 70    | 6.4                         | 6.6  | 7.2  | 6.8  | 4.8  | 5.0  | 7.0   | 14.3  | 14.6  | 11.0  | 8.6   | 7.6  | 100.0 |
|                      | 116   | 6.4                         | 6.6  | 7.2  | 6.8  | 4.8  | 5.0  | 7.0   | 14.3  | 14.6  | 11.0  | 8.6   | 7.6  | 100.0 |
| V <sub>m</sub> [m/s] | 21    | 7.63                        | 7.66 | 7.71 | 7.38 | 7.02 | 8.02 | 9.59  | 10.96 | 10.30 | 9.53  | 8.74  | 8.27 | 8.97  |
|                      | 70    | 7.85                        | 7.83 | 8.05 | 7.69 | 7.39 | 8.37 | 10.03 | 11.54 | 10.86 | 9.95  | 9.09  | 8.56 | 9.37  |
|                      | 116   | 7.96                        | 7.97 | 8.24 | 7.89 | 7.61 | 8.60 | 10.29 | 11.83 | 11.15 | 10.15 | 9.27  | 8.68 | 9.58  |

**Table 55:** Overview results of method 3: Hsu IDW General for the location OWEZ.

| <i>3:Hsu IDW Gen</i> |       | Wind direction sector [deg] |      |      |      |      |      |       |       |       |       |       |      |       |
|----------------------|-------|-----------------------------|------|------|------|------|------|-------|-------|-------|-------|-------|------|-------|
| Par.                 | H [m] | 0                           | 30   | 60   | 90   | 120  | 150  | 180   | 210   | 240   | 270   | 300   | 330  | Total |
| A [m/s]              | 21    | 8.65                        | 8.60 | 8.54 | 8.09 | 7.86 | 8.95 | 10.67 | 12.13 | 11.37 | 10.56 | 9.70  | 9.23 | 9.93  |
|                      | 70    | 8.95                        | 8.90 | 9.00 | 8.49 | 8.35 | 9.42 | 11.23 | 12.87 | 12.05 | 11.14 | 10.14 | 9.58 | 10.43 |
|                      | 116   | 9.09                        | 9.06 | 9.26 | 8.73 | 8.65 | 9.69 | 11.52 | 13.24 | 12.38 | 11.39 | 10.37 | 9.75 | 10.70 |
| k [-]                | 21    | 2.78                        | 2.99 | 2.96 | 2.66 | 2.66 | 2.59 | 2.68  | 2.95  | 2.59  | 2.44  | 2.49  | 2.27 | 2.38  |
|                      | 70    | 2.61                        | 2.96 | 2.99 | 2.63 | 2.71 | 2.52 | 2.57  | 2.77  | 2.43  | 2.34  | 2.34  | 2.16 | 2.27  |
|                      | 116   | 2.57                        | 2.89 | 2.98 | 2.61 | 2.74 | 2.49 | 2.51  | 2.73  | 2.37  | 2.33  | 2.31  | 2.14 | 2.25  |
| f [%]                | 21    | 6.4                         | 6.6  | 7.2  | 6.8  | 4.8  | 5.0  | 7.0   | 14.3  | 14.6  | 11.0  | 8.6   | 7.6  | 100.0 |
|                      | 70    | 6.4                         | 6.6  | 7.2  | 6.8  | 4.8  | 5.0  | 7.0   | 14.3  | 14.6  | 11.0  | 8.6   | 7.6  | 100.0 |
|                      | 116   | 6.4                         | 6.6  | 7.2  | 6.8  | 4.8  | 5.0  | 7.0   | 14.3  | 14.6  | 11.0  | 8.6   | 7.6  | 100.0 |
| V <sub>m</sub> [m/s] | 21    | 7.53                        | 7.53 | 7.58 | 7.25 | 6.90 | 7.86 | 9.39  | 10.74 | 10.11 | 9.38  | 8.62  | 8.19 | 8.81  |
|                      | 70    | 7.79                        | 7.76 | 7.97 | 7.62 | 7.32 | 8.26 | 9.90  | 11.39 | 10.73 | 9.85  | 9.02  | 8.50 | 9.27  |
|                      | 116   | 7.92                        | 7.91 | 8.18 | 7.83 | 7.55 | 8.52 | 10.18 | 11.71 | 11.04 | 10.07 | 9.21  | 8.63 | 9.50  |

**Table 56:** Overview results of method 4: Hsu Cov Shallow for the location OWEZ.

| <i>4:Hsu Cov Sha</i> |       | Wind direction sector [deg] |      |      |      |      |      |       |       |       |       |       |      |       |
|----------------------|-------|-----------------------------|------|------|------|------|------|-------|-------|-------|-------|-------|------|-------|
| Par.                 | H [m] | 0                           | 30   | 60   | 90   | 120  | 150  | 180   | 210   | 240   | 270   | 300   | 330  | Total |
| A [m/s]              | 21    | 8.77                        | 8.73 | 8.64 | 8.17 | 7.93 | 9.08 | 10.92 | 12.45 | 11.66 | 10.76 | 9.85  | 9.33 | 10.11 |
|                      | 70    | 9.01                        | 8.98 | 9.06 | 8.53 | 8.39 | 9.50 | 11.40 | 13.09 | 12.26 | 11.29 | 10.25 | 9.66 | 10.55 |
|                      | 116   | 9.14                        | 9.14 | 9.32 | 8.76 | 8.68 | 9.75 | 11.64 | 13.42 | 12.54 | 11.50 | 10.44 | 9.80 | 10.79 |
| k [-]                | 21    | 2.78                        | 2.97 | 2.94 | 2.69 | 2.71 | 2.55 | 2.66  | 2.93  | 2.57  | 2.42  | 2.47  | 2.26 | 2.35  |
|                      | 70    | 2.61                        | 2.94 | 2.97 | 2.62 | 2.73 | 2.49 | 2.56  | 2.77  | 2.42  | 2.36  | 2.34  | 2.16 | 2.25  |
|                      | 116   | 2.58                        | 2.91 | 3.00 | 2.62 | 2.73 | 2.46 | 2.50  | 2.72  | 2.37  | 2.33  | 2.30  | 2.14 | 2.23  |
| f [%]                | 21    | 6.4                         | 6.6  | 7.2  | 6.8  | 4.8  | 5.0  | 7.0   | 14.3  | 14.6  | 11.0  | 8.6   | 7.6  | 100.0 |
|                      | 70    | 6.4                         | 6.6  | 7.2  | 6.8  | 4.8  | 5.0  | 7.0   | 14.3  | 14.6  | 11.0  | 8.6   | 7.6  | 100.0 |
|                      | 116   | 6.4                         | 6.6  | 7.2  | 6.8  | 4.8  | 5.0  | 7.0   | 14.3  | 14.6  | 11.0  | 8.6   | 7.6  | 100.0 |
| V <sub>m</sub> [m/s] | 21    | 7.63                        | 7.65 | 7.67 | 7.32 | 6.96 | 7.98 | 9.60  | 11.02 | 10.36 | 9.56  | 8.76  | 8.28 | 8.98  |
|                      | 70    | 7.85                        | 7.83 | 8.02 | 7.66 | 7.35 | 8.35 | 10.04 | 11.57 | 10.90 | 9.97  | 9.11  | 8.56 | 9.38  |
|                      | 116   | 7.96                        | 7.97 | 8.22 | 7.86 | 7.58 | 8.59 | 10.29 | 11.86 | 11.18 | 10.17 | 9.28  | 8.68 | 9.59  |

**Table 57:** Overview results of method 5: Hsu Cov General for the location OWEZ.

| <i>3:Hsu Cov Gen</i> |       | Wind direction sector [deg] |      |      |      |      |      |       |       |       |       |       |      |       |
|----------------------|-------|-----------------------------|------|------|------|------|------|-------|-------|-------|-------|-------|------|-------|
| Par.                 | H [m] | 0                           | 30   | 60   | 90   | 120  | 150  | 180   | 210   | 240   | 270   | 300   | 330  | Total |
| A [m/s]              | 21    | 8.67                        | 8.59 | 8.49 | 7.99 | 7.77 | 8.90 | 10.68 | 12.20 | 11.44 | 10.60 | 9.72  | 9.25 | 9.93  |
|                      | 70    | 8.95                        | 8.90 | 8.97 | 8.45 | 8.29 | 9.38 | 11.24 | 12.92 | 12.10 | 11.17 | 10.16 | 9.58 | 10.44 |
|                      | 116   | 9.09                        | 9.05 | 9.23 | 8.69 | 8.62 | 9.67 | 11.53 | 13.29 | 12.41 | 11.41 | 10.38 | 9.76 | 10.70 |
| k [-]                | 21    | 2.79                        | 3.01 | 2.97 | 2.66 | 2.70 | 2.58 | 2.67  | 2.93  | 2.56  | 2.42  | 2.47  | 2.26 | 2.36  |
|                      | 70    | 2.62                        | 2.97 | 3.00 | 2.66 | 2.72 | 2.52 | 2.56  | 2.76  | 2.42  | 2.33  | 2.33  | 2.15 | 2.25  |
|                      | 116   | 2.58                        | 2.89 | 2.99 | 2.62 | 2.78 | 2.49 | 2.51  | 2.73  | 2.37  | 2.33  | 2.30  | 2.14 | 2.23  |
| f [%]                | 21    | 6.4                         | 6.6  | 7.2  | 6.8  | 4.8  | 5.0  | 7.0   | 14.3  | 14.6  | 11.0  | 8.6   | 7.6  | 100.0 |
|                      | 70    | 6.4                         | 6.6  | 7.2  | 6.8  | 4.8  | 5.0  | 7.0   | 14.3  | 14.6  | 11.0  | 8.6   | 7.6  | 100.0 |
|                      | 116   | 6.4                         | 6.6  | 7.2  | 6.8  | 4.8  | 5.0  | 7.0   | 14.3  | 14.6  | 11.0  | 8.6   | 7.6  | 100.0 |
| V <sub>m</sub> [m/s] | 21    | 7.54                        | 7.52 | 7.53 | 7.19 | 6.83 | 7.82 | 9.40  | 10.80 | 10.17 | 9.42  | 8.64  | 8.20 | 8.83  |
|                      | 70    | 7.80                        | 7.75 | 7.94 | 7.58 | 7.27 | 8.24 | 9.91  | 11.43 | 10.77 | 9.87  | 9.03  | 8.51 | 9.28  |
|                      | 116   | 7.92                        | 7.90 | 8.16 | 7.80 | 7.52 | 8.50 | 10.19 | 11.74 | 11.08 | 10.09 | 9.22  | 8.64 | 9.51  |

## B.2 Results FINO-1

**Table 58:** Overview results of measurements for the location FINO-1.

| <i>Measurements</i>        |       | Wind direction sector [deg] |      |       |       |       |      |       |       |       |       |      |      |       |
|----------------------------|-------|-----------------------------|------|-------|-------|-------|------|-------|-------|-------|-------|------|------|-------|
| Par.                       | H [m] | 0                           | 30   | 60    | 90    | 120   | 150  | 180   | 210   | 240   | 270   | 300  | 330  | Total |
| <i>A</i> [m/s]             | 33.5  | 8.75                        | 8.10 | 9.49  | 9.71  | 8.46  | 8.56 | 9.76  | 11.80 | 10.88 | 10.67 | 9.44 | 7.01 | 9.70  |
|                            | 40    | 8.76                        | 8.27 | 9.98  | 10.23 | 9.30  | 9.26 | 10.29 | 12.82 | 11.86 | 11.33 | 9.13 | 7.40 | 10.33 |
|                            | 50    | 8.87                        | 8.47 | 9.70  | 10.08 | 7.88  | 8.22 | 10.29 | 12.56 | 11.43 | 11.04 | 8.93 | 7.35 | 10.24 |
|                            | 60    | 10.47                       | 8.38 | 10.48 | 10.97 | 10.04 | 9.81 | 10.62 | 12.90 | 11.87 | 11.02 | 9.16 | 7.77 | 10.62 |
|                            | 70    | 8.74                        | 4.60 | 9.66  | 10.77 | 9.55  | 9.60 | 10.76 | 12.91 | 11.90 | 11.35 | 9.64 | 6.93 | 10.58 |
|                            | 80    | 9.28                        | 8.78 | 10.46 | 11.14 | 10.34 | 9.97 | 11.19 | 14.05 | 13.15 | 12.23 | 8.81 | 8.64 | 11.21 |
|                            | 90    | 9.37                        | 8.66 | 10.35 | 11.00 | 9.85  | 9.79 | 11.18 | 13.53 | 12.43 | 11.76 | 8.10 | 8.49 | 10.79 |
|                            | 100   |                             |      |       |       |       |      |       |       |       |       |      |      |       |
| <i>k</i> [-]               | 33.5  | 2.29                        | 2.19 | 2.49  | 2.90  | 2.49  | 2.52 | 2.76  | 2.84  | 2.43  | 2.48  | 2.27 | 2.26 | 2.32  |
|                            | 40    | 2.35                        | 2.17 | 2.55  | 3.22  | 2.62  | 2.88 | 2.56  | 2.89  | 2.34  | 2.28  | 2.04 | 2.03 | 2.27  |
|                            | 50    | 2.26                        | 2.27 | 2.67  | 2.67  | 1.72  | 2.46 | 2.65  | 2.76  | 2.39  | 2.36  | 2.05 | 2.07 | 2.25  |
|                            | 60    | 2.40                        | 2.03 | 2.67  | 3.17  | 3.13  | 2.90 | 2.74  | 2.78  | 2.39  | 2.37  | 1.86 | 1.89 | 2.36  |
|                            | 70    | 2.20                        | 1.56 | 2.53  | 2.86  | 2.67  | 2.51 | 2.64  | 2.86  | 2.38  | 2.37  | 2.15 | 2.08 | 2.29  |
|                            | 80    | 2.24                        | 2.22 | 2.46  | 2.80  | 2.99  | 2.75 | 2.58  | 2.95  | 2.41  | 2.28  | 2.03 | 2.11 | 2.28  |
|                            | 90    | 2.26                        | 2.18 | 2.49  | 2.77  | 2.69  | 2.46 | 2.59  | 2.83  | 2.34  | 2.30  | 2.09 | 2.12 | 2.23  |
|                            | 100   |                             |      |       |       |       |      |       |       |       |       |      |      |       |
| <i>f</i> [%]               | 33.5  | 5.0                         | 4.8  | 6.7   | 8.0   | 5.8   | 6.3  | 7.3   | 13.1  | 13.0  | 11.2  | 10.4 | 8.4  | 100.0 |
|                            | 40    | 5.3                         | 4.6  | 5.9   | 7.8   | 5.9   | 7.1  | 8.4   | 15.0  | 12.7  | 10.5  | 9.4  | 7.5  | 100.0 |
|                            | 50    | 6.2                         | 4.1  | 6.0   | 6.5   | 0.4   | 2.6  | 9.5   | 15.8  | 15.5  | 13.0  | 11.6 | 8.9  | 100.0 |
|                            | 60    | 9.2                         | 5.0  | 6.4   | 7.8   | 6.0   | 6.8  | 7.9   | 12.9  | 11.8  | 10.0  | 8.8  | 7.3  | 100.0 |
|                            | 70    | 6.4                         | 0.1  | 0.4   | 9.8   | 6.5   | 7.1  | 8.3   | 14.7  | 14.6  | 12.3  | 11.0 | 8.8  | 100.0 |
|                            | 80    | 5.1                         | 4.3  | 5.2   | 7.4   | 6.3   | 7.0  | 8.5   | 15.3  | 12.7  | 10.6  | 9.7  | 7.9  | 100.0 |
|                            | 90    | 4.9                         | 4.6  | 5.9   | 7.9   | 6.0   | 6.2  | 7.9   | 13.8  | 13.9  | 11.3  | 9.9  | 7.6  | 100.0 |
|                            | 100   |                             |      |       |       |       |      |       |       |       |       |      |      |       |
| <i>V<sub>m</sub></i> [m/s] | 33.5  | 7.72                        | 7.27 | 8.43  | 8.51  | 7.49  | 7.57 | 8.56  | 10.43 | 9.72  | 9.43  | 8.41 | 6.22 | 8.60  |
|                            | 40    | 7.61                        | 7.32 | 8.78  | 8.92  | 8.20  | 8.17 | 9.12  | 11.33 | 10.58 | 10.00 | 8.14 | 6.64 | 9.13  |
|                            | 50    | 7.79                        | 7.49 | 8.48  | 8.83  | 7.06  | 7.19 | 9.01  | 11.08 | 10.22 | 9.78  | 8.00 | 6.55 | 9.05  |
|                            | 60    | 9.13                        | 7.43 | 9.18  | 9.60  | 8.75  | 8.61 | 9.28  | 11.35 | 10.59 | 9.69  | 8.27 | 7.05 | 9.33  |
|                            | 70    | 7.70                        | 4.20 | 8.43  | 9.38  | 8.37  | 8.46 | 9.41  | 11.36 | 10.66 | 10.08 | 8.56 | 6.20 | 9.33  |
|                            | 80    | 8.11                        | 7.78 | 9.18  | 9.74  | 9.02  | 8.80 | 9.88  | 12.39 | 11.73 | 10.83 | 7.92 | 7.72 | 9.88  |
|                            | 90    | 8.22                        | 7.71 | 9.07  | 9.60  | 8.64  | 8.60 | 9.79  | 11.88 | 11.16 | 10.42 | 7.27 | 7.57 | 9.55  |
|                            | 100   |                             |      |       |       |       |      |       |       |       |       |      |      |       |

**Table 59:** Overview results of method 1: Charnock for the location FINO-1.

| <i>1:Charnock</i>    |       | Wind direction sector [deg] |      |      |       |      |      |       |       |       |       |       |       |       |
|----------------------|-------|-----------------------------|------|------|-------|------|------|-------|-------|-------|-------|-------|-------|-------|
| Par.                 | H [m] | 0                           | 30   | 60   | 90    | 120  | 150  | 180   | 210   | 240   | 270   | 300   | 330   | Total |
| A [m/s]              | 33.5  | 7.95                        | 7.51 | 8.62 | 9.06  | 8.55 | 8.62 | 9.57  | 11.72 | 11.30 | 10.35 | 10.08 | 9.75  | 9.81  |
|                      | 40    | 8.03                        | 7.61 | 8.78 | 9.25  | 8.73 | 8.77 | 9.73  | 11.90 | 11.45 | 10.48 | 10.18 | 9.85  | 9.95  |
|                      | 50    | 8.15                        | 7.73 | 9.01 | 9.47  | 8.96 | 8.95 | 9.92  | 12.12 | 11.67 | 10.65 | 10.32 | 9.97  | 10.13 |
|                      | 60    | 8.24                        | 7.83 | 9.15 | 9.68  | 9.14 | 9.09 | 10.09 | 12.30 | 11.84 | 10.79 | 10.42 | 10.06 | 10.28 |
|                      | 70    | 8.33                        | 7.92 | 9.29 | 9.84  | 9.31 | 9.22 | 10.24 | 12.45 | 11.98 | 10.91 | 10.51 | 10.14 | 10.41 |
|                      | 80    | 8.40                        | 7.98 | 9.43 | 9.99  | 9.43 | 9.32 | 10.37 | 12.58 | 12.11 | 11.01 | 10.59 | 10.22 | 10.53 |
|                      | 90    | 8.46                        | 8.04 | 9.55 | 10.10 | 9.55 | 9.44 | 10.49 | 12.70 | 12.23 | 11.10 | 10.65 | 10.28 | 10.63 |
|                      | 100   | 8.53                        | 8.10 | 9.64 | 10.22 | 9.67 | 9.53 | 10.59 | 12.80 | 12.34 | 11.17 | 10.71 | 10.34 | 10.73 |
| k [-]                | 33.5  | 2.10                        | 2.13 | 2.20 | 2.76  | 2.27 | 2.38 | 2.33  | 2.63  | 2.34  | 2.28  | 2.24  | 2.35  | 2.21  |
|                      | 40    | 2.10                        | 2.15 | 2.23 | 2.80  | 2.32 | 2.41 | 2.36  | 2.64  | 2.33  | 2.27  | 2.24  | 2.35  | 2.21  |
|                      | 50    | 2.12                        | 2.16 | 2.30 | 2.83  | 2.39 | 2.43 | 2.38  | 2.66  | 2.33  | 2.26  | 2.23  | 2.35  | 2.22  |
|                      | 60    | 2.13                        | 2.16 | 2.32 | 2.87  | 2.43 | 2.43 | 2.42  | 2.68  | 2.32  | 2.26  | 2.22  | 2.35  | 2.23  |
|                      | 70    | 2.14                        | 2.17 | 2.35 | 2.88  | 2.48 | 2.44 | 2.43  | 2.68  | 2.32  | 2.25  | 2.22  | 2.35  | 2.24  |
|                      | 80    | 2.16                        | 2.16 | 2.39 | 2.89  | 2.50 | 2.44 | 2.45  | 2.69  | 2.31  | 2.25  | 2.22  | 2.36  | 2.25  |
|                      | 90    | 2.17                        | 2.17 | 2.42 | 2.86  | 2.52 | 2.46 | 2.46  | 2.69  | 2.30  | 2.24  | 2.21  | 2.36  | 2.26  |
|                      | 100   | 2.19                        | 2.16 | 2.43 | 2.86  | 2.55 | 2.48 | 2.47  | 2.68  | 2.30  | 2.23  | 2.21  | 2.37  | 2.26  |
| f [%]                | 33.5  | 5.7                         | 4.8  | 5.8  | 7.2   | 6.2  | 5.5  | 6.2   | 11.5  | 14.0  | 12.6  | 11.3  | 9.1   | 100.0 |
|                      | 40    | 5.7                         | 4.8  | 5.8  | 7.2   | 6.2  | 5.5  | 6.2   | 11.5  | 14.0  | 12.6  | 11.3  | 9.1   | 100.0 |
|                      | 50    | 5.7                         | 4.8  | 5.8  | 7.2   | 6.2  | 5.5  | 6.2   | 11.5  | 14.0  | 12.6  | 11.3  | 9.1   | 100.0 |
|                      | 60    | 5.7                         | 4.8  | 5.8  | 7.2   | 6.2  | 5.5  | 6.2   | 11.5  | 14.0  | 12.6  | 11.3  | 9.1   | 100.0 |
|                      | 70    | 5.7                         | 4.8  | 5.8  | 7.2   | 6.2  | 5.5  | 6.2   | 11.5  | 14.0  | 12.6  | 11.3  | 9.1   | 100.0 |
|                      | 80    | 5.7                         | 4.8  | 5.8  | 7.2   | 6.2  | 5.5  | 6.2   | 11.5  | 14.0  | 12.6  | 11.3  | 9.1   | 100.0 |
|                      | 90    | 5.7                         | 4.8  | 5.8  | 7.2   | 6.2  | 5.5  | 6.2   | 11.5  | 14.0  | 12.6  | 11.3  | 9.1   | 100.0 |
|                      | 100   | 5.7                         | 4.8  | 5.8  | 7.2   | 6.2  | 5.5  | 6.2   | 11.5  | 14.0  | 12.6  | 11.3  | 9.1   | 100.0 |
| V <sub>m</sub> [m/s] | 33.5  | 7.12                        | 6.73 | 7.72 | 7.95  | 7.61 | 7.56 | 8.45  | 10.31 | 10.09 | 9.20  | 8.99  | 8.61  | 8.73  |
|                      | 40    | 7.19                        | 6.82 | 7.84 | 8.10  | 7.75 | 7.68 | 8.58  | 10.47 | 10.24 | 9.33  | 9.09  | 8.69  | 8.85  |
|                      | 50    | 7.29                        | 6.92 | 8.00 | 8.29  | 7.92 | 7.84 | 8.74  | 10.66 | 10.44 | 9.48  | 9.21  | 8.79  | 9.00  |
|                      | 60    | 7.36                        | 7.02 | 8.12 | 8.45  | 8.06 | 7.98 | 8.88  | 10.82 | 10.60 | 9.61  | 9.31  | 8.88  | 9.13  |
|                      | 70    | 7.43                        | 7.09 | 8.22 | 8.60  | 8.18 | 8.09 | 9.00  | 10.95 | 10.74 | 9.72  | 9.39  | 8.94  | 9.24  |
|                      | 80    | 7.48                        | 7.15 | 8.32 | 8.73  | 8.28 | 8.18 | 9.11  | 11.07 | 10.87 | 9.82  | 9.47  | 9.00  | 9.34  |
|                      | 90    | 7.52                        | 7.21 | 8.40 | 8.83  | 8.38 | 8.27 | 9.20  | 11.18 | 10.98 | 9.90  | 9.53  | 9.06  | 9.42  |
|                      | 100   | 7.56                        | 7.26 | 8.47 | 8.93  | 8.47 | 8.34 | 9.28  | 11.27 | 11.08 | 9.97  | 9.58  | 9.11  | 9.50  |

### B.3 Results Europlatform

**Table 60:** Overview results of measurements for the location Europlatform.

| <i>Measurements</i>  |       | Wind direction sector [deg] |      |      |      |      |      |      |       |       |      |      |      |       |
|----------------------|-------|-----------------------------|------|------|------|------|------|------|-------|-------|------|------|------|-------|
| Par.                 | H [m] | 0                           | 30   | 60   | 90   | 120  | 150  | 180  | 210   | 240   | 270  | 300  | 330  | Total |
| A [m/s]              | 29.1  | 7.95                        | 7.49 | 7.39 | 7.15 | 6.52 | 6.77 | 8.87 | 10.01 | 10.03 | 8.91 | 9.02 | 9.14 | 8.88  |
| k [-]                | 29.1  | 2.43                        | 2.57 | 2.74 | 2.28 | 2.00 | 2.00 | 2.19 | 2.41  | 2.52  | 1.99 | 2.44 | 2.49 | 2.41  |
| f [%]                | 29.1  | 5.1                         | 7.1  | 7.8  | 6.1  | 5.2  | 4.9  | 8.0  | 15.0  | 15.6  | 10.0 | 8.0  | 7.3  | 100.0 |
| V <sub>m</sub> [m/s] | 29.1  | 6.69                        | 6.53 | 6.44 | 6.34 | 6.01 | 6.12 | 7.93 | 8.99  | 8.91  | 8.14 | 7.76 | 7.80 | 7.67  |

**Table 61:** Overview results of method 1: Charnock for the location Europlatform.

| <i>1:Charnock</i>    |       | Wind direction sector [deg] |      |      |      |      |      |      |      |      |      |      |      |       |
|----------------------|-------|-----------------------------|------|------|------|------|------|------|------|------|------|------|------|-------|
| Par.                 | H [m] | 0                           | 30   | 60   | 90   | 120  | 150  | 180  | 210  | 240  | 270  | 300  | 330  | Total |
| A [m/s]              | 29.1  | 7.17                        | 6.84 | 6.73 | 6.75 | 5.96 | 6.30 | 8.38 | 9.64 | 9.52 | 8.81 | 8.12 | 8.10 | 8.04  |
| k [-]                | 29.1  | 2.25                        | 2.31 | 2.23 | 2.32 | 2.09 | 1.97 | 2.07 | 2.31 | 2.36 | 2.05 | 2.08 | 2.10 | 2.02  |
| f [%]                | 29.1  | 6.9                         | 7.3  | 7.3  | 6.8  | 4.7  | 4.4  | 7.2  | 13.1 | 16.0 | 10.7 | 8.5  | 7.0  | 100.0 |
| V <sub>m</sub> [m/s] | 29.1  | 6.28                        | 5.98 | 5.95 | 5.94 | 5.32 | 5.64 | 7.42 | 8.49 | 8.40 | 7.85 | 7.19 | 7.10 | 7.15  |

**Table 62:** Overview results of method 2: Hsu IDW Shallow for the location Europlatform.

| <i>2:Hsu IDW Sha</i> |       | Wind direction sector [deg] |      |      |      |      |      |      |      |      |      |      |      |       |
|----------------------|-------|-----------------------------|------|------|------|------|------|------|------|------|------|------|------|-------|
| Par.                 | H [m] | 0                           | 30   | 60   | 90   | 120  | 150  | 180  | 210  | 240  | 270  | 300  | 330  | Total |
| A [m/s]              | 29.1  | 7.27                        | 7.01 | 6.95 | 6.95 | 6.19 | 6.59 | 8.58 | 9.74 | 9.62 | 8.90 | 8.18 | 8.15 | 8.20  |
| k [-]                | 29.1  | 2.39                        | 2.45 | 2.38 | 2.50 | 2.20 | 2.12 | 2.25 | 2.52 | 2.58 | 2.19 | 2.17 | 2.19 | 2.16  |
| f [%]                | 29.1  | 6.9                         | 7.4  | 7.3  | 6.8  | 4.7  | 4.4  | 7.3  | 13.1 | 16.0 | 10.7 | 8.5  | 7.0  | 100.0 |
| V <sub>m</sub> [m/s] | 29.1  | 6.35                        | 6.12 | 6.11 | 6.10 | 5.51 | 5.85 | 7.55 | 8.58 | 8.49 | 7.89 | 7.24 | 7.14 | 7.25  |

**Table 63:** Overview results of method 3: Hsu IDW General for the location Europlatform.

| <i>3:Hsu IDW Gen</i> |       | Wind direction sector [deg] |      |      |      |      |      |      |      |      |      |      |      |       |
|----------------------|-------|-----------------------------|------|------|------|------|------|------|------|------|------|------|------|-------|
| Par.                 | H [m] | 0                           | 30   | 60   | 90   | 120  | 150  | 180  | 210  | 240  | 270  | 300  | 330  | Total |
| A [m/s]              | 29.1  | 7.21                        | 6.93 | 6.86 | 6.87 | 6.11 | 6.47 | 8.43 | 9.55 | 9.44 | 8.78 | 8.10 | 8.08 | 8.08  |
| k [-]                | 29.1  | 2.38                        | 2.44 | 2.37 | 2.48 | 2.21 | 2.12 | 2.25 | 2.49 | 2.57 | 2.18 | 2.16 | 2.18 | 2.17  |
| f [%]                | 29.1  | 6.9                         | 7.3  | 7.3  | 6.8  | 4.7  | 4.4  | 7.3  | 13.1 | 16.0 | 10.7 | 8.5  | 7.0  | 100.0 |
| V <sub>m</sub> [m/s] | 29.1  | 6.30                        | 6.06 | 6.04 | 6.03 | 5.44 | 5.75 | 7.43 | 8.42 | 8.34 | 7.80 | 7.18 | 7.09 | 7.16  |

**Table 64:** Overview results of method 4: Hsu Cov Shallow for the location Europlatform.

| <i>4:Hsu Cov Sha</i> |       | Wind direction sector [deg] |      |      |      |      |      |      |      |      |      |      |      |       |
|----------------------|-------|-----------------------------|------|------|------|------|------|------|------|------|------|------|------|-------|
| Par.                 | H [m] | 0                           | 30   | 60   | 90   | 120  | 150  | 180  | 210  | 240  | 270  | 300  | 330  | Total |
| A [m/s]              | 29.1  | 7.28                        | 7.02 | 6.95 | 6.95 | 6.19 | 6.58 | 8.59 | 9.76 | 9.64 | 8.90 | 8.17 | 8.15 | 8.20  |
| k [-]                | 29.1  | 2.40                        | 2.44 | 2.37 | 2.49 | 2.20 | 2.11 | 2.24 | 2.50 | 2.57 | 2.18 | 2.16 | 2.18 | 2.16  |
| f [%]                | 29.1  | 6.9                         | 7.4  | 7.3  | 6.8  | 4.7  | 4.4  | 7.3  | 13.1 | 16.0 | 10.7 | 8.5  | 7.0  | 100.0 |
| V <sub>m</sub> [m/s] | 29.1  | 6.35                        | 6.13 | 6.12 | 6.10 | 5.51 | 5.84 | 7.56 | 8.60 | 8.51 | 7.89 | 7.23 | 7.14 | 7.26  |

**Table 65:** Overview results of method 5: Hsu Cov General for the location Europlatform.

| <i>3:Hsu Cov Gen</i> |       | Wind direction sector [deg] |      |      |      |      |      |      |      |      |      |      |      |       |
|----------------------|-------|-----------------------------|------|------|------|------|------|------|------|------|------|------|------|-------|
| Par.                 | H [m] | 0                           | 30   | 60   | 90   | 120  | 150  | 180  | 210  | 240  | 270  | 300  | 330  | Total |
| A [m/s]              | 29.1  | 7.22                        | 6.94 | 6.86 | 6.87 | 6.10 | 6.45 | 8.44 | 9.58 | 9.47 | 8.79 | 8.10 | 8.08 | 8.09  |
| k [-]                | 29.1  | 2.38                        | 2.43 | 2.35 | 2.47 | 2.20 | 2.10 | 2.24 | 2.49 | 2.57 | 2.18 | 2.16 | 2.18 | 2.16  |
| f [%]                | 29.1  | 6.9                         | 7.4  | 7.3  | 6.8  | 4.7  | 4.4  | 7.3  | 13.1 | 16.0 | 10.7 | 8.5  | 7.0  | 100.0 |
| V <sub>m</sub> [m/s] | 29.1  | 6.30                        | 6.06 | 6.05 | 6.03 | 5.43 | 5.74 | 7.44 | 8.44 | 8.36 | 7.80 | 7.17 | 7.08 | 7.16  |

## B.4 Results K13- $\alpha$

**Table 66:** Overview results of measurements for the location K13- $\alpha$ .

| <i>Measurements</i>  |       | Wind direction sector [deg] |      |      |      |      |      |      |       |       |      |      |      |       |
|----------------------|-------|-----------------------------|------|------|------|------|------|------|-------|-------|------|------|------|-------|
| Par.                 | H [m] | 0                           | 30   | 60   | 90   | 120  | 150  | 180  | 210   | 240   | 270  | 300  | 330  | Total |
| A [m/s]              | 73.8  | 8.46                        | 7.70 | 8.28 | 8.69 | 7.97 | 7.73 | 9.12 | 10.31 | 10.45 | 9.76 | 9.43 | 9.07 | 9.45  |
| k [-]                | 73.8  | 2.57                        | 2.31 | 2.58 | 2.63 | 2.45 | 2.31 | 2.46 | 2.31  | 2.91  | 2.24 | 2.83 | 2.33 | 2.63  |
| f [%]                | 73.8  | 4.7                         | 5.3  | 5.7  | 7.0  | 5.9  | 5.3  | 8.7  | 13.3  | 14.5  | 11.8 | 9.3  | 8.5  | 100.0 |
| V <sub>m</sub> [m/s] | 73.8  | 7.01                        | 6.67 | 7.16 | 7.55 | 6.83 | 6.65 | 7.81 | 9.25  | 8.95  | 8.64 | 7.99 | 7.81 | 8.01  |

**Table 67:** Overview results of method 1: Charnock for the location K13- $\alpha$ .

| <i>1:Charnock</i>    |       | Wind direction sector [deg] |      |      |      |      |      |      |      |      |      |      |      |       |
|----------------------|-------|-----------------------------|------|------|------|------|------|------|------|------|------|------|------|-------|
| Par.                 | H [m] | 0                           | 30   | 60   | 90   | 120  | 150  | 180  | 210  | 240  | 270  | 300  | 330  | Total |
| A [m/s]              | 73.8  | 7.06                        | 7.01 | 7.23 | 7.27 | 6.59 | 6.84 | 8.13 | 9.40 | 9.65 | 9.11 | 8.48 | 8.50 | 8.29  |
| k [-]                | 73.8  | 2.07                        | 2.33 | 2.36 | 2.39 | 2.10 | 1.99 | 1.96 | 2.21 | 2.33 | 2.09 | 2.23 | 2.19 | 2.07  |
| f [%]                | 73.8  | 6.4                         | 5.4  | 5.9  | 6.5  | 5.6  | 5.2  | 8.5  | 13.9 | 13.9 | 11.5 | 9.3  | 7.9  | 100.0 |
| V <sub>m</sub> [m/s] | 73.8  | 6.32                        | 6.13 | 6.36 | 6.37 | 5.88 | 6.06 | 7.36 | 8.41 | 8.55 | 8.20 | 7.52 | 7.44 | 7.38  |

**Table 68:** Overview results of method 2: Hsu IDW Shallow for the location K13- $\alpha$ .

| <i>2:Hsu IDW Sha</i>       |       | Wind direction sector [deg] |      |      |      |      |      |      |      |      |      |      |      |       |
|----------------------------|-------|-----------------------------|------|------|------|------|------|------|------|------|------|------|------|-------|
| Par.                       | H [m] | 0                           | 30   | 60   | 90   | 120  | 150  | 180  | 210  | 240  | 270  | 300  | 330  | Total |
| A [m/s]                    | 73.8  | 7.13                        | 7.09 | 7.37 | 7.45 | 6.80 | 7.03 | 8.36 | 9.55 | 9.69 | 9.18 | 8.51 | 8.52 | 8.42  |
| <i>k</i> [-]               | 73.8  | 2.18                        | 2.43 | 2.47 | 2.55 | 2.23 | 2.10 | 2.16 | 2.45 | 2.50 | 2.24 | 2.34 | 2.30 | 2.24  |
| <i>f</i> [%]               | 73.8  | 6.4                         | 5.4  | 5.9  | 6.5  | 5.6  | 5.2  | 8.5  | 13.9 | 13.9 | 11.5 | 9.3  | 7.9  | 100.0 |
| <i>V<sub>m</sub></i> [m/s] | 73.8  | 6.36                        | 6.20 | 6.49 | 6.51 | 6.03 | 6.20 | 7.48 | 8.49 | 8.58 | 8.23 | 7.54 | 7.44 | 7.45  |

**Table 69:** Overview results of method 3: Hsu IDW General for the location K13- $\alpha$ .

| <i>3:Hsu IDW Gen</i>       |       | Wind direction sector [deg] |      |      |      |      |      |      |      |      |      |      |      |       |
|----------------------------|-------|-----------------------------|------|------|------|------|------|------|------|------|------|------|------|-------|
| Par.                       | H [m] | 0                           | 30   | 60   | 90   | 120  | 150  | 180  | 210  | 240  | 270  | 300  | 330  | Total |
| A [m/s]                    | 73.8  | 7.07                        | 7.03 | 7.29 | 7.36 | 6.71 | 6.93 | 8.22 | 9.37 | 9.55 | 9.07 | 8.43 | 8.45 | 8.31  |
| <i>k</i> [-]               | 73.8  | 2.17                        | 2.43 | 2.47 | 2.55 | 2.23 | 2.11 | 2.15 | 2.43 | 2.51 | 2.25 | 2.34 | 2.30 | 2.24  |
| <i>f</i> [%]               | 73.8  | 6.4                         | 5.4  | 5.9  | 6.5  | 5.6  | 5.2  | 8.5  | 13.9 | 13.9 | 11.5 | 9.3  | 7.9  | 100.0 |
| <i>V<sub>m</sub></i> [m/s] | 73.8  | 6.31                        | 6.15 | 6.41 | 6.43 | 5.96 | 6.11 | 7.36 | 8.35 | 8.46 | 8.13 | 7.47 | 7.38 | 7.36  |

**Table 70:** Overview results of method 4: Hsu Cov Shallow for the location K13- $\alpha$ .

| <i>4:Hsu Cov Sha</i>       |       | Wind direction sector [deg] |      |      |      |      |      |      |      |      |      |      |      |       |
|----------------------------|-------|-----------------------------|------|------|------|------|------|------|------|------|------|------|------|-------|
| Par.                       | H [m] | 0                           | 30   | 60   | 90   | 120  | 150  | 180  | 210  | 240  | 270  | 300  | 330  | Total |
| A [m/s]                    | 73.8  | 7.13                        | 7.09 | 7.37 | 7.46 | 6.80 | 7.04 | 8.38 | 9.57 | 9.69 | 9.18 | 8.51 | 8.52 | 8.43  |
| <i>k</i> [-]               | 73.8  | 2.17                        | 2.43 | 2.46 | 2.53 | 2.21 | 2.08 | 2.14 | 2.43 | 2.50 | 2.24 | 2.34 | 2.30 | 2.23  |
| <i>f</i> [%]               | 73.8  | 6.4                         | 5.4  | 5.9  | 6.5  | 5.6  | 5.2  | 8.5  | 13.9 | 13.9 | 11.5 | 9.3  | 7.9  | 100.0 |
| <i>V<sub>m</sub></i> [m/s] | 73.8  | 6.35                        | 6.20 | 6.49 | 6.51 | 6.04 | 6.22 | 7.51 | 8.51 | 8.58 | 8.22 | 7.54 | 7.44 | 7.46  |

**Table 71:** Overview results of method 5: Hsu Cov General for the location K13- $\alpha$ .

| <i>3:Hsu Cov Gen</i>       |       | Wind direction sector [deg] |      |      |      |      |      |      |      |      |      |      |      |       |
|----------------------------|-------|-----------------------------|------|------|------|------|------|------|------|------|------|------|------|-------|
| Par.                       | H [m] | 0                           | 30   | 60   | 90   | 120  | 150  | 180  | 210  | 240  | 270  | 300  | 330  | Total |
| A [m/s]                    | 73.8  | 7.06                        | 7.03 | 7.28 | 7.37 | 6.71 | 6.94 | 8.25 | 9.40 | 9.55 | 9.07 | 8.43 | 8.45 | 8.32  |
| <i>k</i> [-]               | 73.8  | 2.16                        | 2.42 | 2.46 | 2.54 | 2.21 | 2.09 | 2.14 | 2.42 | 2.50 | 2.25 | 2.34 | 2.30 | 2.23  |
| <i>f</i> [%]               | 73.8  | 6.4                         | 5.4  | 5.9  | 6.5  | 5.6  | 5.2  | 8.5  | 13.9 | 13.9 | 11.5 | 9.3  | 7.9  | 100.0 |
| <i>V<sub>m</sub></i> [m/s] | 73.8  | 6.31                        | 6.15 | 6.41 | 6.44 | 5.97 | 6.13 | 7.39 | 8.37 | 8.46 | 8.12 | 7.47 | 7.38 | 7.36  |

## B.5 Results Noordwijk

**Table 72:** Overview results of measurements for the location Noordwijk.

| <i>Measurements</i>        |       | Wind direction sector [deg] |      |      |      |      |      |      |      |       |      |      |      |       |
|----------------------------|-------|-----------------------------|------|------|------|------|------|------|------|-------|------|------|------|-------|
| Par.                       | H [m] | 0                           | 30   | 60   | 90   | 120  | 150  | 180  | 210  | 240   | 270  | 300  | 330  | Total |
| A [m/s]                    | 27.6  | 7.19                        | 6.70 | 6.61 | 6.60 | 6.36 | 6.10 | 7.04 | 9.88 | 10.10 | 8.95 | 8.96 | 8.64 | 7.88  |
| <i>k</i> [-]               | 27.6  | 2.05                        | 2.61 | 2.16 | 2.51 | 2.80 | 2.59 | 2.22 | 2.58 | 2.79  | 2.22 | 2.29 | 2.18 | 1.92  |
| <i>f</i> [%]               | 27.6  | 5.7                         | 6.1  | 6.6  | 6.9  | 7.0  | 5.6  | 6.1  | 12.3 | 16.1  | 9.4  | 8.7  | 9.4  | 100.0 |
| <i>V<sub>m</sub></i> [m/s] | 27.6  | 6.30                        | 5.72 | 6.10 | 5.78 | 5.58 | 5.41 | 6.34 | 8.64 | 8.74  | 7.85 | 7.70 | 7.49 | 7.18  |

**Table 73:** Overview results of method 1: Charnock for the location Noordwijk.

| <i>1:Charnock</i>          |       | Wind direction sector [deg] |      |      |      |      |      |      |      |       |      |      |      |       |
|----------------------------|-------|-----------------------------|------|------|------|------|------|------|------|-------|------|------|------|-------|
| Par.                       | H [m] | 0                           | 30   | 60   | 90   | 120  | 150  | 180  | 210  | 240   | 270  | 300  | 330  | Total |
| A [m/s]                    | 27.6  | 6.92                        | 6.21 | 6.70 | 6.88 | 6.37 | 6.48 | 8.40 | 9.97 | 10.54 | 9.17 | 8.66 | 7.94 | 8.16  |
| <i>k</i> [-]               | 27.6  | 2.24                        | 2.15 | 2.30 | 2.48 | 2.26 | 2.06 | 2.26 | 2.22 | 2.34  | 1.93 | 2.06 | 1.96 | 1.90  |
| <i>f</i> [%]               | 27.6  | 7.4                         | 6.7  | 6.7  | 7.2  | 5.8  | 5.0  | 7.3  | 11.0 | 15.0  | 10.3 | 9.4  | 8.2  | 100.0 |
| <i>V<sub>m</sub></i> [m/s] | 27.6  | 6.04                        | 5.48 | 5.98 | 6.04 | 5.62 | 5.76 | 7.39 | 8.82 | 9.24  | 8.18 | 7.60 | 7.01 | 7.29  |

**Table 74:** Overview results of method 2: Hsu IDW Shallow for the location Noordwijk.

| <b>2:Hsu IDW Sha</b> |              | <b>Wind direction sector [deg]</b> |      |      |      |      |      |      |       |       |      |      |      |       |
|----------------------|--------------|------------------------------------|------|------|------|------|------|------|-------|-------|------|------|------|-------|
| <b>Par.</b>          | <b>H [m]</b> | 0                                  | 30   | 60   | 90   | 120  | 150  | 180  | 210   | 240   | 270  | 300  | 330  | Total |
| A [m/s]              | 27.6         | 7.07                               | 6.47 | 6.98 | 7.14 | 6.73 | 6.84 | 8.61 | 10.04 | 10.42 | 9.20 | 8.69 | 7.99 | 8.32  |
| k [-]                | 27.6         | 2.44                               | 2.36 | 2.58 | 2.70 | 2.38 | 2.19 | 2.57 | 2.53  | 2.61  | 2.15 | 2.26 | 2.10 | 2.12  |
| f [%]                | 27.6         | 7.4                                | 6.7  | 6.7  | 7.2  | 5.8  | 5.0  | 7.3  | 11.0  | 15.0  | 10.3 | 9.4  | 8.2  | 100.0 |
| V <sub>m</sub> [m/s] | 27.6         | 6.15                               | 5.67 | 6.17 | 6.27 | 5.91 | 6.06 | 7.54 | 8.83  | 9.14  | 8.14 | 7.60 | 7.03 | 7.37  |

**Table 75:** Overview results of method 3: Hsu IDW General for the location Noordwijk.

| <b>3:Hsu IDW Gen</b> |              | <b>Wind direction sector [deg]</b> |      |      |      |      |      |      |      |       |      |      |      |       |
|----------------------|--------------|------------------------------------|------|------|------|------|------|------|------|-------|------|------|------|-------|
| <b>Par.</b>          | <b>H [m]</b> | 0                                  | 30   | 60   | 90   | 120  | 150  | 180  | 210  | 240   | 270  | 300  | 330  | Total |
| A [m/s]              | 27.6         | 6.99                               | 6.39 | 6.87 | 7.05 | 6.61 | 6.72 | 8.42 | 9.82 | 10.22 | 9.04 | 8.57 | 7.90 | 8.19  |
| k [-]                | 27.6         | 2.45                               | 2.37 | 2.56 | 2.71 | 2.40 | 2.22 | 2.57 | 2.51 | 2.60  | 2.13 | 2.24 | 2.09 | 2.13  |
| f [%]                | 27.6         | 7.4                                | 6.7  | 6.7  | 7.2  | 5.8  | 5.0  | 7.3  | 11.0 | 15.0  | 10.3 | 9.4  | 8.2  | 100.0 |
| V <sub>m</sub> [m/s] | 27.6         | 6.08                               | 5.60 | 6.09 | 6.18 | 5.81 | 5.95 | 7.39 | 8.66 | 8.97  | 8.01 | 7.50 | 6.96 | 7.25  |

**Table 76:** Overview results of method 4: Hsu Cov Shallow for the location Noordwijk.

| <b>4:Hsu Cov Sha</b> |              | <b>Wind direction sector [deg]</b> |      |      |      |      |      |      |       |       |      |      |      |       |
|----------------------|--------------|------------------------------------|------|------|------|------|------|------|-------|-------|------|------|------|-------|
| <b>Par.</b>          | <b>H [m]</b> | 0                                  | 30   | 60   | 90   | 120  | 150  | 180  | 210   | 240   | 270  | 300  | 330  | Total |
| A [m/s]              | 27.6         | 7.08                               | 6.46 | 6.96 | 7.10 | 6.67 | 6.83 | 8.62 | 10.09 | 10.49 | 9.23 | 8.71 | 8.00 | 8.33  |
| k [-]                | 27.6         | 2.44                               | 2.37 | 2.58 | 2.71 | 2.42 | 2.22 | 2.55 | 2.51  | 2.59  | 2.13 | 2.26 | 2.09 | 2.10  |
| f [%]                | 27.6         | 7.4                                | 6.7  | 6.7  | 7.2  | 5.8  | 5.0  | 7.3  | 11.0  | 15.0  | 10.3 | 9.4  | 8.2  | 100.0 |
| V <sub>m</sub> [m/s] | 27.6         | 6.15                               | 5.66 | 6.15 | 6.23 | 5.86 | 6.04 | 7.56 | 8.88  | 9.20  | 8.17 | 7.61 | 7.04 | 7.38  |

**Table 77:** Overview results of method 5: Hsu Cov General for the location Noordwijk.

| <b>3:Hsu Cov Gen</b> |              | <b>Wind direction sector [deg]</b> |      |      |      |      |      |      |      |       |      |      |      |       |
|----------------------|--------------|------------------------------------|------|------|------|------|------|------|------|-------|------|------|------|-------|
| <b>Par.</b>          | <b>H [m]</b> | 0                                  | 30   | 60   | 90   | 120  | 150  | 180  | 210  | 240   | 270  | 300  | 330  | Total |
| A [m/s]              | 27.6         | 7.00                               | 6.38 | 6.85 | 7.00 | 6.55 | 6.70 | 8.44 | 9.88 | 10.29 | 9.08 | 8.58 | 7.91 | 8.20  |
| k [-]                | 27.6         | 2.45                               | 2.37 | 2.55 | 2.73 | 2.46 | 2.26 | 2.56 | 2.49 | 2.59  | 2.12 | 2.23 | 2.09 | 2.11  |
| f [%]                | 27.6         | 7.4                                | 6.7  | 6.7  | 7.2  | 5.8  | 5.0  | 7.3  | 11.0 | 15.0  | 10.3 | 9.4  | 8.2  | 100.0 |
| V <sub>m</sub> [m/s] | 27.6         | 6.08                               | 5.60 | 6.07 | 6.15 | 5.76 | 5.92 | 7.40 | 8.71 | 9.03  | 8.04 | 7.52 | 6.96 | 7.26  |

## B.6 Results IJmuiden

**Table 78:** Overview results of measurements for the location IJmuiden.

| <b>Measurements</b>  |              | <b>Wind direction sector [deg]</b> |      |      |      |      |      |      |       |      |      |      |      |       |
|----------------------|--------------|------------------------------------|------|------|------|------|------|------|-------|------|------|------|------|-------|
| <b>Par.</b>          | <b>H [m]</b> | 0                                  | 30   | 60   | 90   | 120  | 150  | 180  | 210   | 240  | 270  | 300  | 330  | Total |
| A [m/s]              | 18.5         | 6.83                               | 6.18 | 7.63 | 6.21 | 4.67 | 5.73 | 6.91 | 10.11 | 9.65 | 8.72 | 8.38 | 7.66 | 7.49  |
| k [-]                | 18.5         | 2.12                               | 2.47 | 3.37 | 2.40 | 2.90 | 3.01 | 2.15 | 2.80  | 2.93 | 2.13 | 2.49 | 1.98 | 1.91  |
| f [%]                | 18.5         | 4.7                                | 6.3  | 4.7  | 11.5 | 5.2  | 6.2  | 9.0  | 13.6  | 14.3 | 10.0 | 7.6  | 7.0  | 100.0 |
| V <sub>m</sub> [m/s] | 18.5         | 6.07                               | 5.48 | 6.69 | 5.62 | 3.95 | 4.89 | 6.19 | 8.80  | 8.26 | 7.77 | 7.20 | 6.94 | 6.84  |

**Table 79:** Overview results of method 1: Charnock for the location IJmuiden.

| <b>1:Charnock</b>    |              | <b>Wind direction sector [deg]</b> |      |      |      |      |      |      |       |       |      |      |      |       |
|----------------------|--------------|------------------------------------|------|------|------|------|------|------|-------|-------|------|------|------|-------|
| <b>Par.</b>          | <b>H [m]</b> | 0                                  | 30   | 60   | 90   | 120  | 150  | 180  | 210   | 240   | 270  | 300  | 330  | Total |
| A [m/s]              | 18.5         | 7.13                               | 6.60 | 5.97 | 5.39 | 4.95 | 6.05 | 8.52 | 10.63 | 10.55 | 9.58 | 8.73 | 8.05 | 8.11  |
| k [-]                | 18.5         | 2.17                               | 2.27 | 2.34 | 2.25 | 2.30 | 1.99 | 2.14 | 2.40  | 2.23  | 2.02 | 2.09 | 1.98 | 1.80  |
| f [%]                | 18.5         | 6.4                                | 6.2  | 6.8  | 7.2  | 5.5  | 5.0  | 7.7  | 12.4  | 15.1  | 11.0 | 8.9  | 7.8  | 100.0 |
| V <sub>m</sub> [m/s] | 18.5         | 6.24                               | 5.80 | 5.30 | 4.85 | 4.40 | 5.38 | 7.55 | 9.31  | 9.32  | 8.49 | 7.72 | 7.18 | 7.30  |

**Table 80:** Overview results of method 2: Hsu IDW Shallow for the location IJmuiden.

| <i>2:Hsu IDW Sha</i>       |       | Wind direction sector [deg] |      |      |      |      |      |      |       |       |      |      |      |       |
|----------------------------|-------|-----------------------------|------|------|------|------|------|------|-------|-------|------|------|------|-------|
| Par.                       | H [m] | 0                           | 30   | 60   | 90   | 120  | 150  | 180  | 210   | 240   | 270  | 300  | 330  | Total |
| A [m/s]                    | 18.5  | 7.22                        | 6.77 | 5.99 | 5.39 | 4.95 | 6.08 | 8.53 | 10.37 | 10.26 | 9.46 | 8.69 | 8.09 | 8.12  |
| <i>k</i> [-]               | 18.5  | 2.33                        | 2.43 | 2.39 | 2.26 | 2.30 | 2.03 | 2.35 | 2.66  | 2.50  | 2.24 | 2.30 | 2.17 | 2.00  |
| <i>f</i> [%]               | 18.5  | 6.4                         | 6.3  | 6.8  | 7.2  | 5.5  | 5.0  | 7.7  | 12.4  | 15.1  | 11.0 | 8.9  | 7.8  | 100.0 |
| <i>V<sub>m</sub></i> [m/s] | 18.5  | 6.32                        | 5.94 | 5.32 | 4.85 | 4.41 | 5.39 | 7.50 | 9.09  | 9.05  | 8.35 | 7.66 | 7.16 | 7.22  |

**Table 81:** Overview results of method 3: Hsu IDW General for the location IJmuiden.

| <i>3:Hsu IDW Gen</i>       |       | Wind direction sector [deg] |      |      |      |      |      |      |       |       |      |      |      |       |
|----------------------------|-------|-----------------------------|------|------|------|------|------|------|-------|-------|------|------|------|-------|
| Par.                       | H [m] | 0                           | 30   | 60   | 90   | 120  | 150  | 180  | 210   | 240   | 270  | 300  | 330  | Total |
| A [m/s]                    | 18.5  | 7.20                        | 6.75 | 5.99 | 5.39 | 4.95 | 6.07 | 8.51 | 10.32 | 10.21 | 9.41 | 8.66 | 8.06 | 8.09  |
| <i>k</i> [-]               | 18.5  | 2.34                        | 2.43 | 2.39 | 2.26 | 2.30 | 2.03 | 2.35 | 2.66  | 2.50  | 2.24 | 2.31 | 2.17 | 2.00  |
| <i>f</i> [%]               | 18.5  | 6.4                         | 6.3  | 6.8  | 7.2  | 5.5  | 5.0  | 7.7  | 12.4  | 15.1  | 11.0 | 8.9  | 7.8  | 100.0 |
| <i>V<sub>m</sub></i> [m/s] | 18.5  | 6.29                        | 5.92 | 5.32 | 4.85 | 4.41 | 5.39 | 7.48 | 9.06  | 9.01  | 8.31 | 7.62 | 7.13 | 7.20  |

**Table 82:** Overview results of method 4: Hsu Cov Shallow for the location IJmuiden.

| <i>4:Hsu Cov Sha</i>       |       | Wind direction sector [deg] |      |      |      |      |      |      |       |       |      |      |      |       |
|----------------------------|-------|-----------------------------|------|------|------|------|------|------|-------|-------|------|------|------|-------|
| Par.                       | H [m] | 0                           | 30   | 60   | 90   | 120  | 150  | 180  | 210   | 240   | 270  | 300  | 330  | Total |
| A [m/s]                    | 18.5  | 7.22                        | 6.76 | 5.99 | 5.39 | 4.95 | 6.07 | 8.55 | 10.44 | 10.34 | 9.51 | 8.73 | 8.11 | 8.14  |
| <i>k</i> [-]               | 18.5  | 2.33                        | 2.44 | 2.40 | 2.27 | 2.31 | 2.03 | 2.34 | 2.66  | 2.48  | 2.24 | 2.29 | 2.17 | 1.98  |
| <i>f</i> [%]               | 18.5  | 6.4                         | 6.3  | 6.8  | 7.2  | 5.5  | 5.0  | 7.7  | 12.4  | 15.1  | 11.0 | 8.9  | 7.8  | 100.0 |
| <i>V<sub>m</sub></i> [m/s] | 18.5  | 6.32                        | 5.93 | 5.31 | 4.85 | 4.41 | 5.39 | 7.51 | 9.15  | 9.13  | 8.40 | 7.69 | 7.17 | 7.25  |

**Table 83:** Overview results of method 5: Hsu Cov General for the location IJmuiden.

| <i>3:Hsu Cov Gen</i>       |       | Wind direction sector [deg] |      |      |      |      |      |      |       |       |      |      |      |       |
|----------------------------|-------|-----------------------------|------|------|------|------|------|------|-------|-------|------|------|------|-------|
| Par.                       | H [m] | 0                           | 30   | 60   | 90   | 120  | 150  | 180  | 210   | 240   | 270  | 300  | 330  | Total |
| A [m/s]                    | 18.5  | 7.20                        | 6.74 | 5.99 | 5.39 | 4.95 | 6.06 | 8.53 | 10.40 | 10.28 | 9.46 | 8.69 | 8.07 | 8.11  |
| <i>k</i> [-]               | 18.5  | 2.34                        | 2.44 | 2.40 | 2.27 | 2.31 | 2.03 | 2.34 | 2.66  | 2.48  | 2.23 | 2.29 | 2.17 | 1.98  |
| <i>f</i> [%]               | 18.5  | 6.4                         | 6.3  | 6.8  | 7.2  | 5.5  | 5.0  | 7.7  | 12.4  | 15.1  | 11.0 | 8.9  | 7.8  | 100.0 |
| <i>V<sub>m</sub></i> [m/s] | 18.5  | 6.30                        | 5.91 | 5.31 | 4.85 | 4.41 | 5.38 | 7.49 | 9.11  | 9.08  | 8.35 | 7.65 | 7.15 | 7.22  |

## B.7 Results Licht Eiland Goeree

**Table 84:** Overview results of measurements for the location Licht Eiland Goeree.

| <i>Measurements</i>        |       | Wind direction sector [deg] |      |      |      |      |      |      |       |       |      |      |      |       |
|----------------------------|-------|-----------------------------|------|------|------|------|------|------|-------|-------|------|------|------|-------|
| Par.                       | H [m] | 0                           | 30   | 60   | 90   | 120  | 150  | 180  | 210   | 240   | 270  | 300  | 330  | Total |
| A [m/s]                    | 38.3  | 7.27                        | 7.50 | 7.52 | 6.65 | 6.73 | 6.58 | 8.71 | 10.14 | 10.05 | 8.90 | 8.97 | 8.76 | 8.60  |
| <i>k</i> [-]               | 38.3  | 2.08                        | 2.52 | 2.71 | 2.06 | 2.83 | 2.08 | 2.68 | 2.93  | 2.54  | 1.97 | 2.43 | 2.29 | 2.29  |
| <i>f</i> [%]               | 38.3  | 4.9                         | 7.7  | 7.7  | 6.4  | 5.4  | 5.3  | 8.2  | 12.9  | 16.5  | 10.5 | 7.7  | 6.8  | 100.0 |
| <i>V<sub>m</sub></i> [m/s] | 38.3  | 6.34                        | 6.52 | 6.52 | 6.10 | 5.72 | 6.00 | 7.56 | 8.79  | 8.91  | 8.14 | 7.72 | 7.58 | 7.52  |

**Table 85:** Overview results of method 1: Charnock for the location Licht Eiland Goeree.

| <i>1:Charnock</i>          |       | Wind direction sector [deg] |      |      |      |      |      |      |      |      |      |      |      |       |
|----------------------------|-------|-----------------------------|------|------|------|------|------|------|------|------|------|------|------|-------|
| Par.                       | H [m] | 0                           | 30   | 60   | 90   | 120  | 150  | 180  | 210  | 240  | 270  | 300  | 330  | Total |
| A [m/s]                    | 38.3  | 6.88                        | 6.54 | 6.66 | 6.54 | 5.84 | 6.27 | 8.30 | 9.69 | 9.52 | 8.57 | 7.89 | 7.77 | 7.88  |
| <i>k</i> [-]               | 38.3  | 2.23                        | 2.26 | 2.46 | 2.40 | 2.15 | 2.13 | 2.16 | 2.40 | 2.34 | 1.95 | 2.02 | 2.05 | 1.99  |
| <i>f</i> [%]               | 38.3  | 7.3                         | 7.3  | 7.2  | 6.8  | 4.8  | 4.5  | 7.2  | 12.3 | 16.2 | 10.7 | 8.5  | 7.0  | 100.0 |
| <i>V<sub>m</sub></i> [m/s] | 38.3  | 6.00                        | 5.75 | 5.84 | 5.78 | 5.22 | 5.57 | 7.36 | 8.53 | 8.40 | 7.68 | 6.98 | 6.82 | 7.02  |

**Table 86:** Overview results of method 2: Hsu IDW Shallow for the location Licht Eiland Goeree.

| <i>2:Hsu IDW Sha</i> |       | Wind direction sector [deg] |      |      |      |      |      |      |      |      |      |      |      |       |
|----------------------|-------|-----------------------------|------|------|------|------|------|------|------|------|------|------|------|-------|
| Par.                 | H [m] | 0                           | 30   | 60   | 90   | 120  | 150  | 180  | 210  | 240  | 270  | 300  | 330  | Total |
| A [m/s]              | 38.3  | 6.97                        | 6.72 | 6.82 | 6.73 | 6.07 | 6.58 | 8.48 | 9.75 | 9.57 | 8.62 | 7.97 | 7.80 | 8.01  |
| k [-]                | 38.3  | 2.35                        | 2.39 | 2.59 | 2.57 | 2.26 | 2.32 | 2.38 | 2.63 | 2.60 | 2.09 | 2.16 | 2.13 | 2.16  |
| f [%]                | 38.3  | 7.3                         | 7.3  | 7.2  | 6.8  | 4.9  | 4.5  | 7.2  | 12.4 | 16.2 | 10.7 | 8.5  | 7.0  | 100.0 |
| V <sub>m</sub> [m/s] | 38.3  | 6.08                        | 5.90 | 5.99 | 5.94 | 5.43 | 5.79 | 7.48 | 8.58 | 8.42 | 7.69 | 7.01 | 6.84 | 7.10  |

**Table 87:** Overview results of method 3: Hsu IDW General for the location Licht Eiland Goeree.

| <i>3:Hsu IDW Gen</i> |       | Wind direction sector [deg] |      |      |      |      |      |      |      |      |      |      |      |       |
|----------------------|-------|-----------------------------|------|------|------|------|------|------|------|------|------|------|------|-------|
| Par.                 | H [m] | 0                           | 30   | 60   | 90   | 120  | 150  | 180  | 210  | 240  | 270  | 300  | 330  | Total |
| A [m/s]              | 38.3  | 6.91                        | 6.65 | 6.74 | 6.65 | 5.98 | 6.44 | 8.34 | 9.58 | 9.40 | 8.51 | 7.90 | 7.74 | 7.90  |
| k [-]                | 38.3  | 2.34                        | 2.40 | 2.60 | 2.58 | 2.27 | 2.32 | 2.39 | 2.62 | 2.60 | 2.09 | 2.15 | 2.13 | 2.16  |
| f [%]                | 38.3  | 7.3                         | 7.3  | 7.2  | 6.8  | 4.9  | 4.5  | 7.2  | 12.4 | 16.2 | 10.7 | 8.5  | 7.0  | 100.0 |
| V <sub>m</sub> [m/s] | 38.3  | 6.03                        | 5.84 | 5.92 | 5.87 | 5.34 | 5.69 | 7.35 | 8.44 | 8.28 | 7.60 | 6.95 | 6.79 | 7.01  |

**Table 88:** Overview results of method 4: Hsu Cov Shallow for the location Licht Eiland Goeree.

| <i>4:Hsu Cov Sha</i> |       | Wind direction sector [deg] |      |      |      |      |      |      |      |      |      |      |      |       |
|----------------------|-------|-----------------------------|------|------|------|------|------|------|------|------|------|------|------|-------|
| Par.                 | H [m] | 0                           | 30   | 60   | 90   | 120  | 150  | 180  | 210  | 240  | 270  | 300  | 330  | Total |
| A [m/s]              | 38.3  | 6.97                        | 6.73 | 6.82 | 6.72 | 6.05 | 6.57 | 8.48 | 9.76 | 9.59 | 8.63 | 7.97 | 7.80 | 8.02  |
| k [-]                | 38.3  | 2.34                        | 2.38 | 2.58 | 2.57 | 2.26 | 2.33 | 2.37 | 2.63 | 2.59 | 2.09 | 2.15 | 2.13 | 2.15  |
| f [%]                | 38.3  | 7.3                         | 7.3  | 7.2  | 6.8  | 4.9  | 4.5  | 7.2  | 12.4 | 16.2 | 10.7 | 8.5  | 7.0  | 100.0 |
| V <sub>m</sub> [m/s] | 38.3  | 6.08                        | 5.91 | 5.99 | 5.93 | 5.41 | 5.78 | 7.48 | 8.58 | 8.45 | 7.70 | 7.02 | 6.85 | 7.11  |

**Table 89:** Overview results of method 5: Hsu Cov General for the location Licht Eiland Goeree.

| <i>3:Hsu Cov Gen</i> |       | Wind direction sector [deg] |      |      |      |      |      |      |      |      |      |      |      |       |
|----------------------|-------|-----------------------------|------|------|------|------|------|------|------|------|------|------|------|-------|
| Par.                 | H [m] | 0                           | 30   | 60   | 90   | 120  | 150  | 180  | 210  | 240  | 270  | 300  | 330  | Total |
| A [m/s]              | 38.3  | 6.91                        | 6.66 | 6.74 | 6.65 | 5.97 | 6.44 | 8.34 | 9.59 | 9.44 | 8.52 | 7.90 | 7.74 | 7.91  |
| k [-]                | 38.3  | 2.34                        | 2.39 | 2.59 | 2.58 | 2.29 | 2.33 | 2.38 | 2.63 | 2.61 | 2.08 | 2.15 | 2.13 | 2.15  |
| f [%]                | 38.3  | 7.3                         | 7.3  | 7.2  | 6.8  | 4.9  | 4.5  | 7.2  | 12.4 | 16.2 | 10.7 | 8.5  | 7.0  | 100.0 |
| V <sub>m</sub> [m/s] | 38.3  | 6.03                        | 5.85 | 5.93 | 5.86 | 5.33 | 5.68 | 7.35 | 8.45 | 8.31 | 7.61 | 6.95 | 6.80 | 7.01  |

## B.8 Results Vlakte van de Raan

**Table 90:** Overview results of measurements for the location Vlakte van de Raan.

| <i>Measurements</i>  |       | Wind direction sector [deg] |      |      |      |      |      |      |      |      |      |      |      |       |
|----------------------|-------|-----------------------------|------|------|------|------|------|------|------|------|------|------|------|-------|
| Par.                 | H [m] | 0                           | 30   | 60   | 90   | 120  | 150  | 180  | 210  | 240  | 270  | 300  | 330  | Total |
| A [m/s]              | 16.5  | 7.06                        | 7.18 | 7.32 | 6.44 | 5.92 | 6.69 | 8.89 | 9.35 | 9.95 | 8.76 | 8.61 | 8.31 | 8.22  |
| k [-]                | 16.5  | 1.96                        | 2.24 | 2.46 | 2.04 | 2.28 | 2.77 | 2.83 | 2.73 | 2.37 | 2.27 | 2.17 | 2.04 | 2.14  |
| f [%]                | 16.5  | 4.7                         | 8.2  | 7.4  | 7.3  | 4.7  | 5.5  | 9.0  | 13.7 | 16.2 | 9.2  | 7.6  | 6.6  | 100.0 |
| V <sub>m</sub> [m/s] | 16.5  | 6.28                        | 6.38 | 6.44 | 6.00 | 5.27 | 5.72 | 7.70 | 8.29 | 8.98 | 7.64 | 7.54 | 7.39 | 7.34  |

**Table 91:** Overview results of method 1: Charnock for the location Vlakte van de Raan.

| <i>1:Charnock</i>    |       | Wind direction sector [deg] |      |      |      |      |      |      |      |      |      |      |      |       |
|----------------------|-------|-----------------------------|------|------|------|------|------|------|------|------|------|------|------|-------|
| Par.                 | H [m] | 0                           | 30   | 60   | 90   | 120  | 150  | 180  | 210  | 240  | 270  | 300  | 330  | Total |
| A [m/s]              | 16.5  | 6.96                        | 6.67 | 6.82 | 6.56 | 5.70 | 6.22 | 8.44 | 9.56 | 9.64 | 8.60 | 8.06 | 7.68 | 7.97  |
| k [-]                | 16.5  | 2.18                        | 2.24 | 2.41 | 2.38 | 2.23 | 2.13 | 2.31 | 2.54 | 2.45 | 1.99 | 2.04 | 2.01 | 2.07  |
| f [%]                | 16.5  | 7.1                         | 7.7  | 7.7  | 6.7  | 4.4  | 4.3  | 7.6  | 12.4 | 16.4 | 10.6 | 8.3  | 6.7  | 100.0 |
| V <sub>m</sub> [m/s] | 16.5  | 6.13                        | 5.91 | 6.01 | 5.83 | 5.09 | 5.55 | 7.43 | 8.40 | 8.50 | 7.66 | 7.12 | 6.77 | 7.07  |

**Table 92:** Overview results of method 2: Hsu IDW Shallow for the location Vlake van de Raan.

| <i>2:Hsu IDW Sha</i>       |       | Wind direction sector [deg] |      |      |      |      |      |      |      |      |      |      |      |       |
|----------------------------|-------|-----------------------------|------|------|------|------|------|------|------|------|------|------|------|-------|
| Par.                       | H [m] | 0                           | 30   | 60   | 90   | 120  | 150  | 180  | 210  | 240  | 270  | 300  | 330  | Total |
| A [m/s]                    | 16.5  | 7.09                        | 6.89 | 6.99 | 6.81 | 6.01 | 6.56 | 8.57 | 9.57 | 9.63 | 8.61 | 8.12 | 7.71 | 8.10  |
| <i>k</i> [-]               | 16.5  | 2.35                        | 2.42 | 2.58 | 2.65 | 2.43 | 2.36 | 2.55 | 2.85 | 2.78 | 2.15 | 2.20 | 2.11 | 2.28  |
| <i>f</i> [%]               | 16.5  | 7.1                         | 7.7  | 7.7  | 6.7  | 4.4  | 4.3  | 7.6  | 12.4 | 16.4 | 10.6 | 8.3  | 6.7  | 100.0 |
| <i>V<sub>m</sub></i> [m/s] | 16.5  | 6.21                        | 6.09 | 6.17 | 6.01 | 5.34 | 5.80 | 7.55 | 8.42 | 8.50 | 7.67 | 7.16 | 6.80 | 7.15  |

**Table 93:** Overview results of method 3: Hsu IDW General for the location Vlake van de Raan.

| <i>3:Hsu IDW Gen</i>       |       | Wind direction sector [deg] |      |      |      |      |      |      |      |      |      |      |      |       |
|----------------------------|-------|-----------------------------|------|------|------|------|------|------|------|------|------|------|------|-------|
| Par.                       | H [m] | 0                           | 30   | 60   | 90   | 120  | 150  | 180  | 210  | 240  | 270  | 300  | 330  | Total |
| A [m/s]                    | 16.5  | 7.05                        | 6.85 | 6.95 | 6.76 | 5.95 | 6.49 | 8.50 | 9.50 | 9.53 | 8.55 | 8.08 | 7.68 | 8.04  |
| <i>k</i> [-]               | 16.5  | 2.33                        | 2.42 | 2.59 | 2.63 | 2.44 | 2.36 | 2.55 | 2.84 | 2.76 | 2.14 | 2.19 | 2.11 | 2.27  |
| <i>f</i> [%]               | 16.5  | 7.1                         | 7.7  | 7.7  | 6.7  | 4.4  | 4.3  | 7.6  | 12.4 | 16.4 | 10.6 | 8.3  | 6.7  | 100.0 |
| <i>V<sub>m</sub></i> [m/s] | 16.5  | 6.19                        | 6.05 | 6.14 | 5.98 | 5.29 | 5.74 | 7.48 | 8.36 | 8.42 | 7.62 | 7.12 | 6.77 | 7.10  |

**Table 94:** Overview results of method 4: Hsu Cov Shallow for the location Vlake van de Raan.

| <i>4:Hsu Cov Sha</i>       |       | Wind direction sector [deg] |      |      |      |      |      |      |      |      |      |      |      |       |
|----------------------------|-------|-----------------------------|------|------|------|------|------|------|------|------|------|------|------|-------|
| Par.                       | H [m] | 0                           | 30   | 60   | 90   | 120  | 150  | 180  | 210  | 240  | 270  | 300  | 330  | Total |
| A [m/s]                    | 16.5  | 7.09                        | 6.90 | 7.00 | 6.81 | 6.00 | 6.54 | 8.57 | 9.59 | 9.66 | 8.62 | 8.12 | 7.71 | 8.10  |
| <i>k</i> [-]               | 16.5  | 2.35                        | 2.40 | 2.57 | 2.64 | 2.44 | 2.36 | 2.54 | 2.84 | 2.77 | 2.15 | 2.19 | 2.10 | 2.27  |
| <i>f</i> [%]               | 16.5  | 7.1                         | 7.7  | 7.7  | 6.7  | 4.4  | 4.3  | 7.6  | 12.4 | 16.4 | 10.6 | 8.3  | 6.7  | 100.0 |
| <i>V<sub>m</sub></i> [m/s] | 16.5  | 6.22                        | 6.10 | 6.18 | 6.01 | 5.33 | 5.79 | 7.55 | 8.43 | 8.53 | 7.68 | 7.16 | 6.80 | 7.16  |

**Table 95:** Overview results of method 5: Hsu Cov General for the location Vlake van de Raan.

| <i>3:Hsu Cov Gen</i>       |       | Wind direction sector [deg] |      |      |      |      |      |      |      |      |      |      |      |       |
|----------------------------|-------|-----------------------------|------|------|------|------|------|------|------|------|------|------|------|-------|
| Par.                       | H [m] | 0                           | 30   | 60   | 90   | 120  | 150  | 180  | 210  | 240  | 270  | 300  | 330  | Total |
| A [m/s]                    | 16.5  | 7.05                        | 6.86 | 6.96 | 6.77 | 5.95 | 6.46 | 8.50 | 9.52 | 9.57 | 8.56 | 8.08 | 7.68 | 8.04  |
| <i>k</i> [-]               | 16.5  | 2.33                        | 2.40 | 2.57 | 2.64 | 2.45 | 2.34 | 2.54 | 2.84 | 2.74 | 2.15 | 2.18 | 2.10 | 2.26  |
| <i>f</i> [%]               | 16.5  | 7.1                         | 7.7  | 7.7  | 6.7  | 4.4  | 4.3  | 7.6  | 12.4 | 16.4 | 10.6 | 8.3  | 6.7  | 100.0 |
| <i>V<sub>m</sub></i> [m/s] | 16.5  | 6.19                        | 6.07 | 6.14 | 5.98 | 5.28 | 5.73 | 7.48 | 8.37 | 8.45 | 7.63 | 7.12 | 6.78 | 7.11  |

## B.9 Results Oosterschelde

**Table 96:** Overview results of measurements for the location Oosterschelde.

| <i>Measurements</i>        |       | Wind direction sector [deg] |      |      |      |      |      |      |      |      |      |      |      |       |
|----------------------------|-------|-----------------------------|------|------|------|------|------|------|------|------|------|------|------|-------|
| Par.                       | H [m] | 0                           | 30   | 60   | 90   | 120  | 150  | 180  | 210  | 240  | 270  | 300  | 330  | Total |
| A [m/s]                    | 16.5  | 6.91                        | 6.89 | 7.07 | 6.65 | 5.48 | 6.21 | 8.09 | 9.37 | 9.56 | 8.50 | 8.09 | 7.60 | 7.81  |
| <i>k</i> [-]               | 16.5  | 2.04                        | 2.37 | 2.60 | 2.38 | 2.14 | 2.65 | 2.58 | 3.03 | 2.74 | 2.44 | 2.24 | 1.91 | 2.16  |
| <i>f</i> [%]               | 16.5  | 5.3                         | 8.1  | 6.6  | 7.6  | 5.4  | 5.0  | 8.9  | 12.4 | 16.3 | 9.7  | 8.0  | 6.8  | 100.0 |
| <i>V<sub>m</sub></i> [m/s] | 16.5  | 6.03                        | 6.08 | 6.15 | 5.96 | 4.99 | 5.32 | 7.08 | 8.13 | 8.37 | 7.34 | 7.11 | 6.91 | 6.95  |

**Table 97:** Overview results of method 1: Charnock for the location Oosterschelde.

| <i>1:Charnock</i>          |       | Wind direction sector [deg] |      |      |      |      |      |      |      |      |      |      |      |       |
|----------------------------|-------|-----------------------------|------|------|------|------|------|------|------|------|------|------|------|-------|
| Par.                       | H [m] | 0                           | 30   | 60   | 90   | 120  | 150  | 180  | 210  | 240  | 270  | 300  | 330  | Total |
| A [m/s]                    | 16.5  | 6.86                        | 6.44 | 6.62 | 6.40 | 5.61 | 6.10 | 8.20 | 9.58 | 9.50 | 8.52 | 7.93 | 7.74 | 7.84  |
| <i>k</i> [-]               | 16.5  | 2.17                        | 2.17 | 2.45 | 2.28 | 2.05 | 2.10 | 2.20 | 2.49 | 2.42 | 1.97 | 2.05 | 2.05 | 2.02  |
| <i>f</i> [%]               | 16.5  | 7.3                         | 7.3  | 7.3  | 6.8  | 4.7  | 4.4  | 7.4  | 12.3 | 16.1 | 10.7 | 8.4  | 7.0  | 100.0 |
| <i>V<sub>m</sub></i> [m/s] | 16.5  | 6.05                        | 5.72 | 5.81 | 5.70 | 5.07 | 5.41 | 7.25 | 8.38 | 8.34 | 7.62 | 6.99 | 6.80 | 6.95  |

**Table 98:** Overview results of method 2: Hsu IDW Shallow for the location Oosterschelde.

| <b>2:Hsu IDW Sha</b> |              | <b>Wind direction sector [deg]</b> |      |      |      |      |      |      |      |      |      |      |      |       |
|----------------------|--------------|------------------------------------|------|------|------|------|------|------|------|------|------|------|------|-------|
| <b>Par.</b>          | <b>H [m]</b> | 0                                  | 30   | 60   | 90   | 120  | 150  | 180  | 210  | 240  | 270  | 300  | 330  | Total |
| A [m/s]              | 16.5         | 6.98                               | 6.67 | 6.80 | 6.65 | 5.92 | 6.45 | 8.38 | 9.58 | 9.47 | 8.55 | 8.00 | 7.79 | 7.97  |
| k [-]                | 16.5         | 2.32                               | 2.36 | 2.61 | 2.53 | 2.24 | 2.33 | 2.46 | 2.75 | 2.69 | 2.12 | 2.20 | 2.16 | 2.22  |
| f [%]                | 16.5         | 7.3                                | 7.3  | 7.3  | 6.8  | 4.7  | 4.5  | 7.4  | 12.3 | 16.1 | 10.7 | 8.4  | 7.0  | 100.0 |
| V <sub>m</sub> [m/s] | 16.5         | 6.14                               | 5.91 | 5.98 | 5.89 | 5.31 | 5.69 | 7.38 | 8.41 | 8.33 | 7.64 | 7.04 | 6.84 | 7.05  |

**Table 99:** Overview results of method 3: Hsu IDW General for the location Oosterschelde.

| <b>3:Hsu IDW Gen</b> |              | <b>Wind direction sector [deg]</b> |      |      |      |      |      |      |      |      |      |      |      |       |
|----------------------|--------------|------------------------------------|------|------|------|------|------|------|------|------|------|------|------|-------|
| <b>Par.</b>          | <b>H [m]</b> | 0                                  | 30   | 60   | 90   | 120  | 150  | 180  | 210  | 240  | 270  | 300  | 330  | Total |
| A [m/s]              | 16.5         | 6.92                               | 6.59 | 6.72 | 6.56 | 5.83 | 6.33 | 8.23 | 9.42 | 9.31 | 8.42 | 7.91 | 7.72 | 7.85  |
| k [-]                | 16.5         | 2.31                               | 2.33 | 2.59 | 2.49 | 2.26 | 2.35 | 2.46 | 2.72 | 2.69 | 2.10 | 2.18 | 2.14 | 2.21  |
| f [%]                | 16.5         | 7.3                                | 7.3  | 7.3  | 6.8  | 4.7  | 4.5  | 7.4  | 12.3 | 16.1 | 10.8 | 8.4  | 7.0  | 100.0 |
| V <sub>m</sub> [m/s] | 16.5         | 6.09                               | 5.84 | 5.92 | 5.83 | 5.23 | 5.58 | 7.25 | 8.28 | 8.19 | 7.54 | 6.97 | 6.79 | 6.95  |

**Table 100:** Overview results of method 4: Hsu Cov Shallow for the location Oosterschelde.

| <b>4:Hsu Cov Sha</b> |              | <b>Wind direction sector [deg]</b> |      |      |      |      |      |      |      |      |      |      |      |       |
|----------------------|--------------|------------------------------------|------|------|------|------|------|------|------|------|------|------|------|-------|
| <b>Par.</b>          | <b>H [m]</b> | 0                                  | 30   | 60   | 90   | 120  | 150  | 180  | 210  | 240  | 270  | 300  | 330  | Total |
| A [m/s]              | 16.5         | 6.99                               | 6.68 | 6.80 | 6.64 | 5.91 | 6.41 | 8.37 | 9.58 | 9.50 | 8.57 | 8.01 | 7.79 | 7.97  |
| k [-]                | 16.5         | 2.32                               | 2.35 | 2.60 | 2.52 | 2.26 | 2.34 | 2.46 | 2.76 | 2.70 | 2.13 | 2.19 | 2.15 | 2.22  |
| f [%]                | 16.5         | 7.3                                | 7.3  | 7.3  | 6.8  | 4.7  | 4.5  | 7.4  | 12.3 | 16.1 | 10.7 | 8.4  | 7.0  | 100.0 |
| V <sub>m</sub> [m/s] | 16.5         | 6.15                               | 5.92 | 5.98 | 5.89 | 5.30 | 5.66 | 7.37 | 8.40 | 8.35 | 7.64 | 7.04 | 6.85 | 7.05  |

**Table 101:** Overview results of method 5: Hsu Cov General for the location Oosterschelde.

| <b>3:Hsu Cov Gen</b> |              | <b>Wind direction sector [deg]</b> |      |      |      |      |      |      |      |      |      |      |      |       |
|----------------------|--------------|------------------------------------|------|------|------|------|------|------|------|------|------|------|------|-------|
| <b>Par.</b>          | <b>H [m]</b> | 0                                  | 30   | 60   | 90   | 120  | 150  | 180  | 210  | 240  | 270  | 300  | 330  | Total |
| A [m/s]              | 16.5         | 6.93                               | 6.60 | 6.72 | 6.55 | 5.80 | 6.29 | 8.22 | 9.41 | 9.34 | 8.43 | 7.92 | 7.72 | 7.85  |
| k [-]                | 16.5         | 2.31                               | 2.33 | 2.59 | 2.49 | 2.26 | 2.36 | 2.46 | 2.74 | 2.70 | 2.11 | 2.18 | 2.14 | 2.21  |
| f [%]                | 16.5         | 7.3                                | 7.3  | 7.3  | 6.8  | 4.7  | 4.5  | 7.4  | 12.3 | 16.1 | 10.8 | 8.4  | 7.0  | 100.0 |
| V <sub>m</sub> [m/s] | 16.5         | 6.10                               | 5.85 | 5.92 | 5.82 | 5.20 | 5.55 | 7.23 | 8.27 | 8.21 | 7.54 | 6.97 | 6.79 | 6.95  |



## C Surface roughness classes

**Table 102:** Roughness classes as defined for the LNG3+ database [50] [25]. Note that not all 46 classes are given in this table.

| <b>ID</b> | $z_0$ [m] | <b>Class names</b>                    |
|-----------|-----------|---------------------------------------|
| 0         | 0.03      | no data                               |
| 1         | 0.03      | grass                                 |
| 2         | 0.17      | maize                                 |
| 3         | 0.07      | potatoes                              |
| 4         | 0.1       | beets                                 |
| 5         | 0.16      | cereals                               |
| 6         | 0.04      | other agricultural crops              |
| 8         | 0.1       | greenhouses                           |
| 9         | 0.39      | orchards                              |
| 10        | 0.1       | bulb cultivation                      |
| 11        | 0.75      | deciduous forest                      |
| 12        | 0.75      | coniferous forest                     |
| 16        | 0.001     | fresh water                           |
| 17        | 0.001     | salt water                            |
| 18        | 1.6       | continuous urban area                 |
| 19        | 0.5       | built-up in rural area                |
| 20        | 1.1       | deciduous forest in urban area        |
| 21        | 1.1       | coniferous forest in urban area       |
| 22        | 2         | built-up area with dense forest       |
| 23        | 0.03      | grass in built-up area                |
| 24        | 0.001     | bare soil in built-up area            |
| 25        | 0.1       | main roads and railways               |
| 26        | 0.5       | buildings in rural area               |
| 27        | 0.0003    | runways                               |
| 28        | 0.1       | parking lots                          |
| 30        | 0.0002    | salt marshes                          |
| 31        | 0.0003    | beaches and dunes                     |
| 32        | 0.06      | sparsely vegetated dunes              |
| 33        | 0.02      | vegetated dunes                       |
| 34        | 0.03      | heathlands in dune areas              |
| 35        | 0.0003    | shifting sands                        |
| 36        | 0.03      | heathlands                            |
| 37        | 0.04      | heathlands with minor grass influence |
| 38        | 0.06      | heathlands with major grass influence |
| 39        | 0.06      | raised bogs                           |
| 40        | 0.75      | forest in raised bogs                 |
| 41        | 0.03      | miscellaneous swamp vegetation        |
| 42        | 0.1       | reed swamp                            |
| 43        | 0.75      | forest in swamp areas                 |
| 44        | 0.07      | swampy pastures in peat areas         |
| 45        | 0.03      | herbaceous vegetation                 |
| 46        | 0.001     | bare soil in natural areas            |